

12

AFGL-TR-86-0073

AD-A173 990

**MULTIPLE SCATTERING TREATMENT FOR USE IN
THE LOWTRAN AND FASCODE MODELS**

R. G. Isaacs
W.-C. Wang
R. D. Worsham
S. Goldenberg

DTIC
ELECTE
NOV 04 1986
S D

Atmospheric and Environmental Research, Inc.
840 Memorial Drive
Cambridge, Massachusetts 02139

7 April 1986

Final Report
1 January 1984 - 31 March 1986

APPROVED FOR PUBLIC RELEASE; DISTRIBUTION UNLIMITED

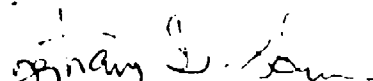
DTIC FILE COPY

AIR FORCE GEOPHYSICS LABORATORY
AIR FORCE SYSTEMS COMMAND
UNITED STATES AIR FORCE
HANSOM AIR FORCE BASE, MASSACHUSETTS 01731

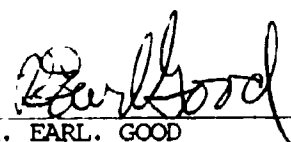
86 11 3_037

This technical report has been reviewed and is approved for publication.


FRANCIS X. KNEIZYS
Contract Manager


BERTRAM D. SCHURIN
Branch Chief

FOR THE COMMANDER


R. EARL GOOD
Acting Division Director

This report has been reviewed by the ESD Public Affairs Office (PA) and is releasable to the National Technical Information Service (NTIS).

Qualified requestors may obtain additional copies from the Defense Technical Information Center. All others should apply to the National Technical Information Service.

If your address has changed, or if you wish to be removed from the mailing list, or if the addressee is no longer employed by your organization, please notify AFGL/DAA, Hanscom AFB, MA 01731. This will assist us in maintaining a current mailing list.

DISCLAIMER NOTICE

**THIS DOCUMENT IS BEST QUALITY
PRACTICABLE. THE COPY FURNISHED
TO DTIC CONTAINED A SIGNIFICANT
NUMBER OF PAGES WHICH DO NOT
REPRODUCE LEGIBLY.**

Unclassified

SECURITY CLASSIFICATION OF THIS PAGE (When Data Entered)

REPORT DOCUMENTATION PAGE		READ INSTRUCTIONS BEFORE COMPLETING FORM
1. REPORT NUMBER AFGL-TR-86-0073	2. GOVT ACCESSION NO. AD-A173990	3. RECIPIENT'S CATALOG NUMBER
4. TITLE (and Subtitle) Multiple Scattering Treatment for Use in the LOWTRAN and FASCODE Models		5. TYPE OF REPORT & PERIOD COVERED Final Report 1 Jan. 1984 - 31 Mar. 1986
		6. PERFORMING ORG. REPORT NUMBER P95F
7. AUTHOR(s) R. G. Isaacs W.-C. Wang		8. CONTRACT OR GRANT NUMBER(s) F19628-84-C-0028
9. PERFORMING ORGANIZATION NAME AND ADDRESS Atmospheric and Environmental Research, Inc. (AER) 840 Memorial Drive Cambridge, MA 02139		10. PROGRAM ELEMENT, PROJECT, TASK AREA & WORK UNIT NUMBERS 62101F 767009AT
11. CONTROLLING OFFICE NAME AND ADDRESS Air Force Geophysics Laboratory Hanscom AFB, Massachusetts 01731 Contract Manager: F. Kneizys/OPI		12. REPORT DATE 7 April 1986
		13. NUMBER OF PAGES 234
14. MONITORING AGENCY NAME & ADDRESS (if different from Controlling Office)		15. SECURITY CLASS. (of this report) Unclassified
		15a. DECLASSIFICATION/DOWNGRADING SCHEDULE
16. DISTRIBUTION STATEMENT (of this Report) APPROVED FOR PUBLIC RELEASE; DISTRIBUTION UNLIMITED		
17. DISTRIBUTION STATEMENT (of the abstract entered in Block 20, if different from Report)		
18. SUPPLEMENTARY NOTES		
19. KEY WORDS (Continue on reverse side if necessary and identify by block number) Radiance Transmission Scattering Model Solar Atmosphere Thermal Aerosol Atmosphere		
20. ABSTRACT (Continue on reverse side if necessary and identify by block number) An evaluation of available approaches to treat the coupled processes of multiple-scattering due to atmospheric molecules and aerosols, and nongray absorption due to atmospheric gases is performed. Based on the evaluation and consideration of the requirements of efficiency, accuracy and code structure of LOWTRAN and FASCODE models, we recommend that an approach based on the stream approximation together with the k-distribution method is best suited for implementation into these models. The parameterization is unique in the (over)		

sense that the k-distribution method decouples the multiple-scattering from the treatment of non-gray gaseous absorption so that the stream approximation can be used to treat multiple scattering in both the LOWTRAN and FASCODE models. The stream approximation is extremely attractive since it retains the analytical simplicity (and hence, efficiency) of single scattering while improving the treatment of multiple-scattering (and hence, accuracy). Therefore, the parameterization is a uniform approach for solar, thermal and microwave regimes and can provide a general methodology to treat multiple-scattering due to aerosols, clouds and precipitation in the presence of gaseous absorption within the LOWTRAN/FASCODE formalism.

Calculations are performed to compare the accuracy of the stream approximation to numerical multiple scattering treatments for solar, thermal, and microwave spectral regions. Results indicate the approach can achieve RMS accuracies of about 20 percent in radiance for domains of optical properties characteristic of realistic atmospheric models.

The multiple scattering parameterization is implemented in both FASCODE and LOWTRAN models. FASCODE and LOWTRAN multiple scattering radiance results are compared to exact treatments. These results indicate that the new multiple scattering versions of these models provide more accurate simulations of the path dependent radiance than do their nonscattering counterparts. To insure consistency, multiple scattering versions of LOWTRAN and FASCODE are compared to one another.

Finally, recommendations are presented to further exploit the capabilities introduced here.

TABLE OF CONTENTS

	Page
1. INTRODUCTION	5
1.1 Background	5
1.2 Objective of the Present Study	6
2. MULTIPLE SCATTERING APPROACH	7
2.1 Stream Approximation	7
2.2 Theory	8
2.2.1 Radiance and Source Function	8
2.2.2 Layer Fluxes	14
2.2.3 Flux Adding Method.....	16
2.2.4 Band Model Considerations	17
3. IMPLEMENTATION OF MULTIPLE SCATTERING PARAMETERIZATION	20
3.1 FASCODE Implementation of the Stream Approximation for Multiple Scattering	20
3.1.1 Overview	20
3.1.2 Adding Method	23
3.1.2.1 Upward Adding Pass	25
3.1.2.2 Downward Pass	27
3.1.3 Stream Approximation, Source Function, Radiance ..	28
3.1.4 Description of FASCODE2 with Multiple Scattering	30
3.1.5 Notes on the Operation of FASCODE2 with Multiple Scattering	45
3.2 LOWTRAN Implementation	50
3.2.1 Overview	50
3.2.2 k-Distribution Method	50
3.2.3 Inhomogeneous Atmosphere	50
3.2.4 Stream Approximation, Source Function, and Radiance Calculation	59
3.2.5 Description of LOWTRAN6 with Multiple Scattering	60
3.2.6 Notes on the Operation of LOWTRAN6 with Multiple Scattering	64
4. RESULTS OF INTERCOMPARISON OF IMPLEMENTED MULTIPLE SCATTERING APPROACH WITH EXACT CALCULATIONS	66
4.1 Comparison of FASCODE Multiple Scattering Results to Exact Calculations	66
4.2 Comparison of LOWTRAN Multiple Scattering Results to Exact Calculations	77

For	
A&I	<input checked="" type="checkbox"/>
3	<input type="checkbox"/>
ed	<input type="checkbox"/>
1	
4	
5	
6	
7	
8	
9	
10	
11	
12	
13	
14	
15	
16	
17	
18	
19	
20	
21	
22	
23	
24	
25	
26	
27	
28	
29	
30	
31	
32	
33	
34	
35	
36	
37	
38	
39	
40	
41	
42	
43	
44	
45	
46	
47	
48	
49	
50	
51	
52	
53	
54	
55	
56	
57	
58	
59	
60	
61	
62	
63	
64	
65	
66	
67	
68	
69	
70	
71	
72	
73	
74	
75	
76	
77	
78	
79	
80	
81	
82	
83	
84	
85	
86	
87	
88	
89	
90	
91	
92	
93	
94	
95	
96	
97	
98	
99	
100	

ability Codes

Dist	Avail and/or Special
A-1	



TABLE OF CONTENTS (Cont.)

4.2.1	Solar Multiple Scattering	77
4.2.2	Thermal Multiple Scattering	78
5.	SUMMARY AND CONCLUSIONS	93
5.1	Summary	93
5.2	Recommendations	94
6.	ACKNOWLEDGEMENTS	96
7.	REFERENCES	97

APPENDICES

- A: REVIEW AND TRADE-OFF ANALYSIS OF MULTIPLE SCATTERING
PARAMETERIZATIONS
- B: FASCODE TEST CASE
- C: LOWTRAN TEST CASES

1. INTRODUCTION

1.1 Background

Optimal design and deployment of electro-optical (EO) remote sensing and communication systems requires accurate modeling and prediction of the effects of the ambient environment on atmospheric transmission. Atmospheric transmittance/radiance models such as AFGL's LOWTRAN (Kneizys et al., 1983) and FASCODE (Clough et al., 1986) have been developed within this context to provide the capability to assess potential adverse environmental impacts on EO system performance.

In order to accurately predict atmospheric effects on the propagation of visible, infrared and microwave radiation, it is necessary to treat the extinction mechanisms including molecular scattering and absorption, and particle (aerosols, clouds and precipitation) scattering and absorption, characterizing the ambient atmosphere. In the present AFGL transmittance/radiance models, these processes are adequately included in the treatment of path transmission. However, simplified treatments are employed to simulate the effects of scattering on the calculation of radiance. For thermal infrared and microwave radiation, for example, particle scattering in LOWTRAN has been treated as an enhancement to extinction but not as a source term. This approach leads to an underestimate of radiance for paths where multiple scattering is important (Ben-Shalom et al., 1980). LOWTRAN uses the single scattering approximation for evaluating solar radiances (Ridgway et al., 1982). While the single scattering implementation is straightforward, its application introduces errors which are functions of wavelength, sun/sensor geometry, and surface optical properties (cf. Isaacs and Özkaynak, 1980; Dave, 1981). These errors are primarily due to neglecting higher order scattering and surface reflection. In FASCODE, particle scattering has been treated as equivalent to absorption. All scattered radiation is thus re-emitted as if it were absorbed, i.e., the scattered radiation is conserved. This conservative scattering approach can lead to an overestimate of radiance.

In order to provide a more realistic simulation of radiation in spectral regions and along atmospheric paths where multiple scattering (MS) is a significant contribution to the source function, an efficient and accurate scattering parameterization has been incorporated into the LOWTRAN and FASCODE models.

1.2 Objective of the Present Study

A two-year research program supported by AFGL/OPI was undertaken at Atmospheric and Environmental Research, Inc. (AER). The overall program objective was to incorporate a uniform, compatible, accurate and efficient multiple scattering scheme into the present LOWTRAN/FASCODE models so that the multiple scattering effects due to particulates could be realistically treated. The first phase of the program was to study and evaluate the available multiple-scattering parameterizations and recommend the most appropriate one for its incorporation into the transmittance/radiance models. Constraints of efficiency, accuracy, and code structure of LOWTRAN/FASCODE were the key considerations of the evaluation processes. The results of a trade-off analysis to determine an appropriate approach are summarized in Appendix A. The second phase of the study was to implement the most suitable multiple scattering parameterization into the LOWTRAN and FASCODE models, test the resulting multiple scattering versions and document the codes.

This report summarizes the work accomplished in the second phase of the overall effort. Following this introduction, the selected approach for multiple scattering is described in detail (Section 2). In Section 3, the implementation of the multiple scattering parameterization within the LOWTRAN/FASCODE models is discussed in detail. Comparisons of the implemented code are made to exact treatments and to one another in Section 4. Finally, recommendations are provided in Section 5 for enhancing the multiple scattering capability provided here.

2. MULTIPLE SCATTERING APPROACH

2.1 Stream Approximation

Selection of an appropriate treatment of multiple scattering (MS) for application to the LOWTRAN and FASCODE models is severely constrained by competing requirements of desired efficiency and accuracy, and limitations imposed by the inherent code structures of these models. Additionally, it is desired to provide an approach which is uniformly applicable to all spectral regions considered and equally appropriate for implementation within both LOWTRAN and FASCODE. Based on these considerations, the MS parameterization selected consisted of a finite stream approach (using two streams for simplicity) to approximate the scattering source function.

This approach could be implemented directly in FASCODE since it is essentially a monochromatic calculation. It is known, however, that there exist difficulties in calculating the transmittance/radiance averaged over a finite spectral interval in a nongray gaseous absorber with multiple scattering because the commonly-used band models are not applicable (cf. Stephens, 1984). Such is the case for implementing an MS treatment within LOWTRAN. The best approach to solve this problem is the use of the k-distribution method, which decouples the multiple scattering from the gaseous spectral integration so that the available (monochromatic) multiple scattering algorithms can be used directly. For LOWTRAN, the stream approximation is performed through an interface routine consisting of the k-distribution method. For practical purposes, this consists of decomposing the band model determined optical properties into a set of equivalent monochromatic calculations which are then summed to give the spectrally averaged results. The configuration of the multiple scattering approach for LOWTRAN and FASCODE is summarized in Figure 2-1.

As mentioned earlier, the multiple scattering parameterization has to be accommodated by the present LOWTRAN and FASCODE code structures. This constraint is particularly important for FASCODE. In the FASCODE application, gaseous absorption is evaluated directly from the line-by-line calculation. Fluxes required for the stream approximation are calculated via the parameterized adding method. The adding method is particularly consistent with the code structure of both radiance/transmittance models since they treat one layer at a time.

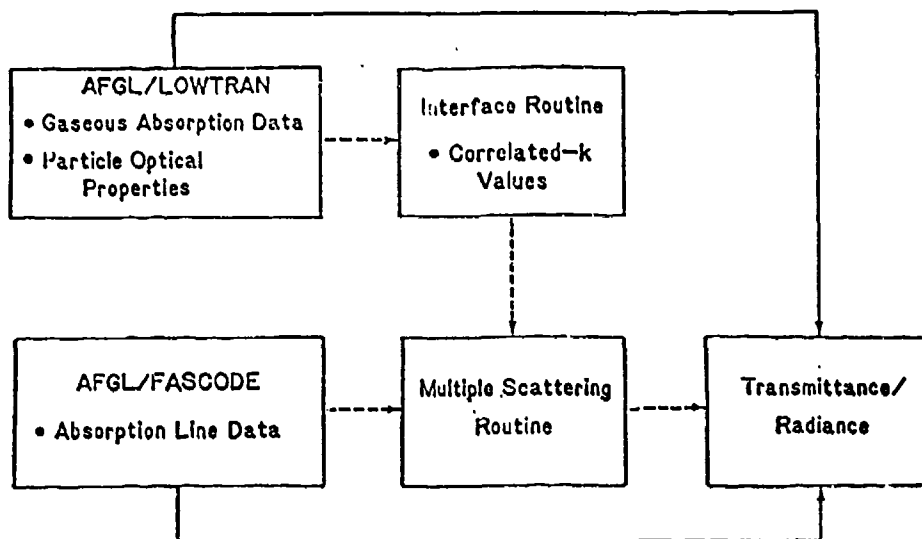


Fig. 2-1. AFGL transmittance/radiance code structure -- present models (solid line) with MS parameterization (dashed line).

In the FASCODE model, for example, the evaluation of layer optical properties always commences with that level in the selected path with the highest pressure and the selected spectral sampling interval decreases with pressure. This approach insures that the layer spectral resolution is consistent with the decrease of Voight line widths at higher altitudes. From the perspective of the line-by-line calculation, this method is computationally quite efficient. However, it is inconsistent with monochromatic multiple scattering treatments. In order to accomodate the sampling requirements of both the line-by-line and multiple scattering calculations, the FASCODE implementation employs the adding formalism to aid in the merging of the scattered fluxes from successive layers.

2.2 Theory

We provide a generic outline of the basic theory here. This prescription is modified slightly for specific application to the LOWTRAN and FASCODE models. Details of the specific model implementations are described in Section 3.

2.2.1 Radiance and Source Function

The desired radiance I_ν at wavenumber ν for an arbitrary path with zenith angle cosine and azimuth angle (μ, ϕ) is given by the solution to the radiative transfer equation (RTE):

$$\mu \frac{d}{dt} I_V(\tau, \mu, \phi) = I_V(\tau, \mu, \phi) - J_V(\tau, \mu, \phi). \quad (2.1)$$

Here τ_V is the optical thickness, μ is then cosine of the path zenith angle, and ϕ is the azimuth angle relative to the sun's azimuth. Vertical optical depth, τ_V , will depend on the relevant mechanisms determining the extinction of electromagnetic radiation for the spectral region characterized by wavenumber, ν . In general these mechanisms include: (a) molecular absorption, k_a , (b) molecular scattering, k_s , (c) particulate absorption, σ_a , and (d) particulate scattering, σ_s . Optical depth is given by integrating the relevant vertical extinction coefficient profiles according to:

$$\tau_V(z) = \int_z^{\infty} [k_a(z) + k_s(z) + \sigma_a(z) + \sigma_s(z)] dz$$

The general source function, J_V , including scattering of solar radiation and thermal emission, is given by:

$$J(\tau, \mu, \phi) = J_O(\tau, \mu, \phi) + J_{MS}(\tau, \mu, \phi) \quad (2.2)$$

where

$$J_O(\tau, \mu, \phi) = \frac{\omega_O(\tau)}{4\pi} \pi F e^{-\tau/\mu_O} P(\Omega; -\Omega_O) + [1 - \omega_O(\tau)] B[\Theta(\tau)] \quad (2.3)$$

and

$$J_{MS}(\tau, \mu, \phi) = \frac{\omega_O(\tau)}{4\pi} \int_{\Omega} P(\Omega; \Omega') I(\tau, \Omega') d\Omega'. \quad (2.4)$$

Here, ω_O is the single scattering albedo, P is the appropriate angular scattering or phase function, and B is the Planck function at temperature Θ . The extraterrestrial solar irradiance is given by F and the path and solar directions are given by Ω and Ω_O , respectively. The first term in Equation (2.3) is the single scattering of solar radiation while the second is the local thermal emission.

Radiance solutions to the RTE (Eq. (2.1)) are subject to boundary conditions at the top of the atmosphere ($\tau = 0.0$) for downward radiance and at the earth's surface ($\tau = \tau^*$) for upward radiance. At $\tau = 0.0$, downward diffuse radiance from space is zero (the direct solar irradiance is accounted for via the primary source function) resulting in:

$$I_b(0, -\mu, \phi) = 0.0 \quad (2.5)$$

(At millimeter wave frequencies a contribution due to emission at the cosmic background effective temperature of 2.7 K may be included when high accuracy is required.)

Boundary conditions at the surface will depend on the nature of the surface reflectance/emittance properties. The most common assumption is that of Lambert reflectance, i.e. the upward isotropic flux given by a constant surface albedo, r , times the downward flux. Upward and downward fluxes $F^\pm(\tau)$ at optical depth τ , are defined respectively as:

$$F^\pm(\tau) = \int_0^{2\pi} \int_0^1 I(\tau, \pm\mu, \phi) \mu d\mu d\phi \quad (2.6)$$

This results in a lower boundary condition upward radiance of:

$$I_b(\tau^*, \mu, \phi) = \frac{r}{\pi} \left[\pi F_{\downarrow 0} \exp(-\tau^*/\mu_0) + \int_0^{2\pi} \int_0^1 I(\tau^*, -\mu, \phi) \mu d\mu d\phi \right] + (1-r) B[T_s] \quad (2.7)$$

The three terms on the R.H.S. of (2.7) are respectively: (a) reflectance of attenuated solar irradiance (in UV, visible, near IR spectral regions), (b) reflectance of downward scattered radiance field, and (c) thermal emission due to the surface at temperature, T_s . The surface emissivity is unity minus the surface albedo, i.e., $(1-r)$. LOWTRAN requires that the surface albedo be specified, while FASCODE asks for the surface emissivity.

General radiance solutions to the RTE for upward and downward radiances, respectively, are:

$$I(\tau, +\mu, \phi) = I_b(\tau^*, \mu, \phi) e^{-(\tau^*-\tau)/\mu} + \int_{\tau}^{\tau^*} J(t, \mu, \phi) e^{-(t-\tau)/\mu} \frac{dt}{\mu} \quad (2.8)$$

$$I(\tau, -\mu, \phi) = I_b(0, -\mu, \phi) e^{-\tau/\mu} + \int_0^{\tau} J(t, \mu, \phi) e^{-(\tau-t)/\mu} \frac{dt}{\mu} \quad (2.9)$$

where the I_b are given by the boundary conditions (2.7) and (2.5) above, respectively. Incorporating these boundary conditions, the radiance solutions become:

$$I(\tau, \mu, \phi) = \left\{ \frac{\tau}{\pi} \left[\pi \mu_0 F e^{-\tau^*/\mu_0} + \int_0^1 \int_0^{2\pi} I(\tau^*, -\mu, \phi) \mu d\mu d\phi \right] \right. \\ \left. + (1-\tau) B[T(\tau^*)] \exp[-(\tau^*-\tau)/\mu] + \int_{\tau}^{\tau^*} J(t, \mu, \phi) e^{-(t-\tau)/\mu} \frac{dt}{\mu} \right\} \quad (2.10)$$

$$I(\tau, -\mu, \phi) = \int_0^{\tau} J(t, \mu, \phi) e^{-(\tau-t)/\mu} \frac{dt}{\mu} \quad (2.11)$$

In the stream approximation, the multiple scattering contribution to the source function (Eq. (2.4) above) is approximated by assuming constant scattered radiances I^+ and I^- over upward (Ω^+) and downward (Ω^-) hemispheres, respectively, or from Eq. (2.4):

$$J_{MS}(\tau, \mu, \phi) \approx \frac{\omega_0(\tau)}{4\pi} \left[I^+(\tau) \int_{\Omega^+} P(\Omega, \Omega^+) d\Omega^+ \right. \\ \left. + I^-(\tau) \int_{\Omega^-} P(\Omega, \Omega^-) d\Omega^- \right]. \quad (2.12)$$

Integrating over the angular scattering functions for the resulting azimuthally averaged backscatter fractions, $\beta(\mu)$, as a function of zenith angle cosine and substituting the corresponding fluxes:

$$I^{\pm}(\tau) \approx F^{\pm}(\tau)/\pi \quad (2.13)$$

results in

$$J_{MS}(\tau, \pm\mu, \phi) \approx \frac{\omega_0(\tau)}{\pi} \{ F^{\pm}(\tau) [1-\beta(\mu)] + F^{\mp}(\tau) \beta(\mu) \}. \quad (2.14)$$

This simple expression for the multiple scattered contribution to the source function is added to the single scattering and thermal emission contributions for the general source function, J (Eq. (2.2)). The source function is then integrated along with the desired path (as in Eqs. (2.10) or (2.11)) to obtain the desired total radiance including the approximated MS contribution.

The evaluation of the approximated MS source function (Eq. (2.14)) requires local fluxes F^+ , F^- , backscatter fractions, $\beta(u)$, and single scattering albedos, ω_0 . The backscatter fractions are given as functions of zenith angle cosine and asymmetry factor by Wiscombe and Grams (1976) (see Figure 2-2). A small error is introduced by assuming these backscatter fractions for the equivalent Henyey-Greenstein phase function rather than integrating the actual function. The single scattering albedo, $\omega_0(\tau)$, for a given layer with total optical thickness $\Delta\tau$ is:

$$\omega_0(\tau) = \Delta\tau_g / \Delta\tau \quad (2.15)$$

where $\Delta\tau_g$ is the total scattering optical thickness of the layer. Discretizing equation (2.14) for a given layer, N , the contribution of multiple scattering is approximated as:

$$J_{SA}^N(\pm\mu) = J_0 + \frac{\omega_0^N}{\pi} \{ F_N^\pm [1 - \beta^N(\mu, g^N)] + F_N^\mp \beta^N(\mu, g^N) \}. \quad (2.16)$$

Here the fluxes are taken as the layer mean quantities evaluated at a level halfway through the layer. The asymmetry factor, g , is a measure of the directional scattering and can be evaluated from the phase function.

Once the source function is approximated, the path radiance can be evaluated. Along a path consisting of layers (N) and the layer above ($N+1$) with transmissions T_N and T_{N+1} , respectively, for example, the emission, E , depends on the path integral of the total source function:

$$E_{N+1}^+ = E_N^+ T_{N+1} + J_{SA}^{N+1}(+\mu)(1 - T_{N+1}) \quad (2.17)$$

for downward looking and

$$E_{N+1}^- = E_N^- + (1 - T_{N+1}) J_{SA}^{N+1}(-\mu) T_N \quad (2.18)$$

for upward looking, where the intrinsic layer emission is

$$E_N^\pm = (1 - T_N) J_{SA}^N(\pm\mu). \quad (2.19)$$

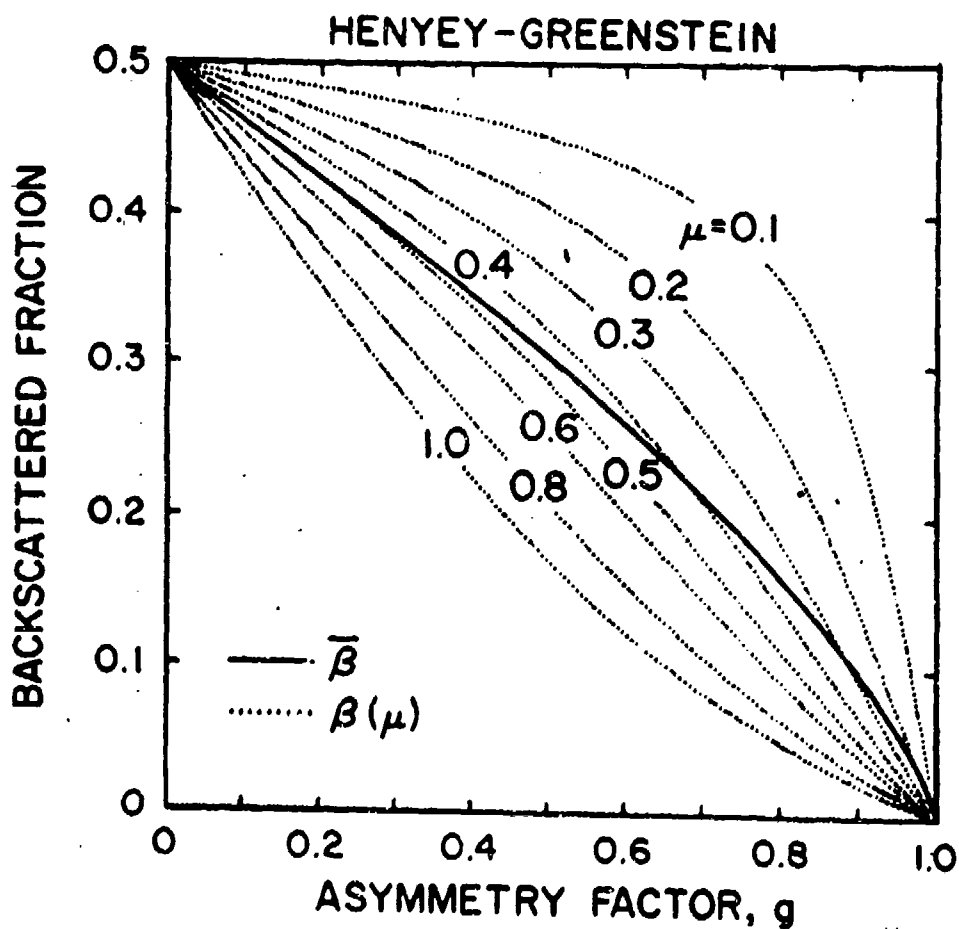


Figure 2-2. Backscattered fractions $\bar{\beta}$ and $\beta(\mu)$ for the Henyey-Greenstein phase function versus the asymmetry factor g for a range of values of μ (Wiscombe and Grams, 1976).

2.2.2 Layer Fluxes

Fluxes approximate the required radiances for evaluation of the multiply scattered source function. Upward and downward fluxes (F^+ and F^- , respectively) for individual isolated layers are evaluated using an appropriate flux parameterization. For example, for solar scattering, the hybrid modified delta eddington approximation (Meador and Weaver, 1980) is used. The chosen flux parameterization also provides intrinsic layer reflection and transmission functions, R and T . These fluxes are calculated using standard two stream parameterization approaches. To accommodate the flux parameterizations, optical properties for the whole atmosphere (i.e., surface to space) are required. The approach for calculating fluxes thus consists of two steps: (1) evaluating local layer (i.e., intrinsic) fluxes for each atmospheric layer, and (2) combining these to obtain the actual flux profiles using the adding method.

Upward and downward layer fluxes for solar radiation are given by:

$$F^+ = Ae^{k\tau} + Be^{-k\tau} + Ce^{-\tau/\mu_o} \quad (2.20)$$

$$F^- = \frac{1}{\gamma_2} \{ A(\gamma_1 - k)e^{k\tau} + B(\gamma_1 + k)e^{-k\tau} + Ye^{-\tau/\mu_o} \} \quad (2.21)$$

where the appropriate constants are given by:

$$\begin{aligned} k &= (\gamma_1^2 - \gamma_2^2)^{1/2} \\ A &= [B(\gamma_1 + k) + Y] / (k - \gamma_1) \\ B &= (E_1 e^{k\tau^*} + E_2 e^{-\tau^*/\mu_o}) / (E_3 e^{k\tau^*} + E_4 e^{-k\tau^*}) \\ C &= \pi \omega_o \left\{ \frac{\beta(\mu_o)}{\mu_o} - \gamma_1 \beta(\mu_o) - \gamma_2 [1 - \beta(\mu_o)] \right\} \left(\frac{\mu_o^2}{1 - k^2 \mu_o^2} \right) \\ Y &= C(\gamma_1 + \frac{1}{\mu_o}) - \pi F \omega_o \beta(\mu_o) \end{aligned} \quad (2.22)$$

$$\begin{aligned}
E_1 &= Y[1/(\gamma_1 - k) - r/\gamma_2] \\
E_2 &= [-C + \pi F \mu_o r + \frac{rY}{\gamma_2}] \\
E_3 &= (\gamma_1 + k)[1/(k - \gamma_1) + r/\gamma_2] \\
E_4 &= [1 - r(\gamma_1 + k)/\gamma_2] \\
\gamma_1 &= \frac{-\{1 - g^2 - \omega_o(4 - 3g) - \omega_o g^2(4\beta_o + 3g - 4)\}}{4[1 - g^2(1 - \mu_o)]} \\
\gamma_2 &= \frac{\{7 - 3g^2 - \omega_o(4 + 3g) + \omega_o g^2(4\beta_o + 3g)\}}{4[1 - g^2(1 - \mu_o)]}
\end{aligned} \tag{2.23}$$

Here, r is the Lambert surface albedo and the solar zenith angle cosine is μ_o

The transmission and reflection functions used later in the flux adding are given by:

$$\begin{aligned}
R &= F^+/\mu_o \pi F \\
T &= F^-/\mu_o \pi F + \exp(-\tau/\mu)
\end{aligned} \tag{2.24}$$

For the thermal fluxes, a linear Planck function relation across an atmospheric layer is used. In so doing, the parameterized two-stream solutions for emission from the layer top and layer bottom, and for total transmission and reflection are

$$\begin{aligned}
F^+ &= a(PB_t - mQ - B_b)/D \\
F^- &= a(PB_b + mQ - B_t)/D \\
T &= a/D \\
R &= uv(e^{\tau^1} - e^{\tau^1})/D
\end{aligned} \tag{2.25}$$

where B_t and B_b are the Planck intensity at the layer top and bottom and

$$\begin{aligned}
 a^2 &= 1 - \omega_0 \\
 m &= (B_b - B_t)/\tau \\
 P &= ve^{\tau_1} + ue^{-\tau_1} \\
 Q &= ve^{\tau_1} - ue^{-\tau_1} - a \\
 D &= v^2 e^{\tau_1} - u^2 e^{-\tau_1} \\
 u &= (1-a)/2 \\
 v &= (1+a)/2 \\
 \tau_1 &= \sqrt{3} \text{ at}
 \end{aligned} \tag{2.26}$$

The optical thickness τ and the single scattering albedo ω_0 are given by

$$\begin{aligned}
 \tau &= ku + \tau_s(1 - g) + \tau_a \\
 \omega_0 &= \tau_s(1 - g)/\tau
 \end{aligned} \tag{2.27}$$

Here k is the gas absorption coefficient (for a particular wavelength and probability interval), u is the gas amount, τ_s is the scattering optical thickness, τ_a is the absorption optical thickness and g is the asymmetry factor for the particulate matter in the layer.

2.2.3 Flux Adding Method

To obtain the actual flux profile throughout the atmosphere, intrinsic layer fluxes are combined algebraically using the adding method. In this method, fluxes, reflections, and transmissions are used to add individual layers together. Composite upward fluxes, $^1F_N^+$, and reflection functions R_N^+ , obtained upon adding two isolated layers, N and $(N-1)$ are given by:

$$^1F_N^+ = F_N^+ + T_N(^1F_{N-1}^+ + F_N^- R_{N-1}^+)(1 - R_N R_{N-1}^+)^{-1} \tag{2.28}$$

$$R_N^+ = R_N + R_{N-1}^+ T_N^2 (1 - R_N R_{N-1}^+)^{-1}. \tag{2.29}$$

Analogous equations provide composite downward fluxes and reflection functions, ${}^1F_N^-$ and R_N^- , respectively. The composite upward and downward fluxes provide the actual upward and downward fluxes at layer interfaces including the effects of all layers above and below. For example, the upward and downward fluxes at the boundary between layers N and (N+1) are given by:

$${}^2F_N^+ = ({}^1F_N^+ + {}^1F_{N+1}^- R_N^+)(1 - R_N^+ R_{N+1}^-)^{-1}, \quad (2.30)$$

$${}^2F_{N+1}^- = ({}^1F_{N+1}^- + {}^1F_N^+ R_{N+1}^-)(1 - R_N^+ R_{N+1}^-)^{-1}. \quad (2.31)$$

Once obtained, these fluxes are substituted into Eq. (2.16) above to provide the approximation of the MS source function.

2.2.4 Band model considerations

For LOWTRAN, it is necessary to integrate the spectral radiance values over a finite spectral interval ($\sim 20 \text{ cm}^{-1}$). The basic problem encountered in the calculation of radiative transfer in low spectral resolution in a hazy or cloudy atmosphere is the coupling between the processes of scattering and absorption due to cloud/aerosol particles and absorption by atmospheric gases. The main difficulty is that the integration over frequency cannot be properly accounted for by the usual band model technique for gaseous absorption because they do not allow for multiple-scattering. A direct line-by-line integration over frequency would be very time consuming. One alternative way of carrying out the frequency integration is to use the "k-distribution method" for homogeneous layers (Arking and Grossman, 1972) and the "correlated k-distribution approximation" for inhomogeneous atmospheres (cf. Wang and Ryan, 1983).

For gaseous absorption, the k-distribution method is comparable to line-by-line calculations (Arking and Grossman, 1972). This method is equivalent to the exponential-sum fitting method (see Wiscombe and Evans, 1977) and to the path length distribution method (see Bakan et al., 1978). However, in general, the latter two methods use scaling approximations to account for atmospheric inhomogeneity while the correlated-k approximation assumes certain relationship between k values at different pressure and temperature levels. The accuracy of the approximation is excellent for the $9.6 \text{ } \mu\text{m}$ O_3 band thermal radiation calculations (see Lacis et al., 1979).

Yamamoto et al. (1970, 1971) used finite sums of exponentials to describe the non-gray nature of water vapor absorption and carried out solutions of the equation of transfer for homogeneous band layers using both Chandrasekhar's principles of invariance as well as the discrete ordinate technique. Both techniques require extensive numerical calculations. On the other hand, two-stream approximations together with the correlated-k approximation have been used to study the radiative effects of aerosols (see Hansen et al., 1980). As best summarized recently by Stephens on efficient and accurate radiation parameterizations (1984, p. 862 of the paper): "... only the k-distribution approach can be readily incorporated into scattering models..."

In a homogenous gas layer, the k-distribution function is formerly related to the mean transmission function $T_{\Delta\nu}(u)$,

$$\begin{aligned} T_{\Delta\nu}(u) &\equiv \frac{1}{\Delta\nu} \int_{\Delta\nu} e^{-ku} dv \equiv \int_0^{\infty} f(k) e^{-ku} dk \\ &\equiv \int_0^1 e^{-ku} dg \approx \sum_{i=1}^n e^{-k_i u} \Delta g_i \end{aligned} \quad (2.32)$$

where $\Delta\nu$ is the narrow repeated interval (20 cm^{-1} in LOWTRAN) and u is the gas amount. The $f(k)$ for a given gas at a specified $\Delta\nu$ is the probability density function such that $f(k)dk$ is the fraction of the frequency interval for which the absorption coefficient is between k and $k+dk$. Eq. (2.32) reveals that the transmission depends on the distribution of k -values within $\Delta\nu$, but not on the ordering of the values. The cumulative k -distribution function is $g(k)$, while $(k_i, \Delta g_i)$ are the discrete sets of values to approximate the integral.

By expressing the band model transmission as the sum of exponentials, the multiple scattering calculation for each component can be performed independently as if it were a monochromatic problem. These are weighted and summed (as in Equation (2.32) to recover the essential band model character of the problem.

The fit of Wiscombe and Evans (1977) has been used for the two LOWTRAN transmission functions of water vapor/uniformly mixed gases, and ozone. The accuracy of the fitting is in general within a few percent for $T > 0.1$. For inhomogeneous atmospheres, we adopt the same scaling approximation used in LOWTRAN, i.e.,

$$k_1(P, \theta) = k_1(P_0, \theta_0) \frac{P}{P_0} \sqrt{\frac{\theta_0}{\theta}}. \quad (2.33)$$

where θ_0 , P_0 are reference temperatures and pressures, respectively.

3. IMPLEMENTATION OF MULTIPLE SCATTERING PARAMETERIZATION

3.1 FASCODE Implementation of the Stream Approximation for Multiple Scattering

3.1.1 Overview

The existing code structure of the FASCODE line-by-line algorithm presents a constraint for the implementation of a multiple scattering capability. In order to optimize computational efficiency and minimize online storage requirements, FASCODE program logic calculates path transmittance and radiance in a single unidirectional pass through the desired atmospheric path. This pass commences with the highest pressure sublayer (i.e., that requiring the least spectral resolution) and progresses monotonically to the lowest pressure sublayer requiring the highest spectral resolution. Cumulative quantities with spectral structure (such as transmittance and radiance) are evaluated by merging the lower resolution results from the previous layer with the higher resolution results of the current layer. While this procedure is appropriate for nonscattered radiance where the local source function for a layer consists solely of contributions from local thermal emission, the methodology is not valid in the presence of multiple scattering. Fundamentally, the local multiply-scattered (MS) source function is composed of contributions scattered from layers, both above and below the current layer in addition to local thermal emission. Therefore, a modification of the FASCODE program logic is required to incorporate the stream approximation (SA) for multiple scattering within FASCODE. The SA efficiently provides an estimate of the local multiply-scattered source function given the availability of a suitable estimate of the profiles of upward and downward flux. Evaluation of the flux profile, however, requires a priori total atmospheric properties such as optical depth and single scattering albedo profiles. This is not possible with the current layer by layer FASCODE algorithm. Once obtained, the source function for the multiply-scattered radiance may be summed along the desired path in analogy to the approach currently used within FASCODE to obtain the thermal emission via summation of the local Planck function contributions.

This apparent inconsistency of FASCODE with multiple scattering is resolved by combining the stream approximation approach with the adding method to obtain the required MS flux profiles. In the adding method, properties of individual layers (such as emission, transmission, and reflection) are

combined algebraically to yield the overall properties of the combined layers. A typical application of the adding method consists of two opposite unidirectional passes throughout the atmosphere. In the FASCODE implementation, the existing upward pass is exploited to set up one part of the adding calculation. This is done subsequent to the existing calculation of optical depths via the combined line-by-line gas absorption and LOWTRAN-based aerosol extinction routines. The upward pass also provides an opportunity to evaluate and merge radiance contributions due to thermal emission only. A downward pass, unique to MS cases, completes the calculation. During the downward pass, actual fluxes will be calculated for each layer, layer multiply-scattered source function evaluated using the stream approximation, and multiply-scattered radiances summed along the desired path. These radiances will be merged with the nonscattered radiance contributions evaluated during the upward pass to yield total cumulative multiply-scattered radiance.

The combined stream approximation/adding method approach for FASCODE is summarized in the flow chart presented in Figure 3-1. The shaded areas denote modifications to FASCODE to accommodate multiple scattering. The unshaded code segment on the left-hand side of the diagram represents the existing non-MS FASCODE algorithm. Within the shaded portion during the upward pass are code modifications to calculate: (a) layer single scatter albedo, ω_0^N , and phase function asymmetry factor, g^N ; (b) layer reflection and transmission functions, R_N , T_N , respectively and intrinsic upward and downward fluxes F_N^\pm using the two stream approximation; (c) beginning of the adding method for composite upward fluxes and reflection, $^1F^+$, R^+ , respectively; and (d) layer and merged values of the thermal radiance contribution E_N^0 based on the J_N^0 source function described above. The downward pass completes the adding method. Details will be described in the following sections. Notably, the time-consuming line-by-line calculations are done once only during the upward pass. The downward pass is a simple merging of precalculated and stored quantities based on algebraic manipulations.

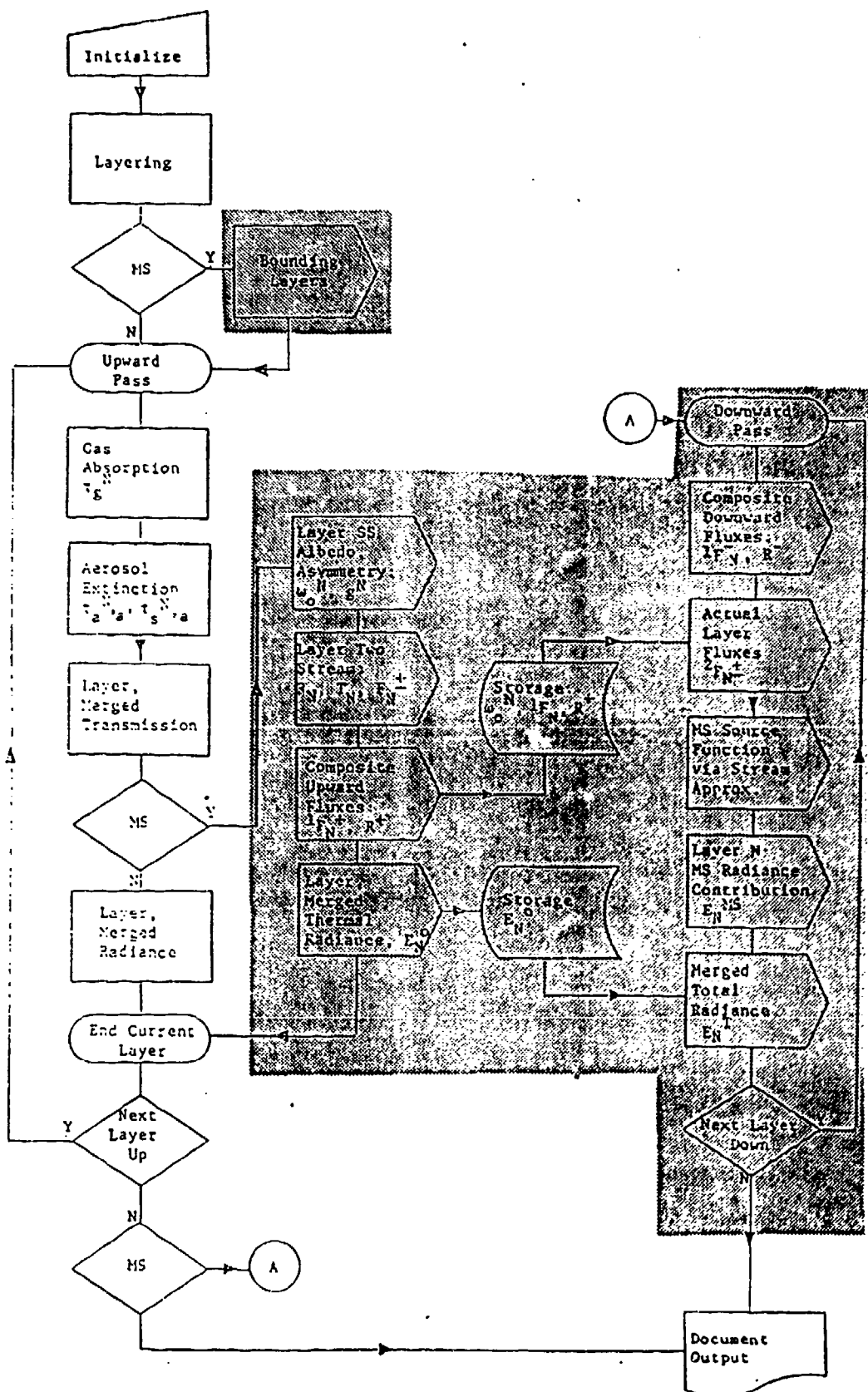


Figure 3-1. FASCODE implementation of stream approximation/adding method.

3.1.2 Adding Method

To illustrate the application of the adding method to calculate the actual flux profiles, consider the layered atmosphere illustrated in Figure 3-2. There are four layers (N-1), (N), (N+1), and (N+2) above an emitting surface (N-2). As each layer is treated during the existing FASCODE upward pass, the following quantities are evaluated:

N+2	$T_{N+2}, T_{N+2}, F_{N+2}^{\pm}$
N+1	$R_{N+1}, T_{N+1}, F_{N+1}^{\pm}$
N	R_N, T_N, F_N^{\pm}
N-1	$R_{N-1}, T_{N-1}, F_{N-1}^{\pm}$
N-2	$/// /// /// /// /// R_{N-2}, F_{N-2}^+$

Figure 3-2. Schematic of FASCODE model atmosphere layers.

τ_g^N	gas absorption optical depth via line-by-line
$\tau_{g,s}^N$	molecular scattering via LOWFAS
$\tau_{a,a}^N$	aerosol absorption optical depth via LOWFAS
$\tau_{a,s}^N$	aerosol scattering optical depth via LOWFAS
θ^N	mean layer thermodynamic temperature via FASCODE layering.

For a multiple scattering (MS) calculation, the shaded branch of the upward path in Figure 3-1 is selected and the following two additional quantities are calculated:

ω_o^N	single scattering albedo = $(\tau_{a,s}^N + \tau_{g,s}^N) / (\tau_g^N + \tau_{a,a}^N + \tau_{a,s}^N + \tau_{g,s}^N)$
g^N	phase function asymmetry factor

The asymmetry factor is obtained from a look-up table for the appropriate aerosol model, wavenumber domain, and level.

The asymmetry factor is obtained from a look-up table for the appropriate aerosol model, wavenumber domain, and level.

Next, a simple two-stream approximation is used to evaluate the intrinsic layer fluxes, F_N^{\pm} , transmission function (direct and diffuse), T_N , and reflection function, R_N . The intrinsic layer fluxes, F_N^{\pm} are the upward flux at the top and the downward flux from the bottom of the Nth isolated layer, respectively. These are analytical transformations of the form:

$$\{\tau_g^N, \tau_{a,a}^N, \tau_{a,s}^N, g^N, \theta^N\} \longrightarrow \{F_N^+, F_N^-, R_N, T_N\}. \quad (3.1)$$

Specific two stream flux formulations for solar and thermal scattering are given in Section 2.2.2. These are evaluated once during the upward pass through FASCODE at increasing spectral resolution with decreasing layer mean pressure, i.e., $\Delta\nu(N+1) < \Delta\nu(N)$ where N is layer index numbered consecutively from surface to space, and $\Delta\nu$ is the spectral resolution for each layer determined by the FASCODE algorithm.

Surface emission is treated as the zeroth layer with:

$$\begin{aligned} F_0^+ &= \pi \epsilon_s B(\theta_s) \\ R_0 &= (1 - \epsilon_s) \\ F_0^-, T_0 &= 0 \end{aligned} \quad (3.2)$$

where θ_s is the surface temperature and ϵ_s is the surface emissivity. Likewise, a target at the top of the path may be treated as the Mth layer with:

$$\begin{aligned} F_M^- &= \pi \epsilon_t B(\theta_t) \\ R_M &= (1 - \epsilon_t) \\ F_M^+, T_M &= 0 \end{aligned} \quad (3.3)$$

Similar considerations can be applied to treat nonscattering layers above and below the scattering layer system. As noted in the flow chart (Figure 3.1), an additional modification necessitated in order to accomplish a multiple scattering calculation is the consideration of bounding layers above and below the altitudes of the nodes of the specified path (i.e., H1 and H2). A minimum of one layer extending from the surface to H1 and from H2 to 15 km (assuming

H2 < 15 km) is included. In order to illustrate application of the adding method, the required relations for the system illustrated in Figure 3-2 are presented explicitly. It has been assumed that multiple scattering contributions above 15 km will be negligible.

3.1.2.1 Upward Adding Pass

The loop begins by adding layer (N-1) to layer (N-2). Subsequent layers are added one at a time until layer (N+2) is reached. The modified upward flux from the combination of (N-2) and (N-1), ${}^1F_N^+$, consists of three contributions (see Figure 3-2):

- i. the intrinsic upward flux from layer (N-1), F_{N-1}^+
- ii. the multiple reflection of the intrinsic upward flux from layer (N-2), F_{N-2}^+ , transmitted through layer (N-1):

$$\text{i.e., } F_{N-2}^+ + T_{N-1} + F_{N-2}^+ T_{N-1} R_{N-1} R_{N-2} +$$

$$F_{N-2}^+ T_{N-1} (R_{N-1} R_{N-2})^2 + \dots$$

$$= F_{N-2}^+ T_{N-1} (1 - R_{N-1} R_{N-2})^{-1}$$

- iii. the multiple reflection of the intrinsic downward flux from layer (N-1), F_{N-1}^- , reflected from layer (N-2) and transmitted through layer (N-1):

$$\text{i.e., } F_{N-1}^- T_{N-1} R_{N-2} + F_{N-1}^- T_{N-1} R_{N-2} (R_{N-1} R_{N-2}) + \dots$$

$$= F_{N-1}^- T_{N-1} R_{N-2} (1 - R_{N-1} R_{N-2})^{-1}$$

These will sum to the composite flux:

$${}^1F_{N-1}^+ = F_{N-1}^+ + T_{N-1} (F_{N-2}^+ + F_{N-1}^- R_{N-2}) (1 - R_{N-1} R_{N-2})^{-1} \quad (3.4)$$

Similar considerations lead to the composite reflection of layers (N-1) and (N-2):

$$R_{N-1}^+ = R_{N-1} + R_{N-2} T_{N-1}^2 (1 - R_{N-1} R_{N-2})^{-1} \quad (3.5)$$

Next layer N is added to the composite of (N-1, N-2), resulting in composite values for layer N:

$${}^1F_N^+ = F_N^+ + T_N ({}^1F_{N-1}^+ + F_N^- R_{N-1}^+) (1 - R_N R_{N-1}^+)^{-1} \quad (3.6)$$

$$R_N^+ = R_N + R_{N-1}^+ T_N^2 (1 - R_N R_{N-1}^+)^{-1} \quad (3.7)$$

This process is repeated for layer (N+1):

$${}^1F_{N+1}^+ = F_{N+1}^+ + T_{N+1} ({}^1F_N^+ + F_{N+1}^- R_N^+) (1 - R_{N+1} R_N^+)^{-1} \quad (3.8)$$

$$R_{N+1}^+ = R_{N+1} + R_N^+ T_{N+1}^2 (1 - R_{N+1} R_N^+)^{-1} \quad (3.9)$$

and layer (N+2):

$${}^1F_{N+2}^+ = F_{N+2}^+ + T_{N+2} ({}^1F_{N+1}^+ + F_{N+2}^- R_{N+1}^+) (1 - R_{N+2} R_{N+1}^+)^{-1} \quad (3.10)$$

$$R_{N+2}^+ = R_{N+2} + R_{N+1}^+ T_{N+2}^2 (1 - R_{N+2} R_{N+1}^+)^{-1} \quad (3.11)$$

Since there are no layers above (N+2), the upward composite ${}^1F_{N+2}^+$ is identically the actual upward flux, i.e.,

$${}^2F_{N+2}^+ = {}^1F_{N+2}^+ \quad (3.12)$$

Calculated composite layer values are required for the evaluation of the composite values of the subsequent layers. These intermediate quantities are merged to the next higher layer's spectral resolution and stored for subsequent use on the downward pass. At the termination of the upward pass, the following quantities have been calculated for each layer and stored for use during the downward pass: (a) the intrinsic layer values, ω_o^N , R_N , T_N , F_N^- (the intrinsic upward fluxes are not required), (b) the composite quantities, ${}^1F_N^+$, R_N^+ , and the nonscattered contribution to emission, E_N^0 . These values are stored only at local layer resolution to minimize total memory requirements.

3.1.2.2 Downward Pass

The downward pass is devoted exclusively to the adding method and stream approximation. No additional line-by-line calculations are performed. In analogy to its upward counterpart, downward composite fluxes, ${}^1F_1^-$ and reflectance functions, R_N^- , are calculated during the unidirectional downward pass. However, in addition both actual upward and downward fluxes, ${}^2F_N^\pm$, are calculated from the composite fluxes and reflection functions.

For the topmost layer, no downward composite fluxes are possible (unless there are nonscattering layers above N+2). Therefore, the actual upward and downward fluxes at the interface of layers (N+1) and (N+2) are:

$${}^2F_{N+1}^+ = ({}^1F_{N+1}^+ + F_{N+2}^- R_{N+1}^+)(1 - R_{N+2} R_{N+1}^+)^{-1} \quad (3.13)$$

$${}^2F_{N+2}^- = ({}^1F_{N+2}^- + {}^1F_{N+1}^+ R_{N+2})(1 - R_{N+2} R_{N+1}^+)^{-1} \quad (3.14)$$

At this point, actual upward and downward fluxes are available at the boundaries of layer (N+2), facilitating calculation of the multiply-scattered source function, J_{N+2}^{MS} , using the stream approximation (see Equation (2.14)). This source function provides the layer contribution to multiply-scattered emission, E_{N+2}^{MS} . This is added to the thermal contribution E_{N+2}^O evaluated during the upward pass.

Proceeding downward, the composite quantities are first calculated by adding the next layer down to the composite above it, for example, the downward composite flux emerging from layer (N+1) and the corresponding downward composite reflection are:

$${}^1F_{N+1}^- = F_{N+1}^- + T_{N+1}(F_{N+2}^- + F_{N+1}^+ R_{N+2})(1 - R_{N+2} R_{N+1}^+)^{-1} \quad (3.15)$$

$$R_{N+1}^- = R_{N+1} + R_{N+2} T_{N+1}^2 (1 - R_{N+1} R_{N+2})^{-1} \quad (3.16)$$

Actual fluxes at the interface of layers N and (N+1) are then obtained from the composite values:

$${}^2F_N^+ = ({}^1F_N^+ + {}^1F_{N+1}^- R_N^+)(1 - R_N^+ R_{N+1}^-)^{-1} \quad (3.17)$$

$$^2F_{N+1}^- = (^1F_{N+1}^- + ^1F_N^+ R_{N+1}^-)(1 - R_N^+ R_{N+1}^-)^{-1} \quad (3.18)$$

For the next layer, N, the procedure is identical, resulting in the composites:

$$^1F_N^- = F_N^- + T_N(^1F_{N+1}^- + F_N^+ R_{N+1}^-)(1 - R_N^+ R_{N+1}^-)^{-1} \quad (3.19)$$

$$R_N^- = R_N + R_{N+1}^- T_N^2 (1 - R_N^+ R_{N+1}^-)^{-1} \quad (3.20)$$

and actual fluxes:

$$^2F_{N-1}^+ = (^1F_{N-1}^+ + ^1F_N^- R_{N-1}^+)(1 - R_{N-1}^+ R_N^-)^{-1} \quad (3.21)$$

$$^2F_N^- = (^1F_N^- + ^1F_{N-1}^+ R_N^-)(1 - R_{N-1}^+ R_N^-)^{-1} \quad (3.22)$$

Finally, the procedure terminates at the surface layer (N-2), layer (N-1) interfaces where:

$$^1F_{N-1}^- = F_{N-1}^- + T_{N-1}(^1F_N^- + F_{N-1}^+ R_N^-)(1 - R_{N-1}^+ R_N^-)^{-1} \quad (3.23)$$

$$R_{N-1}^- = R_{N-1} + R_N^- T_{N-1}^2 (1 - R_{N-1}^+ R_N^-)^{-1} \quad (3.24)$$

Then:

$$^2F_{N-2}^+ = (F_{N-2}^+ + ^1F_{N-1}^- R_{N-2}^+)(1 - R_{N-2}^+ R_{N-1}^-)^{-1} \quad (3.25)$$

$$^2F_{N-1}^- = (^1F_{N-1}^- + F_{N-2}^+ R_{N-1}^-)(1 - R_{N-2}^+ R_{N-1}^-)^{-1} \quad (3.26)$$

In this last step, the upward surface emission flux, F_{N-2}^+ , and reflection function, R_{N-2} , are composite quantities since there are no layers below. This completes the downward pass and the multiply-scattered radiance calculation.

3.1.3 Stream Approximation, Source Function, Radiance

Using the stream approximation (SA), the multiply-scattered source function at optical depth, τ , for a path with zenith angle, $\cos^{-1} \mu$, will be given by (see Equation (2.16)):

$$J_{SA}(\tau, \pm\mu) = [1 - \omega_o(\tau)]B(\theta) + \frac{\omega_o(\tau)}{\pi} \{F^\pm(\tau)[1 - \beta(\mu)] + F^\mp\beta(\mu)\} \quad (3.27)$$

The plus sign is for downward looking paths ($\mu > 0$) while the minus sign is for upward looking paths ($\mu < 0$). In the expression above, $\omega_o(\tau)$ is the single scattering albedo, $B(\theta)$ is the Planck function, and $\beta(\mu)$ is the backscatter fraction for path zenith angle μ . The backscatter fraction is a function of the particulate asymmetry factor at level τ , $g(\tau)$, and is available from Wiscombe and Grams (1976).

For level N, the level source function is given by:

$$J_N^{SA}(\pm\mu) = (1 - \omega_o^N) B(\theta_N) + \frac{\omega_o^N}{\pi} \{F_N^\pm[1 - \beta^N(\mu, g^N)] + F_N^\mp\beta^N(\mu, g^N)\} \quad (3.28)$$

The first term above is due to nonscattered thermal emission, while the second term is due to multiple scattering. Thus, the source function can be written as:

$$J_N^{SA} = J_N^o(\omega_o^N, \theta_N) + J_N^{MS}(\mu, \omega_o^N, g^N, F_N^\pm) \quad (3.29)$$

where the thermal emission term J_N^o depends only on local layer properties, and the multiply-scattered term J_N^{MS} requires, in addition to local properties, the local fluxes which depend on the overall path properties. The first term is a generalization of the nonscattering thermal emission source function currently evaluated within FASCODE and may be treated in a like manner.

The path radiance or emission with multiple-scattering is obtained by summing radiance contributions along the path essentially as is currently done with no scattering. Along a path consisting of two layers, layer N and the layer above, N + 1, the emission depends on the path integral of the source function and is given by:

$$E_{N+1}^+ = E_N^+ T_{N+1} + J_{SA}^{N+1}(+\mu)(1 - T_{N+1}) \quad (3.30)$$

for downward looking and:

$$E_{N+1}^- = E_N^- + (1 - T_{N+1}) J_{SA}^{N+1}(-\mu) T_N \quad (3.31)$$

for upward looking where:

$$E_N^\pm = (1 - T_N) J_{SA}^N(\pm\mu). \quad (3.32)$$

With no scattering, $\omega_0^{N, N+1} = 0$ and the source function for each layer reduces to the Planck function as in the original FASCODE, i.e.,:

$$\lim_{\omega_0 \rightarrow 0} J_{SA}^N = B(\theta_N). \quad (3.33)$$

As described above, the thermal emission source J_N^0 can be summed along the path in analogy to the current nonscattering radiance calculation to provide the path thermal emission E_N^0 . Evaluation of the multiply-scattered radiance contribution E_N^{MS} for each layer is accomplished via the adding algorithm on the complementary downward pass where it is merged with the previously calculated nonscattered contributions to obtain total radiance.

3.1.4. Description of FASCODE2 with Multiple Scattering

In implementing multiple scattering into FASCODE2, the main considerations were in maintaining the integrity of the existing program, and in making the resultant code as transparent to the user as possible. The first and most constraining element of the existing code, was the use of panels in doing the radiance calculation. This necessitated that any multiple scattering implementation also be adjusted to utilize this methodology.

All of the routines to be listed below, utilize the existing FASCODE method of working with only a "panel" of numbers at a time. This necessitates a great deal of I/O for doing any calculation with multiple scattering, but allows for complete compatibility with the existing structure and execution of FASCODE. Another benefit of this approach, is that the program is compartmentalized, and the user should find no difference in run time for this program with multiple scattering turned off, and the previous version of FASCODE2.

As discussed above, flux adding, used in conjunction with the stream approximation was implemented as the best approach. This involved the extensive

modification of EMINIT, and RADMRG. These routines were modified to merge the composite fluxes and drive the flux-adding during the radiance calculation. The primary additions to the code, were the subroutines FLXADD, FLXDWN, and SRCFCN. FLXADD calculates and adds fluxes for each of the FASCODE layers. This routine is called within the layer loop from both EMINIT, and RADMRG. FLXDWN drives the downward flux adding, and is called from XLAYER after the FASCODE upward path is completed. SRCFCN evaluates the multiple scattered source function, and is called from FLXDWN.

Several secondary routines that were added were MSEMIS, TLEMIS, XLAYMS, FLUXLP, MSIN, and MSOUT. MSEMIS merges the multiple scattered contribution to the radiance for each layer. TLEMIS merges the total multiple scattered radiance contribution obtained from MSEMIS and merges it with the total single scattered radiance calculated within FASCODE. XLAYMS drives the calculation of the radiance contribution from layers above the desired path. FLUXLP merges the fluxes and drives the flux-adding for layers in which radiances are not evaluated. The purpose of these last two routines will be discussed in Section 3.1.5. MSIN reads merged fluxes from the previous layer while MSOUT writes out the merged fluxes for the current layer.

Some minor additions were the functions BETABS, and E3. BETABS evaluates the backscattered fraction for a given angle and asymmetry factor. E3 evaluates the exponential integral $E_3(x)$. Some minor changes were also made to EMIN, GETEXT, AERF, EXTDTA, EXABIN, AEREXT, TRANS, LOWTRN, and ATMPH. EMIN was modified to evaluate the thermal emission, for multiple scattering cases. GETEXT buffers in the asymmetry factors along with the extinction and scattering coefficients. AERF calculates the scattering optical thickness, and the asymmetry factor from the buffered quantities. EXTDTA now contains the asymmetry factors for each of the LOWTRAN models. EXABIN does the level weighting for the asymmetry factors. AEREXT evaluates the asymmetry factors for each wavenumber. TRANS does the weighted average for the final asymmetry factor result. LOWTRN was modified to read in the asymmetry factors for user-defined aerosols. ATMPH was modified to determine the multiple scattering path. This will be discussed in the next section.

A flowchart for FASCODE2 with multiple scattering is illustrated in Table 3-1. The structure of FASCODE2 with multiple scattering is outlined in Table 3-2 giving, also, brief descriptions of the altered and added routines. The segment load file and file usage are shown in Tables 3-3 and 3-4, respectively.

Table 3-1

Flowchart of FASCODE Multiple Scattering Routines

Underlined subroutines are modified from the existing FASCODE;
others are new subroutines

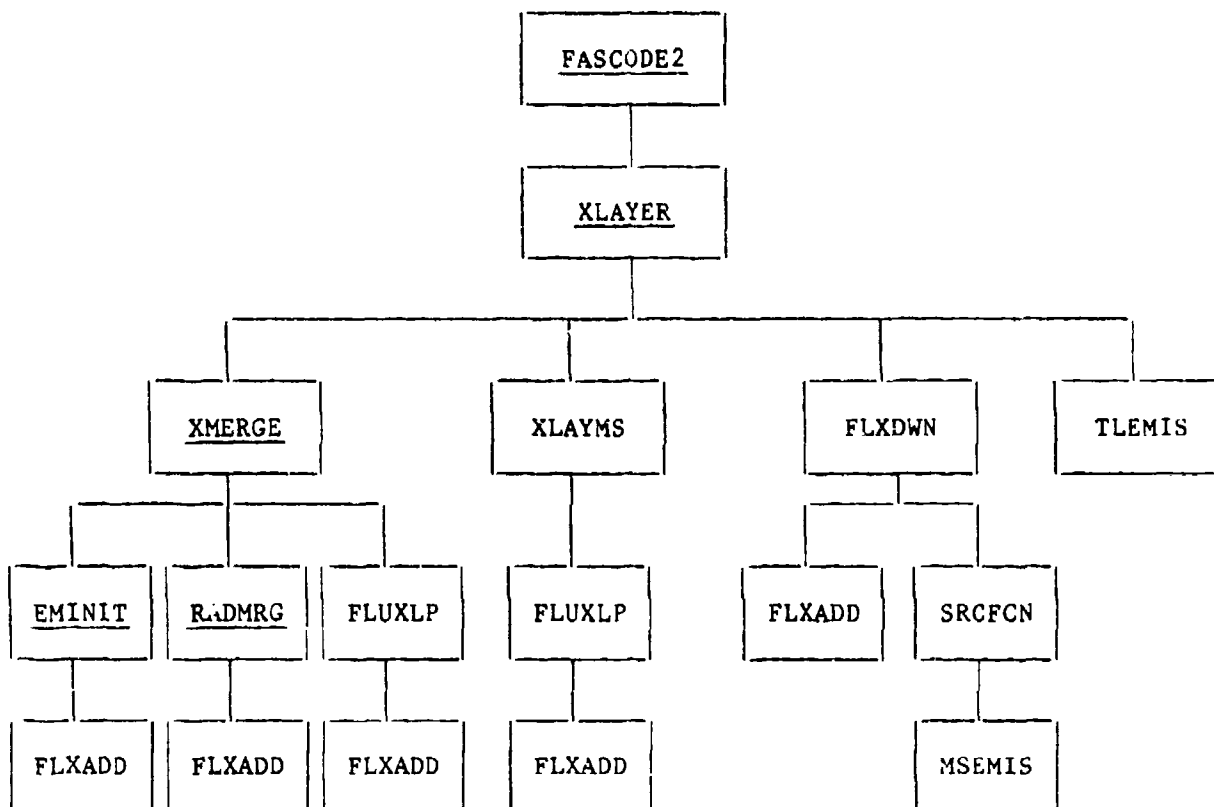


Table 3-2

Description and Segment Load Grouping of FASCODE2 Subroutines

(This listing will contain all the FASCODE routines but will only describe the routines pertinent to the multiple scattering calculation.)

FASCOD2*	Fast Atmospheric Signature Code
	/ADRIVE/ /CONSTS/ /FILHDR/ /IFIL / /LANCHN/ /LASIV / /MAIN / /MSACCT/* Multiple Scattering files and parameters /MSCONS/* Multiple Scattering flags and constants BUFIN BUFOUT COPYFL ENDFIL SKIPFL
FLTRFN	CNVFLT RDSCAN
LASER	
PLTFAS	/AXISXY/ /NAME / /PLTHDR/ /POINTS/ /TITLOC/ /YCOM / ENDPLT EXPT FSCLIN LINT MNMX TEMPFN TENLOG XNTLOG

Legend: /Common Blocks/
 (Block Data)
 Subroutines

NOTE: "*" designates routines added or modified in the implementation of Multiple Scattering by AER.

Table 3-2 (Cont.)

AXES		
AXISL		
AXLOG		
AX2		
BBSCLE		
FPLINE		
HEADER		
SCANFN	CKPRNT CNVREC CONVSC INTER PANLSC RDSCAN SHAPEG SHAPET SHRKSC SINCSQ	
TEST	(BTEST)	
XLAYER*		Controls Layer by Layer Calculation
/ABSORA/		
/ASYMMA/*		Aerosol Asymmetry Factors
/LINHDR/		
/MLTSCT/*		General Labeled Common for Multiple Scattering
/SCATTA/		
/RMRG /		
/XBLF /		
MSCOPY*		Copies Multiple Scattering output files by panels
FLXDWN*		Controls Layer by Layer Downward Flux Adding
AERF*		Evaluates Extinction, Scattering, and Asymmetry
BBFN		Computes Black Body Function
E3*		Computes Exponential Integral E3
FLXADD*		Calculates and does Adding of Fluxes for Current Layer
GETEXT*		Reads Extinction, Absorption, and Asymmetry
MSIN*		Reads Merged Fluxes from Previous Layer
MSOUT*		Writes Merged Fluxes for Current Layer
RADFN		Computes Radiation Function
SRCFCN*		Evaluates Multiple Scattering Source Function and Radiance
BETABS*		Calculates Back-Scattering Fraction
MSEMIS*		Merges Multiple Scattered Radiance

Table 3-2 (Cont.)

OPDPTH	/ABSORB/ /SCATTR/ /LBLF /
CONTNM	XINT
FRNCO2	(BFCO2)
FRN296	(BFH2O)
N2CONT	(BN2)
O2CONT	(O2C)
O3CHAP	(O3CH)
O3HHT0	(O3HHO)
O3HHT1	(O3HH1)
O3HHT2	(O3HH2)
SL296	(BS296)
SL260	(BS260)
HIRAC1	/FNSH / (BHIRAC) (BMOLEC) (BSHAPEL) (VOICON) ABSOUT CNVFNV MOLEC PANEL QV RDLIN R1PRNT SHAPEG SHAPEL VERFN XINT

Table 3-2 (Cont.)

LBLF4	(BMOLEC) (VOICON) CONVF4 MOLEC QV RDLIN4 SHRINK	
NONLTE	/VBNLTE/	
HIRACQ	/FNSQ / (BH IRAQ) (BMOLEC) (BSHAPEL) (VOICON) ABSOUT CNVFNQ MOLEC PANELQ QV RDLIN R1PRNT SHAPEG SHAPEL VERFN XINT	
VIBPOP		
VIBTMP		
OPPATH*	/BNDRIES/ /CNTRL / /PATHD /	
FSCATM*	/BNDRY / /CONSTN/ /DEAMT / /HMOLS / /PARMTR/ /ZOUTP / (ATMCON) ATMPH* PACK WATVAP	Obtains Refractive Path and Calculates Absorber Atmospheric Path Driver

Table 3-2 (Cont.)

FSCGEO

ALAYER
AMERGE
ANDEX
AUTLAY
EXPINT
FDBETA
FINDSH
FNDHNM
HALFWD
RADREF
REDUCE
RFPATH
SCALHT

MDLATM*

Sets up selected Atmosphere

/MDLATM/
/TRAC /
(MCATMB)
CONVRT
DEFAULT
NSMDL
RDUNIT

LOWTRN*

LOWTRAN Driver for Aerosols

/CNSTNS/
/LCRD1 /
/LCRD2 /
/LCRD3 /
/LCRD4 /
/MART /
/MDLZ /
/MODEL /
/RAIN /
/TITL /
/USRDTA/
/ZVSALY/
(TITLE)

AERNSM

/MDATA /
(MARDTA)
(MDTA)
(PRFDTA)
AERPRF
MARINE
STDMDL

CIRRUS

Table 3-2 (Cont.)

EXABIN*	Loads the Aerosol Extinction, Absorption and Asymmetry Coefficients for the desired Model
/EXTD /*	Stores all the Aerosol Attenuation Coefficients
(EXTDTA)*	Contains all the Aerosol Attenuation Coefficients
AB	
AITK	
DEBYE	
DOP	
GAMFOG	
GMRAIN	
INDX	
GEO	
/PARMLT/	
/RFRPTH/	
ANDEX	
EXPINT	
FDBETL	
FILL	
FINDSL	
FNDHML	
GEOINL	
LOLAYR	
PACKL	
RADREF	
REDUCL	
RFPATL	
SCALHT	
NEWMDL	
TRANS*	Outputs Aerosol Optical Properties for Path
AB	
AEREXT*	Interpolates Aerosol Attenuation Coefficients for values at Wavenumber ν
AITK	
DEBYE	
DOP	
GAMFOG	
GMRAIN	
INDX	
TNRAIN	
VSA	
PATH	
TELEMIS*	Merges Multiple Scattered and Single Scattered Radiance for the Total Path
EMOUT	Writes Merged Radiance and Transmittance Results

Table 3-2 (Cont.)

XLAYMS*		Controls Layer by Layer Calculation for Contributing Scattering Layers Above Desired Path
	AERF*	Evaluates Extinction, Scattering, and Asymmetry
	BBFN	Computes Black Body Function
	EMIN*	Reads Optical Depths and Calculates τ_{gas}
	E3*	Computes Exponential Integral E3
	FLUXLP*	Merges Fluxes from Previous and Current Layer
	FLXADD*	Calculates and does Adding of Fluxes for Current Layer
	GETEXT*	Reads Extinction, Absorption, and Asymmetry
	MSIN*	Reads Merged Fluxes from Previous Layer
	MSOUT*	Writes Merged Fluxes for Current Layer
	RADFN	Computes Radiation Function
XMERGE*		Driver for Merging Options
	GETEXT*	Reads Extinction, Absorption, and Asymmetry
	RADFN	Computes Radiation Function
	XMERGI	Driver for Merging Routines using RADINT
ABINIT		Initializes Optical Depth Calculation
	ABSOUT	Writes Merged Optical Depth Results
ABSINT		Merges Optical Depths using General 4-point Interpolation
	ABSOUT	Writes Merged Optical Depth Results
ABSMRG		Merges Optical Depths using Lagrange 4-point Interpolation
	ABSOUT	Writes Merged Optical Depth Results
ADARSL		Adds Absorption and Scattering to Common Blocks for use in a Transmittance Run
	AERF*	Evaluates Extinction, Scattering, and Asymmetry
	GETEXT*	Reads Extinction, Absorption, and Asymmetry
EMINIT*		Initializes Radiance Calculation with First Layer and Drives Layer Flux Calculation
	AERF*	Evaluates Extinction, Scattering, and Asymmetry
	BBFN	Computes Black Body Function
	EMIN*	Reads Optical Depths and Calculates τ_{gas}
	EMOUT	Writes merged Radiance and Transmittance Results
	E3*	Computes Exponential Integral E3
	FLXADD*	Calculates and does Adding of Fluxes for Current Layer
	MSIN*	Reads Merged Fluxes from Previous Layer
	MSOUT*	Writes Merged Fluxes for Current Layer

Table 3-2 (Cont.)

FLUXLP*	AERF*	Drives Layer Flux Calculation without Radiance
	BBFN	Evaluates Extinction, Scattering, and Asymmetry
	EMIN*	Computes Black Body Function
	E3*	Reads Optical Depths and Calculates τ_{gas}
	FLXADD*	Computes Exponential Integral E3
		Calculates and does Adding of Fluxes for Current Layer
RADINT	MSIN*	Reads Merged Fluxes from Previous Layer
	MSOUT*	Writes Merged Fluxes for Current Layer
		Merges Radiance and Transmittance using General 4-point Interpolation
	AERF*	Evaluates Extinction, Scattering, and Asymmetry
	BBFN	Computes Black Body Function
	EMBND	Evaluates Boundary Contribution to Radiance
RADMRG*	EMIN*	Reads Optical Depths and Calculates τ_{gas}
	EMOUT	Writes Merged Radiance and Transmittance Results
		Merges Radiance and Transmittance using Lagrange 4-point Interpolation, and also Drives Layer Flux Calculation
	AERF*	Evaluates Extinction, Scattering, and Asymmetry
	BBFN	Computes Black Body Function
	EMIN*	Reads Optical Depths and Calculates τ_{gas}
	EMOUT	Writes merged Radiance and Transmittance Results
	E3*	Computes Exponential Integral E3
	FLXADD*	Calculates and does Adding of Fluxes for Current Layer
	MSIN*	Reads Merged Fluxes from Previous Layer
	MSOUT*	Writes Merged Fluxes for Current Layer

Table 3-3
Segment Load File for FASCODE2 with Multiple Scattering

FASCODE	TREE	FASCOD2-(LAYRS,LASER,SCANFN,PLOTT,
	,FLTRFN,TEST)	
FASCOD2	GLOBAL	CONSTS,FILHDR,MAIN,IFIL,LAMCHN,LASIV,ADRIE,
	,MSACCT,MSCONS	
FASCOD2	INCLUDE	FASCOD2,BUFIN,BUFOUT
*		
LAYRS	TREE	XLAYER-(OPPATHS,OPDPHS,XMERGES,FLUXES,TLEMIS,XLAYMS)
XLAYER	GLOBAL	LINHDR,XBLF,ABSORA,SCATTA,ASYMMA,RMRG,MLTSCT
XLAYER	INCLUDE	XLAYER,MSCOPY
*		
OPPATHS	TREE	OPPATH-(FSCATMA,LOWT,PATH)
OPPATH	GLOBAL	CNTRL,BNDRIES,PATHD-SAVE
OPPATH	INCLUDE	OPPATH
*		
FSCATMA	TREE	FSCATM-(FSCGEO,MDLATM)
FSCATM	INCLUDE	FSCATM,ATMPH,ATMCON,PACK,WATVAP
FSCATM	GLOBAL	CONSTN,HMOLS,PARMTR,DEAMT,ZOUTP,BNDRY-SAVE
FSCGEO	INCLUDE	RFPATH,ALAYER,AUTLAY,EXPINT,FINDSH,SCALHT,ANDEX,
	,RADREF,HALFWD,FSCGEO,FDBETA,FNDHMN,REDUCE,AMERGE	
MDLATM	INCLUDE	MDLATM,NSMDL,MLATMB,CONVRT,RDUNIT,DEFAULT
MDLATM	GLOBAL	MLATM,TRAC-SAVE
*		
FLUXES	TREE	FLXDWN-(SRCFCN)
FLXDWN	INCLUDE	FLXDWN,RADFN,GETEXT,FLXADD,MSIN,MSOUT,E3,AERF,BBFN
*		
LOWT	TREE	LOWTRN-(GEO,EXABIN,TRANS,AERNS,VSA,CIRRUS,NEWMDL)
LOWTRN	INCLUDE	TITLE
LOWTRN	GLOBAL	LCRD1,LCRD2,LCRD3,LCRD4,MODEL,CNSTNS,
	,MDLZ,ZVSALY,MART,USRDTA,TITL,RAIN-SAVE	
GEO	INCLUDE	GEO,GEOINL,REDUCL,EXPINT,RADREF,SCALHT,ANDEX,
	,RFPATL,FDBETL,FNDHML,FINDSL,FILL,LOLAYR,PACKL	
GEO	GLOBAL	PARMLT,RFRPTH-SAVE
EXABIN	INCLUDE	EXABIN,EXTDTA,INDX,DEBYE,DOP,AB,CAMFOG,
	,AITK,GMRAIN	
EXABIN	GLOBAL	EXTD
TRANS	INCLUDE	TRANS,AEREXT,TNRAIN,DEBYE,DOP,INDX,AB,
	,CAMFOG,AITK,GMRAIN	
AERNS	TREE	AERNSM
AERNSM	INCLUDE	AERNSM,AERPRF,PRFDTA,MARINE,MARDTA,STDMDL,MDTA
AERNSM	GLOBAL	MDATA-SAVE
*		
PATH	INCLUDE	PATH
*		
XMERGES	TREE	XMERGE-(ABINIT,ABSMRG,ABSINT,EMINIT,RADMRG,RADINT,
	,ADARSL,FLUXLP)	
XMERGE	INCLUDE	RADFN,XMERGE,GETEXT,XMERGI
ADARSL	INCLUDE	ADARSL,GETEXT,AERF

Table 3-3 (Cont.)

```

*
OPDPTHS  TREE      OPDPTH-(HIRAC1,LBLF4,CONTNW,NLTE)
OPDPTH   GLOBAL    LBLF,ABSORB,SCATTR
*
HIRAC1   INCLUDE   HIRAC1,SHAPEL,SHAPEG,VOICON,RDLIN,CNVFNV,PANEL,MOLEC,
,QV,ABSOUT,VERFN,R1PRNT,XINT,BMOLEC,BHIRAC,BSHAPEL
HIRAC1   GLOBAL    FNSH-SAVE
*
LBLF4    INCLUDE   LBLF4,RDLIN4,CONVF4,MOLEC,QV,SHRINK,VOICON,BMOLEC
*
CONTNW   TREE      CONTNM-(SL296,SL260,FRN296,FRNCO2,
,N2CONT,O3CHAP,O3HHTO,O3HHT1,O3HHT2,O2CONT)
CONTNM   INCLUDE   CONTNM,XINT
O3CHAP   INCLUDE   O3CHAP,O3CH
O3HHTO   INCLUDE   O3HHTO,O3HHO
O3HHT1   INCLUDE   O3HHT1,O3HH1
O3HHT2   INCLUDE   O3HHT2,O3HH2
O2CONT   INCLUDE   O2CONT,O2C
SL296    INCLUDE   SL296,BS296
SL260    INCLUDE   SL260,BS260
FRN296   INCLUDE   FRN296,BFH20
FRNCO2   INCLUDE   FRNCO2,BFCO2
N2CONT   INCLUDE   N2CONT,BN2
*
NLTE     TREE      NONLTE-(HIRACQ,VIBTMP,VIBPOP)
NONLTE   GLOBAL    VBNLTE
HIRACQ   INCLUDE   HIRACQ,SHAPEL,SHAPEG,VOICON,RDLIN,CNVFNQ,PANELQ,
,MOLEC,QV,ABSOUT,VERFN,R1PRNT,XINT,BMOLEC,BHIRAQ,BSHAPEL
HIRACQ   GLOBAL    FNSQ-SAVE
*
ABINIT   INCLUDE   ABINIT,ABSOUT
*
ABSMRG   INCLUDE   ABSMRG,ABSOUT
ABSINT   INCLUDE   ABSINT,ABSOUT
*
EMINIT   INCLUDE   EMINIT,EMIN,EMOUT,MSIN,MSOUT,BBFN,AERF,FLXADD,E3
*
RADMRG   INCLUDE   RADMRG,EMIN,EMOUT,MSIN,MSOUT,BBFN,AERF,FLXADD,E3
*
RADINT   INCLUDE   RADINT,EMIN,EMOUT,BBFN,AERF,EMBND
*
SRCFCN   INCLUDE   SRCFCN,BETABS,MSEMIS
*
TLEMIS   INCLUDE   TLEMIS,EMOUT
*
XLAYMS   INCLUDE   XLAYMS,GETEXT,RADFN,FLUXLP,MSIN,MSOUT,EMIN,EMOUT,
,FLXADD,BBFN,AERF,E3
*
FLUXLP   INCLUDE   FLUXLP,FLXADD,MSIN,MSOUT,BBFN,AERF,EMIN,E3
*
SCANFN   INCLUDE   SCANFN,SHAPEG,RDSCAN,SHRKSC,SHAPET,CONVSC,PANLSC,
,CNVREC,SINCSQ,CKPRNT,INTER

```

Table 3-3 (Cont.)

*		
FLTRFN	INCLUDE	FLTRFN,RDSCAN,CNVFLT
*		
TEST	INCLUDE	TEST,BTEST
*		
PLOTT	TREE	PLTFAS-(BBSCLE,HEADER,AXEST,FPLINE)
PLTFAS	GLOBAL	PLTHDR,AXISXY,YCOM,POINTS,TITLOC,NAME
PLTFAS	INCLUDE	PLTFAS,LINT,EXPT,XNTLOG,TEMPFN,TENLOG,MNMX,FSCLIN,
,ENDPLT		
*		
AXEST	TREE	AXES-(AXISL,AXLOG,AX2)
	END	FASCOD2

Table 3-4
File Usage

UNIT NAMES:

TAPE5	-	INPUT
TAPE6	-	OUTPUT
TAPE10	-	Output file containing gas optical depths for current layer. Labeled KFILE.
TAPE11	-	Output file. For FASCODE runs without MS, it contains merged results from previous layer. For multiple scattering runs, it contains the merged total radiance and transmittance for the path. Label alternates between LFILE and MFILE. Always labeled LFILE for final output.
TAPE12	-	Output file. For FASCODE runs without MS, it contains the final merged results. For multiple scattering runs, this file contains the total thermal emission radiance. Label alternates between MFILE and LFILE. Always labeled MFILE for final output.
TAPE19	-	Intermediate output file, containing aerosol coefficients for path above desired path. Only used if upper path is defined. Labeled IMSFIL.
TAPE20	-	Intermediate output file, containing aerosol coefficients for desired path. Labeled IEXFIL.
TAPE21	-	Intermediate output file, containing total layer flux values. Label alternates between ISFILE and LSFILE.
TAPE22	-	Intermediate output file, containing composite layer flux values. Label alternates between JSFILE, KSFILE, and MSFILE.
TAPE23	-	Intermediate output file, containing composite layer flux values. Label alternates between JSFILE, KSFILE, and MSFILE.
TAPE24	-	Intermediate output file, containing total layer flux values. Label alternates between ISFILE and LSFILE.
TAPE25	-	Intermediate output file, containing composite layer flux values. Label alternates between JSFILE, KSFILE, and MSFILE.
TAPE26	-	Intermediate output file. This file holds optical properties for upper path for the upward adding loop, and for the downward loop it contains the final multiple scattered contribution to the radiance for the FASCODE path. Initially labeled IEFIL, labeled KEFILE at end of run.
TAPE27	-	Intermediate output file, containing the multiple scattered contribution to the radiance. Label alternates between IEFIL, JEFIL, and KEFILE.
TAPE28	-	Intermediate output file, containing the multiple scattered contribution to the radiance. Label alternates between IEFIL, JEFIL, and KEFILE.

Note: TAPE10 - TAPE28 are in buffered binary format.

Table 3-4 (Cont.)

UNIT NAMES

KFILE	-	Contains gas optical depths for current layer.
LFILE	-	Contains results of previous layer for FASCODE runs without multiple scattering. Contains final merged results for multiple scattering run.
MFILE	-	Contains final merged results for FASCODE runs without multiple scattering. Contains total single scattered results for multiple scattering runs.
IMSFIL	-	Contains aerosol coefficients for path above desired path.
IEXFIL	-	Contains aerosol coefficients for desired path.
ISFILE	-	Contains total composite fluxes for previous layer.
JSFILE	-	Contains downward composite fluxes for current layer.
KSFILE	-	Contains upward composite fluxes for previous layers during upward adding loop. Contains downward composite fluxes for previous layer during downward adding loop.
LSFILE	-	Contains total composite fluxes for current layer.
MSFILE	-	Contains upward composite fluxes for current layer during upward adding loop. Contains upward composite fluxes for all layers during downward adding loop.
IEFILE	-	Contains τ_{gas} for upper path during upward adding loop. Contains multiple scattering contribution to the radiance from the current layer during downward adding loop.
JEFILE	-	Contains multiple scattering contribution to the radiance from the previous layers.
KEFILE	-	Contains total multiple scattering contribution to the path radiance.

3.1.5 Notes on the Operation of FASCODE2 with Multiple Scattering

In order to use FASCODE2 with multiple scattering, it would be helpful to understand a little about how and why it does the calculation the way it does. Supplemental user instructions are listed in Table 3-5. The first thing that the user will note, is that a new flag appears in Card 1.2. This flag is for turning off and on the multiple scattering sections of the program. As outlined in the user instructions, various other parameters must also be set so that a) aerosols are included, b) radiance is calculated, c) FSCATM is called, and d) normal merging is done.

The next card, is where an understanding of how the calculation is performed can be very useful. Card 1.2a is a new card which is only read if IMS=1. This card includes four quantities, a) TGRND, which is the temperature of the ground (at 0.0 km), b) SEMIS, which is the emissivity of the surface

(at 0.0 km), c) HMINMS, the minimum height for multiple scattering (default = 0.0 km), and d) HMAXMS, the maximum height for multiple scattering (default = 15.0 km). HMINMS and HMAXMS determine the bounds that are placed on the multiple scattering calculation. HMINMS determines the height at which multiple scattering will start. HMAXMS determines the height above which multiple scattering paths are not calculated. If the maximum of the desired path is below HMAXMS, the program will define a path from the maximum of the desired path to HMAXMS. If the maximum of the desired path is above HMAXMS, then HMAXMS is ignored, but the entire path is calculated using multiple scattering. This means that HMAXMS only checks to see if the contribution from above should be added, but does not cut off the multiple scattering calculation at that height. For the case where the minimum of the desired path is above HMAXMS, then no multiple scattering is performed for that path.

For example, if the user defined a slant path from 4.0 to 10.0 km, with HMINMS = 0.0 km and HMAXMS = 15.0 km, the program would first define a new path from 10.0 to 15.0 km, to obtain the downward flux contribution. Secondly, a path from 0.0 to 4.0 km would be defined to obtain the contribution from the layers below 4 km. Then lastly the program would define the path from 4.0 to 10.0 km and calculate the desired radiances, adding in any contributions obtained from the first two calculations. It should therefore be clear that a simple path from 4.0 to 10.0 km using multiple scattering, may actually involve the execution of FASCODE for THREE separate paths. This therefore can increase the run time proportionally.

This example just described, is the worst case scenario. Another case could consider a path from 10 to 30 km, with HMINMS and HMAXMS as before. The program would first define a path from 0.0 to 10.0 km to obtain the contribution from below, and would then do the path from 10 to 30 km using multiple scattering. Yet another possibility, is to define a path from 0.0 to 10.0 km, with HMINMS and HMAXMS as before. The program would first do a path from 10 to 15 km to obtain the contribution from above, and then do the path from 0.0 to 10.0 km. The final possible case, is to define a path from 0.0 to 20.0 km with HMINMS and HMAXMS still set to 0.0 and 15.0 km respectively. This would result in only one path from 0.0 to 20.0 km calculating the multiply scattered radiances.

One thing the user should note, is that in the preceeding examples there was no mention of angles, or tangent paths. That is because this methodology is true without regard to the angle for slant paths, and is true for all tangent paths. For example, if you want to consider a tangent path starting at 25 km with a minimum at 10 km, and a range of 1000 km, leaving HMINMS and HMAXMS as previously defined. The program would first do the slant path from 0.0 to 10 km to obtain the contribution from below, and would then do the desired tangent path.

The following items should be noted by the user:

- 1) When doing a multiple scattering run, the input file is rewound so it is not possible to string multiple scattering jobs together.
- 2) Additional paths which are defined by the multiple scattering parameters will increase run time proportionally.
- 3) Some coding notes:
 - a) The coding which sets and determines the multiple scattering paths is contained in ATMPTH.
 - b) The two routines, XLAYMS & FLUXLP were written for the multiple scattering paths which don't require the calculation of radiances.

A test case for FASCODE along with the input and output files is described in Appendix B.

Table 3-5
**Supplemental User Instructions for Using FASCODE2
 with Multiple Scattering**

The following user instruction cards are not a complete FASCODE2 user deck, but only present the changes to existing cards and/or the addition of new cards required for Multiple Scattering runs.

1) CARD 1.2 now appears as follows:

```

IHIRAC, ILBLF4, ICNTNM, IAERSL, IEMIT, ISCAN, IFILTR, IPLOT,
   5,      10,      15,      20,      25,      30,      35,      40,
4X,11, 4X,11, 4X,11, 4X,11, 4X,11, 4X,11, 4X,11, 4X,11,

ITEST,  IATM,  IMRG,  ILAS,  IMS,  IRAD,  MPTS,  NPTS
  45,    50,    55,    60,    65,    70, 71-75, 76-80
4X,11, 4X,11, 4X,11, 4X,11, 4X,11, 4X,11,    15,    15
  
```

where each of the parameters is as defined in the FASCODE2 user instructions, excluding the new flag, IMS which is used for turning on the multiple scattering sections of FASCODE2.

```

IMS (0,1)  flag for multiple scattering
           = 0  normal FASCODE run, no scattering
           = 1  FASCODE run with multiple scattering
  
```

NOTE: the following must also be true for multiple scattering:

- a) IAERSL = 1 or 7
- b) IEMIT = 1
- c) IATM = 1
- d) IMRG = 0

2) CARD 1.2a (this card directly follows Card 1.2)

**** Required if IMS = 1, otherwise omit.

```

TGRND,      SEMIS,      HMINMS,      HMAXMS

  1-10,      11-20,      21-30,      31-40
E10.3,      E10.3,      E10.3,      E10.3
  
```

Table 3-5 (Cont.)

TGRND	Temperature of surface (degrees Kelvin) (no default value)
SEMIS	Emissivity of surface (no default value)
HMINMS	Minimum height for Multiple Scattering (default = 0.0 km)
HMAXMS	Maximum height for Multiple Scattering (default = 15.0 km)

3) CARD 3.6 (optional card for LOWTRN subroutine) now appears as follows:

(1 to 16) (DUMMY,EXTC(1,1),ABSC(1,1),ASYM(1,1),(I=1,47))

Format (3(F6.2,2F7.5,F6.4))

where EXTC, and ABSC are as defined in FASCODE2 user instructions, and ASYM is the Aerosol Asymmetry Factor which is required for multiple scattering calculations.

NOTE: When multiple scattering runs are performed, subsequent runs cannot be done using only one input deck. This is due to the rewinding of the input deck during multiple scattering execution. It is therefore required that each multiple scattering run, necessitates its own input deck.

3.2 LOWTRAN Implementation

3.2.1 Overview

In this section, we describe the technical details of incorporating into LOWTRAN 6 the multiple scattering treatment together with the k-distribution method. The procedure and the new code structure are also presented. The existing LOWTRAN 6 program structure is shown in Figure 3-3 (Figure 27 of Kneizys et al., 1983). For simplicity of implementation, we have added only two new subroutines, MSRAD and FLXADD, to handle the k-distribution and multiple scattering. The subroutine FLXADD is called from MSRAD. The functions of MSRAD and FLXADD are shown in Figure 3-4, while the individual elements are described below.

3.2.2 k-Distribution Method

Because of the complicated molecular absorption band structure of the gases, a rigorous frequency integration would require a line-by-line integration which clearly is very time consuming and thus not acceptable for LOWTRAN. Our approach to this problem is the application of the absorption coefficient (k) distribution method (cf. Wang and Ryan, 1983; Stephens, 1984). In a homogeneous gas layer, the k-distribution function is formally related to the mean transmission function $T_{\Delta\nu}(u)$,

$$\begin{aligned} T_{\Delta\nu}(u) &\equiv \frac{1}{\Delta\nu} \int_{\Delta\nu} e^{-ku} dv \equiv \int_0^\infty f(k) e^{-ku} dk \\ &\equiv \int_0^1 e^{-k_i u} dg = \sum_{i=1}^n e^{-k_i u} \Delta g_i \end{aligned} \quad (3.34)$$

where $\Delta\nu$ is the narrow repeated interval (20 cm^{-1} in LOWTRAN) and u is the gas amount. The $f(k)$ for a given gas at a specified $\Delta\nu$ is the probability density function such that $f(k)dk$ is the fraction of the frequency interval for which the absorption coefficient is between k and $k + dk$. Eqn. (3.34) reveals that the transmission depends on the distribution of k -values within $\Delta\nu$ but not on the ordering of the values. The cumulative k-distribution function is $g(k)$, while $(k_i, \Delta g_i)$ are the discreet sets of values to approximate the integral.

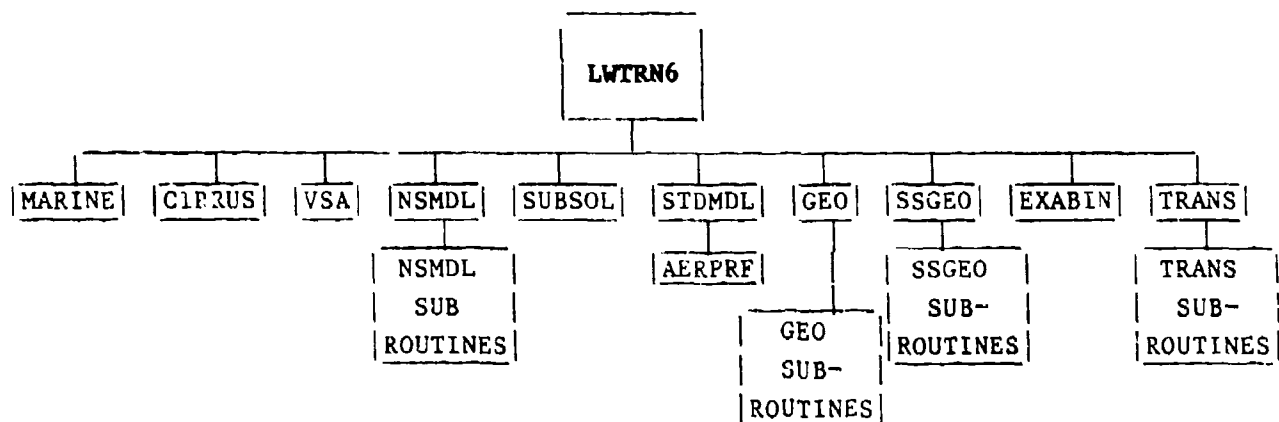


Figure 3-3. LOWTRAN 6 Main Program Structure

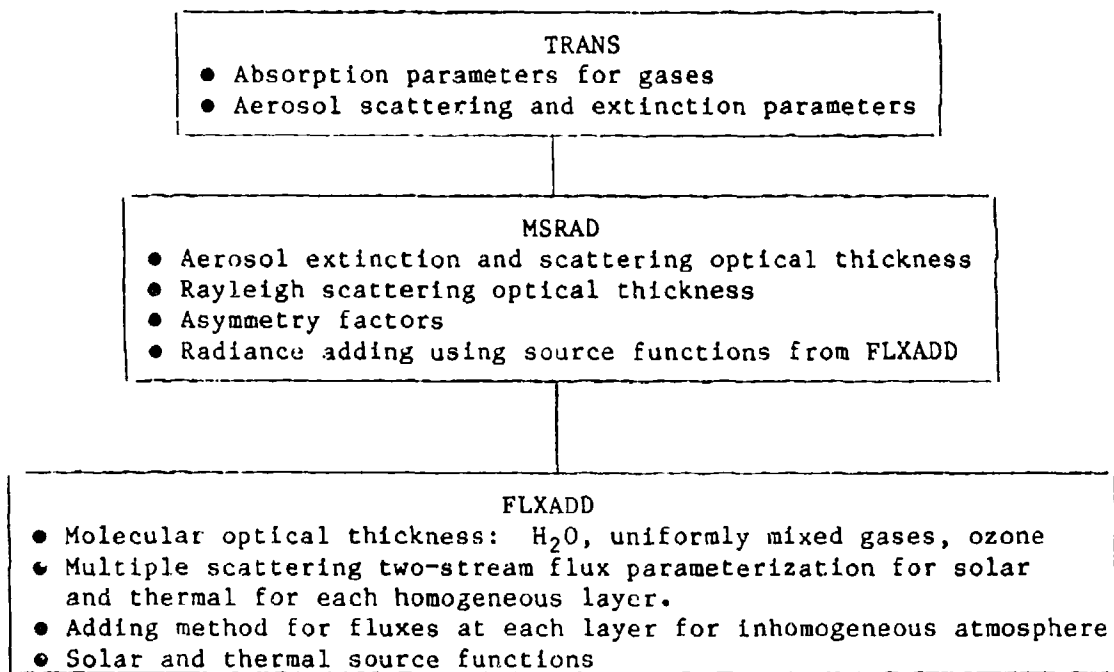


Figure 3-4. Functions of subroutine TRANS, MSRAD, and FLXADD used in the LOWTRAN implementation of multiple scattering.

For the summation in Eq. (3.34) to be useful with LOWTRAN, values for k and Δg must be found to fit the LOWTRAN transmission data for water vapor/uniformly mixed gases (H_2O^+) and ozone (O_3). The transmission for water vapor/uniformly mixed gases and ozone may be expressed as

$$T_1 = T(H_2O^+) = \sum_{i=1}^M e^{-k_i u_1} \Delta g_i \quad (3.35)$$

$$T_2 = T(O_3) = \sum_{j=1}^N e^{-k_j u_2} \Delta g_j. \quad (3.36)$$

The problem of fitting LOWTRAN transmission data as an exponential sum has been handled successfully by Wiscombe and Evans (cf. Wiscombe and Evans, 1977), using 10 k and Δg values for H_2O^+ and six for O_3 . Their k values and associated Δg values are listed in Table 3-6. Plots of the percent transmission error of their fit relative to the LOWTRAN data for both H_2O^+ and O_3 as a function of \log_{10} of the effective optical depth are shown in Figures 3-5 and 3-6.

Making use of the Wiscombe and Evans exponential sum fit of the LOWTRAN transmission data yields values of k_i , k_j , and Δg_i , Δg_j for $M = 10$, $N = 6$. However, if $M \neq N$ and $\Delta g_i \neq \Delta g_j$, it is necessary to perform multiple scattering calculations separately for water vapor/uniformly mixed gases (H_2O^+) and ozone (O_3) using two probability (k) loops. This problem is avoided by choosing either the 10 H_2O^+ or 6 O_3 Δg_i values and then expressing the transmission of both H_2O^+ and O_3 as the sum of either 10 or 6 terms. Run time efficiency concerns suggest that both transmissions be expressed as the sum of six exponentials, using the Δg_j values for the ozone fit shown in Table 3-6. Thus, in the LOWTRAN implementation, the transmission function for water vapor is refit to the Δg values for ozone for each path. The transmission as a function of probability is shown in Figure 3-7. (Figure is illustrative only -- actual values are not plotted.)

TRANSMITTANCE PERCENT ERROR WATER VAPOR AND UNIFORMLY MIXED GASES

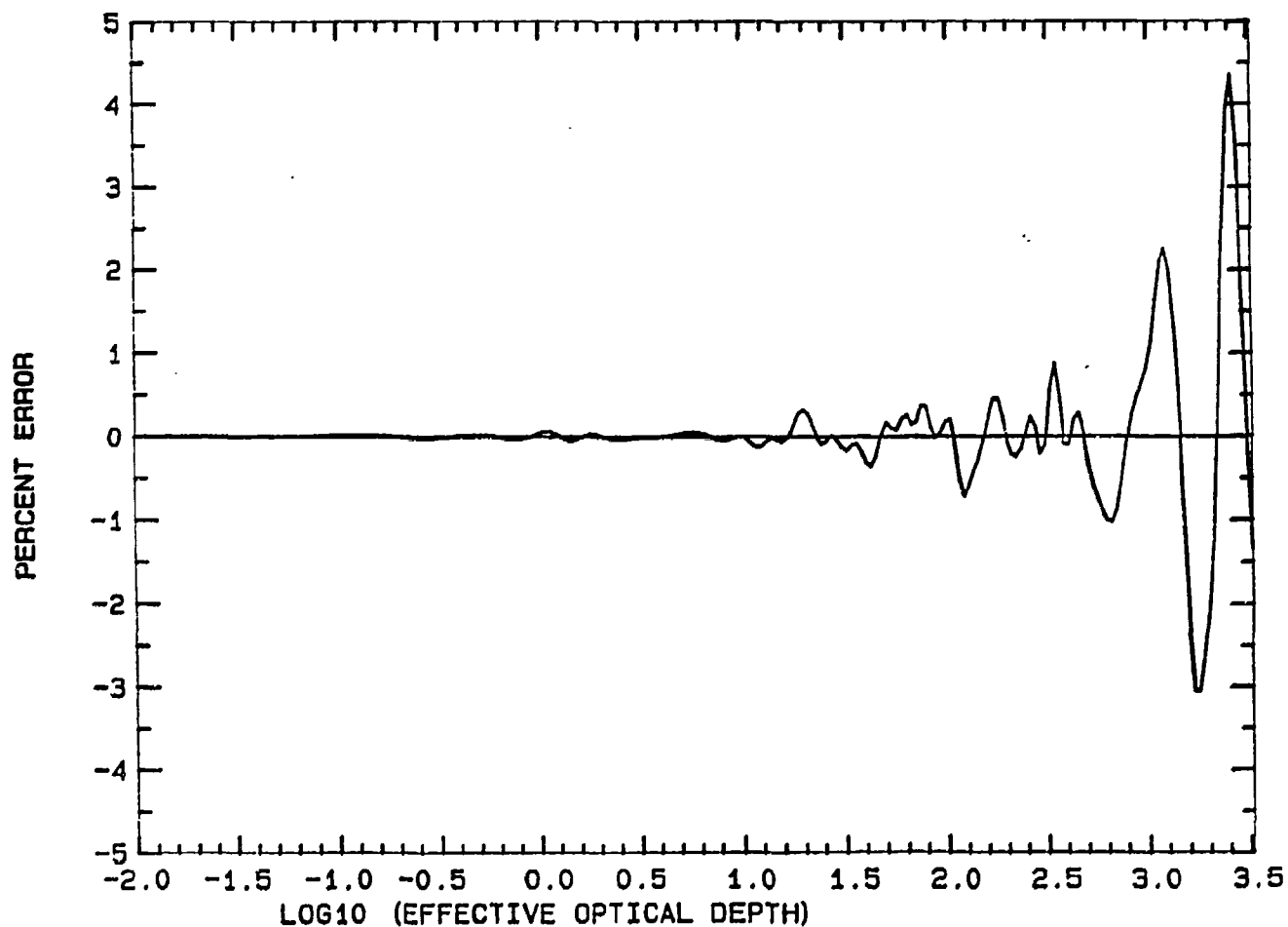


Fig. 3-5 Percent error of transmittance fit for water vapor and uniformly mixed gases relative to LOWTRAN values. Transmittance fit is based on Wiscombe and Evans, 1977

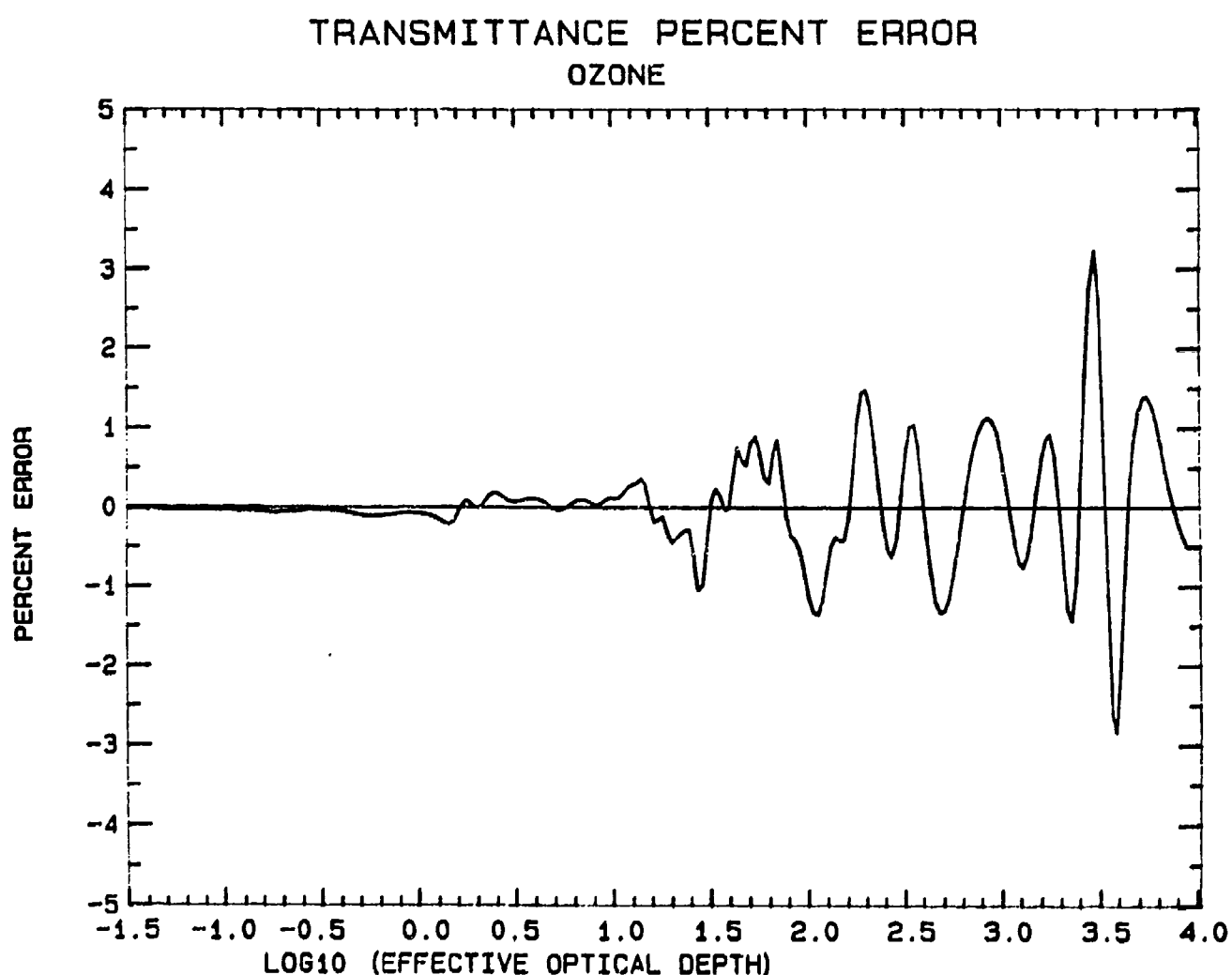
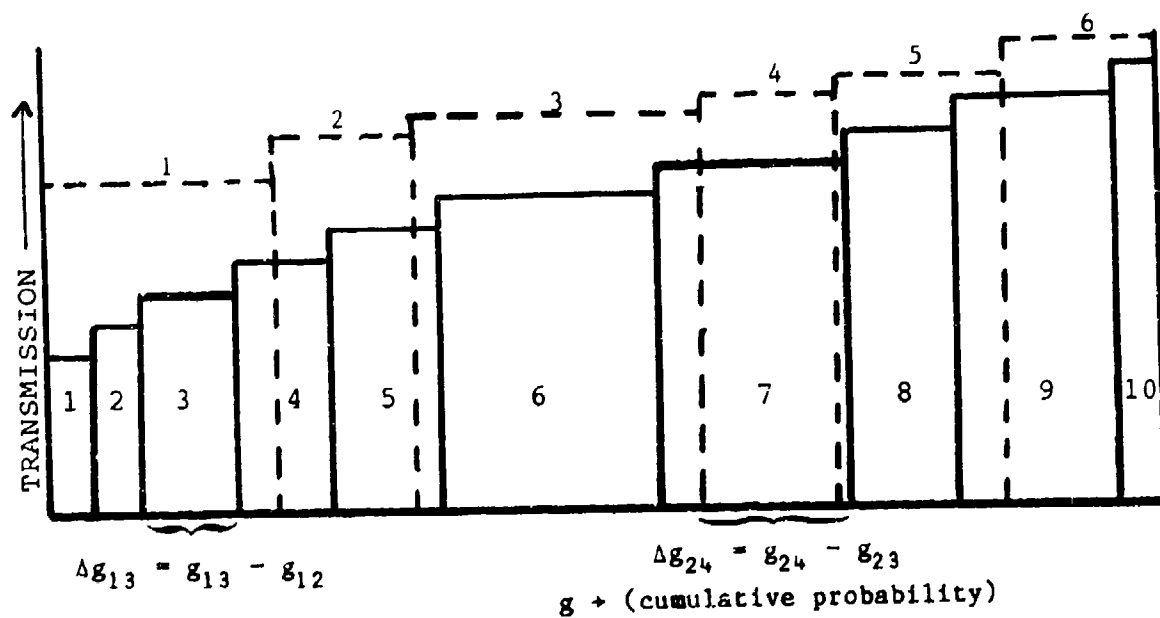


Fig. 3-6 Percent error transmittance fit for ozone relative to LOWTRAN values. Transmittance fit is based on Wiscombe and Evans, 1977.



Legend

—— H_2O^+

---- O_3

g_{1i} = cumulative probability for H_2O^+

g_{2j} = cumulative probability for O_3

Figure 3-7. Transmission vs. cumulative probability for Wiscombe and Evans (1977) fit to LOWTRAN H_2O^+ and O_3 transmission values. (Figure does not depict actual transmission values.)

As an example, the refit H_2O^+ transmission for the first of six components may be expressed as

$$T'_{11} = [T_{11} \Delta g_{11} + T_{12} \Delta g_{12} + T_{13} \Delta g_{13} + T_{14}(g_{21} - g_{13})] / \Delta g_{21}, \quad (3.37)$$

where $T_{1i} = e^{-k_i u_1}$, $i = 1, 10$, so that $T(H_2O^+) = T_1 = \sum_{i=1}^6 T'_{1i} \Delta g_i$. The total molecular transmission for H_2O^+ and O_3 for a particular layer for some small frequency interval is now

$$T_1 \cdot T_2 = \left[\sum_{i=1}^6 e^{-k_i u_1} \Delta g_i \right] \cdot \left[\sum_{i=1}^6 e^{-k_i u_2} \Delta g_i \right]. \quad (3.38)$$

Assuming no overlap of gas absorption, the many cross terms may be eliminated, resulting in

$$T_1 \cdot T_2 \equiv \sum_{i=1}^6 e^{-(k_i u_1 + k_i u_2)} \Delta g_i. \quad (3.39)$$

Figure 3-8 compares the product of the water vapor and ozone obtained from: (1) the intrinsic LOWTRAN band model, (2) the k-distribution fit including overlap terms (Eqn. (3.38)), and (3) the k-distribution fit assuming no overlap terms (Eqn. (3.39)), i.e., eliminating cross terms. This calculation is for the near surface layer of a US standard atmosphere run and covers the spectral range from about 6.7 to 20 μm . It can be seen that there is some difference between the calculated transmission but very little of practical consequence for the multiple scattering calculation.

The individual components of the combined gas ($H_2O^+ + O_3$) molecular absorption transmission can thus be expressed by

$$T_i = T'_{1i} \cdot T_{2i}, \quad i = 1, 2, \dots, 6. \quad (3.40)$$

The j th component of the optical thickness of a given layer due to molecular absorption is

$$\tau_u = -\ln(T_j). \quad (3.41)$$

T_j is added to the molecular continuum, aerosol extinction, and molecular scattering optical thickness to determine the total optical thickness for each k value and layer in FLXADD.

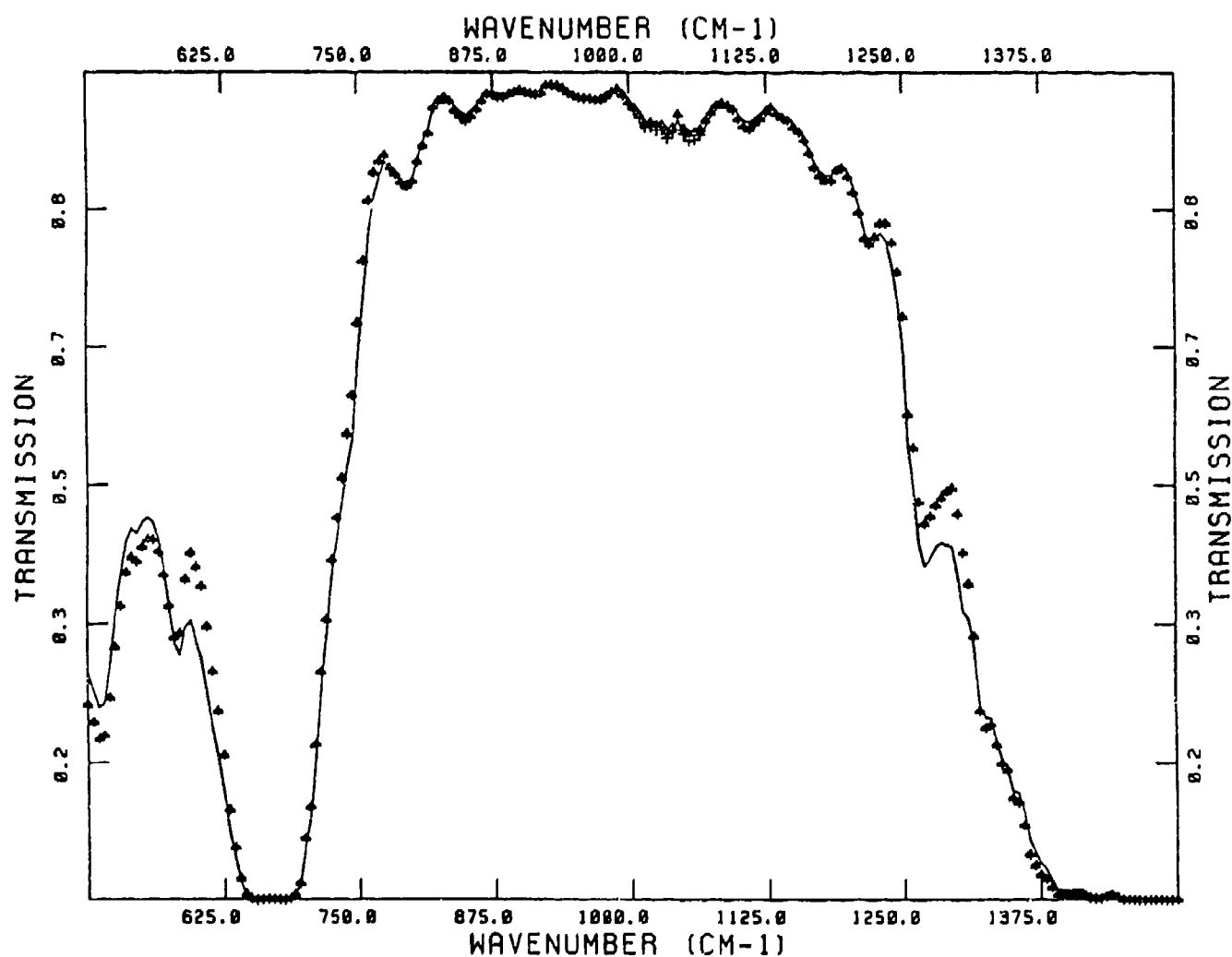


Fig. 3-8. Comparison of LOWTRAN transmission (line) to that calculated from the k-distribution model assuming no overlap (+) and including overlap (Δ).

It is important to note that the k-distribution transmittances are employed only in the determination of the multiply scattered source function. The adding of radiances based on the source function depends on the original LOWTRAN transmissions. Thus, errors in the combined k-distribution/stream approximation approach for multiple scattering are not propagated beyond the approximate multiple scattering approach.

Table 3-6
The Set of k_1 and Δg_1 Values Used to Approximate the
LOWTRAN 6 Transmission Data

i	k_1	Δg_1
I. Water Vapor/Uniformly Mixed Gases		
1	1.718754×10^{-2}	1.233690×10^{-4}
2	2.490766×10^{-1}	4.614758×10^{-3}
3	2.328222	2.404693×10^{-2}
4	7.744676×10^{-1}	2.772890×10^{-2}
5	2.229876×10^{-1}	5.409872×10^{-2}
6	4.438688×10^{-2}	2.119191×10^{-1}
7	1.081388×10^{-2}	2.776904×10^{-1}
8	3.054533×10^{-3}	3.089278×10^{-1}
9	1.258653×10^{-3}	9.072606×10^{-2}
10	0.000000	1.240893×10^{-4}
II. Ozone		
1	4.736517×10^{-1}	7.395116×10^{-2}
2	3.823806×10^{-2}	5.557539×10^{-1}
3	7.424869×10^{-3}	2.476504×10^{-1}
4	1.785435×10^{-3}	8.688930×10^{-2}
5	4.336295×10^{-4}	3.565867×10^{-2}
6	0.000000	1.385517×10^{-4}

3.2.3 Inhomogeneous Atmosphere

For inhomogeneous atmospheres, we adopt the same scaling approximation used in LOWTRAN (see Eqn. 2.21):

$$k_i(P, \theta) = k_i(P_o, \theta_o) \frac{P}{P_o} \sqrt{\theta_o / \theta}$$

We use the same adding method discussed in Section 3.1.2 to calculate the thermal radiation flux in an inhomogeneous atmosphere. Basically, the parameters used are F^+ , F^- , T , and R , as presented in Section 3.1.2.

3.2.4 Stream Approximation, Source Function, and Radiance Calculation

Again, we use the same procedures discussed in Section 3.1.3. to calculate the radiance from the source function and stream approximation.

The multiple scattered contribution to the source function is approximated by (Eqn. 2.14, 2.2, 2.3, 2.10, 2.11).

$$J_{MS}(\tau, \mu, \phi) = \frac{\omega_o(\tau)}{\pi} \{ F^+(\tau) [1 - \beta(\mu)] + F^-(\tau) \beta(\mu) \}. \quad (2.14)$$

The total source function is:

$$J(\tau, \mu, \phi) = J_o(\tau, \mu, \phi) + J_{MS}(\tau, \mu, \phi) \quad (2.2)$$

where:

$$J_o(\tau, \mu, \phi) = \frac{\omega_o(\tau)}{4\pi} \pi F e^{-\tau/\mu_o} P(\Omega; -\Omega_o) + [1 - \omega_o(\tau)] B[\Theta(\tau)] \quad (2.3)$$

The single scattered contribution to J_o above is taken directly from the existing LOWTRAN single scattering coding. (Actually the summed multiply scattered radiance is added to the summed singly scattered radiance.)

One essential difference between the multiple scattering radiance implementation and the previous single scattering version is the treatment of surface reflection. Through the surface boundary condition, surface reflection affects the flux profile and hence source function throughout the atmosphere. From the radiance solutions:

$$I(\tau, \mu, \phi) = \left\{ \frac{\tau}{\pi} \left[\pi \mu_0 F e^{-\tau^*/\mu_0} + \int_0^1 \int_0^{2\pi} I(\tau^*, -\mu, \phi) \mu d\mu d\phi \right] \right. \\ \left. + (1-r) B[\theta(\tau^*)] \exp(-\tau^*/\mu) + \int_{\tau}^{\tau^*} J(\tau, \mu, \phi) e^{-(\tau-\tau)/\mu} \frac{d\tau}{\mu} \right\} \quad (2.10)$$

$$I(\tau, -\mu, \phi) = \int_0^{\tau} J(\tau, \mu, \phi) e^{-(\tau-\tau)/\mu} \frac{d\tau}{\mu} \quad (2.11)$$

It can be seen that surface reflection can increase both upward and downward radiances through the source function. For upward radiances, there is a more drastic difference between the standard LOWTRAN treatment and the implemented multiple scattering version. This concerns reflection of downward scattered radiance from the surface and back to a downward looking observer (the second term in the brackets in Equation (2.10)). This contribution is not included in standard LOWTRAN although the reflected attenuated direct solar term is (i.e., the first term in Equation (2.10)).

3.2.5 Description of LOWTRAN6 with Multiple Scattering

The addition of multiple scattering to LOWTRAN6 has been made with a minimum of changes to the source code and input deck. Only one new input parameter, IMULT, has been added. IMULT, read as the last input on card 1, is set to zero for the original LOWTRAN6 with single scattering and one for the AER LOWTRAN6 with multiple scattering. If aerosols are not included (clear sky case), the original LOWTRAN6 is executed, independent of the value of IMULT.

Source code changes were made primarily in the main program LWTRN6 and in subroutines TRANS, with some additions to EXABIN, AEREXT, EXTDTA, and RFPATH. Subroutines MSRAD, FLXADD, and ALEVEL and functions BETABS and PLANCK were added.

The main program has been altered to allow the path geometry calculations (called from subroutine GEO) to be accessed twice, once for the original LOWTRAN single scatter path and once for the entire atmosphere, required for computation of the multiply scattered radiance. The reason for the second path geometry call is that the thermal and solar source functions used to determine the multiply scattered radiance contribution are functions of the

upward and downward flux at each layer. The multiply scattered flux at a given layer will, in part, be determined by radiation from all atmospheric layers, even those above or below the layers between the observer and target. To calculate the fluxes at each layer, it is therefore necessary to add the flux contributions from the surface up to space, and back down to the surface again. This adding procedure, executed in the new subroutine FLXADD, is discussed in detail in Sections 3.1.2.1 and 3.1.2.2.

A flag (variable ITEST) has been incorporated into RFPATH for the purpose of isolating the refracted viewing path zenith angle for each layer, as opposed to the solar zenith angle, calculated for the solar cases in a later pass through RFPATH.

A number of changes were incorporated into subroutine TRANS. After calculating the cumulative path parameters used in the original LOWTRAN6, it calls MSRAD, where the aerosol scattering and extinction, H₂O continuum and Rayleigh scattering optical thickness for each layer are calculated. The asymmetry factor for each layer is also calculated based on model extinction and absorption data added to EXABIN, AEREXT, and EXTMTA, and aerosol effective absorber amounts for the four vertically spaced aerosol regions. MSRAD calls subroutine FLXADD.

Subroutine FLXADD calculates the six degraded k components of the H₂O/ uniformly mixed gas transmission for each layer, as well as the molecular absorption optical thickness. It is then added to the continuum, aerosol extinction, and molecular scattering optical thickness from MSRAD to provide the total optical thickness for each layer and k-value, as well as the corresponding single scatter albedo. The diffuse flux contribution for each isolated layer and k-value is computed from the applicable two-stream approximation, either solar or thermal, and combined in the flux adding routine to determine the total upward and downward flux for each layer for each k value. The diffuse solar downward flux is summed over k value and returned to evaluate the surface reflected downward diffuse solar flux. Function PLANCK returns the black body radiance for a particular wavenumber and temperature in units of $\text{Wcm}^{-2} \text{sterad}^{-1}/\text{cm}^{-1}$, while subroutine ALEVEL returns the layer number corresponding to a particular height, the top layer of the atmosphere being layer 1. Knowing the upward and downward fluxes as well as the backscatter parameter β returned from function BETABS, the multiple scattered source function can be determined.

Returning to MSRAD, the radiance is summed over the viewing path (between H1 and H2) and k-values to provide the multiply scattered diffuse radiance contribution. For a downward looking (upward radiance) calculation, the multiply scattered radiance at the upper boundary may be expressed by

$$I^+(n_t) = \sum_{k=1}^6 \{ (1 - T_{n_t}^i) S(k, n_t) + \sum_{i=n_t}^{n_b-1} (T_{i+1}^i - T_i^i) S(k, i+1) \} \Delta g_k + I_s \quad (3.39)$$

where n_b is the bottom layer, n_t the top layer, $S(k, i)$ the source function for a particular k value and layer i. T_i^i is the transmission from the upper boundary (H2) through layer i along the viewing path. The total upward radiance also includes I_s , a direct solar reflection surface contribution or surface thermal emission term, which for the new AER LOWTRAN includes the contribution due to the reflection of the single and multiple scattered solar radiance. For a thermal case,

$$I_s = B_s T_t \epsilon \quad (3.40)$$

where B_s is the black body function for a given surface temperature and frequency, T_t is the total atmospheric transmissivity, and ϵ is the surface emissivity. For the old LOWTRAN (single scatter) solar case,

$$I_s = a_s \mu_o T_t S / \pi, \quad (3.41)$$

where a_s is the surface albedo, μ_o the cosine of solar zenith angle at the surface, and S the direct solar intensity at the surface. With multiple scattering (IMULT=1), the single and multiple scatter reflection terms are added, so that

$$I_s = a_s \mu_o T_t S / \pi + a_s F_s^- T_t / \pi, \quad (3.42)$$

where F_s^- is the downward diffuse flux at the surface.

For an upward looking (downward radiance) case, the multiply scattered radiance is expressed by

$$I^-(n_b) = \sum_{k=1}^6 \{ (1 - T_{n_b}^i) S(k, n_b) + \sum_{i=n_b}^{n_t+1} (T_i^i - T_{i-1}^i) S(k, i-1) \} \Delta g_k, \quad (3.43)$$

where T_i^i is the transmission from the lower boundary (H1) through layer i along the viewing path. At this point, the LOWTRAN6 path parameters are reloaded, and TRANS is executed once more for the single scatter LOWTRAN6 case. The single scatter diffuse radiance is added to the multiple scatter

term and the boundary radiance contributions (if any) to yield the total thermal radiance, while the solar/lunar radiance is the sum of the single and multiple scatter terms plus a surface reflection term where applicable. MSRAD and FLXADD are not called for the LOWTRAN6 single scatter case.

Figures 3-9 and 3-10 are flow charts of subroutines TRANS, MSRAD, and FLXADD.

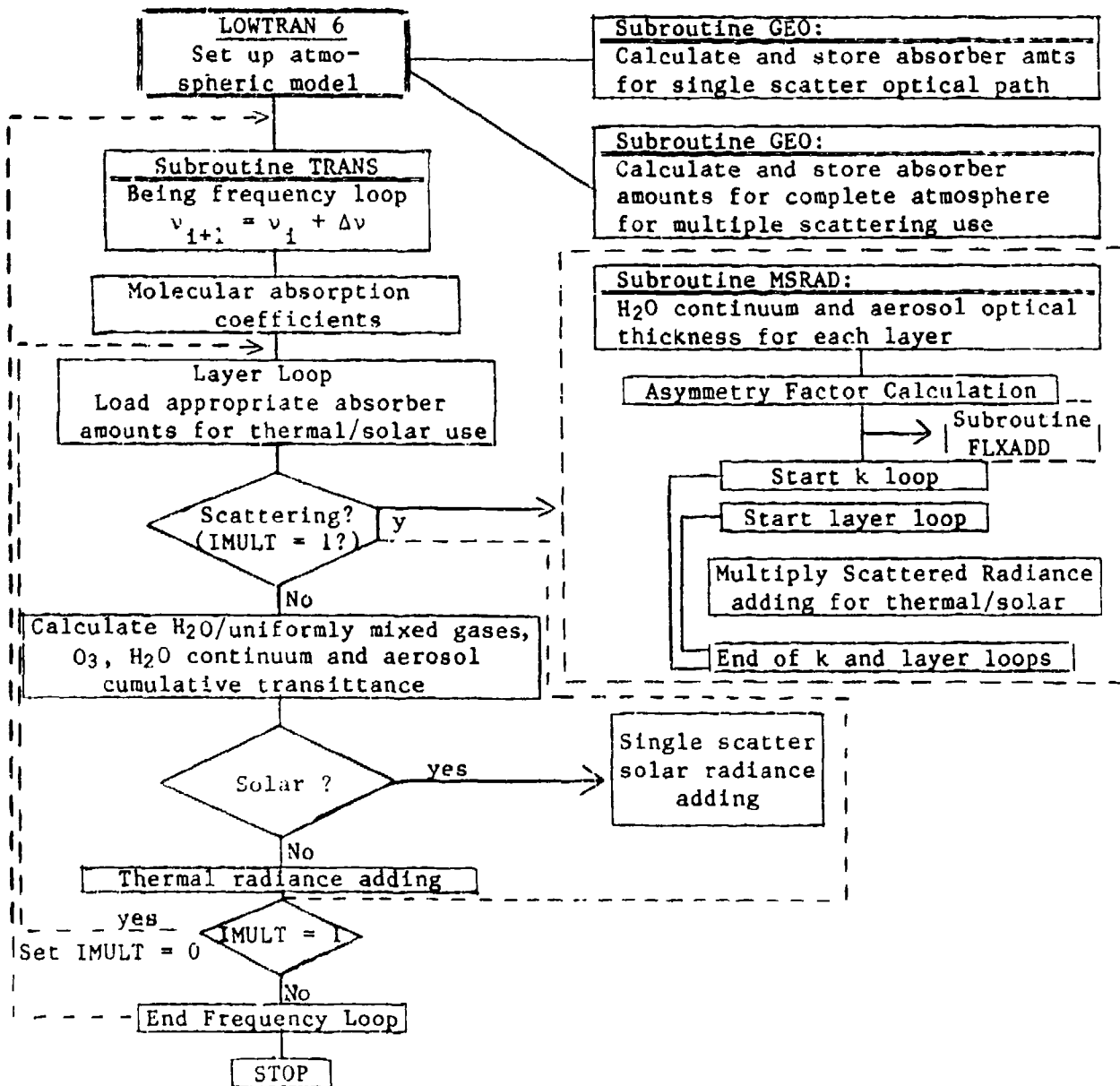
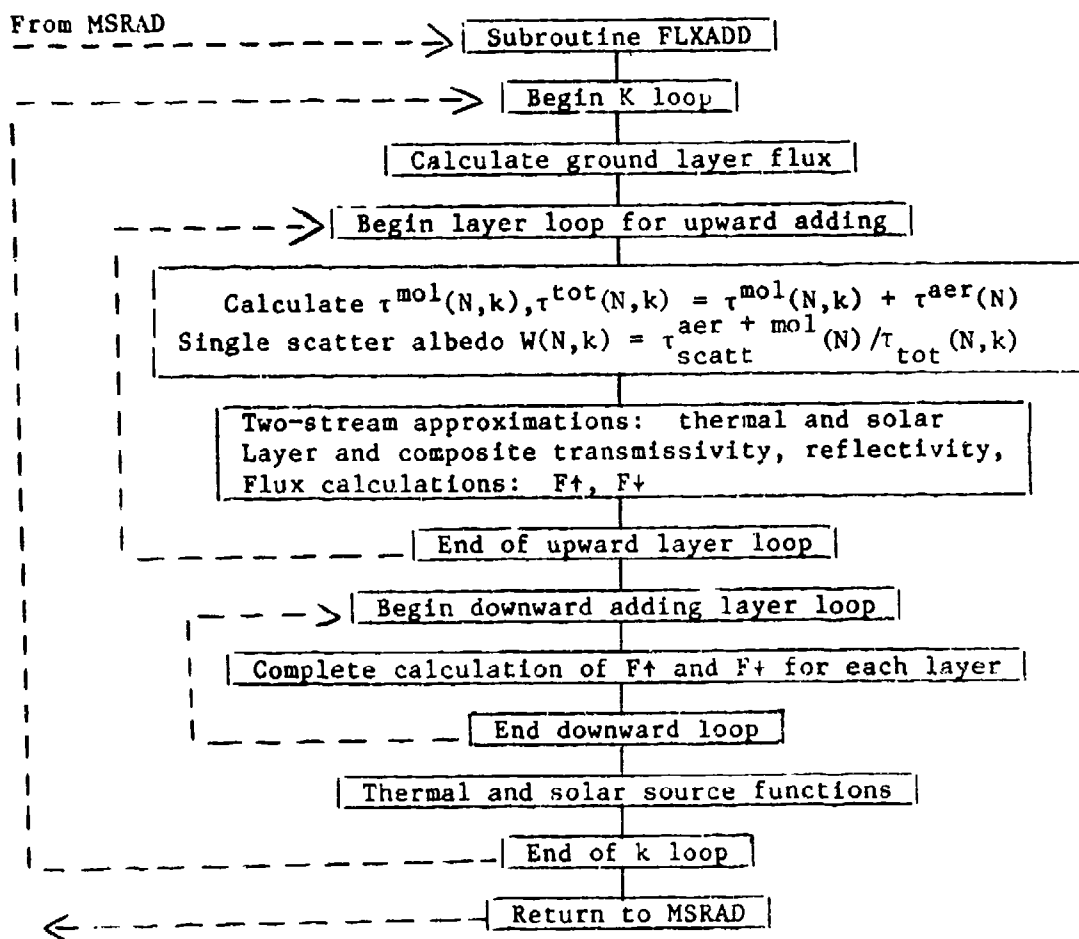


Figure 3-9. Flowchart of Subroutines TRANS and MSRAD.



3.2.6 Notes on the Operation of LOWTRAN6 with Multiple Scattering

As previously discussed, the only change to the LOWTRAN input card images occurs in card 1 with the addition of the input parameter IMULT used to turn multiple scattering on or off. Card 1 is now read as follows:

```

MODEL, ITYPE, IEMSCT, M1, M2, M3, IM, NOPRNT, TBOUND, SALB, IMULT
15 , 15 , 15 , 15, 15, 15, 15, 15 , F10.3 , F10.3, 15

```

As previously mentioned, setting IMULT = 1 initiates multiple scattering, while IMULT = 0 provides single scattering or clear sky results.

Unlike the original LOWTRAN6, the new LOWTRAN6 requires a complete atmospheric profile (surface to space) to properly calculate the multiple scattering contribution to the radiance. For a calculation involving a path from 0-1 km, for example, it is still necessary to choose the desired stratospheric as well as higher level aerosol distribution set by IVULCN on card 2. For a 3-20 km path, the boundary layer aerosols, set using IHAZE, on card 2 or user-defined via card 2D, will now affect the calculated radiance. The original LOWTRAN performing single scattering required aerosol information only along the path between observer and target.

As currently set up, LOWTRAN6 will not do multiple Rayleigh scattering for IHAZE = 0 but will instead default to the original LOWTRAN6 single scattering calculation. To perform a multiple Rayleigh scattering calculation without boundary layer aerosols, choose IHAZE > 0 and set the visibility (VIS on card 3) to a large value such as 300 km to effectively eliminate the effect of these aerosols.

When LOWTRAN6 is run in its original form (single scattering only, IMULT = 0), the output for a solar case includes the reflected attenuated direct solar radiance under the heading GROUND REFLECTED. However, in many cases, the ground reflected diffuse radiance due to single and multiple scattering is on the same order of magnitude as the direct reflected radiance. The output for new LOWTRAN6 (IMULT = 1) has therefore been altered to include both the total (diffuse single and multiple scattered and direct) and direct reflection terms. Since the original single scatter LOWTRAN does not calculate downward radiance at the surface for an upward radiance case, the single scattered diffuse reflection term cannot currently be calculated.

Running LOWTRAN6 with multiple scattering results in a several-fold increase in CPU time. The atmospheric profile and path being used may not produce a significant multiple scattering contribution, possibly resulting in wasted computer time. A new feature has therefore been added to the solar output. Both the total (single and multiple) and single scattered radiance are now included under the heading "PATH SCATTERED RADIANCE." If in doubt, the user may now run a multiple scatter LOWTRAN run to determine the relative size(s) of the single and multiple scatter contributions. If multiple scattering is negligible, future calculations may be made with the more economical single scatter (IMULT = 0) option.

Test cases for LOWTRAN are provided in Appendix C.

4. RESULTS OF INTERCOMPARISON OF IMPLEMENTED MULTIPLE SCATTERING APPROACH WITH EXACT CALCULATIONS

4.1 Comparison of FASCODE Multiple Scattering Results to Exact Calculations

The detailed approach described in the previous sections was employed to develop a multiple scattering version of FASCODE based on the stream approximation and adding method. In order to verify the operation of the code, a number of test cases were run. To validate the results, these test cases were also run with the discrete ordinate code (DOM) for multiple scattering. Additionally, the existing nonscattering version of FASCODE was run for comparison. The optical properties for these test cases and corresponding radiance results are given in Table 4-1(a)-(c). Three test cases were selected. Case I is based on a FASCODE run at 900 cm^{-1} with a rural haze and 5 km visibility. This resulted in an optical depth of 0.357 and a single scattering albedo of 0.126. With this small albedo, the effects of scattering are expected to be small and results for all three methods should be comparable. In order to enhance the scattering effects and emphasize the differences between approaches, the number density of aerosol was increased to nonphysical amounts to yield single scattering albedos in the vicinity of 0.5 (case II) and 0.9 (case III). Note that the FASCODE models include the effect of atmospheric refraction while the discrete ordinate method code is strictly a plane parallel model. Comparisons of these results for zenith angles in the domain from 65 to 115 degrees should be made with this in mind.

Results are plotted in Figures 4-1 to 4-6. Upward and downward emergent radiances for Case I are shown in Figures 4-1 and 4-2, respectively. Here FASCODE, FASCODEMS, and the DOM are shown to give approximately the same magnitude and angular distribution of radiance. A slight tendency for FASCODE to underestimate the upward radiance and overestimate the downward radiance can be noted. At a higher optical depth and single scattering albedo (case II), this effect becomes obvious (Figures 4-3 and 4-4, respectively.) Here it can be seen that FASCODEMS does a clearly superior job at representing the angular radiance distribution. For a situation where multiple scattering dominates over gas absorption (case III, Figures 4-5 and 4-6), the deficiency of the absorption only FASCODE model is obvious.

Table 4-1

Scattering Comparisons for FASCODE Multiple Scattering Runs

(WAVELENGTH = 900 CM-1 , RADIANCES = ERG SEC-1 CM-2 (CM-1)-1 STR-1)

(a) CASE I. SMALL SCATTERING

TAU=0.357, OMEGA0=0.126, ASYMMETRY FACTOR=0.6985

ZENITH ANGLE (DEGREES)	AFGL FASCODE (NO MS)	AER FASCODE (MS)	DISCRETE ORDINATE METHOD (MS)
UPWARD RADIANCES			
0.000	101.29	102.55	106.24 †
8.349	100	102.42	103.07
19.165	100	101.84	102.45
30.045	100	100.69	101.23
40.939	97.29	98.75	99.18
51.839	94.02	95.58	95.81
62.741	88.62	90.23	90.09
73.644 *	79.17	80.66	79.61
84.548 *	68.23	68.29	60.96
DOWNWARD RADIANCES			
95.452 *	65.16	63.44	68.51
106.356 *	46.79	44.37	46.72
117.259	35.15	32.85	34.09
128.161	28.48	26.36	27.12
139.061	24.43	22.48	23.01
149.955	21.92	20.11	20.49
160.835	20.41	18.70	19.00
171.651	19.64	17.98	18.24
180.000	19.47	17.81	14.69 †

†This point extrapolated in discrete ordinate method.

*FASCODE path is refracted while discrete ordinate method is plane parallel.
These zenith angles are affected.

(2) CASE II. INTERMEDIATE SCATTERING

TAU=0.555, OMEGA0=0.498, ASYMMETRY FACTOR=0.6985

ZENITH ANGLE (DEGREES)	AFGL FASCODE (NO MS)	AER FASCODE (MS)	DISCRETE ORDINATE METHOD (MS)
UPWARD RADIANCES			
0.000	94.73	101.62	103.52 †
8.349	94.55	101.48	101.43
19.165	93.77	100.85	100.69
30.045	92.25	99.63	99.21
40.939	89.79	97.53	96.68
51.839	86.00	94.02	92.50
62.741	80.24	88.21	85.45
73.644 *	71.93	78.66	73.33
84.548 *	68.01	68.06	55.37
DOWNWARD RADIANCES			
95.452 *	66.48	59.53	70.14
106.356 *	56.04	44.76	50.95
117.259	45.63	34.02	37.25
128.161	38.49	27.40	29.14
139.061	33.78	23.35	24.28
149.955	30.72	20.89	21.32
160.835	28.84	19.46	19.58
171.651	27.87	18.71	18.70
180.000	27.65	18.55	16.80 †

(c) CASE III. LARGE SCATTERING

TAU=0.308, OMEGA0=0.897, ASYMMETRY FACTOR=0.6985

ZENITH ANGLE (DEGREES)	AFGL FASCODE (NO MS)	AER FASCODE (MS)	DISCRETE ORDINATE METHOD (MS)
UPWARD RADIANCES			
0.000	103.31	112.24	119.78 †
8.349	102.97	112.19	113.19
19.165	102.45	111.96	112.81
30.045	101.46	111.49	112.03
40.939	99.78	110.53	110.58
51.839	97.01	108.57	107.87
62.741	92.28	104.51	102.49
73.644 *	83.37	95.13	90.55
84.548 *	68.85	68.79	62.28
DOWNWARD RADIANCES			
95.452 *	63.04	46.54	57.61
106.356 *	41.52	21.81	28.65
117.259	30.60	12.71	16.29
128.161	24.75	8.72	10.68
139.061	21.33	6.78	7.84
149.955	19.24	5.83	6.31
160.835	18.00	5.37	5.48
171.651	17.37	5.14	5.09
180.000	17.23	5.09	---- †

In order to gain some insight into the differences between the FASCODE and FASCODEMS results, a radiance budget has been computed for one upward and one downward zenith angle corresponding to case II. These radiance budgets are presented in Table 4-2 and provide the magnitude of contributions to the total radiance from surface emission, atmospheric emission, and the scattering source function, as applicable. Radiance values are rounded for simplicity.

Table 4-2

Case II Radiance Budgets [unattenuated surface emission corresponds to 120 radiance units; units = $\text{erg s}^{-1} \text{cm}^{-2} \text{str}^{-1} (\text{cm}^{-1})^{-1}$].

	FASCODE	FASCODEMS	DOM
(a) Upward Radiance (zenith angle 8.3 degrees)			
Surface emission	65	65	
Atmospheric emission	30	16	
Scattering source		20	
Total	95	101	101
(b) Downward Radiance (zenith angle 171.7 degrees)			
Atmospheric emission	28	12	
Scattering source	-	8	
Total	28	20	19

Examination of Table 4-2 indicates that FASCODE over estimates atmospheric emission in the presence of scatterers since it assumes that scattering extinction is equivalent to absorption. In this case radiation absorbed is re-emitted. While scatterers may absorb and re-emit, some fraction of the extinction due to their presence (i.e., that given by their single scattering albedo) is simply redirected. In the case of the upward intensity in Table 4-2, forward scattering of some of the surface emission lost due to extinction more than compensates for the decreased atmospheric emission. Thus the non-scattering version of FASCODE underestimates the radiance. For the downward radiance in Table 4-2, the small scattering source does not compensate for the decrease in atmospheric emission due to the treatment of scattering. In this case FASCODE overestimates the actual radiance.

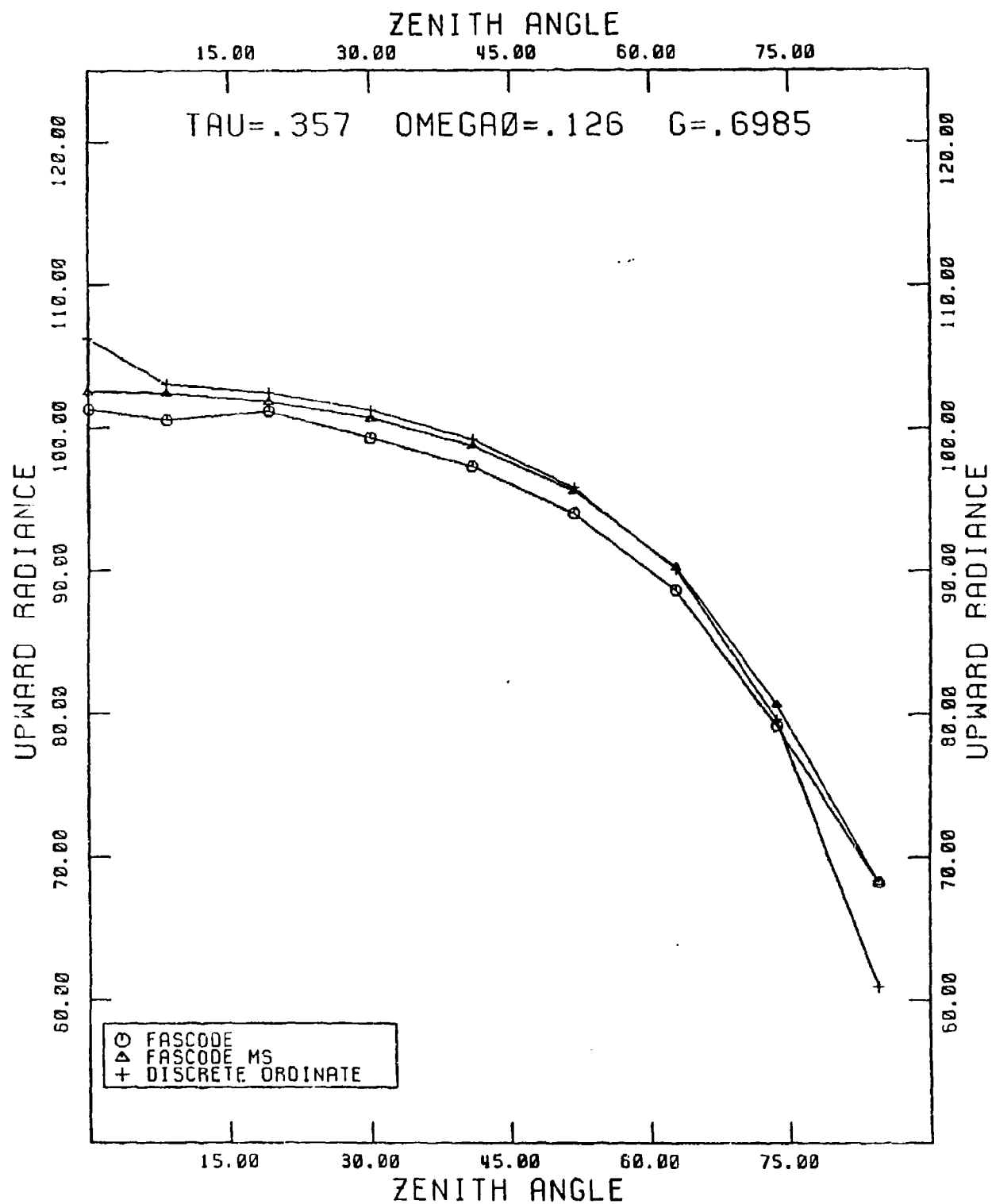


Figure 4-1. Comparison of FASCODE, FASCODEMS, and DOM for upward radiance
[units: $\text{ergs sec}^{-1} \text{cm}^{-2} \text{str}^{-1} (\text{cm}^{-1})^{-1}$]

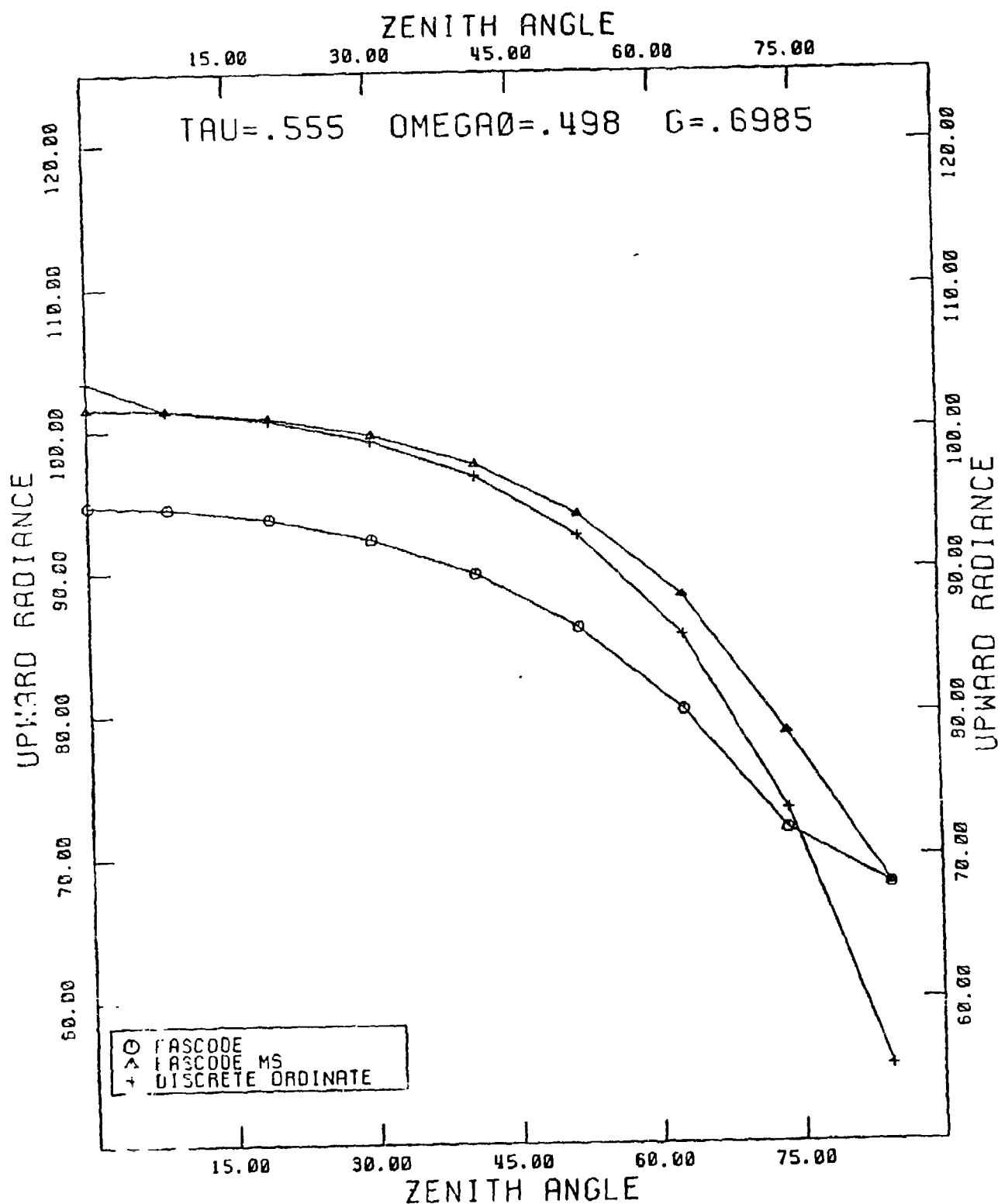


Figure 4-3. Comparison of FASCODE, FASCODEMS, and DOM for upward radiance
[units: $\text{ergs sec}^{-1} \text{cm}^{-2} \text{str}^{-1} (\text{cm}^{-1})^{-1}$]

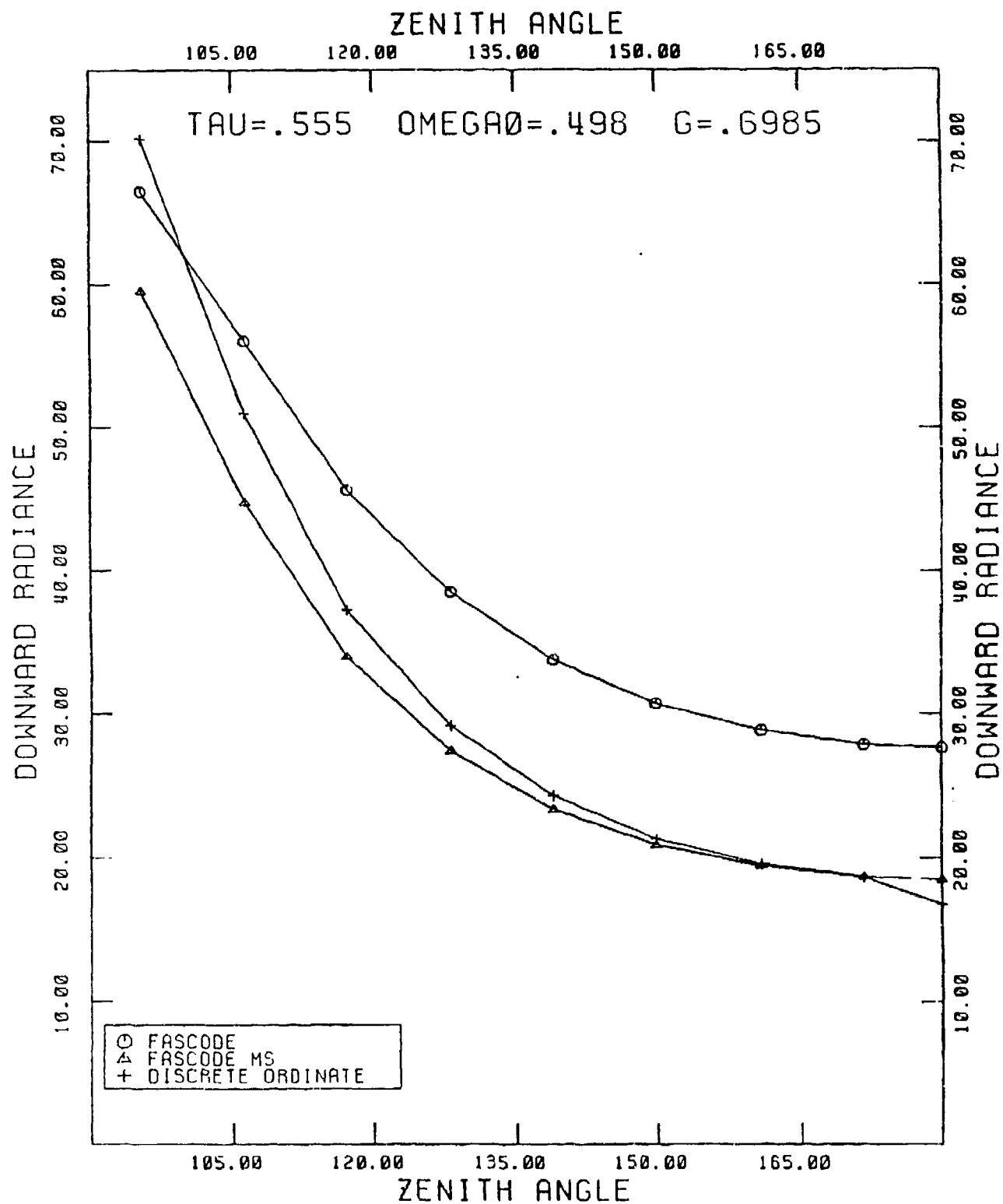


Figure 4-4. Comparison for FASCODE, FASCODEMS, and DOM for downward radiance [units: $\text{ergs sec}^{-1} \text{cm}^{-2} \text{str}^{-1} (\text{cm}^{-1})^{-1}$]

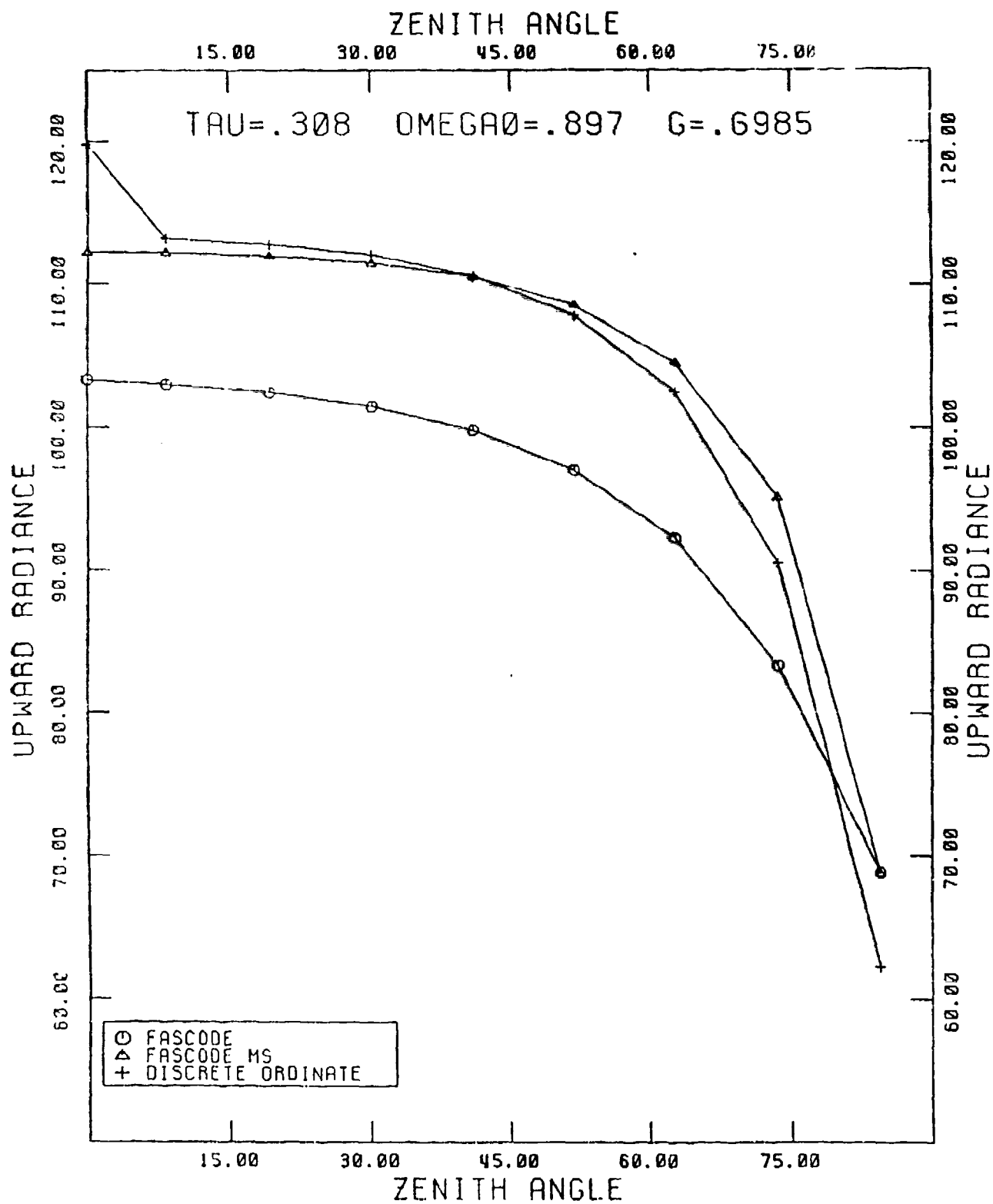


Figure 4-5. Comparison of FASCODE, FASCODEMS, and DOM for upward radiance
[units: $\text{ergs sec}^{-1} \text{cm}^{-2} \text{str}^{-1} (\text{cm}^{-1})^{-1}$]

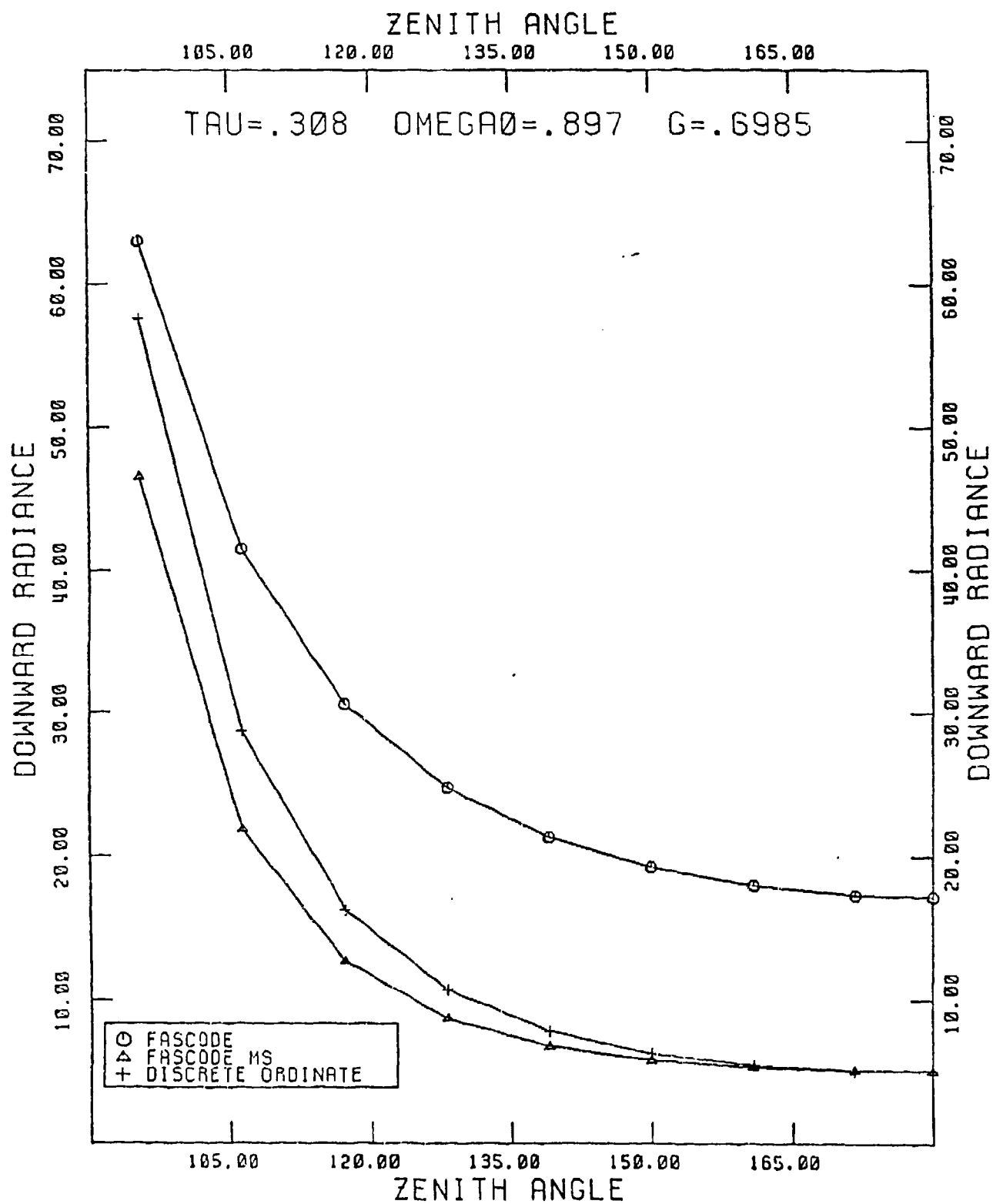


Figure -6. Comparison for FASCODE, FASCODEMS, and DOM for downward radiance [units: $\text{ergs sec}^{-1} \text{cm}^{-2} \text{str}^{-1} (\text{cm}^{-1})^{-1}$]

4.2 Comparison of LOWTRAN Multiple Scattering Results to Exact Calculations

4.2.1 Solar Multiple Scattering

In order to verify the correct operation of the implemented LOWTRAN multiple scattering treatment for both solar and thermal regimes, comparisons were made to exact results.

In the case of solar multiple scattering, exact results were obtained for a variety of cases during the trade-off analysis summarized in Appendix A. Exact solutions to the radiative transfer equation for solar multiple scattering were obtained using the Gauss-Seidel iterative method based on a code by Dave (1972). This algorithm evaluates the fluxes and radiances for inhomogeneous atmospheres with arbitrary vertical distributions of anisotropically scattering aerosol overlying a Lambert reflecting surface. Emergent fluxes and radiances from this code were compared to those obtained from LOWTRAN for three values of total optical thickness (0.25, 0.50, 1.00) and two values of surface albedo (0.0, 0.4).

A number of special modifications of LOWTRAN were necessary to accommodate the comparison. These included reading in the same aerosol extinction and absorption coefficients, asymmetry factor, and phase function as were used for the Dave model runs, and forcing LOWTRAN to use the quantities with the same vertical distribution as the Dave code. (Ordinarily, user supplied aerosol data read into LOWTRAN will only be used in the lowest 2 km of the atmosphere.) These changes made the comparison as close as possible to a direct one. The LOWTRAN code was run at $0.55 \mu\text{m}$ with the sun at a zenith angle of 60° .

The first test of the LOWTRAN implementation is whether the adding method is calculating the correct fluxes for use in the stream approximation of the multiply scattered source function. Table 4.3 compares the emergent fluxes calculated by the exact code and LOWTRAN. For simplicity all fluxes and radiances plotted here have been normalized to correspond to π units of incident solar irradiance. To obtain the appropriate engineering units ($\text{watts/cm}^2 \text{ cm}^{-1}$, and $\text{watts/cm}^2 \text{ str cm}^{-1}$, for flux and radiance, respectively), the normalized values can be multiplied by 1.719×10^{-6} . As can be seen from the results, the solar two stream approximation and flux adding procedure in LOWTRAN is reproducing the exact values quite well throughout the range of

optical thicknesses and surface albedos examined. The errors, on the order of a few percent, are to be expected from the two stream approximation.

Figures 4-9 through 4-12 illustrate the comparison between the exact radiance calculation as a function of path zenith angle (θ) and those obtained from LOWTRAN using either the solar single scattering option (LOWTRAN) or the new multiple scattering option (LOWTRAN MS). Plotted are the normalized emergent upward and downward radiances for an optical depth of 0.5 and surface albedos of 0.0 and 0.4. The plots extend to a maximum zenith angle of 60° since at larger angles the effects of refraction in the LOWTRAN code make it difficult to compare to the plane parallel exact results. In all cases it can be seen that the introduction of the multiply scattered contribution to path radiance in LOWTRAN MS has considerably improved the simulation as compared to that obtained from the exact code. The improvement is considerable, especially for upward radiance when there is surface reflection (see Figure 4-11). This is because although the single scatter version of LOWTRAN included the surface reflection of the attenuated direct solar beam, it contained no provision to treat the reflected downward scattered radiance. This contribution (which is the second term in the brackets in Equation (2.10)) may be considerable when multiple scattering is a factor and is included in the LOWTRAN MS version since the downward scattered flux is calculated as a result of the adding method.

The relative accuracies as a function of path zenith angle expressed as percent errors obtained in the comparison between LOWTRAN MS and the exact calculations for all optical depths evaluated are summarized in Figures 4-13 and 4-14, for surface albedos of 0.0 and 0.4, respectively. In general, the solar multiple scattering approach implemented within LOWTRAN underestimates radiance by 10 or 20 percent. These accuracies are consistent with those obtained off line in the trade-off analysis (see Appendix A, Table A-5.)

4.2.2 Thermal Multiple Scattering

Proper operation of the code for thermal multiple scattering was verified by comparing LOWTRAN MS to corresponding FASCOD MS results. FASCOD MS has been compared to exact multiple scattering using the discrete ordinate method in Section 4.1. The case chosen was a vertical path from the surface to 20 km using a U.S. Standard atmosphere (MODEL 6) and a rural aerosol model

with 5 km visual range (HAZE 2). The spectral domain for both runs was 850-1150 cm^{-1} . Figures 4-15a, b illustrate this comparison for upward and downward radiance, respectively. The FASCODE MS results have been degraded to 5 cm^{-1} for consistency with the LOWTRAN MS values. In general both models agree quite well within this spectral region. The slight discrepancy between degraded FASCODE and LOWTRAN spectra (especially for downward radiance) in this region is not due to multiple scattering effects, but rather to differences in the corresponding clear air spectra. This is illustrated by Figure 4-16 where all aerosols have been removed from the calculation.

One problem with the previous treatment of thermal scattering within LOWTRAN was the failure to provide a source function to introduce multiply scattered radiance contributions along the observed path. As a consequence of this ad hoc approach, LOWTRAN seriously underestimated path radiance for long paths such as those near the horizon where multiple scattering could contribute significantly (Ben-Shalom et al., 1980). This deficiency is corrected with the implementation of the multiple scattering approach described here. To illustrate, radiances have been simulated for a ground based observer scanning the sky between 8.0 and 13.5 μm . Figures 4-17, 4-18, and 4-19 illustrate the calculated results, for observing zenith, 10° above the horizon, and the horizon, using the standard LOWTRAN, the Ben-Shalom modification (Ben-Shalom et al, 1980), and LOWTRAN MS. For comparison, the black body function of the lowest atmospheric layer is also plotted. The calculation has assumed a mid-latitude summer atmosphere and 5 km visual range.

As can be seen in Figure 4-17, there is very little difference in the results among the three approaches when observing zenith when multiple scattering effects are minimized. For larger air mass factors, however, the three approaches diverge, with the LOWTRAN MS result bounded below by the standard LOWTRAN and above by the Ben-Shalom modified version (see Figure 4-18). This is understandable since standard LOWTRAN removes all scattered radiance from the path radiance and the Ben-Shalom modification assumes that all scattered radiance is returned to the path radiance (i.e., the scattering is conservative). Actually some of the scattered radiance is returned to the path radiance through the scattering source function. The fraction returned depends on the single scattering albedo and through the scattering phase function, on the viewing geometry. At the horizon (Figure 4-19), the standard LOWTRAN result

significantly underestimates the radiance level expected qualitatively, i.e., that approximating the emission of the lowest atmospheric layer.

In Figure 4-20a are plotted LOWTRAN MS results for the case described above with the observer path at various elevation angles. For comparison, Figure 4-20c reproduces a set of radiance measurements taken with qualitatively similar conditions (Bell et al, 1960). Note that the wavelength range of these measurements is much broader than that illustrated in Figure 4-20a and the vertical scales are different. Additionally, the ambient temperature when the measurements were taken is about 5 K higher than that of the surface layer of the midlatitude summer model used in the LOWTRAN MS simulation. In spite of these differences, the simulated and measured radiances exhibit similar magnitudes and dependence on path elevation angle.

Table 4-3

Comparison of solar multiply scattered emergent fluxes
(normalized to π units of incident irradiance) from
LOWTRAN FLXADD subroutine (L) and exact calculation (E).

π^*	Upward Flux F^+ ($\pi = 0$)		Downward Flux F^- ($\pi = \pi^*$)	
	$r = 0.0$ L / E	$r = 0.4$ L / E	$r = 0.0$ L / E	$r = 0.4$ L / E
0.25	.188 / .191	.611 / .634	.323 / .316	.367 / .371
0.50	.244 / .256	.562 / .584	.503 / .489	.536 / .544
1.00	.316 / .324	.492 / .515	.599 / .567	.605 / .615

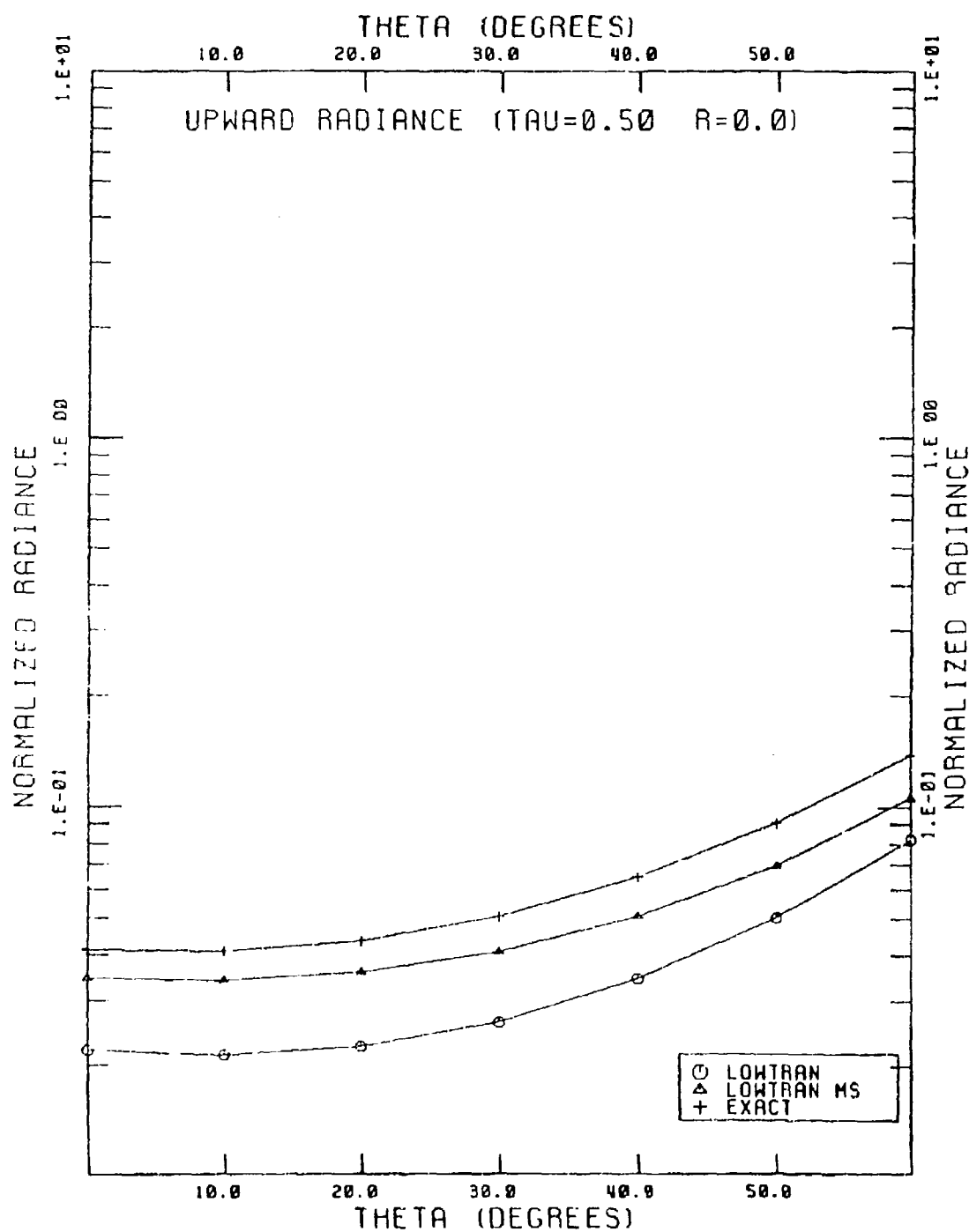


Figure 4-9. LOWTRAN6 upward radiance (solar, .55 μ m) with and without multiple scattering compared to exact (Dave) results. Solar zenith angle is 60°.

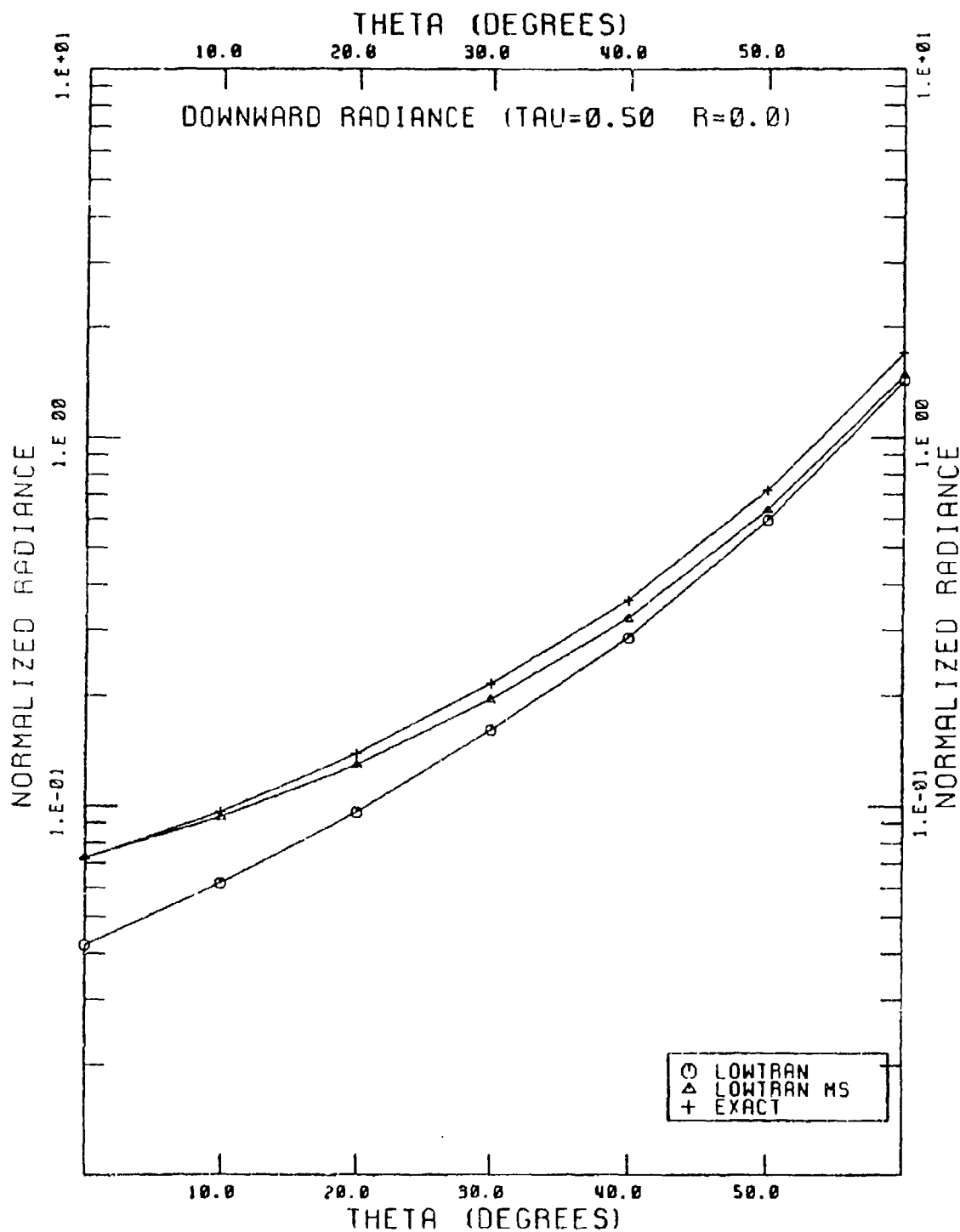


Figure 4-10. LOWTRAN6 downward radiance (solar, .55 μm) with and without multiple scattering compared to exact (Dave) results. Solar zenith angle is 60° .

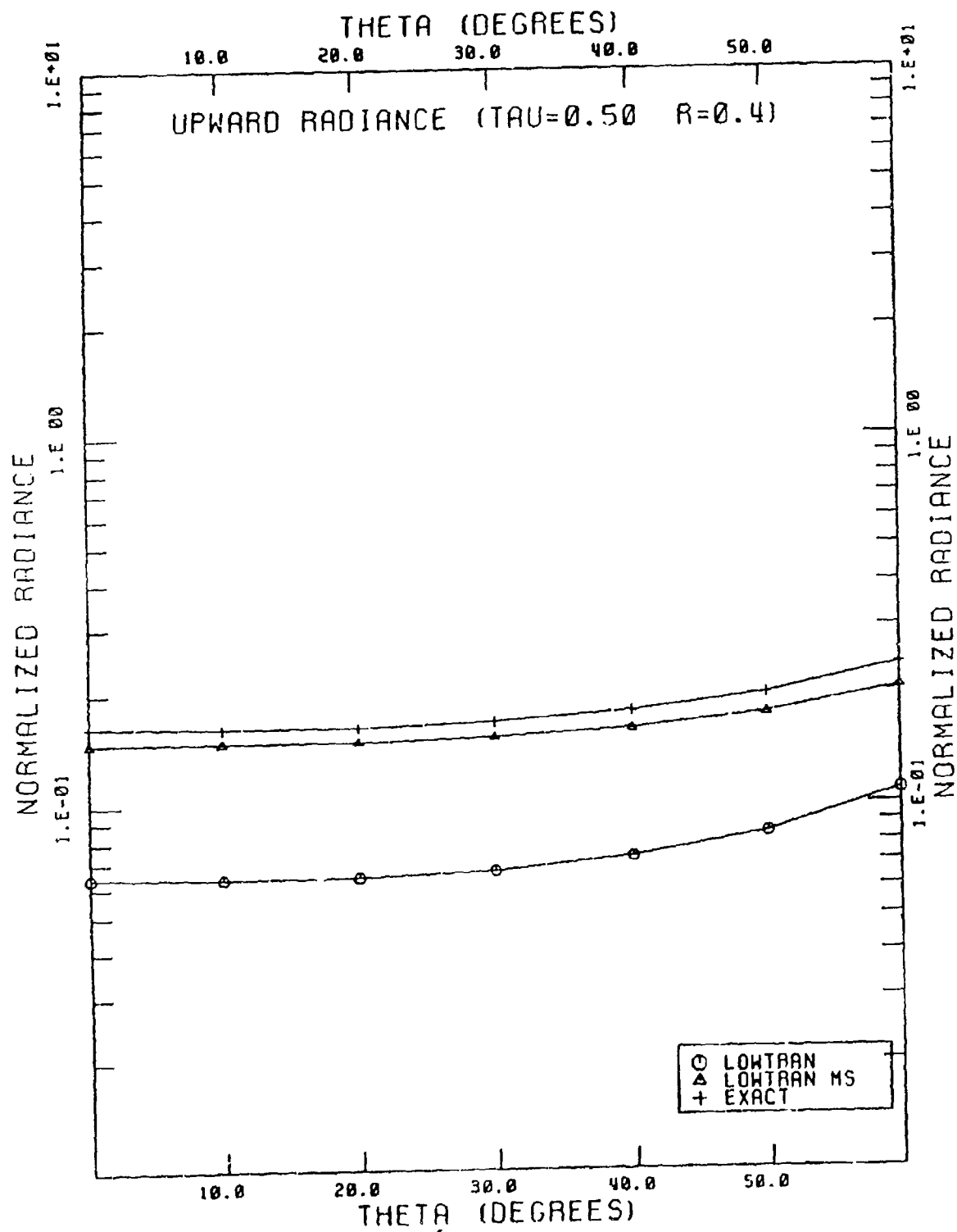


Figure 4-11. LOWTRAN6 upward radiance (solar, $0.55 \mu\text{m}$) with and without multiple scattering compared to exact (Dave) results. Solar zenith angle is 60° .

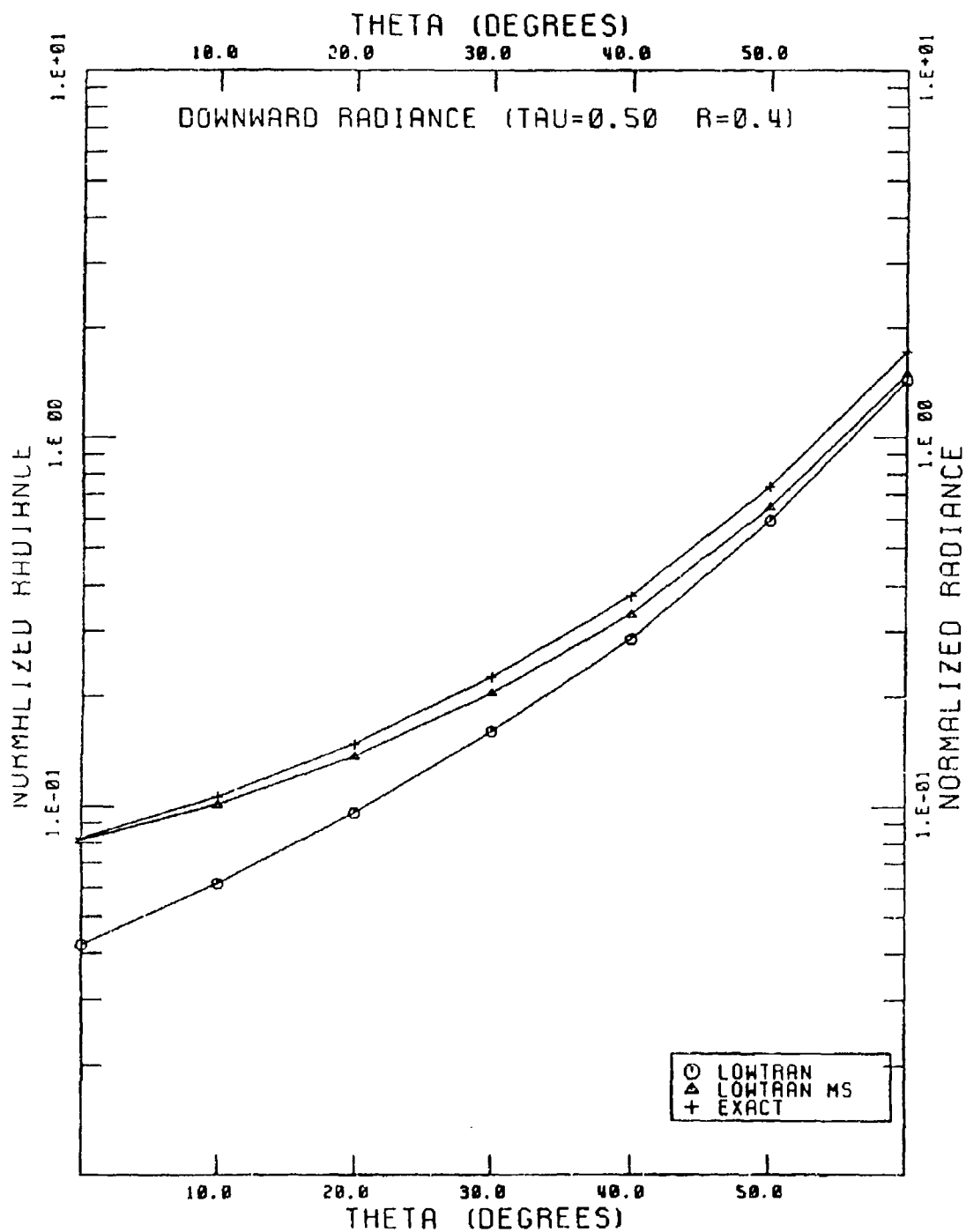


Figure 4-12. LOWTRAN6 downward radiance (solar, .55 μm) with and without multiple scattering compared to exact (Dave) results. Solar zenith angle is 60° .

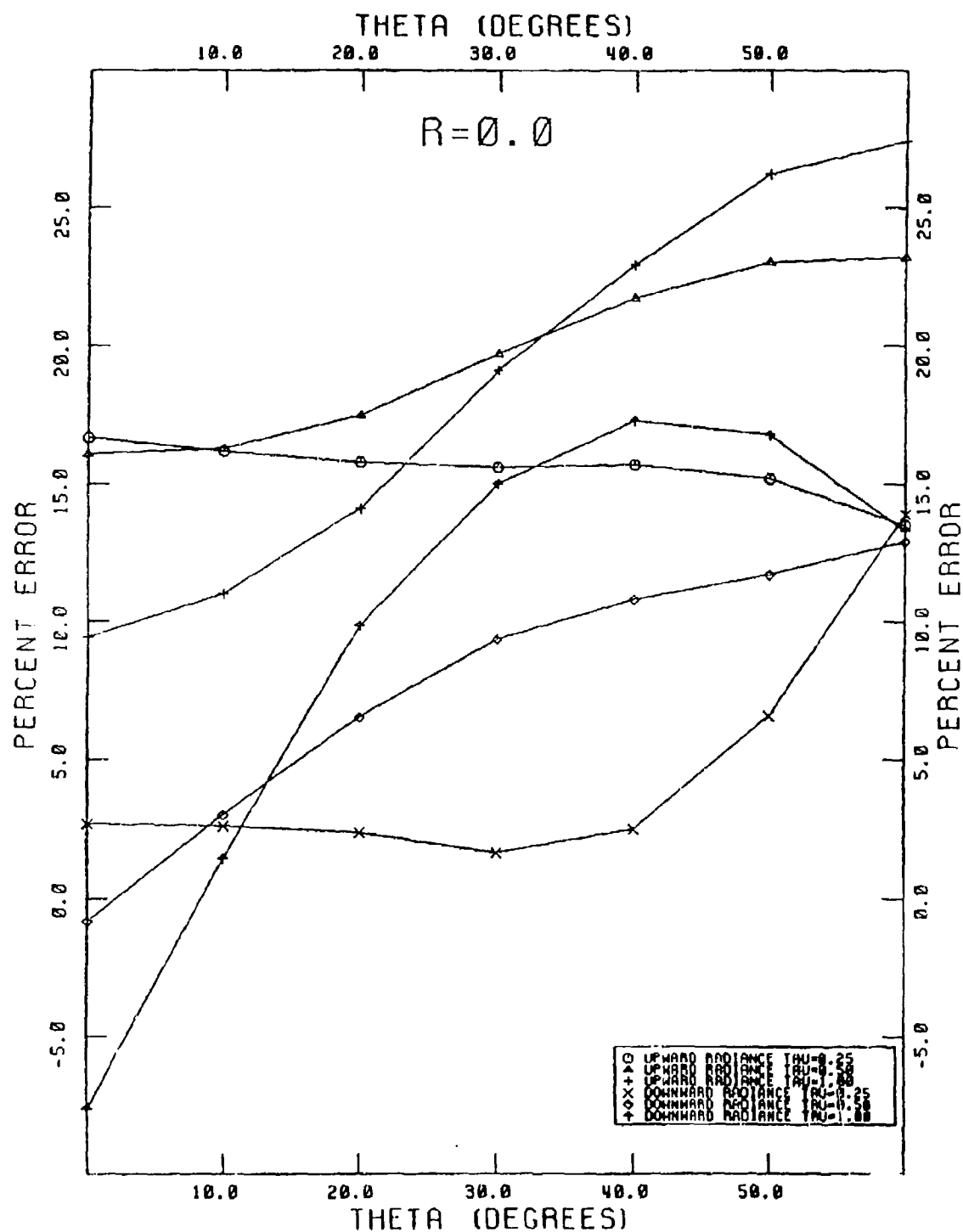


Figure 4-13. Percent error of LOWTRAN6 multiple scatter calculations relative to exact (Dave) results for optical depths between 0.25 and 1.00 with a surface reflectance of 0.0.

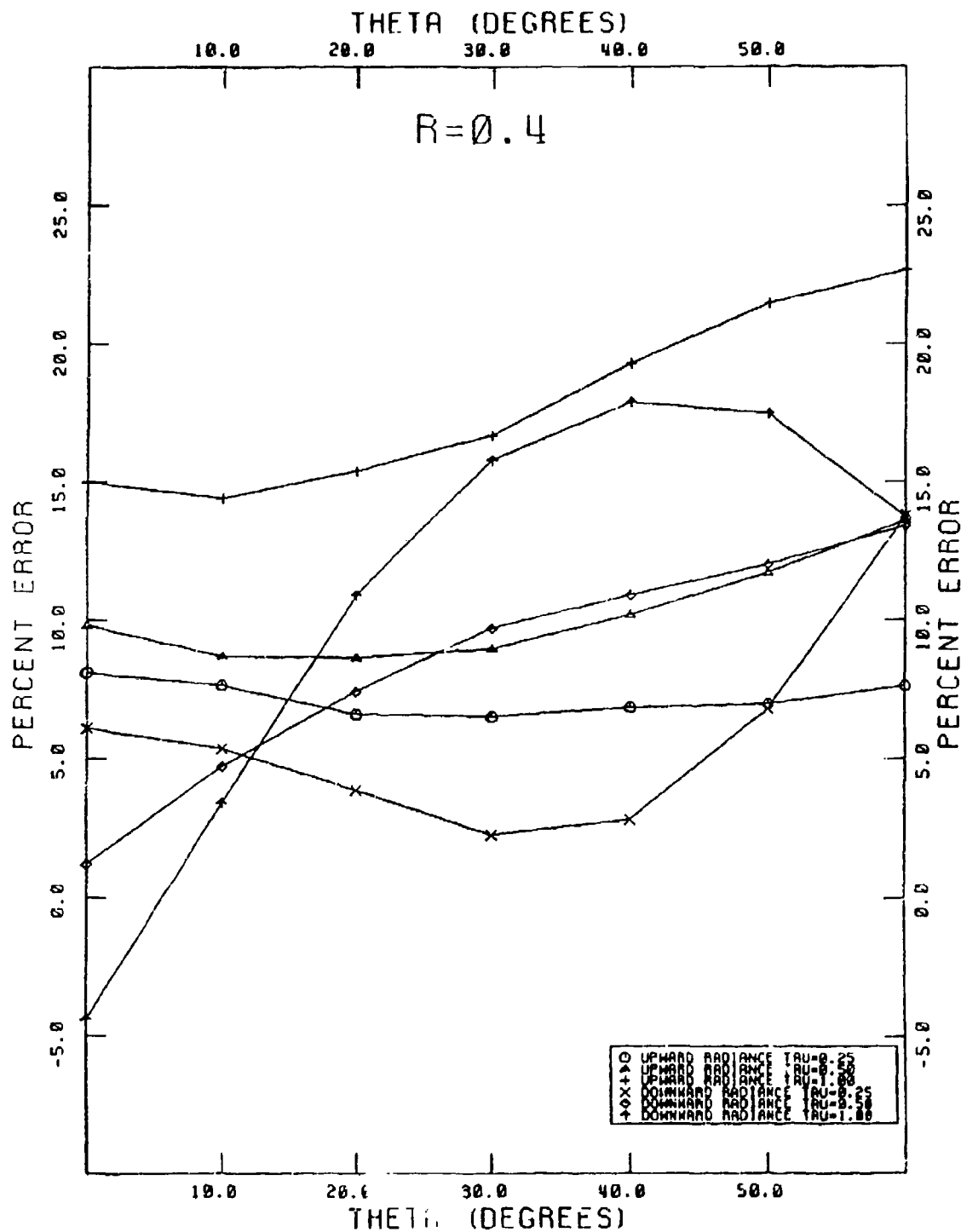


Figure 4-14. Percent error of LOWTRAN6 multiple scatter calculations relative to exact (Dave) results for optical depths between 0.25 and 1.00 with a surface reflectance of 0.4.

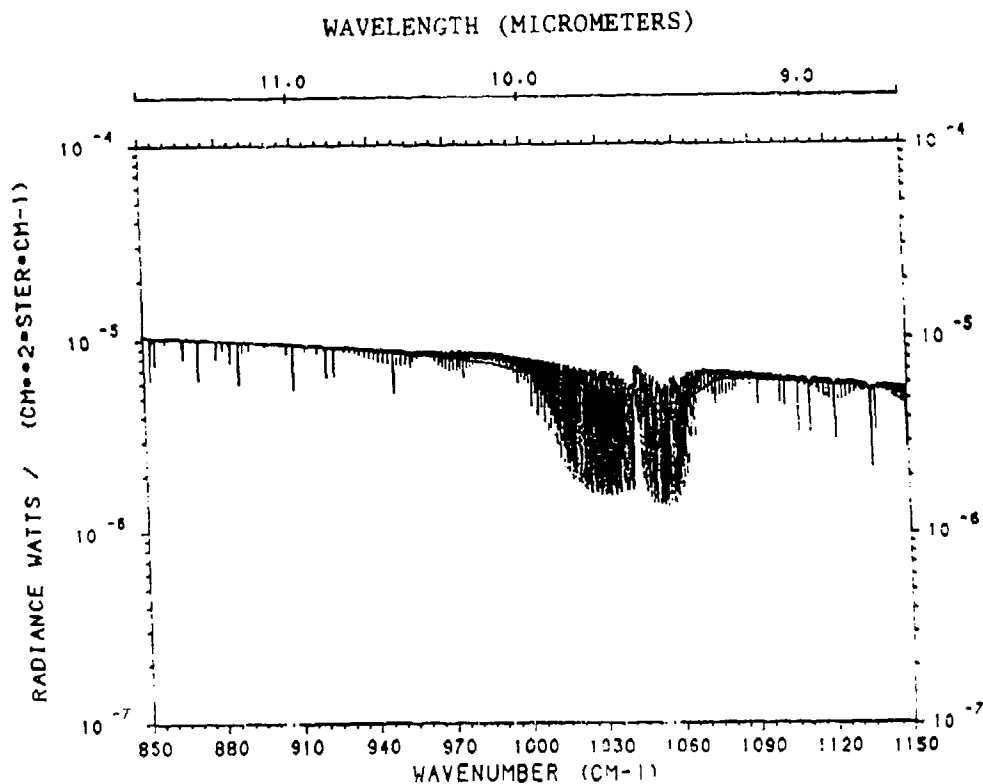


Figure 4-15a. Comparisons of LOWTRAN and FASCODE upward thermal radiance (with multiple scattering) between 850 and 1150 cm^{-1} .

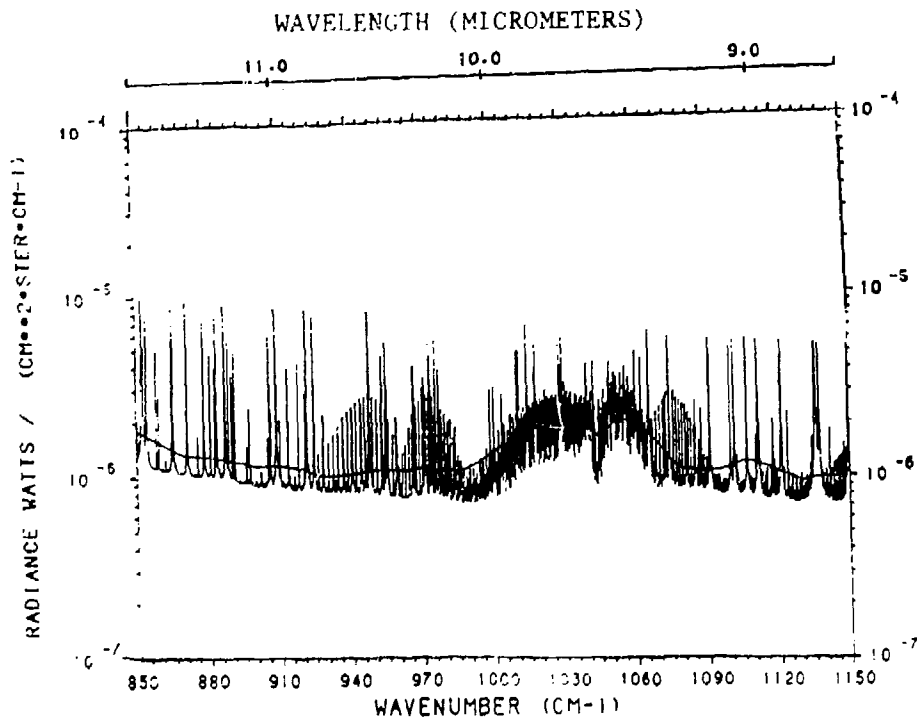


Figure 4-15b. Comparison of LOWTRAN and FASCODE downward thermal radiance (with multiple scattering) between 850 and 1150 cm^{-1} .

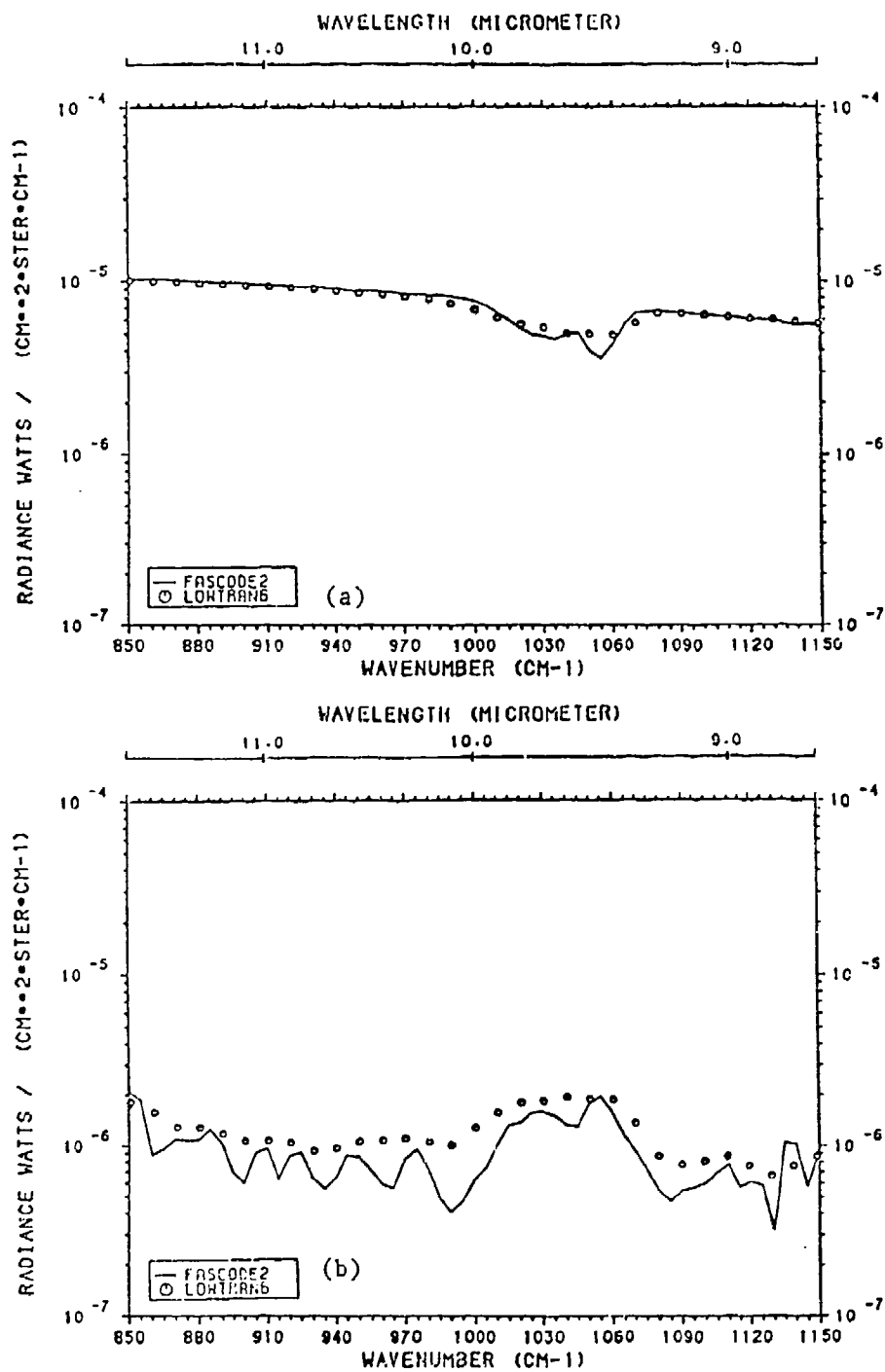


Figure 4.16. Comparisons of clear sky upward (a) and downward (b) radiances between LOWTRAN6 and FASCODE2.

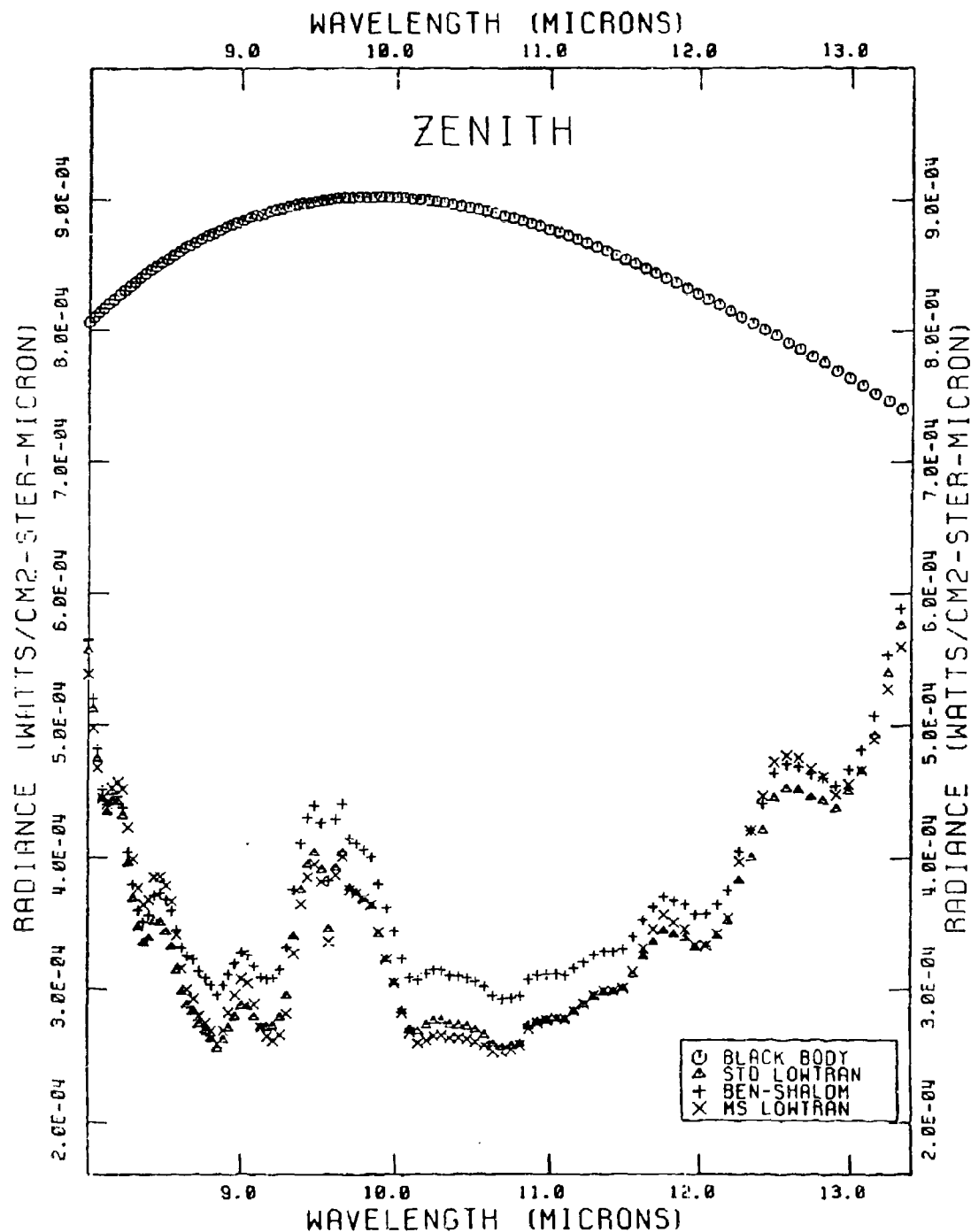


Figure 4-17. Downward thermal radiance comparison between 8 and 13.5 μm : Black body radiance of lowest atmospheric layer, standard LOWTRAN (without multiple scattering), Ben-Shalom calculations, and new LOWTRAN (with multiple scattering). Viewing path is from surface to zenith.

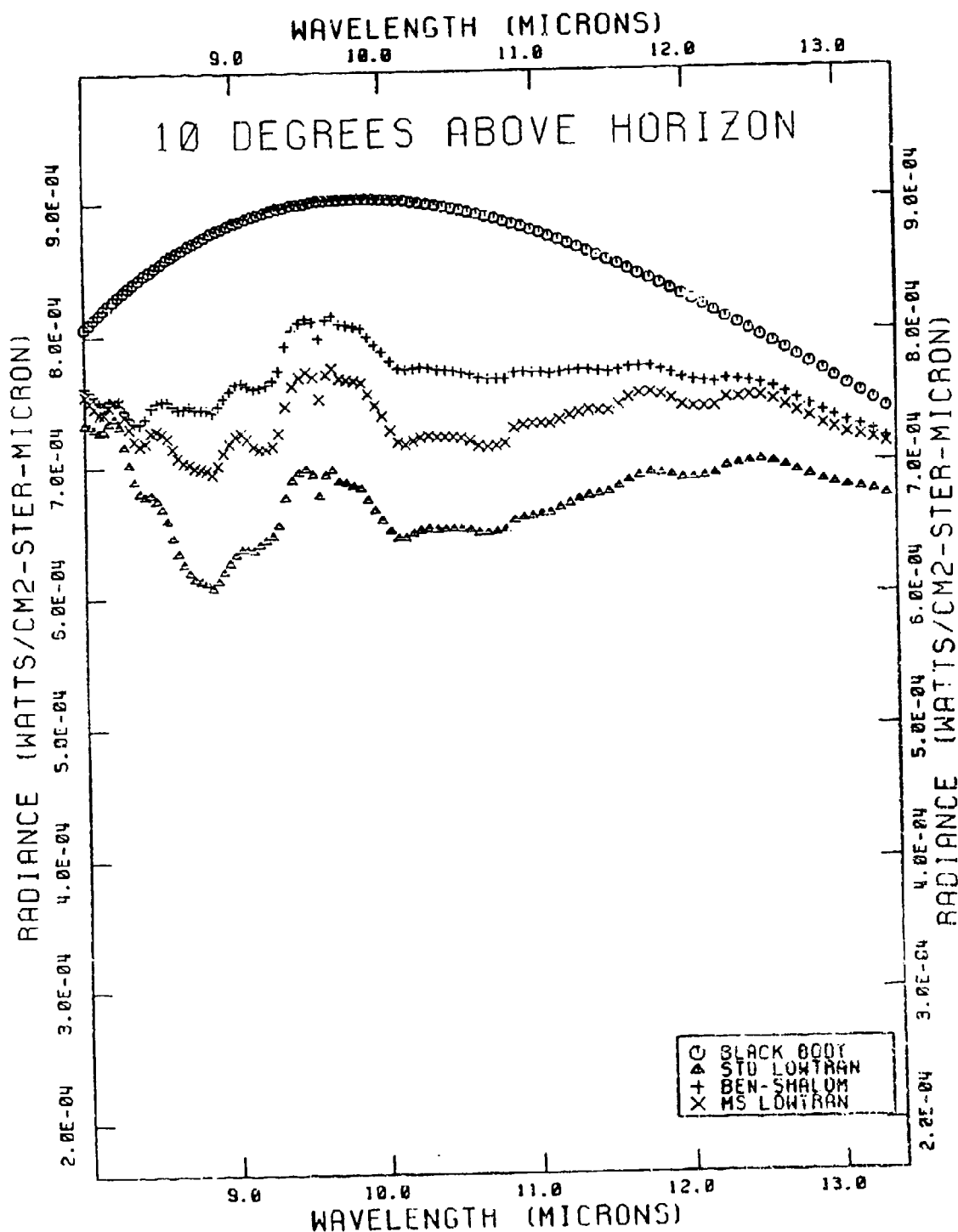


Figure 4-18. Downward thermal radiance comparison between 8 and 13.5 μm : Black body radiance of lowest atmospheric layer, standard LOWTRAN (without multiple scattering), Ben-Shalom calculations, and new LOWTRAN (with multiple scattering). Viewing path is from the surface to space with a zenith angle of 80° (10° above horizon).

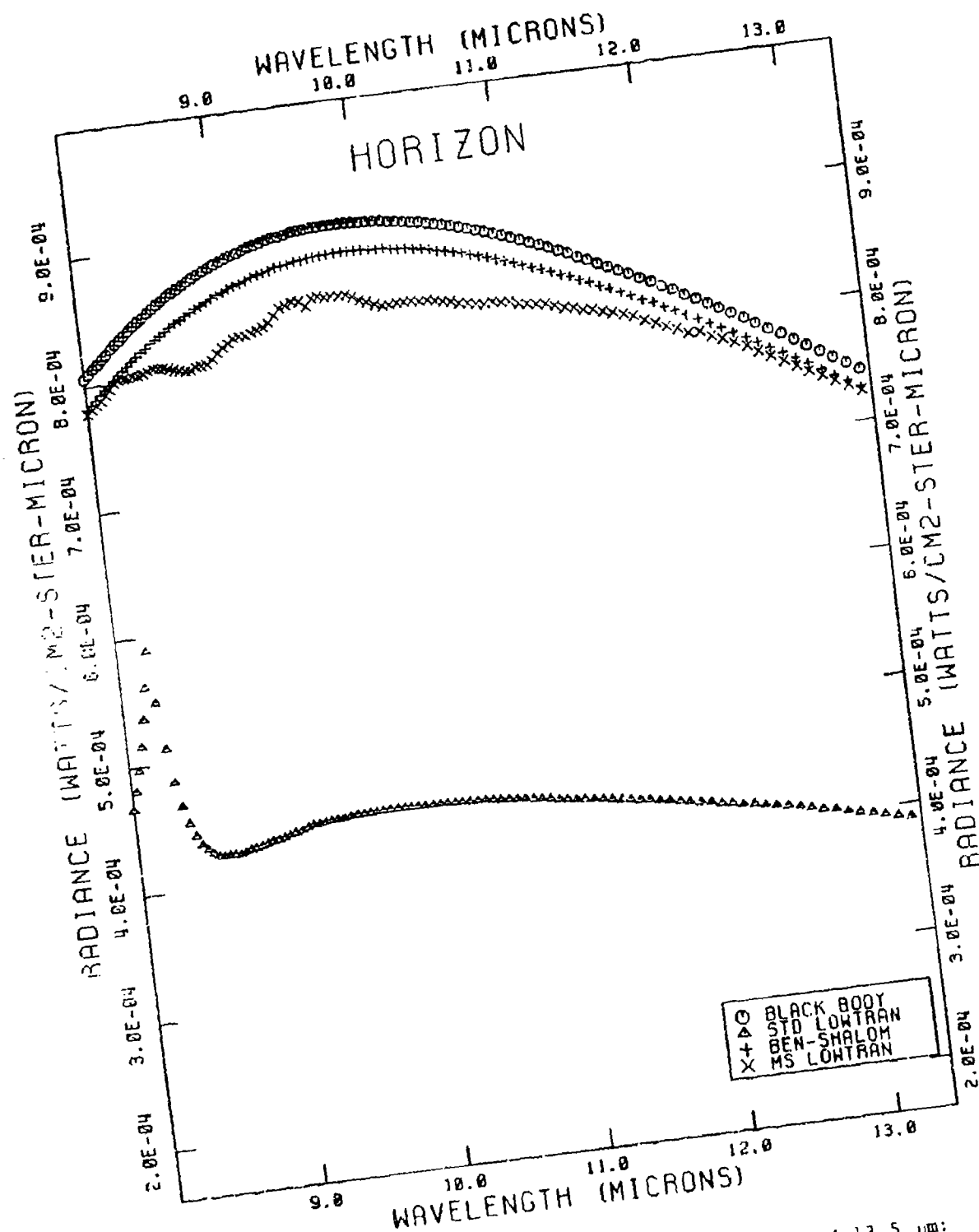


Figure 4-19. Downward thermal radiance comparison between 8 and 13.5 μ m: Black body radiance of lowest atmospheric layer, standard LOWTRAN (without multiple scattering), Ben-Shalom calculations, and new LOWTRAN (with multiple scattering). Viewing path is from the surface to the horizon.

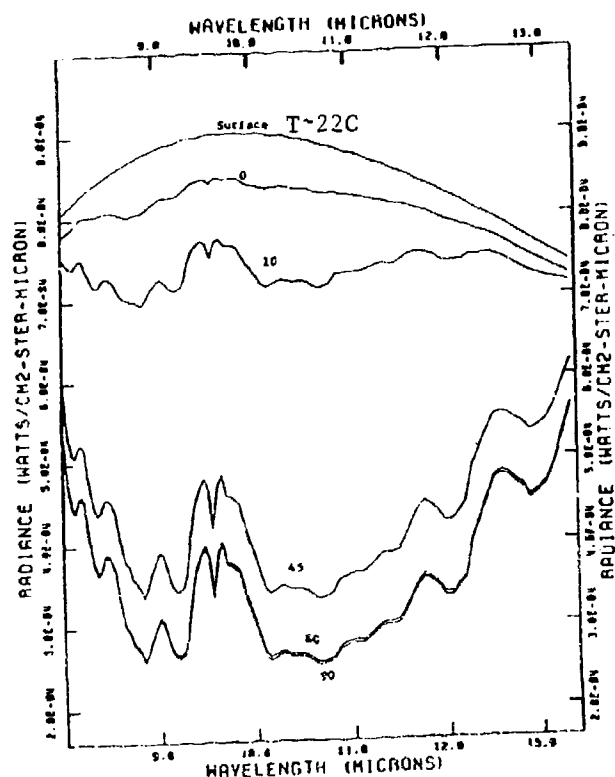


Figure 4-20a.

Downward thermal radiance results from LOWTRAN with multiple scattering (8.0 to 13.5 μm). Viewing path elevation angle varies between 0 to 90°. Also included is the black body radiance of the lowest atmospheric layer ($\sim 22^\circ\text{C}$).

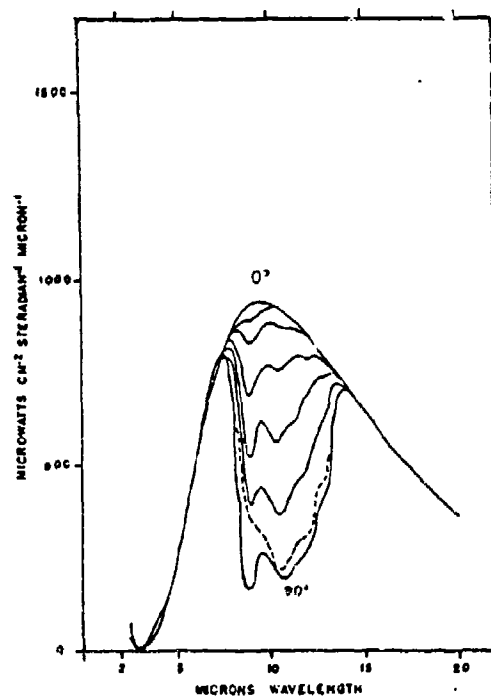


Figure 4-20b.

Downward radiance measurements for various viewing angles under atmospheric conditions qualitatively similar to those of Figure 4.20a (from Bell et al., 1960).

5. SUMMARY AND CONCLUSIONS

5.1 Summary

The goal of this research has been to provide a suitable parameterization of multiple scattering for implementation within the LOWTRAN and FASCODE atmospheric transmittance/radiance models developed at AFGL. Due to the comprehensive spectral domains treated by these models it was desired to develop a uniform approach applicable to spectral regions from the ultraviolet to the millimeter wave. Furthermore for consistency, analogous approaches were desired for implementation in LOWTRAN and FASCODE. The specific nature of the chosen approach was also constrained by the requirements of desired accuracy and computational efficiency of these models and additionally by their inherent code structure. Code structure requirements were particularly limiting with respect to the FASCODE model.

After reviewing the relevant radiative transfer literature two potential candidate multiple scattering parameterizations were selected for testing. These were a stream approximation and a successive order of scattering approach. Extensive intercomparison tests were conducted to compare the accuracy and efficiency of these candidate approaches to exact numerical treatments in the solar, thermal, and microwave/millimeter wave scattering regimes. Based on the results of these intercomparisons it was decided that the stream approximation would provide the required degree of accuracy and the least computational level of effort.

Two additional considerations were factors in formulating appropriate approaches to introduce multiple scattering into the LOWTRAN and FASCODE models. First, in the case of LOWTRAN it was necessary to provide an interface between the molecular absorber band model treatment and the multiple scattering parameterization. To accomplish this task the k-distribution method was introduced. The k-distribution method effectively decouples the multiple scattering from the LOWTRAN treatment of a gray gas absorption so that the spectral integration can be done properly.

Secondly, although multiple scattering approaches generally begin with a knowledge of the monochromatic optical properties of the entire path of interest, both LOWTRAN and FASCODE perform transmittance and radiance calculations on a layer-by-layer basis. Thus, in these models, the properties of the

overall path are not known until the end of the calculation. To further complicate matters, the spectral resolution of each FASCODE layer is determined by the appropriate pressure dependent average line width. Thus, for a given desired spectral domain, the resolution of each FASCODE layer increases with decreasing pressure and monochromatic optical data on the entire desired scattering path is never available. These characteristics of the FASCODE code structure led to the adoption of a layer adding approach in order to accommodate both the stream approximation and the layer-by-layer nature of the calculation.

Path dependent radiances at 900 cm^{-1} were calculated using the FASCODE implementation of the multiple scattering parameterization (FASCODEMS), the original FASCODE, and the discrete ordinate method. Comparison of these results indicates that the multiple scattering version of FASCODE provides more accurate radiance distribution in the presence of aerosol scattering. Our parametric studies indicate that accuracies of 15 to 20 percent should be expected. However, this increase in accuracy incurs an additional cost in code execution time. In our timing test, CPU execution times for a multiple scattering run in a three-hundred wave number region ($800\text{--}1100\text{ cm}^{-1}$), took about 3-1/2 times longer than a standard FASCODE run. Most of this additional time was due to the required spectral merging of stored quantities rather than calculations of the stream approximation. Additionally, multiple scattering runs of FASCODE require three times the temporary storage of regular FASCODE runs. The program size is increased by about 15 percent.

To insure consistency, LOWTRAN and FASCODE multiple scattering results were also compared. A much closer agreement is found between AER LOWTRAN and FASCODE (both use multiple scattering) than those between LOWTRAN6 (uses single scattering) and FASCODE.

5.2 Recommendations

This report has described recommendations and implementations of an approach to provide the LOWTRAN and FASCODE models with a unified treatment of multiple scattering consistent with described levels of accuracy and their respective code structures. Introduction of this capability has a number of implications which require additional consideration. These form the basis of our recommendations.

For FASCODE, the question of solar multiple scattering remains an open issue. Certainly, the line parameter compilation provides the capability to exercise FASCODE well below 2500 cm^{-1} where solar effects can influence path radiance. We did not introduce solar scattering into FASCODE since the necessary solar irradiance and single scattering routines from LOWTRAN are not yet a part of FASCODE2. If solar multiple scattering is desired in FASCODE, these routines and the capability to calculate the direct solar contribution and the scattering phase function (i.e., the solar path transmission) should be added to FASCODE, then a suitable coupling to the stream approximation/flux adding code segments could be implemented.

Likewise, although this report has illustrated the applicability of the scattering parameterization to the microwave and millimeterwave region for scattering by precipitation, the FASCODE model does not provide the necessary optical properties for such calculations. Attenuation (i.e., extinction) coefficients for rain are available in FASCODE; however, information on single scattering albedo (or alternatively, the scattering coefficients) and asymmetry factor are not. It would seem a simple matter to provide this data. A simple parameterization of these values in the domain between 19.35 and 231 GHz ($0.65 - 7.7\text{ cm}^{-1}$) is available in the interim (Isaacs et al., 1985).

With regard to LOWTRAN, we recommend that the k-values should be part of the laboratory experiments, i.e., they be provided directly from fitting the laboratory measurements of transmission values. The present setup of LOWTRAN can easily accommodate the updated k-values of different gases. The scaling approximation to treat inhomogeneous atmospheric effects needs to also be revised, perhaps utilizing the correlated-k techniques published by Wang and Ryan (1983).

Finally, it is worth noting that although the choice of the stream approximation for multiple scattering for implementation within the LOWTRAN and FASCODE models was not an arbitrary one, other approaches are possible. One criteria which the user may wish to consider is the trade-off between accuracy and computational level of effort. As implemented, the multiple scattering enhancements described here will provide emergent radiances with percent errors generally in the range of 10 to 30 percent for solar scattering and less than 10 percent for thermal scattering. Internal radiances, i.e., those evaluated for paths within the atmosphere, will be somewhat less accurate. These accuracies should be adequate for many simulation requirements. For users requiring higher accuracies, the code changes to LOWTRAN and FASCODE to accommodate multiple scattering have made it possible for experienced users of these models to access the necessary optical properties profiles for input to numerical multiple scattering algorithms. This can be accomplished by further modifying the LOWTRAN and FASCODE models to produce output files of the profiles of optical thickness, single scattering albedo, asymmetry factor, and/or angular scattering function which are used in the set up of the current stream approximation calculation.

Other possible options which may interest knowledgeable users include output of emergent fluxes or flux profiles (made possible by the inclusion of the two stream/adding step done in the stream approximation) and substituting other multiple scattering approximations (such as higher order stream approximations) within the code to obtain more accuracy. One application which we have not explored is the applicability of the implemented code changes to evaluation of multiply scattered visible and infrared radiances by clouds. A variety of exciting avenues are opened with the inclusion of the multiple scattering capability within LOWTRAN and FASCODE.

6. ACKNOWLEDGEMENTS

The authors thank F. Kneizys, S. A. Clough, E. Shettle, L. Abreu, J. Chetwynd, and G. Anderson of AFGL for their help and encouragement during the tenure of this work.

7. REFERENCES

- Arking, A. and K. Grossman (1972) The influence of line shape and band structure on temperatures in planetary atmospheres. J. Atmos. Sci., 29, 937.
- Bakan, S., P. Koepke and H. Quenzel (1978) Radiation calculations in absorption bands: Comparison of exponential series and path length distribution method. Beit. Physics der. Atmos., 51, 28-30.
- Bell, E., L. Eisner, J. Young, and R. Oetjen (1960) Spectral radiance of sky and terrain at wavelengths between 1 and 20 microns. II. Sky measurements. J. Opt. Soc. Am., 50, 1313-1320.
- Bellman, R. E., R. E. Kalaba and G. M. Wing (1960) J. Math. Phys., 1, 280.
- Ben-Shalom, A., B. Barzilia, D. Cabib, A. D. Devir, S. G. Lipson and U. P. Oppenheim (1980) Applied Optics, 19, 6, 838.
- Bergstrom, R. W., B. L. Babson, and T. P. Ackerman (1981) Calculation of multiply-scattered radiation in clean atmospheres. Atmos. Env., 15, 10/11, 1821-1826.
- Bergstrom, R. W., Jr. and R. Viskanta (1972) School of Mech. Eng., Purdue Univ., W. Lafayette, IN.
- Burke, H. K. and N. D. Sze (1977) A comparison of variational and discrete ordinate methods of solving radiative transfer problems. J. Quant. Spectrosc. Radiat. Trans., 12, 783-793.
- Carlstedt, J. L., T. W. Mullikan (1966) Chandrasekhar's X and Y functions. Astroph. J. Suppl., 12, 113, 449.
- Chandrasekhar, S. (1960) Radiative Transfer. Dover Publications.
- Clough, S. A., F. X. Kneizys, E. P. Shettle, and G. P. Anderson (1986) Atmospheric radiance and transmittance: FASCOD2. Proceedings, Sixth Conference on Atmospheric Radiation, 13-16 May 1986, Williamsburg, VA, pp. 141-144.
- Collins, D. G. and M. B. Wells (1965) Rep. RRA-174, Radiation Research Assoc., Inc., Fort Worth, TX.
- Coulson, K. L., J. V. Dave and Z. Sekera (1960) Tables related to radiation emerging from a planetary atmosphere with Rayleigh scattering. University of California Press.
- Cuzzi, J. N., T. P. Ackerman, L. C. Helmle (1982) The delta-four-stream approximation for radiative flux transfer. J. Atmos. Sci., 39, 917-925.
- Dave, J. V. (1970) Intensity and polarization of radiation emerging from a plane parallel atmosphere containing monodispersed aerosols. Appl. Opt., 9, 2673-2684.

- Dave, J. V. (1972) Development of programs for computing characteristics of ultraviolet radiation. Programs I - IV. Final Report, Contract No. NAS5-21680, NASA Goddard Space Flight Center, Greenbelt, MD 20771.
- Dave, J. V. (1981) Transfer of visible radiation in the atmosphere. Atmos. Env., 15, 10/11, 1805-1820.
- Dave, J. V. and J. Canosa (1974) J. Atmos. Sci., 31, 1089-1101.
- Deirmendjian, D. (1969) Electromagnetic Scattering on Spherical Polydispersions. American Elsevier Publ.
- Elterman, L. (1970) Vertical Attenuation Model with Eight Surface Meteorological Ranges 2 to 13 Kilometers. Report No. AFCRL-70-0200, March 1970, Air Force Cambridge Research Laboratories.
- Goody, R. M. (1964) Atmospheric Radiation: Theoretical Basis. Clarendon Press, 436 pp.
- Guthrie, R. (1986) Preliminary results from a 2-D model with coupled chemistry, radiation, temperature, and dynamics. Paper presented at the NASA Upper Atmosphere Theory and Data Analysis Program, Seattle, Washington, June 23-27, 1986.
- Hansen, J. E. (1969a) Astrophys. J., 155, 565-573.
- Hansen, J. E. (1969b) J. Atmos. Sci., 36, 478-487.
- Hansen, J. E. and L. D. Travis (1974) Light scattering in planetary atmospheres. Space Sci. Rev., 16, 527-610.
- Hansen, J. E., A. A. Lacis, P. Lee, and W.-C. Wang (1980) Climatic effects of atmospheric aerosol. Aerosols: Anthropogenic and natural sources and transport. Ann. N.Y. Acad. Sci., 338, 575-587.
- Hansen, J., A. Lacis, D. Rind, G. Russell, P. Stone, I. Fung, R. Ruedy and J. Lerner (1984) Climate sensitivity: Analysis of feedback mechanisms. Geophys. Mono., 29, Maurice Ewing, 5, Hansen and Takahashi (Eds.)
- Heney, L. G. and Greenstein, J. L. (1941) Diffuse radiation in the galaxy. Ap. J., 93, 70-83.
- Hering, W. S. (1981) An operational technique for estimating visible spectrum contrast transmittance. University of California at San Diego, Scripps Institution of Oceanography, Visibility Laboratory, SIO Ref. 82-1, AFGL-TR-81-0198. ADA 111823
- Herman, B. M. and S. R. Browning (1965) J. Atmos. Sci., 22, 559-566.
- Hovenier, J. W. (1971) Multiple scattering of polarized light in planetary atmospheres. Astr. Astrophys., 13, 7-29.
- Irvine, W. M. (1965) Astrophys. J., 142, 1563.

- Irvine, W. M. (1968) Multiple scattering by large particles: II. Optically thick layers. J. Astrophys., 152, 823-834.
- Isaacs, R. G. (1981) Role of radiative transfer theory in visibility modeling: Efficient approximate techniques. Atmos. Env., 15, 10/11, 1827-1834.
- Isaacs, R. G., G. Deblonde, R. D. Worsham, and M. Livshite (1985) Millimeter-wave Moisture Sounder Feasibility Study: The Effect of Cloud and Precipitation on Moisture Retrievals. AFGL TR-85-0040. ADA 162 231
- Isaacs, R. G. and H. Özkaynak (1980) Uncertainties associated with the implementation of radiative transfer theory within visibility models. Second Joint Conference on Applications of Air Pollution Meteorology, New Orleans, LA, 24-27 March, 362-369. American Meteorological Society, Boston, MA.
- Kaufman, Y. J. (1979) Effect of the earth's atmosphere on the contrast for Zenith observation. J. Geophys. Res., 84, 3165.
- Kaufman, Y. J. (1982) Solution of the equation of transfer for remote sensing over nonuniform surface reflectivity. J. Geophys. Res., 87, C6, 4137-4147.
- Kneizys, F. X., E. P. Shettle, W. O. Gallery, J. H. Chetwynd, Jr., L. W. Abreu, J. E. A. Selby, R. W. Fenn and R. A. McClatchey (1983) Atmospheric transmittance/radiance: Computer code LOWTRAN6. AFGL-TR-83-0287. ADA137786. Air Force Geophysics Laboratory, Hanscom AFB, MA 01731.
- Lacis, A. A., and J. E. Hansen (1974) A parameterization for the absorption of solar radiation in the earth's atmosphere. J. Atmos. Sci., 31, 118-133.
- Lacis, A. A., W. C. Wang and J. E. Hansen (1979) Correlated K-distribution method for radiative transfer in climate models: Application to effect of cirrus cloud on climate. NASA Publ. 2076, E. R. Kreins, Ed., 416pp.
- Lenoble, J. (1977) Standard procedures to compute atmospheric radiative transfer in a scattering atmosphere. IAMAP, Boulder, CO.
- Liou, K. N. (1973) A numerical experiment on Chandrasekhar's discrete-ordinate method for radiative transfer: Applications to cloudy and hazy atmospheres. J. Atmos. Sci., 30, 1303-1326.
- Liou, K. N. (1974) Analytic two-stream and four-stream solutions for radiative transfer. J. Atmos. Sci., 31, 1473-1475.
- Liou, K. N. (1980) An Introduction to Atmospheric Radiation. Academic Press, NY, 392 pp.
- Meador, W. E. and W. R. Weaver (1980) Two-stream approximations to radiative transfer in planetary atmospheres: A unified description of existing methods and a new improvement. J. Atmos. Sci., 37, 630-643.
- Nagel, M. R., H. Quenzel, W. Kweta and R. Wendling (1978) Daylight Illumination Color Contract Tables. Academic Press.

- Piotrowski, S. (1956) Asymptotic case of the diffusion of light through an optically thick scattering layer. Acta Astron., 6, 61-73.
- Plass, G. N. and G. W. Kattawar (1968) Appl. Opt., 7, 1129-1135.
- Rasool, S. I., and S. H. Schneider (1971) Atmospheric carbon dioxide and aerosols: Effects of large increase on global climate. Science, 173, 138-141.
- Ridgway, W. L., R. A. Moose and A. C. Cogley (1982) Single and multiple scattered solar radiation. AFGL-TR-82-0299. ADA 126 323
- Rosenwald, R. D., H. Hill, and J. Logan (1984) Radiative transfer: Gaussian quadrature formulas for integrals with the weight functions $\text{EXP}(-|x-t|)$ and $E_n(|x-t|)$. J. Quant. Spectrosc. Radiat. Transfer, 31, 3, 221-236.
- Sagan, C., and J. B. Pollack (1967) Anisotropic non-conservative scattering and the clouds of Venus. J. Geophys. Res., 72, 469-477.
- Savage, R. (1978) Radiative properties of hydrometeors at microwave frequencies. J. Appl. Meteorol., 17, 904-911.
- Schuster, A. (1905) Radiation through a foggy atmosphere. Ap. J., 21, 1-22.
- Schwarzschild, K. (1906) On the equilibrium of the Sun's atmosphere. Nachr. Gesell. Wiss. Gottingen, Math.-Phys. Kl., 195, 41-53.
- Shettle, E. P. and J. G. Kuriyan (1975) Atmospheric radiative transfer theory (visible and UV). CIAP Monograph 1-DOT-TST-75-51.
- Stephens, G. (1984) The parameterization of radiation for numerical weather prediction and climate models. Mon. Weather Rev., 112, 826-867.
- Stogryn, A. (1975) A note on brightness temperature at millimeter wavelengths. IEEE Trans. Geo. Sci. Electron., GE13, 81-84.
- Sze, N. D. (1976) Variational methods in radiative transfer problems. J. Quant. Spectrosc. Radiat. Trans., 16, 763-780.
- Sze, N. D., R. G. Isaacs, M. Ko, M. B. McElroy (1981) Atmospheric studies related to aerospace activities and remote sensing technology. NASA CR 3410, NASA Langley Research Center.
- van de Hulst, H. C. (1948) Ap. J., 107, 235.
- van de Hulst, H. C. (1963) A New Look at Multiple Scattering. Science Report, NASA/GISS, NY, 81 pp.
- van de Hulst, H. C. (1971) J. Quant. Spectrosc. Radiat. Trans., 11, 785-795.
- van de Hulst, H. C. and K. Grossman (1968) In The Atmosphere of Venus and Mars. J. C. Brandt and M. B. McElroy (Eds.), Gordon and Breach, NY, pp. 35-55.
- Wang, W.-C. and G. A. Domoto (1974) The radiative effects of aerosols in the Earth's atmosphere. J. Appl. Meteorol., 13, 521-534.

- Wang, W. C. and P. B. Ryan (1983) Overlapping effect of atmospheric H₂O, CO₂ and O₃ on the CO₂ radiative effect. Tellus, 35B, 81-91.
- Waters, J. W. (1976) Absorption and emission by atmospheric gases. Methods of Experimental Physics, 12, B, Academic Press, 142-176.
- Wiscombe, W. J. (1976) On initialization error, and flux conservation in the doubling method. J. Quant. Spectros. Radiat. Transfer, 16, 637.
- Wiscombe, W. J. (1977) The delta-Eddington approximation for a vertically inhomogeneous atmosphere. NCAR TN-121+STR.
- Wiscombe, W. J. and J. W. Evans (1977) Exponential-sum fitting of radiative transmission functions. J. Comput. Phys., 24, 416-444.
- Wiscombe, W. J. and G. W. Grams (1976) the backscattered fraction in two-stream approximations. J. Atmos. Sci., 33, 2440-2451.
- Yamamoto, G., M. Tanaka, and S. Asano (1970) Radiative transfer in water clouds in the infrared region. J. Atmos. Sci., 27, 282-292.
- Yamamoto, G., M. Tanaka, and S. Asano (1971) Radiative heat transfer in water clouds in the infrared radiative. J. Quant. Spectrosc. Radiat. Transfer, 11, 697-708.

APPENDIX A

REVIEW AND TRADE-OFF ANALYSIS OF MULTIPLE SCATTERING PARAMETERIZATIONS

A.1 Review of Multiple Scattering Parameterizations

Radiative transfer theory provides the mathematical description of the interaction between both external (e.g., incident solar) and internal (e.g., emitted thermal) sources of electromagnetic radiation and the optically active atmospheric constituents of gases and particulates (e.g., aerosols, clouds, and precipitation). The solution to the radiative transfer equation for a scattering atmosphere (Chandrasekhar, 1960; Goody, 1964; Liou, 1980) generally requires a numerical solution. An extensive variety of exact numerical methods have been developed to solve these equations over the years, and excellent review are available (Hansen and Travis, 1974; Shettle and Kuriyan, 1975; Lenoble, 1977). This section will focus on approximate multiple scattering methods which can be used as parameterizations applicable to both LOWTRAN and FASCODE models.

A.1.1 Solar Radiation

For practical purposes it is useful to categorize the extensive hierarchy of available computational procedures based on both the relative accuracy of the results required and the expenditure of computational resources incurred. A subjective evaluation according to these criteria results in four classes of method based on resultant accuracy characterized as either exact or approximate and computational methodologies denoted as either numerical or analytical. Exact methods are defined as those which agree among themselves to some acceptable degree of accuracy when applied to a variety of diverse problems. All other methods are approximate. The most recent intercomparison of exact methods suggests that about 1% accuracy in radiance can be expected (Lenoble, 1977). A variety of exact, numerical methods are listed in Table A-1 along with representative literature citations. The essential difference between numerical and analytical approaches is that the latter generally require less computer time. Analytical approaches are those which are generally implementable using simple algebraic relations supported by a priori specifiable parameters, i.e., there are no recurrent or iterative calculations and no convergence criteria. Exact analytical methods are available only for

Table A-1

Exact Numerical Multiple Scattering Computation Techniques

Name	Representative References
Successive Orders of Scattering*	van de Hulst (1948) Irvine (1955) Nagel et al. (1978)
Gauss-Seidel	Herman and Browning (1965) Dave (1972)
Doubling and Adding	van de Hulst (1963, 1971) Hansen (1969a,h)
Monte Carlo*	Collins and Wells (1965) Plass and Kattawar (1968)
Discrete Ordinates	Chandrasekhar (1960) Liou (1973)
Spherical Harmonics*	Bergstrom and Viskanta (1972) Dave and Canosa (1974)
Invariant Imbedding	Bellman, Kalaba, and Wing (1960)
Variational-iterative [†]	Sze (1976) Burke and Sze (1977)

*Represented in IAMAP Radiation Commission intercomparison, Lenoble, 1977)

[†]Isotropic scattering only

a few cases which are, unfortunately, not immediately applicable to general terrestrial radiance simulation situations. These cases include, for the most part, approaches based on Chandrasekhar's H functions for semi-infinite atmospheres ($\tau = \infty$) and X and Y functions for finite atmospheres (Chandrasekhar, 1960). For the former set of problems, for example, solutions are available for isotropic, Rayleigh and various anisotropic phase functions. For finite atmospheres, solutions are available only for isotropic (Carlstedt and Mullikan, 1966) and Rayleigh scattering (Coulson et al., 1960). These exact treatments, often obtainable in the form of lookup tables, are useful as checks for the accuracy of both exact numerical methods and proposed approximate methods when applied to degenerate cases (such as isotropic scattering).

Approximate methods include those based on evaluating the first few tractable terms or orders of more extensive exact numerical treatments and those formulated specifically as approximations. In the former class of approximate methods, the philosophy is to accept the known risk of increased error for a specific application in order to benefit from reduced computer run time. Examples include terminating successive order of scattering approaches after a few scatterings (see Nagel et al., 1978), reducing the number of Legendre polynomials carried in the expansion of an angular scattering function, and limiting the number of quadrature angles in the discrete ordinate method. The method is approximate since the user knows a priori that the full available power of the exact numerical method at hand is not being exercised. For the simplest cases, these approaches often result in analytical solutions which may themselves be useful such as single and double scattering solutions (Deirmendjian, 1969; Hovenier, 1971), the two- and four-stream approximations based on the discrete ordinate method (Liou, 1973, 1974), and the two-step function approach based on general variational methods (Sze, 1976; Burke and Sze, 1977).

Multiple scattering methods formulated as intrinsically approximate have a common heritage in the estimation of radiation fluxes within larger numerical models (see Stephens, 1984). This applies both to the use of similarity relations to reduce anisotropic problems to isotropic equivalents (van de Hulst and Grossman, 1968) and various so-called two-stream approximations (Meader and Weaver, 1980). Notably, it is only recently that various investigators have sought approaches to treat the approximation of

multiply scattered radiances by augmenting a single scattering solution with an estimate of the multiply scattered radiance field based on a suitable flux parameterization. Included among these are: (a) the "diffuse field" approximation described by Bergstrom et al. (1981) for use in visibility impact models, (b) a path radiance approximation based on the delta-Eddington approach by Hering (1981) which was implemented within an operational visible contrast transmittance model, and (c) Kaufman's (1979) radiance approximation for applications to remote sensing. Kaufman has primarily applied his approximate scheme as a device to evaluate multiply scattered contributions to upward radiance within the context of multidimensional remote sensing (cf. Kaufman, 1982). Analogous solutions for downward radiance were derived by Isaacs (1981) for application to visibility model related radiance evaluation.

This overview of computational methods applicable to the simulation of radiances due to the multiple scattering of solar radiation suggests that a suitable parameterization may be found among one of the approximate approaches described above. In order to quantify this assessment, radiance comparisons were made between representative methods from each of the categories described above for a set of model atmospheres with aerosol content varying from ultra-clear to hazy conditions. Table A-2 summarizes the scattering treatments selected in this comparison. The Gauss-Seidel multiple scattering (MS) approach was selected to provide exact numerical radiance results for reference purposes (Dave and Gazdag, 1970). The algorithm used (Dave, 1972) evaluates fluxes and radiances for atmospheres with arbitrary vertical distribution of anisotropic aerosol extinction overlying a Lambert reflecting surface. When applied to pure molecular scattering cases, radiance results from the code reproduce the exact analytical tabulations of Coulson et al. (1960) based on Chandrasekhar's X and Y functions for Rayleigh scattering to high accuracy.

Three parameterization approaches were investigated. These include: (a) single scattering (SS), (b) a stream approximation (SA), and (c) successive orders of scattering (SOS). The SOS method (which is presently solved numerically) was formulated to treat the single scattered radiance exactly and to approximate higher order scattering by an isotropic angular scattering function. These approaches are summarized in Table A-3. Results of the test case comparisons are discussed in Section A.2.

Table A-2

Methods Selected for Intercomparison

Accuracy	Computational Effort	
	Numerical	Analytical
Exact	Gauss-Seidel [MS] (Dave and Gazdag, 1970; Dave, 1972)	X,Y functions* (Chandrasekhar, 1960; Coulson et al., 1960)
Approximate	Successive Order of Scattering [SOS]	Single Scattering [SS] Stream Approximation [SA] (Kaufman, 1979)

*Rayleigh scattering only

Table A-3

Summary of Source Function, J , and Radiance, R , Evaluation Approaches for Three Candidate Approximation
 (θ = temperature, T = transmittance, τ = optical depth)

	Single Scattering (SS)	Stream Approximation (SA)	Successive Scatterings (SOS)
Source Function, J	$J_0 = \frac{\omega}{4} r e^{-\tau/\mu_0} P(\Omega, -\Omega_0)$	$J^\pm = J_0 + \frac{\omega}{\pi} [r^\pm (1-\beta)]$	$J^n = J_0 + \frac{\omega}{2} \int_0^{\tau^*} K(t, \tau) J^{n-1} dt$
	$+ (1-\omega_0) B(\theta)$	$+ \beta F^\pm$	$K(t, \tau) = E_1(t-\tau) + 2\tau E_2(\tau^*-t)$ $+ E_2(\tau^*-\tau)$
Radiance, R	$R = J_B T_b + \int_{T_b}^1 J(\tau) d\tau$	same	same
Boundary Term J_B	$J_B = r \mu_0 F e^{-\tau/\mu_0}$ $+ (1-r) B(\theta_b)$	$J_B = r [\mu_0 F e^{-\tau/\mu_0} + \frac{F(T_b)}{\pi}]$ $+ (1-r) B(\theta_b)$	$J_B = r [\mu_0 F e^{-\tau/\mu_0}$ $+ 2 \int_0^{\tau^*} E_2(\tau^*-t) J(t) dt]$ $+ (1-r) B(\theta_b)$

A.1.2 Thermal Radiation

The detailed numerical schemes described in the previous section can be used to perform thermal radiation calculations by including the thermal emission term. For example, the doubling method has been extended by Wiscombe to include an inhomogeneous internal source (see Wiscombe, 1976 and the cited references for other detailed methods). Although these methods are useful for reference calculations, from practical considerations, the study of particle multiple scattering on atmospheric transmittance has to rely heavily on parameterizations. This is especially true for the LOWTRAN/FASCODE models.

Studies of the effects of aerosol multiple scattering on atmospheric infrared transmittance have emphasized the calculation of fluxes rather than radiances. The two-stream approach has been the commonly-used parameterization. In general, the two-stream approximation is a method of representing the radiation field in two streams in one-dimensional radiation transfer problems. The approximation, proposed by Schuster (1905) and Schwarzschild (1906), is to assume that the intensity in the positive direction is isotropic and that in the negative direction has a different value but is also isotropic. Chandrasekhar (1960) has used the Gaussian quadrature to approximate the integral over angle, terming this the "discrete ordinate" method. The first approximation of the discrete ordinate method results in the same form as the Schuster-Schwarzschild approximation except for different constant coefficients due to Gaussian division.

Sagan and Pollack (1967) and Piotrowski (1956) compared the approximation with the exact solutions for the cases of conservative and non-conservative isotropic scattering. The results show 5-10% accuracy in absolute values. A survey paper by Irvine (1968) has investigated several approximation methods, including two-stream, Eddington and modified two-stream approximation. Uses of two-stream approximation for treating multiple scattering in thermal radiation are numerous (e.g., Rasool and Schneider, 1971; Wang and Domoto, 1974; Hansen et al., 1984). This parameterization has been used for climate application such as investigation of climatic effect due to aerosols (Hansen et al., 1980).

A.2 Trade-off Analysis of Exact and Approximate Treatments

A series of computer codes was written to support an intercomparison of angle dependent radiances from single scattering (SS), stream approximation

(SA), and successive orders of scattering (SOS) parameterizations with those evaluated using accurate numerical multiple scattering treatments. For the stream approximation, two independent flux treatments were employed, one for solar radiation and one for thermal radiation. The intercomparison calculations were performed by parametrically varying the relevant optical properties of optical depth, single scattering albedo, and asymmetry factor. Thus, they were offline from either the LOWTRAN or FASCODE models.

Furthermore, these calculations assumed single homogeneous scattering layers.

Assessment criteria include accuracy defined in terms of computer execution times for a set of test cases and accuracy measured by intercomparison with numerical results.

A.2.1 Solar Scattering

For solar scattering, six model atmospheres were used in a comparison test consisting of one Rayleigh scattering case and five atmospheres including increasing amounts of aerosol. The vertical distribution of molecular density was that of the AFGL midlatitude summer model while that for the aerosol was Elterman's (1970) distribution. The turbidity weighting factor (defined as the ratio of total aerosol scattering optical depth to total scattering optical depth) varied from zero to near unity with corresponding surface visual ranges decreasing to about 1.2 km in haze. The optical properties of these model atmospheres are given in Table A-4. For each of the six test cases radiances were calculated using the SS, SOS, and SA methods at nine values of zenith angle, three values of azimuth angle, and two surface reflectances for both upward viewing from the surface and downward viewing from space (i.e., a total of 108 values). The solar zenith angle for all cases was 60°. Corresponding exact multiple scattering (MS) cases were evaluated using the Gauss-Seidel iterative method (Dave, 1972). The phase function used was based on the radiance values from the exact method, $R(\text{MS})$ and each approximate method [$R(A)$, $A=\text{SS, SOS, SA}$], percent errors were calculated for the corresponding i th viewing angle, surface reflectance pair according to:

$$PE_i(A) = \left[\frac{R(\text{MS}) - R(A)}{R(\text{MS})} \right] \times 100\% \quad (\text{A.1})$$

Table A-4

Optical Properties of Model Atmospheres used in Solar Scattering Comparison Tests ($\lambda = 0.55 \mu\text{m}$)

Model Atmosphere	Optical Thicknesses			Turbidity Factor	Single Scattering Albedo	Visual Range (km)
	Rayleigh	Aerosol Scattering	Aerosol Absorption			
Rayleigh	0.1	0.0	0.0	0.1	0.00	319.1*
Case 1	0.1	0.1220	0.0281	0.25	0.5494	34.9
Case 2	0.1	0.3252	0.0749	0.50	0.7648	14.0
Case 3	0.1	0.7317	0.1686	1.00	0.8798	6.4
Case 4	0.1	1.5446	0.3558	2.00	0.9392	3.1
Case 5	0.1	3.9836	0.91767	5.00	0.97551	1.2

*Assuming no earth curvature effects and a Rayleigh scattering coefficient (for dry air at STP) of 0.01226 km^{-1} (Goody, 1964, p. 414).

Additionally in order to provide a measure of overall accuracy for each case, root mean square errors, RMS, were evaluated for each approximate method, A, and surface reflectance, r, according to:

$$\text{RMS}(A,r) = \left(\sum_{i=1}^{54} \frac{1}{54} [\text{PE}_i(A)]^2 \right)^{1/2} \quad (\text{A.2})$$

A comparison of RMS error according to Equ. (A.2) is summarized in Table A-5. For each of the approximations (single scattering, stream approximation, successive orders of scattering), RMS errors are provided for the six model atmospheres and two selected values of surface reflectance ($r = 0.0, 0.4$). The magnitude of RMS errors reported in Table A-5 for single scattering approximate those which would be obtained using the LOWTRAN6 single scattering option (IEMSCT = 2) for a like sun/observer geometry. Examining Table A-5, it is notable that the increase of RMS error with optical thickness is considerably less for the stream approximation and successive scattering method than for the single scatter parameterization. This is not surprising since the latter does not treat the multiply scattered radiance contribution which becomes increasingly important at larger optical thicknesses. At a moderate optical thickness (say 1.0, corresponding to an approximate visual range of 6.4 km) and zero surface reflectance the SOS and SA approaches are better by factors of about 1.5 and 2.0, respectively.

In order to provide a measure of efficiency for each approximation, execution times were tabulated for calculation of scattered radiances for the ensemble of eighteen upward and downward zenith angles, three azimuth angles, and two values of surface reflectance. These results are presented in Table A-6. The codes to evaluate each approximation were run on AER's Harris H800 and while not optimized for speed were configured for consistency with the layered atmosphere code structure of the LOWTRAN/FASCODE models. The exact multiple scattering (MS) execution times were obtained from comparison runs made on the AFGL CYBER. To provide a basis for comparison, Harris equivalent execution times (the values in parentheses) were estimated for each case using a benchmark execution of the Dave code from each machine to obtain a conversion factor of about 2.1. It is important to note that these times apply to the evaluation of the radiances from prespecified profiles of optical parameters and do not include time spent calculating atmospheric transmission.

Table A-5

Comparison RMS Errors for Single Scattering (SS),
Stream Approximation (SA), and Successive
Orders of Scattering (SOS)

Optical Thickness/ Reflectivity		SS	SA	SOS
0.10 (Rayleigh)	/0.0	13.5	4.3	4.5
	/0.4	29.2	10.4	3.6
0.25 (Case 1)	/0.0	33.4	12.2	17.9
	/0.4	41.8	4.9	18.8
0.50 (Case 2)	/0.0	50.4	17.2	29.5
	/0.4	57.6	9.4	31.9
1.00 (Case 3)	/0.0	67.0	29.1	43.3
	/0.4	72.5	23.2	48.6
2.00 (Case 4)	/0.0	80.8	34.0	58.1
	/0.4	83.3	30.3	63.5
5.00 (Case 5)	/0.0	90.0	39.1	73.1
	/0.4	90.5	40.1	73.7

It is interesting to compare execution times relative to the corresponding single scattering values. The stream approximation takes about two times longer regardless of optical thickness. This is of interest since the successive scattering execution times increase with increasing optical thickness and are at best eight times larger, although this could probably be shortened by careful optimization. Except for the Rayleigh case (which could be solved exactly anyway), multiple scattering execution times are at least an order of magnitude larger and increase slightly with optical thickness.

A.2.2 Thermal Scattering

A set of model atmosphere test cases was employed to compare each multiple scattering parameterization for thermal scattering with an exact numerical treatment. Spectral regions of interest included the infrared where scattering by aerosol and cloud can be a factor in determining the radiance

Table A-6

Comparison Execution Times for Single Scattering (SS),
Stream Approximation of (SA), and Successive
Order of Scattering (SOS) Methods

Optical Thickness	Execution Time (sec)			
	SS ¹	SA ¹	SOS ¹	MS ^{2,3}
0.10 (Rayleigh)	3.4	7.8	27.4	2.45 (5.1)
0.25 (Case 1)	3.4	7.8	37.6	47.64 (100.1)
0.50 (Case 2)	3.4	7.8	47.6	48.79 (102.5)
1.00 (Case 3)	3.4	7.8	63.4	50.14 (105.3)
2.00 (Case 4)	3.4	7.8	90.6	51.98 (109.2)
5.00 (Case 5)	3.4	7.8	107.8	52.92 (111.13)

¹Harris H800 CPU time to evaluate radiances for eighteen upward and downward zenith angles, three azimuth angles and two values of surface reflectance, i.e., a total of 108 atmospheric paths.

²AFGL CYBER CPU execution time in seconds for multiple scattering (Dave, 1975) solution of same 108 atmospheric paths.

³Parentheses contain estimated Harris H800 execution times for comparison (the Rayleigh scattering case is actual) based on an H800/CYBER time factor of 2.1 obtained from a common benchmark run of the Dave code.

field and the microwave/millimeter wave where scattering is due largely to precipitation. Calculations were performed for similar sets of optical properties for the stream approximation (SA), successive orders of scattering (SOS), and an accurate numerical method for multiple scattering, the discrete ordinate method (DOM).

In order to maximize the effects of aerosol scattering in the infrared, a spectral region was selected (900 cm^{-1}) where gaseous absorption is relatively weak. This window region, influenced primarily by water vapor continuum absorption, is used for remote sensing purposes such as surface temperature retrieval. The test comparisons were done parametrically with optical thicknesses in the range from 0.05 to 1.00, single scattering albedos between 0.5 and 0.9, and asymmetry factors between 0.6 and 0.8. These ranges were chosen both to include values representative of the 10-12 μm window for typical haze conditions and to push the effect of scattering to unrealistically high values for testing purposes. The optical properties of the model atmospheres used in the thermal scattering comparison are summarized in Table A-7.

Table A-7
Optical Properties of Model Atmospheres
Used in Thermal Scattering Comparison

	Optical Thickness	Single Scattering Albedo	Asymmetry Factor
Infrared Region ($\nu = 900\text{ cm}^{-1}$)			
Case 1 a,b	0.05	0.50, 0.75, 0.90	0.6, 0.7, 0.8
Case 2 a,b	0.25	0.50, 0.75, 0.90	0.6, 0.7, 0.8
Case 3 a,b	0.50	0.50, 0.75, 0.90	0.6, 0.7, 0.8
Case 4 a,b	1.00	0.50, 0.75, 0.90	0.6, 0.7, 0.8
Microwave/millimeter wave ($f = 19.35, 37.00\text{ GHz}$)			
Case 5 a,b (19.35 GHz)	0.906	0.21 (M-P, Rain rate 15 mmhr^{-1})	Phase Function
Case 6 a,b (37.00 GHz)	3.20	0.39 (M-P, Rain rate 15 mmhr^{-1})	Phase Function
a: Isothermal	$T_s = 288\text{K}, T_a = 283\text{K}$		
b: Gradient	$T_s = 286\text{K}, \bar{T}_a = 283\text{K}$		

The surface temperature for all calculations was assumed to be 288 K. Two types of atmospheric temperature profile were investigated: an isothermal atmosphere with a temperature of 283 K and an atmosphere with a 10 K temperature gradient from top to bottom and a mean temperature of 283 K. These are called the isothermal and gradient atmospheres, respectively.

Microwave/millimeter wave calculations were done for cases with similar surface temperatures and temperature profiles. Two frequencies, 19.35 and 37.0 GHz (1.55 and 0.81 cm, respectively) corresponding to those used for satellite remote sensing were investigated. For these cases (see Table A-7), scattering was assumed due to a Marshall-Palmer distribution of rain with a rain rate of 15 mm/h. Precipitation scattering properties such as the extinction coefficient, single scattering albedo, and angular scattering function were evaluated from a parameterization of the Mie theory calculations of Savage (1978) developed for a millimeter wave simulation model (Isaacs et al., 1985).

The discrete ordinate method (DOM) (Liou, 1973) provided numerical solutions as a standard for comparison. A sixteen stream version of the DOM code was used. Radiance results were thus given at eight upward and eight downward zenith angles within the domains from 0 to 90 degrees (upward radiance) and 90 to 180 degrees (downward radiance). The endpoints of these ranges (i.e., 0, 90, and 180 degrees) are extrapolated from internal points and are thus not accurate values. To facilitate calculation of the required Legendre polynomial expansion of the angular scattering function, Henyey-Greenstein phase functions with the desired asymmetry factors were employed.

Results of the multiple scattering parameterization intercomparison were tabulated as radiances, percent errors as a function of zenith angle, and percent root mean squared (RMS) errors. The latter quantity was evaluated over all zenith angles used in the intercomparison. Sample results are shown in Figures A-1 to A-4. Figure A-1(a) and (b) illustrate the comparison between upward and downward emergent radiances, respectively, for the SA and SOS parameterizations and the exact DOM solution. This particular calculation is for an optical depth of 0.25, single scattering albedo of 0.9, and an asymmetry factor of 0.8. The SOS approach underestimates upward radiance and overestimates downward radiance compared to the DOM due to the assumption of isotropic scattering. The SA, however, reasonably reproduces the multiply scattered radiance field, except near the horizon (zenith angles approaching 90°).

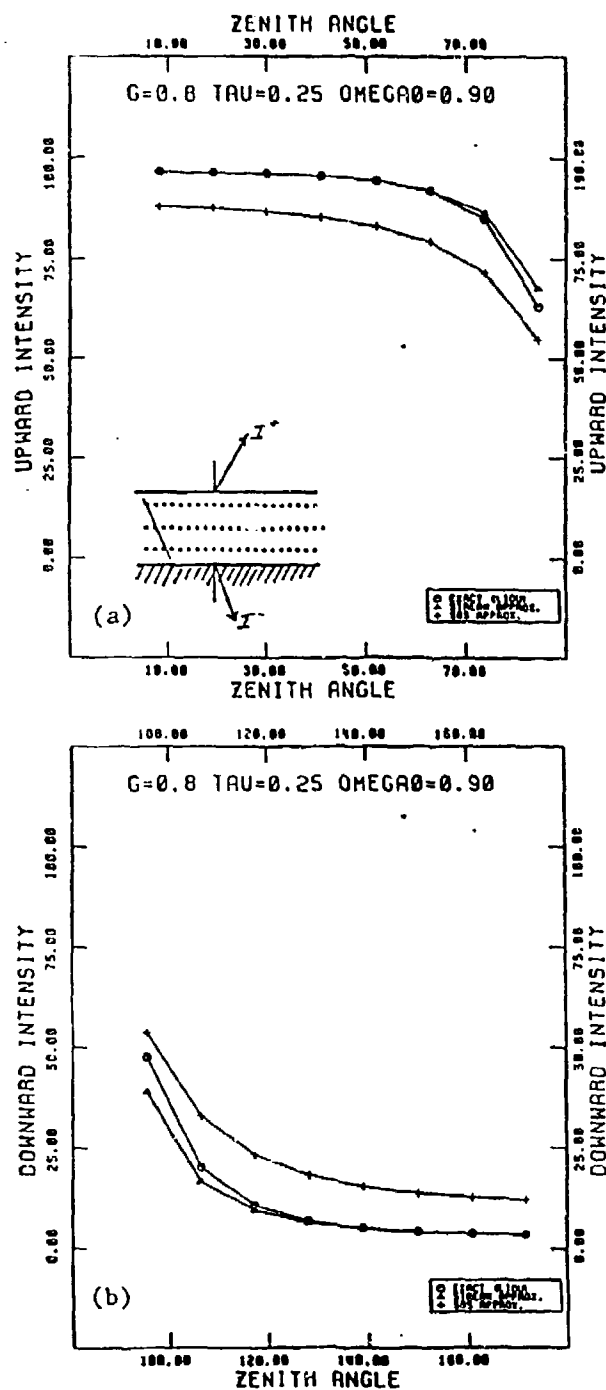


Figure A-1. Comparison of emergent radiances from DOM, SA, and SOS for $g = 0.8$, $\tau = 0.25$, $\omega_0 = 0.9$: (a) upward radiances, (b) downward radiances (units: $\text{erg sec}^{-1} \text{cm}^{-1} \text{str}^{-1} (\text{cm}^{-1})^{-1}$)

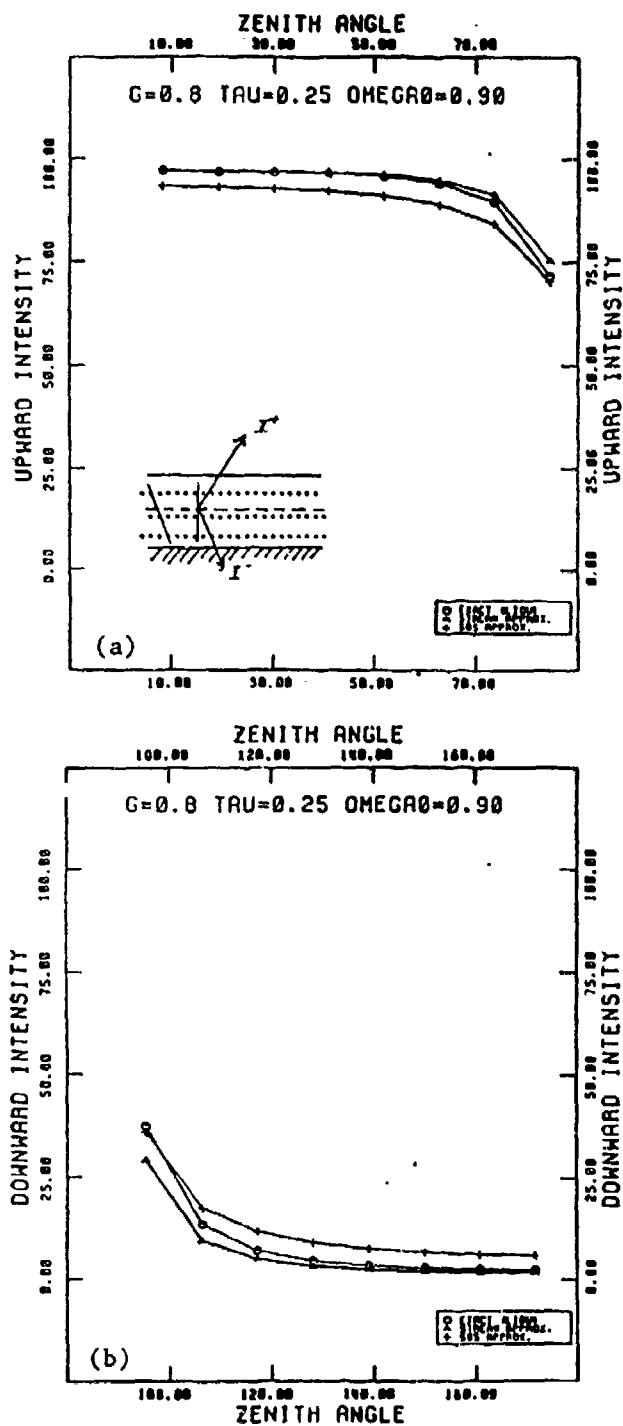


Figure A-2. Comparison of internal radiances from DOM, SA, and SOS for $g = 0.8$, $\tau = 0.25$, $\omega_0 = 0.9$: (a) upward radiances, (b) downward radiances (units: $\text{erg sec}^{-1} \text{cm}^{-1} \text{str}^{-1} (\text{cm}^{-1})^{-1}$)

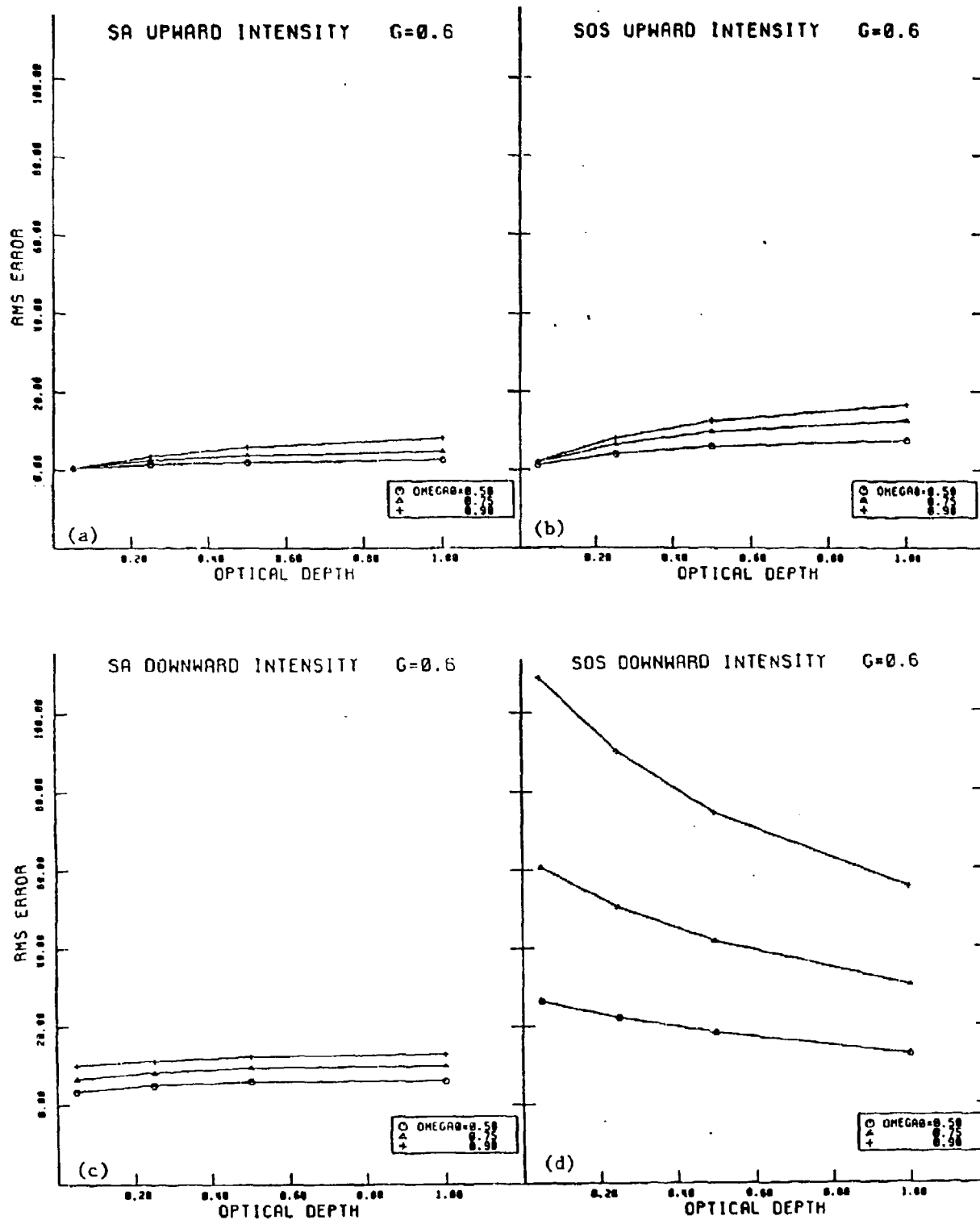


Figure A-3. Percent RMS errors for SA and SOS compared to DOM as a function of optical depth and single scattering albedo for $g = 0.6$: (a) SA upward radiance, (b) SOS upward radiance, (c) SA downward radiance, and (d) SOS downward radiance.

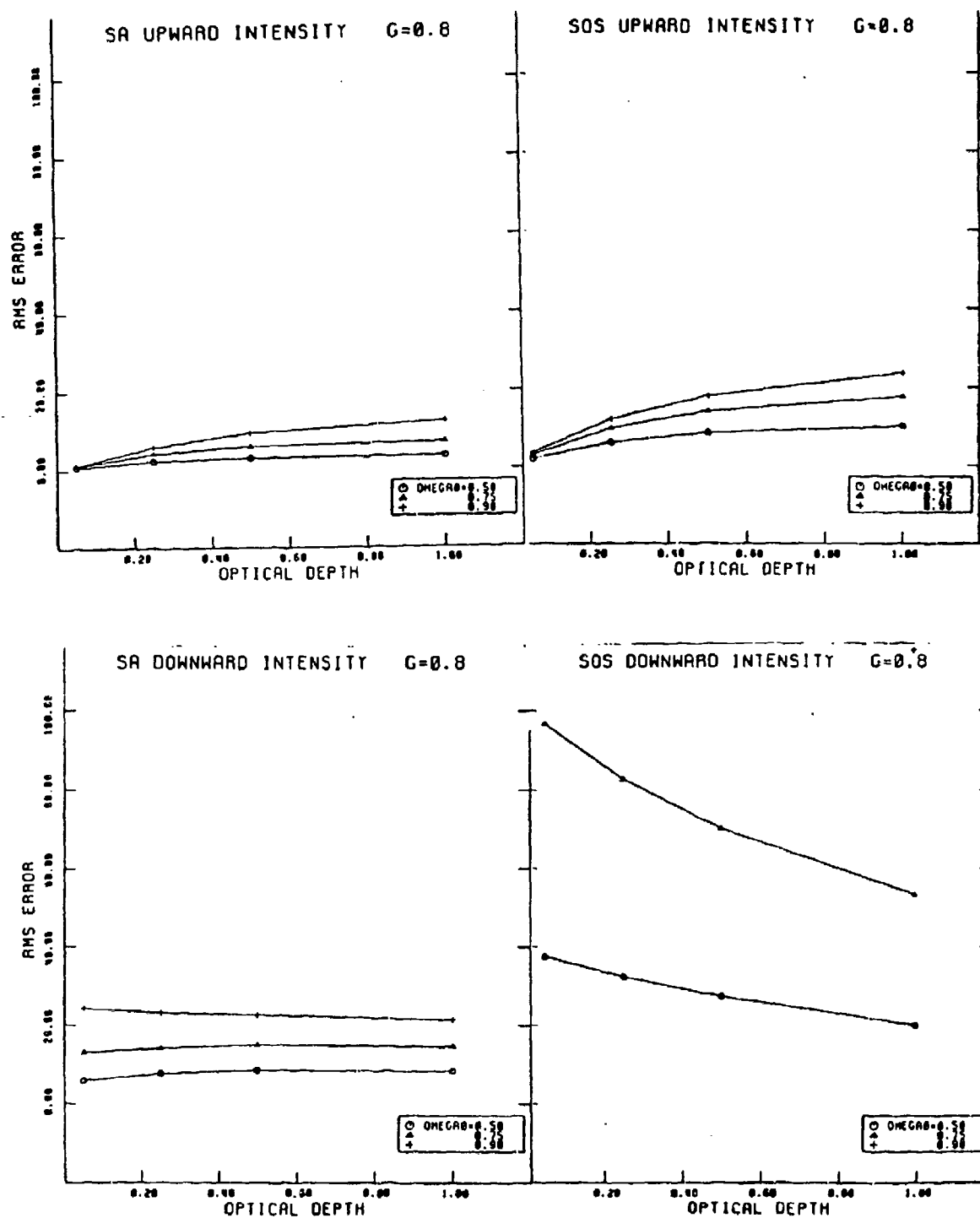


Figure A-4. Percent RMS errors for SA and SOS compared to DOM as a function of optical depth and single scattering albedo for $g = 0.8$:
 (a) SA upward radiance, (b) SOS upward radiance, (c) SA downward radiance, and (d) SOS downward radiance.

Similar conclusions can be drawn by looking at the internal upward and downward radiances halfway through the layer at an optical depth of 0.125 (Figures A-2(a) and (b), respectively).

Figures A-3 and A-4 illustrate the percent RMS error for the stream approximation and successive orders of scattering compared to the discrete ordinate solutions for all optical depths, and single scattering albedos, and scattering asymmetry factors of 0.6 and 0.8, respectively. While the SOS approach provides reasonable upward radiances with errors only slightly greater than the SA, SOS derived downward radiances are quite inaccurate. Downward radiances are a real test of the scattering parameterization since upward radiances are largely determined by the uniform surface emission at these optical depths. Notably, RMS errors for the stream approximation are weakly dependent on optical depth and are at most about 25 percent. Errors are largest for high single scattering albedo and asymmetry factor, i.e., when the scattering effect is maximum and when the angular scattering function is strongly forward scattering. This is expected due to the nature of the approximation used.

Computer execution times were also tabulated for each thermal scattering test case ensemble to ascertain their relative efficiency. Execution times are given in Table A-8. Times for the SOS and DOM are comparable while the SA was about 40 times faster than the DOM. These results suggest that the SA is the candidate parameterization of choice.

A.3 Recommendations for LOWTRAN and FASCODE

Based on these results, the stream approximation was selected for implementation for thermal scattering as well as solar scattering in the LOWTRAN and FASCODE models. Based on the evaluation and consideration of the requirements of efficiency, accuracy and code structure of LOWTRAN and FASCODE models, the parameterization of the stream approximation together with the correlated-k approximation is best suited for implementation into these models. The parameterization is unique in the sense that the correlated-k approximation decouples the multiple scattering from the treatment of nongray

Table A-8
Thermal Results

Execution Time (sec)	SA	SOS	DOM (Liou)*
Optical Thickness			
Tau = 0.05			
(g = 0.6, ω_0 = 0.50)	.35	6.28	5.76
(12.10)			
(g = 0.6, ω_0 = 0.90)	.35	6.28	5.79
(12.10)			
Tau = 0.25			
(g = 0.6, ω_0 = 0.50)	.34	7.55	5.79
(12.16)			
(g = 0.6, ω_0 = 0.90)	.34	10.17	5.81
(12.19)			
Tau = 0.50			
(g = 0.6, ω_0 = 0.50)	.34	8.87	5.72
(12.02)			
(g = 0.6, ω_0 = 0.90)	.34	12.79	5.79
(12.15)			
Tau = 1.00			
(g = 0.6, ω_0 = 0.50)	.34	10.14	5.74
(12.06)			
(g = 0.6, ω_0 = 0.90)	.36	16.69	5.82
(12.22)			

*Runs were made on AFGL's Cyber 750 system. All other runs on AER's Harris H800 system. Times in parenthesis are Harris equivalents for runs made on the Cyber, using a benchmark factor of 2.1.

gaseous absorption so that the stream approximation can be used to treat multiple scattering in both the LOWTRAN and FASCODE models. The stream approximation is extremely attractive since it retains the analytical simplicity (and hence, efficiency) of single scattering while improving the treatment of multiple-scattering (and hence, accuracy).

Appendix B

EXAMPLE OF FASCODE OUTPUT

A case is included as a test for FASCODE with multiple scattering. The input cards for the case are listed in Table B-1 and the listing of the file TAPE 6 is in Table B-2. The next section will discuss the output for the test case. Only those details which differ from the standard FASCODE output will be discussed.

This case demonstrates the new multiple scattering calculation for thermal scattering of downward radiance. The parameters selected for this case are as follows: the atmospheric profile is the 1962 U.S. Standard and the boundary layer aerosol model is RURAL with 5 km meteorological range. The path is a slant path from the ground to 20 km with a zenith angle at the ground of 0.0 degrees.

The output for this case shown in Table B-2 will now be described. The first difference is in CARD 2, which now contains another quantity, IMS. IMS is the eleventh variable printed on CARD 2, and is the flag for multiple scattering. When IMS is 1, the multiple scattering features of the program will be used. The next difference which occurs in the output, is a print of the path parameters which occurs on pages 2 and 3. This occurs due to a call to FSCGEO which is needed to determine whether or not the user defined path starts at or intersects the ground, and whether or not HMINMS and HMAXMS are contained within the user defined path. (This is explained further in the user instructions in Section 3.1.4. If additional paths were determined to be necessary in order to accommodate the multiple scattering calculation, these paths would be run and the corresponding output would appear in the calculations at this point. The user defined path would be the last path that would appear in the output.)

The next 25 pages in the output shown in Table B-2 are identical to those in the output for a run without multiple scattering. The following 21 pages which output the optical depths, radiance, and transmittance for each FASCODE layer are different for the multiple scattering runs. The differences will be discussed for one layer, since each layer has the same output. The first difference is that the radiance that is printed is the thermal emission and not the conservative scattering radiance supplied with the standard FASCODE

run. The second difference is that after the radiance and transmittance is printed, the composite upward flux and reflectance for that layer is also printed. These quantities are intermediate results used by the multiple scattering sections of the code, and are printed for the users benefit to see what the multiple scattering is doing.

That would conclude the output for the standard FASCODE run, but for the multiple scattering run, we still need to add the fluxes from the top down in order to determine the multiple scattered contribution. The next 21 pages are printout from the downward adding of the fluxes. The first page starts off with the composite downward flux and reflectance for layer 10. Then the total upward and downward flux for the top of layer 10 is printed. The next page prints out the composite downward flux and reflectance for layer 9. Then the total upward and downward flux for the top of layer 9 is printed. The next page starts with the output of the source function for the multiple scattering contribution to the radiance from Layer 10 (this quantity is actually the MS emission from layer 10). This is followed by the composite downward flux and reflectance for layer 8, followed by the total upward and downward flux for the top of layer 8. The source function for layer 9 appears at the top of the next page, and is followed by the total multiple scattered emission from both layer 9 and 10. This output scheme is continued such that on the last of the 21 pages the final MS emission that is printed is the total multiple scattering emission for the path.

The next and final page in the output is the total radiance for the FASCODE run and consists of the multiple scattered emission added to the thermal emission.

TABLE B-1

INPUT CARDS FOR THE FASCODE TEST CASE

Test Case

```

AER TEST CASE - MULTIPLE SCATTERING - RURAL AEROSOL - 900 - 910 CM-1
HI=1 F4=1 CN=1 AE=1 EM=1 SC=0 FI=0 PL=0 TS=0 AT=1 HG=0 LS=0 MS=1 RA=0 5 5
200.20 1.000 0.0 15.0
900.000 910.000 .000 .000 .000 .000 .000 .000
0.000 1.000
6 2 0 1 0 7 0 .000 .000 .000 .000
00.000 20.000 000.000 .000 .000 0 .000 .000
.000 .000 .000 .000 .000 .000 .000
2 0 0 0 0 0 .000 .000 .000 .000

```

TABLE B-2

FASCODE OUTPUT FOR CASE 1

AER TEST CASE - MULTIPLE SCATTERING - RURAL AEROSOL * 999 - 910 CM-1 FASCODE2 96/87/15 16.84.54
 TIME ENTERING FASCODE 71.7848
 MIRAC LBLF4 1
 CMYMM 1
 AERSL 1
 EMISS 1
 SCNFM 8
 FILTR 8
 PLOT 8
 TEST 8
 IATH 1
 IMRG 8
 ILAS 8
 SCAT 1

TABLE B-2 (Cont.)

16.04.56.

86/87/15.

*****PROGRAM FSCATH*****

CONTROL CARD 2.1: MODEL AND OPTIONS

MODEL	=	6
ITYPE	=	2
IBMAX	=	8
NOZERO	=	1
NOPRINT	=	0
MMOL	=	7
IPUNCH	=	0
RE	=	.000 KM
HSPACE	=	.000 KM
VBAR	=	.000 CM-1

CONTROL CARD 2.1 PARAMETERS WITH DEFAULTS:

MODEL	=	6
ITYPE	=	2
IBMAX	=	8
NOZERO	=	1
NOPRINT	=	0
MMOL	=	7
IPUNCH	=	0
RE	=	6371.238 KM
HSPACE	=	160.000 KM
VBAR	=	985.000 CM-1

SLANT PATH SELECTED. ITYPE = 2

CONTROL CARD 2.2: SLANT PATH PARAMETERS

H1	=	.0000 KM
H2	=	20.0000 KM
ANGLE	=	.0000 DEG
RANGE	=	.0000 KM
BETA	=	.0000 DEG
LEN	=	R

AUTOLAYERING SELECTED

AVTRAT	=	2.00
TDIFF1	=	10.00
TDIFF2	=	15.00
ALTD1	=	.00
ALTD2	=	100.00

CASE 2A: GIVEN H1, H2, ANGLE

TABLE B-2 (Cont.)

SLANT PATH PARAMETERS IN STANDARD FORM

H1	1	0000	KH
H2	2	0000	KZ
ANGLE	-	0000	DEG
PH1	-	1000	KH
PH2	-	0000	KH
PH3	-	0000	KH
PH4	-	0000	KH
PH5	-	0000	KH

***** LOWTRAN 6 (MODIFIED) *****

CARG 3.1 ***

MODEL ATMOSPHERE NO.

61010 - 1

• 遊戲

、

●

...

三

TABLE B-2 (Cont.)

CLOUD AND OR RAIN TYPE CHOSEN IS				NO CLOUD		M IS SET TO		7		AEROSOL PROFILE	
Z (KM)	P (MB)	T (K)	REL H (%)	H2O (GM M-3)	CLD AMT (GM M-3)	RAIN RATE (MM HR-1)	TYPE				
.000	1013.000	288.20	45.92	5.904E+00	.000E+00	.000E+00	RURAL			RURAL	
1.000	898.000	281.70	49.07	4.201E+00	.000E+00	.000E+00	RURAL			RURAL	
2.000	795.000	275.20	52.03	2.901E+00	.000E+00	.000E+00	RURAL			RURAL	
3.000	701.200	268.70	50.70	1.800E+00	.000E+00	.000E+00	TROPOSPHERIC			TROPOSPHERIC	SPRING-SUMMER
4.000	616.000	262.20	50.10	1.100E+00	.000E+00	.000E+00	TROPOSPHERIC			TROPOSPHERIC	SPRING-SUMMER
5.000	540.500	255.70	48.43	6.402E-01	.000E+00	.000E+00	TROPOSPHERIC			TROPOSPHERIC	SPRING-SUMMER
6.000	472.200	249.20	49.25	3.801E-01	.000E+00	.000E+00	TROPOSPHERIC			TROPOSPHERIC	SPRING-SUMMER
7.000	411.100	242.70	48.22	2.101E-01	.000E+00	.000E+00	TROPOSPHERIC			TROPOSPHERIC	SPRING-SUMMER
8.000	356.500	236.20	50.61	1.200E-01	.000E+00	.000E+00	TROPOSPHERIC			TROPOSPHERIC	SPRING-SUMMER
9.000	308.000	229.70	37.14	4.602E-02	.000E+00	.000E+00	TROPOSPHERIC			TROPOSPHERIC	SPRING-SUMMER
10.000	265.000	223.30	28.73	1.800E-02	.000E+00	.000E+00	TROPOSPHERIC			TROPOSPHERIC	SPRING-SUMMER
11.000	227.000	216.80	27.47	8.202E-03	.000E+00	.000E+00	BACKGROUN	STRATO		BACKGROUN	STRATO
12.000	194.000	216.70	12.54	3.700E-03	.000E+00	.000E+00	BACKGROUN	STRATO		BACKGROUN	STRATO
13.000	165.000	216.70	6.10	1.800E-03	.000E+00	.000E+00	BACKGROUN	STRATO		BACKGROUN	STRATO
14.000	141.700	216.70	2.85	8.403E-04	.000E+00	.000E+00	BACKGROUN	STRATO		BACKGROUN	STRATO
15.000	121.100	216.70	2.85	6.050E-04	.000E+00	.000E+00	BACKGROUN	STRATO		BACKGROUN	STRATO
16.000	103.500	216.70	1.39	4.091E-04	.000E+00	.000E+00	BACKGROUN	STRATO		BACKGROUN	STRATO
17.000	89.500	216.70	1.16	3.409E-04	.000E+00	.000E+00	BACKGROUN	STRATO		BACKGROUN	STRATO
18.000	75.650	216.70	.98	2.895E-04	.000E+00	.000E+00	BACKGROUN	STRATO		BACKGROUN	STRATO
19.000	64.670	216.70	.84	2.491E-04	.000E+00	.000E+00	BACKGROUN	STRATO		BACKGROUN	STRATO
20.000	55.290	216.70	.73	2.157E-04	.000E+00	.000E+00	BACKGROUN	STRATO		BACKGROUN	STRATO
21.000	47.290	217.60	.57	1.873E-04	.000E+00	.000E+00	BACKGROUN	STRATO		BACKGROUN	STRATO
22.000	40.470	218.60	.44	1.632E-04	.000E+00	.000E+00	BACKGROUN	STRATO		BACKGROUN	STRATO
23.000	34.670	219.60	.35	1.437E-04	.000E+00	.000E+00	BACKGROUN	STRATO		BACKGROUN	STRATO
24.000	29.720	220.60	.27	1.256E-04	.000E+00	.000E+00	BACKGROUN	STRATO		BACKGROUN	STRATO
25.000	25.490	221.60	.21	1.104E-04	.000E+00	.000E+00	BACKGROUN	STRATO		BACKGROUN	STRATO
27.500	17.460	224.04	.11	7.731E-05	.000E+00	.000E+00	BACKGROUN	STRATO		BACKGROUN	STRATO
30.000	11.970	226.50	.06	5.414E-05	.000E+00	.000E+00	BACKGROUN	STRATO		BACKGROUN	STRATO
32.500	8.293	231.45	.03	3.738E-05	.000E+00	.000E+00	METEORIC DUST			METEORIC DUST	
35.000	5.746	236.50	.01	2.501E-05	.000E+00	.000E+00	METEORIC DUST			METEORIC DUST	
37.500	4.062	243.35	.00	1.795E-05	.000E+00	.000E+00	METEORIC DUST			METEORIC DUST	
40.000	2.871	250.40	.00	1.249E-05	.000E+00	.000E+00	METEORIC DUST			METEORIC DUST	
100.000	.000	195.10	.00	1.209E-10	.000E+00	.000E+00	METEORIC DUST			METEORIC DUST	

PROGRAM WILL COMPUTE RADIANCE

ATMOSPHERIC MODEL
 TEMPERATURE = 6 1962 U S STANDARD
 WATER VAPOR = 6 1962 U S STANDARD
 OZONE = 6 1962 U S STANDARD

SLANT PATH. H1 TO H2
 H1 = .000 KM
 H2 = 20.000 KM

TABLE B-2 (Cont.)

ANGLE =	.000 DEG
RANGE =	.000 KM
BETA =	.000 DEG
LEN =	B
FREQUENCY RANGE	
V1 =	900.0 CM-1 (11.11 MICROMETERS)
V2 =	910.0 CM-1 (10.99 MICROMETERS)
DV =	5.0 CM-1

TABLE B-2 (Cont.)

ATMOSPHERIC PROFILES

I	Z (KM)	P (MB)	T (K)	QNTMFM MOL/CM2	WV KM	WV CM/KM	WV (-)	AEROSOL 1 (-)	AEROSOL 2 (-)	AEROSOL 3 (-)	AEROSOL 4 (-)	AEROSOL 5 (-)	CIRRUS (-)	RH (PERCENT)
1	1.00	1013.000	288.2	.000E+00	.000E+00	.000E+00	.000E+00	.000E+00	.000E+00	.000E+00	.000E+00	.000E+00	.000E+00	.000E+00
2	1.00	898.800	281.7	.000E+00	.000E+00	.000E+00	.000E+00	.000E+00	.000E+00	.000E+00	.000E+00	.000E+00	.000E+00	.000E+00
3	2.00	795.000	275.2	.000E+00	.000E+00	.000E+00	.000E+00	.000E+00	.000E+00	.000E+00	.000E+00	.000E+00	.000E+00	.000E+00
4	3.00	701.200	268.7	.000E+00	.000E+00	.000E+00	.000E+00	.000E+00	.000E+00	.000E+00	.000E+00	.000E+00	.000E+00	.000E+00
5	4.00	616.600	262.2	.000E+00	.000E+00	.000E+00	.000E+00	.000E+00	.000E+00	.000E+00	.000E+00	.000E+00	.000E+00	.000E+00
6	5.00	540.500	255.7	.000E+00	.000E+00	.000E+00	.000E+00	.000E+00	.000E+00	.000E+00	.000E+00	.000E+00	.000E+00	.000E+00
7	6.00	472.200	249.2	.000E+00	.000E+00	.000E+00	.000E+00	.000E+00	.000E+00	.000E+00	.000E+00	.000E+00	.000E+00	.000E+00
8	7.00	411.100	242.7	.000E+00	.000E+00	.000E+00	.000E+00	.000E+00	.000E+00	.000E+00	.000E+00	.000E+00	.000E+00	.000E+00
9	8.00	356.500	236.2	.000E+00	.000E+00	.000E+00	.000E+00	.000E+00	.000E+00	.000E+00	.000E+00	.000E+00	.000E+00	.000E+00
10	9.00	308.000	229.7	.000E+00	.000E+00	.000E+00	.000E+00	.000E+00	.000E+00	.000E+00	.000E+00	.000E+00	.000E+00	.000E+00
11	10.00	265.000	223.3	.000E+00	.000E+00	.000E+00	.000E+00	.000E+00	.000E+00	.000E+00	.000E+00	.000E+00	.000E+00	.000E+00
12	11.00	227.000	216.8	.000E+00	.000E+00	.000E+00	.000E+00	.000E+00	.000E+00	.000E+00	.000E+00	.000E+00	.000E+00	.000E+00
13	12.00	194.000	210.7	.000E+00	.000E+00	.000E+00	.000E+00	.000E+00	.000E+00	.000E+00	.000E+00	.000E+00	.000E+00	.000E+00
14	13.00	165.800	216.7	.000E+00	.000E+00	.000E+00	.000E+00	.000E+00	.000E+00	.000E+00	.000E+00	.000E+00	.000E+00	.000E+00
15	14.00	141.700	216.7	.000E+00	.000E+00	.000E+00	.000E+00	.000E+00	.000E+00	.000E+00	.000E+00	.000E+00	.000E+00	.000E+00
16	15.00	121.100	216.7	.000E+00	.000E+00	.000E+00	.000E+00	.000E+00	.000E+00	.000E+00	.000E+00	.000E+00	.000E+00	.000E+00
17	16.00	103.500	216.7	.000E+00	.000E+00	.000E+00	.000E+00	.000E+00	.000E+00	.000E+00	.000E+00	.000E+00	.000E+00	.000E+00
18	17.00	89.500	216.7	.000E+00	.000E+00	.000E+00	.000E+00	.000E+00	.000E+00	.000E+00	.000E+00	.000E+00	.000E+00	.000E+00
19	18.00	75.650	216.7	.000E+00	.000E+00	.000E+00	.000E+00	.000E+00	.000E+00	.000E+00	.000E+00	.000E+00	.000E+00	.000E+00
20	19.00	64.670	216.7	.000E+00	.000E+00	.000E+00	.000E+00	.000E+00	.000E+00	.000E+00	.000E+00	.000E+00	.000E+00	.000E+00
21	20.00	55.290	216.7	.000E+00	.000E+00	.000E+00	.000E+00	.000E+00	.000E+00	.000E+00	.000E+00	.000E+00	.000E+00	.000E+00
22	21.00	47.290	217.6	.000E+00	.000E+00	.000E+00	.000E+00	.000E+00	.000E+00	.000E+00	.000E+00	.000E+00	.000E+00	.000E+00
23	22.00	40.470	218.6	.000E+00	.000E+00	.000E+00	.000E+00	.000E+00	.000E+00	.000E+00	.000E+00	.000E+00	.000E+00	.000E+00
24	23.00	34.670	219.6	.000E+00	.000E+00	.000E+00	.000E+00	.000E+00	.000E+00	.000E+00	.000E+00	.000E+00	.000E+00	.000E+00
25	24.00	29.720	220.6	.000E+00	.000E+00	.000E+00	.000E+00	.000E+00	.000E+00	.000E+00	.000E+00	.000E+00	.000E+00	.000E+00
26	25.00	25.490	221.6	.000E+00	.000E+00	.000E+00	.000E+00	.000E+00	.000E+00	.000E+00	.000E+00	.000E+00	.000E+00	.000E+00
27	27.50	17.460	224.0	.000E+00	.000E+00	.000E+00	.000E+00	.000E+00	.000E+00	.000E+00	.000E+00	.000E+00	.000E+00	.000E+00
28	30.00	11.970	226.5	.000E+00	.000E+00	.000E+00	.000E+00	.000E+00	.000E+00	.000E+00	.000E+00	.000E+00	.000E+00	.000E+00
29	32.50	8.293	231.4	.000E+00	.000E+00	.000E+00	.000E+00	.000E+00	.000E+00	.000E+00	.000E+00	.000E+00	.000E+00	.000E+00
30	35.00	5.746	236.5	.000E+00	.000E+00	.000E+00	.000E+00	.000E+00	.000E+00	.000E+00	.000E+00	.000E+00	.000E+00	.000E+00
31	37.50	4.062	243.4	.000E+00	.000E+00	.000E+00	.000E+00	.000E+00	.000E+00	.000E+00	.000E+00	.000E+00	.000E+00	.000E+00
32	40.00	2.871	250.4	.000E+00	.000E+00	.000E+00	.000E+00	.000E+00	.000E+00	.000E+00	.000E+00	.000E+00	.000E+00	.000E+00
33	100.00	.000	195.1	.000E+00	.000E+00	.000E+00	.000E+00	.000E+00	.000E+00	.000E+00	.000E+00	.000E+00	.000E+00	.000E+00

TABLE B-2 (Cont.)

16.04.59.

06/07/15.

*****PROGRAM FSCATH*****

CONTROL CARD 2.1: MODEL AND OPTIONS

MODEL = 6
 ITYPE = 2
 I8MAX = 0
 NOZERO = 1
 NOPRINT = 0
 NMOL = 7
 IPUNCH = 0
 RE = 6371.230 KM
 HSPACE = 100.000 KM
 VBAR = 905.000 CM-1

CONTROL CARD 2.1 PARAMETERS WITH DEFAULTS:

MODEL = 6
 ITYPE = 2
 I8MAX = 0
 NOZERO = 1
 NOPRINT = 0
 NMOL = 7
 IPUNCH = 0
 RE = 6371.230 KM
 HSPACE = 100.000 KM
 VBAR = 905.000 CM-1

SLANT PATH SELECTED. ITYPE = 2

CONTROL CARD 2.2: SLANT PATH PARAMETERS

H1 = .0000 KM
 H2 = 20.0000 KM
 ANGLE = .0000 DEG
 RANGE = .0000 KM
 BETA = .0000 DEG
 LEN = 0

ATMOSPHERIC PROFILE SELECTED IS: M - 6 U. S. STANDARD, 1976

I	Z (KM)	P (MB)	T (K)	REFRACT INDEX-1 +1.0E5	AIR	H2O	CO2	O3	N2O	CO	CH4	O2
1	.000	1013.00000	288.26	271.94	2.55E+19	1.97E+17	0.41E+15	6.78E+11	8.15E+12	3.82E+12	4.33E+13	5.33E+18
2	1.000	898.00000	281.70	246.92	2.31E+19	1.40E+17	7.60E+15	6.78E+11	7.40E+12	3.35E+12	3.93E+13	4.82E+18
3	2.000	795.00000	275.20	223.62	2.09E+19	9.70E+16	6.91E+15	6.78E+11	6.70E+12	2.93E+12	3.56E+13	4.38E+18
4	3.000	701.00000	268.70	202.05	1.89E+19	6.02E+16	6.24E+15	6.27E+11	6.05E+12	2.55E+12	3.21E+13	3.95E+18
5	4.000	616.00000	262.20	182.11	1.70E+19	3.68E+16	5.63E+15	5.77E+11	5.45E+12	2.22E+12	2.90E+13	3.56E+18
6	5.000	540.00000	255.70	163.71	1.53E+19	2.14E+16	5.06E+15	5.77E+11	4.90E+12	1.99E+12	2.50E+13	3.20E+18
7	6.000	472.00000	249.20	146.76	1.37E+19	1.27E+16	4.53E+15	5.65E+11	4.39E+12	1.78E+12	2.30E+13	2.87E+18
8	7.000	411.00000	242.70	131.20	1.23E+19	7.02E+15	4.05E+15	6.15E+11	3.91E+12	1.54E+12	2.09E+13	2.57E+18
9	8.000	356.00000	236.20	116.91	1.09E+19	4.01E+15	3.61E+15	6.57E+11	3.50E+12	1.31E+12	1.86E+13	2.29E+18
10	9.000	308.00000	229.70	103.87	9.71E+18	1.54E+15	3.21E+15	8.91E+11	3.11E+12	1.07E+12	1.65E+13	2.03E+18
11	10.000	265.00000	223.30	91.93	8.60E+18	6.02E+14	2.84E+15	1.13E+12	2.73E+12	8.60E+11	1.45E+13	1.80E+18
12	11.000	227.00000	216.80	81.11	7.58E+18	2.74E+14	2.50E+15	1.63E+12	2.38E+12	6.83E+11	1.27E+13	1.59E+18
13	12.000	194.00000	210.70	69.35	6.48E+18	1.24E+14	2.14E+15	2.01E+12	2.01E+12	5.19E+11	1.08E+13	1.35E+18
14	13.000	165.00000	205.70	59.27	5.54E+18	6.02E+13	1.83E+15	2.33E+12	1.69E+12	3.60E+11	9.12E+12	1.16E+18
15	14.000	141.00000	200.70	50.65	4.74E+18	2.81E+13	1.56E+15	2.38E+12	1.42E+12	2.37E+11	7.71E+12	9.90E+17
16	15.000	121.00000	206.70	43.29	4.05E+18	2.03E+13	1.34E+15	2.63E+12	1.19E+12	1.62E+11	6.50E+12	8.46E+17
17	16.000	103.50000	216.70	37.00	3.46E+18	1.37E+13	1.11E+15	2.31E+12	9.95E+11	1.04E+11	5.48E+12	7.24E+17
18	17.000	88.50000	216.70	31.64	2.96E+18	1.14E+13	9.72E+14	3.51E+12	8.24E+11	7.40E+10	4.60E+12	6.10E+17
19	18.000	75.65000	216.70	27.04	2.53E+18	9.68E+12	8.35E+14	4.05E+12	6.76E+11	5.06E+10	3.85E+12	5.29E+17
20	19.000	64.67000	216.70	23.12	2.16E+18	8.33E+12	7.14E+14	4.39E+12	5.47E+11	3.24E+10	3.22E+12	4.52E+17
21	20.000	55.29000	216.70	19.76	1.85E+18	7.21E+12	6.10E+14	4.77E+12	4.37E+11	2.40E+10	2.63E+12	3.80E+17
22	21.000	47.29000	217.60	16.83	1.57E+18	6.26E+12	5.20E+14	4.77E+12	3.46E+11	1.89E+10	2.13E+12	3.29E+17
23	22.000	40.47000	218.60	14.34	1.34E+18	5.46E+12	4.43E+14	4.89E+12	2.75E+11	1.61E+10	1.71E+12	2.80E+17
24	23.000	34.67000	219.60	12.23	1.14E+18	4.80E+12	3.70E+14	4.77E+12	2.25E+11	1.49E+10	1.36E+12	2.39E+17
25	24.000	29.72000	220.60	10.44	9.76E+17	4.20E+12	3.22E+14	4.52E+12	1.83E+11	1.37E+10	1.07E+12	2.09E+17
26	25.000	25.49000	221.60	8.91	8.33E+17	3.69E+12	2.75E+14	4.27E+12	1.46E+11	1.33E+10	8.80E+11	1.74E+17
27	26.000	224.000	224.00	6.03	5.64E+17	2.58E+12	1.86E+14	3.27E+12	8.96E+10	1.02E+10	5.57E+11	1.18E+17
28	27.000	19.97000	226.50	4.09	3.83E+17	1.81E+12	1.26E+14	2.51E+12	5.42E+10	7.66E+09	3.50E+11	8.00E+16
29	28.000	17.43000	230.00	2.70	2.52E+17	1.22E+12	8.33E+13	1.86E+12	2.94E+10	5.72E+09	2.09E+11	5.20E+16
30	29.000	15.00000	236.50	1.80	1.76E+17	8.63E+11	5.81E+13	1.38E+12	1.63E+10	4.49E+09	1.31E+11	3.69E+16
31	30.000	12.75000	242.90	1.32	1.24E+17	6.13E+11	4.09E+13	9.66E+11	8.29E+09	3.59E+09	8.19E+10	2.59E+16
32	31.000	10.71000	250.40	.89	8.30E+16	4.10E+11	2.74E+13	6.07E+11	3.75E+09	4.99E+09	4.69E+10	1.74E+16
33	32.000	9.26000	257.30	.62	5.80E+16	2.99E+11	1.91E+13	3.50E+11	1.60E+09	5.16E+09	2.68E+10	1.21E+16
34	33.000	8.00000	264.20	.44	4.09E+16	2.14E+11	1.35E+13	2.15E+11	6.51E+08	5.39E+09	1.49E+10	9.45E+15
35	34.000	7.00000	270.60	.31	2.92E+16	1.53E+11	9.64E+12	1.20E+11	2.74E+08	5.71E+09	8.10E+09	6.10E+15
36	35.000	6.25000	276.70	.22	2.13E+16	1.12E+11	7.05E+12	6.62E+10	1.02E+09	6.19E+09	4.49E+09	4.46E+15
37	36.000	5.65000	280.80	.13	1.18E+16	6.02E+10	3.90E+12	2.13E+10	2.23E+07	5.32E+09	1.95E+09	2.47E+15
38	37.000	5.19000	287.00	.07	6.42E+15	3.05E+10	2.12E+12	7.07E+09	4.52E+06	4.50E+09	8.38E+08	1.34E+15
39	38.000	4.80000	293.20	.04	3.28E+15	1.42E+10	1.12E+12	2.37E+09	8.54E+05	4.48E+09	3.50E+08	7.00E+14
40	39.000	4.45000	299.60	.02	1.72E+15	6.03E+09	5.69E+11	5.17E+08	1.54E+05	4.31E+09	1.42E+09	3.60E+14
41	40.000	4.10000	306.40	.01	8.34E+14	2.36E+09	2.75E+11	2.09E+08	2.62E+04	2.86E+09	5.49E+07	1.74E+14
42	41.000	3.80000	313.60	.00	3.83E+14	7.86E+08	1.26E+11	1.15E+08	4.22E+03	1.98E+09	2.01E+07	8.01E+13
43	42.000	3.50000	321.00	.00	1.71E+14	2.28E+08	5.65E+10	8.56E+07	6.60E+02	1.17E+09	7.19E+06	3.50E+13

TABLE B-2 (Cont.)

44 98.000 .00184 186.90 .00 7.13E+13 6.07E+07 2.35E+10 5.08E+07 9.64E+01 7.14E+08 2.40E+06 1.49E+13
 45 95.000 .00076 188.40 .00 2.92E+13 1.58E+07 9.65E+09 2.05E+07 1.38E+01 3.00E+08 7.85E+05 6.08E+12
 46 100.000 .00032 195.10 .00 1.19E+13 4.04E+06 3.92E+09 4.76E+06 1.97E+00 1.25E+08 2.55E+05 2.38E+12

CASE 2A: GIVEN H1, H2, ANGLE

SLANT PATH PARAMETERS IN STANDARD FORM

H1 = .000 KM
 H2 = 20.000 KM
 ANGLE = .000 DEG
 PH1 = 180.000 DEG
 HMIN = .000 KM
 LEN = 0

FASCODE LAYER BOUNDARIES PRODUCED BY THE AUTOMATIC LAYERING ROUTINE AUTLAY

THE USER SHOULD EXAMINE THESE BOUNDARIES AND MODIFY THEM IF APPROPRIATE
 THE FOLLOWING PARAMETERS ARE USED:

AVTRAT = 2.00 = MAX RATIO OF VOIGT WIDTHS
 TOIFF1 = 10.00 = MAX TEMP DIFF AT 0. KM
 TOIFF2 = 15.00 = MAX TEMP DIFF AT 100. KM
 ALZERO = .100 CM-1 = AVERAGE LORENTZ WIDTH AT STP
 AVMWT = 36.00 = AVERAGE MOLECULAR WEIGHT
 VBAR = 905.00 CM-1 = AVERAGE WAVENUMBER

I	Z (KM)	P (MB)	T (K)	LORENTZ (CM-1)	DOPPLER (CM-1)	ZETA	VOIGT (CM-1)	VOIGT RATIO	TEMP DIFF (K)
1	1.000	1013.00000	288.20	.00132	.00092	.991	.00132	1.18	9.8
2	1.500	845.30033	278.45	.00601	.00090	.990	.00602	1.18	9.8
3	3.000	701.20000	268.70	.00263	.00089	.986	.00264	1.19	9.8
4	4.500	577.29741	258.95	.00091	.00087	.986	.00093	1.20	9.8
5	6.000	472.20000	249.20	.00079	.00085	.983	.00080	1.21	9.8
6	7.500	382.82783	239.45	.00081	.00084	.980	.00082	1.22	9.8
7	9.000	308.00000	229.70	.00451	.00082	.977	.00453	1.25	10.3
8	10.000	241.49018	219.40	.00268	.00080	.972	.00271	1.98	2.7
9	15.000	121.10000	216.70	.00397	.00080	.946	.00401	1.98	.0
10	19.400	60.74078	216.70	.00201	.00080	.898	.00210	1.98	3.9
11	24.000	29.72000	220.60	.00340	.00080	.809	.00358	2.01	5.6
12	29.700	12.52214	226.20	.00141	.00081	.635	.00178	1.50	11.1
13	35.300	5.52596	237.27	.00061	.00083	.423	.00119	1.15	11.3
14	39.400	3.13044	248.60	.00034	.00085	.284	.00104	1.07	11.5
15	43.500	1.81014	260.06	.00019	.00087	.190	.00097	1.09	1.2
16	55.700	.38733	258.87	.00004	.00087	.045	.00009	1.04	12.4
17	60.200	.21097	246.45	.00002	.00085	.026	.00006	1.03	12.6
18	64.800	.11208	233.85	.00001	.00083	.015	.00003	1.03	12.9
19	69.500	.05619	220.97	.00001	.00080	.008	.00001	1.03	13.2
20	75.300	.02284	207.81	.00000	.00078	.003	.00000	1.04	13.5
21	82.200	.00770	194.33	.00000	.00075	.001	.00000	1.00	.8

TABLE B-2 (Cont.)

CALCULATION OF THE REFRACTED PATH THROUGH THE ATMOSPHERE

I	ALTITUDE TO FROM (KM)	THETA (DEG)	D RANGE (KM)	R RANGE (KM)	DBETA (DEG)	BETA (DEG)	PHI (DEG)	BEND (DEG)	SBAR (MB)	TBAR (K)	RHOBAR (MOL CM-3)
M1 TO M2											
1	1.000	1.000	1.000	1.000	.000	.000	180.000	.000	955.683	284.998	2.43E+19
2	1.800	.000	.500	1.500	.000	.000	180.000	.000	872.882	280.885	2.25E+19
3	1.500	.000	.500	2.000	.000	.000	100.000	.000	828.105	276.835	2.15E+19
4	2.000	.000	1.000	3.000	.000	.000	180.000	.000	747.913	271.992	1.99E+19
5	3.000	.000	1.000	4.000	.000	.000	180.000	.000	658.727	265.493	1.80E+19
6	4.000	.000	.500	4.500	.000	.000	180.000	.000	596.908	259.586	1.66E+19
7	4.500	.000	.500	5.000	.000	.000	180.000	.000	558.868	257.336	1.57E+19
8	5.000	.000	1.000	6.000	.000	.000	180.000	.000	506.284	252.495	1.45E+19
9	6.000	.000	1.000	7.000	.000	.000	180.000	.000	441.516	245.996	1.30E+19
10	7.000	.000	.500	7.500	.000	.000	180.000	.000	396.932	241.087	1.19E+19
11	7.500	.000	.500	8.000	.000	.000	180.000	.000	369.634	237.837	1.13E+19
12	8.000	.000	1.000	9.000	.000	.000	180.000	.000	332.137	232.999	1.03E+19
13	9.000	.000	1.000	10.000	.000	.000	180.000	.000	286.399	226.550	9.14E+18
14	10.000	.000	.500	10.500	.000	.000	180.000	.000	253.215	221.369	8.20E+18
15	10.500	.000	.400	11.000	.000	.000	180.000	.000	234.235	218.188	7.78E+18
16	11.000	.000	1.000	12.000	.000	.000	180.000	.000	216.499	216.751	7.02E+18
17	12.000	.000	1.000	13.000	.000	.000	180.000	.000	179.908	216.700	5.80E+18
18	13.000	.000	1.000	14.000	.000	.000	180.000	.000	153.750	216.700	5.13E+18
19	14.000	.000	1.000	15.000	.000	.000	180.000	.000	131.480	216.700	4.38E+18
20	15.000	.000	1.000	16.000	.000	.000	180.000	.000	112.380	216.700	3.75E+18
21	16.000	.000	1.000	17.000	.000	.000	180.000	.000	96.802	216.700	3.23E+18
22	17.000	.000	1.000	18.000	.000	.000	180.000	.000	82.875	216.700	2.74E+18
23	18.000	.000	1.000	19.000	.000	.000	180.000	.000	70.168	216.700	2.34E+18
24	19.000	.000	.400	19.400	.000	.000	180.000	.000	62.705	216.700	2.10E+18
25	19.400	.000	.600	20.000	.000	.000	180.000	.000	58.815	216.700	1.94E+18

TABLE B-2 (Cont.)

INTEGRATED ABSORBER AMOUNTS BY LAYER

1	2	3	4	5	6	7	8	9	10	11	12	13	14	15	16	17	18	19	20	21	22	23	24	25	TOTAL
LAYER BOUNDARIES FROM TO		INTEGRATED AMOUNTS (MOL CM-2)																							
		AIR	H ₂ O	CO ₂	O ₃	H ₂ O	CO	CH ₄																	
1	1.000	2.426E+24	1.673E+22	0.814E+20	6.779E+16	7.772E+17	3.583E+17	4.129E+18	5.876E+23																
2	1.000	1.127E+24	6.410E+21	3.723E+20	3.390E+16	3.610E+17	1.622E+17	1.918E+18	2.358E+23																
3	1.500	1.073E+24	5.327E+21	3.542E+20	3.389E+16	3.435E+17	1.516E+17	1.825E+18	2.244E+23																
4	2.000	1.990E+24	7.711E+21	6.578E+20	6.822E+16	6.370E+17	2.738E+17	3.384E+18	4.161E+23																
5	3.000	1.795E+24	4.751E+21	5.926E+20	6.819E+16	5.747E+17	2.300E+17	3.053E+18	3.753E+23																
6	4.000	8.293E+23	1.611E+21	2.780E+20	2.086E+16	2.655E+17	1.079E+17	1.411E+18	1.734E+23																
7	4.500	7.862E+23	1.229E+21	2.596E+20	2.086E+16	2.518E+17	1.073E+17	1.337E+18	1.644E+23																
8	5.000	1.450E+24	1.668E+21	4.708E+20	5.709E+16	4.643E+17	1.866E+17	2.467E+18	3.033E+23																
9	6.000	1.298E+24	9.586E+20	4.207E+20	5.895E+16	4.152E+17	1.657E+17	2.208E+18	2.715E+23																
10	7.000	5.960E+23	3.863E+20	1.890E+20	3.122E+16	1.989E+17	7.303E+16	1.013E+18	1.247E+23																
11	7.500	5.626E+23	2.315E+20	1.898E+20	3.216E+16	1.802E+17	6.877E+16	9.559E+17	1.177E+23																
12	8.000	1.031E+24	2.581E+20	3.405E+20	7.657E+16	3.299E+17	1.107E+17	1.749E+18	2.555E+23																
13	9.000	9.142E+23	9.979E+19	3.819E+20	1.806E+17	2.915E+17	9.609E+16	1.545E+18	1.555E+23																
14	10.000	4.968E+23	2.879E+19	1.641E+20	7.582E+16	1.579E+17	4.820E+16	8.363E+17	1.039E+23																
15	10.600	3.111E+23	1.209E+19	1.027E+20	6.867E+16	9.799E+16	2.862E+16	5.220E+17	6.500E+22																
16	11.000	7.020E+23	1.891E+19	2.318E+20	1.613E+17	2.199E+17	5.973E+16	1.172E+18	1.460E+23																
17	12.000	6.001E+23	8.815E+18	1.982E+20	2.870E+17	1.845E+17	4.350E+16	9.931E+17	1.255E+23																
18	13.000	5.128E+23	4.211E+18	1.694E+20	2.256E+17	1.552E+17	2.944E+16	8.394E+17	1.073E+23																
19	14.000	4.383E+23	2.396E+18	1.447E+20	2.507E+17	1.309E+17	1.971E+16	7.086E+17	9.166E+22																
20	15.000	3.746E+23	1.675E+18	1.237E+20	2.819E+17	1.891E+17	1.308E+16	5.974E+17	7.834E+22																
21	16.000	2.202E+23	1.250E+18	1.057E+20	3.256E+17	9.872E+16	8.809E+15	5.024E+17	6.697E+22																
22	17.000	2.738E+23	1.051E+18	9.040E+19	3.759E+17	7.473E+16	6.156E+15	4.211E+17	5.725E+22																
23	18.000	2.340E+23	8.986E+17	7.720E+19	4.200E+17	6.809E+16	4.085E+15	3.515E+17	4.894E+22																
24	19.000	8.381E+22	3.237E+17	2.767E+19	1.786E+17	2.802E+16	1.223E+15	1.232E+17	1.793E+22																
25	19.400	1.163E+23	4.519E+17	3.039E+19	2.791E+17	2.807E+16	1.580E+15	1.676E+17	2.431E+22																
TOTAL	.000	2.834E+25	4.737E+22	6.710E+21	3.538E+18	6.412E+18	2.369E+18	3.423E+19	4.255E+24																

SUMMARY OF THE GEOMETRY CALCULATION

MODEL - U. S. STANDARD, 1976
 H1 - .000 KM
 H2 - 20.000 KM
 ANGLE - .000 DEG
 RANGE - 20.000 KM
 BETA - .000 DEG
 PHI - 100.000 DEG
 MIN - .000 KM
 BENDING - .000 KM
 LEN - 0
 AIRMAS - .945 RELATIVE TO A VERTICAL PATH, GROUND TO SPACE

FINAL SET OF LAYERS FOR INPUT TO FASCODE
 A LAYER AMOUNT MAY BE SET TO ZERO IF THE CUMULATIVE AMOUNT FOR THAT LAYER AND ABOVE IS LESS THAN .1 PERCENT
 OF THE TOTAL AMOUNT. THIS IS DONE ONLY FOR THE FOLLOWING CASES
 1. IEMIT = 0 (TRANSMITTANCE)
 2. IEMIT = 1 (RADIANCE) AND IPATH = 3 (PATH LOOKING UP)

O2 IS NOT INCLUDED
 IF THE AMOUNTS FOR ALL THE MOLECULES BUT O2 ARE ZEROED, THE REMAINING LAYERS ARE ELIMINATED

TABLE B-2 (Cont.)

L	LAYER BOUNDARIES FROM (KM)	IPATH	PBAR (MB)	TBAR (K)	INTEGRATED AMOUNTS (MOLS CM-2)								
					AIR	H2O	CO2	O3	N2O	CO	CH4	O2	
1	.000	1.500	3	929.14027	283.43	3.55E+24	2.31E+22	1.17E+21	1.02E+17	1.14E+18	5.20E+17	6.05E+18	7.43E+23
2	1.500	3.000	3	773.19998	273.69	3.06E+24	1.30E+22	1.01E+21	9.91E+16	9.31E+17	4.25E+17	5.21E+18	6.43E+23
3	3.000	4.500	3	639.19247	263.94	2.62E+24	6.36E+21	8.66E+20	8.91E+16	8.40E+17	3.46E+17	4.46E+18	5.49E+23
4	4.500	6.000	3	524.71482	254.20	2.24E+24	2.90E+21	7.30E+20	8.60E+16	7.16E+17	2.91E+17	3.00E+18	4.68E+23
5	6.000	7.500	3	427.48751	244.45	1.89E+24	1.26E+21	6.26E+20	9.02E+16	6.07E+17	2.40E+17	3.22E+18	3.96E+23
6	7.500	9.000	3	345.37569	234.71	1.59E+24	4.90E+20	5.26E+20	1.05E+17	5.10E+17	1.67E+17	2.70E+18	3.33E+23
7	9.000	10.600	3	274.71517	224.73	1.41E+24	1.29E+20	4.66E+20	1.76E+17	4.49E+17	1.44E+17	2.38E+18	2.95E+23
8	10.600	15.000	3	181.34791	216.08	2.56E+24	4.72E+19	8.47E+20	9.25E+17	7.07E+17	1.81E+17	4.24E+18	5.36E+23
9	15.000	19.400	3	90.91292	216.70	1.29E+24	5.20E+18	4.25E+20	1.58E+18	3.56E+17	3.24E+16	2.00E+18	2.69E+23
10	19.400	20.000	3	58.01539	216.70	1.16E+23	4.52E+17	3.84E+19	2.79E+17	2.81E+16	1.50E+15	1.60E+17	2.43E+22

NEW HEIGHT

1 .000
 2 1.500
 3 3.000
 4 4.500
 5 6.000
 6 7.500

TABLE B-2 (Cont.)

18.688
15.888
19.488
20.088

7 0 9 10 11

TABLE B-2 (Cont.)

***** LOWTRAN 5 (MODIFIED) *****

[illegible]

SUMMARY OF THE GEOMETRY CALCULATION

WIND	-	210	KM	210	DEG
WAVE	-	20	000	KM	20
ANGLE	-	210	DEG	210	DEG
RANGE	-	20	000	KM	20
BETA	-	202	DEG	202	DEG
PMI	-	180	000	DEG	180
MMIN	-	000	KM	000	KM
BENDING	-	000	DEG	000	DEG
PM	-	0		0	

EQUIVALENT SEA LEVEL TOTAL ABSORBED AMOUNTS

	AER 1	AER 2	AER 3	CIPRUS	MEAN RM
1960-1970	1.0	1.0	1.0	1.0	1.0
1971-1980	1.0	1.0	1.0	1.0	1.0
1981-1990	1.0	1.0	1.0	1.0	1.0
1991-2000	1.0	1.0	1.0	1.0	1.0
2001-2010	1.0	1.0	1.0	1.0	1.0
2011-2020	1.0	1.0	1.0	1.0	1.0
2021-2030	1.0	1.0	1.0	1.0	1.0
2031-2040	1.0	1.0	1.0	1.0	1.0
2041-2050	1.0	1.0	1.0	1.0	1.0
2051-2060	1.0	1.0	1.0	1.0	1.0
2061-2070	1.0	1.0	1.0	1.0	1.0
2071-2080	1.0	1.0	1.0	1.0	1.0
2081-2090	1.0	1.0	1.0	1.0	1.0
2091-2100	1.0	1.0	1.0	1.0	1.0

TABLE B-2 (Cont.)

(PRCNT)

49.24

.000E+00

.000E+00

4.990E-03

8.149E-02

1.102E+00

7.573E+00

FINAL LOWTRAN LAYERS

ZLO	ZMI	AER1	AER2	AER3	CIRCU3	RHRT	RHPTM
1.500	283.33	1.057E+00	.000E+00	.000E+00	.000E+00	.000E+00	1.500E+00
3.000	273.58	1.241E-01	1.730E-02	.000E+00	.000E+00	.000E+00	1.500E+00
4.500	263.83	.000E+00	3.376E-02	.000E+00	.000E+00	.000E+00	1.500E+00
6.000	254.08	.000E+00	1.431E-02	.000E+00	.000E+00	.000E+00	1.500E+00
7.500	244.33	.000E+00	9.686E-03	.000E+00	.000E+00	.000E+00	1.500E+00
9.000	234.58	.000E+00	4.537E-03	.000E+00	.000E+00	.000E+00	1.500E+00
10.500	224.55	.000E+00	1.901E-03	1.438E-04	.000E+00	.000E+00	1.600E+00
12.000	218.85	.000E+00	9.120E-05	2.446E-05	.000E+00	.000E+00	4.400E+00
13.500	216.70	.000E+00	.000E+00	2.040E-05	.000E+00	.000E+00	4.400E+00
15.000	216.70	.000E+00	.000E+00	3.520E-04	.000E+00	.000E+00	6.000E+00

LOWTRAN WAVELENGTH INTERVAL ** 890.000 920.000 5.000

FREQUENCY WAVELENGTH TOTAL RAIN

890.0	11.236	.8509	1.0000
895.0	11.173	.8496	1.0000
900.0	11.111	.8483	1.0000
905.0	11.050	.8470	1.0000
910.0	10.989	.8457	1.0000
915.0	10.929	.8441	1.0000
920.0	10.870	.8424	1.0000

INTEGRATED ABSORPTION FROM 890.000 TO 920.000 CM-1 = 4.59 CM-1
AVERAGE TRANSMITTANCE = .8469

TABLE B-2 (Cont.)

16.05.86.

86/07/15.

*****PROGRAM FSCATM*****

CONTROL CARD 2.1: MODEL AND OPTIONS

MODEL = 6
 ITYPE = 2
 IRLAX = 22
 NOZERO = 1
 NOPRINT = 0
 NMOL = 7
 IPUNCH = 0
 RE = 6371.238 KM
 HSPACE = 100.000 KM
 VBAR = 985.000 CM-1

CONTROL CARD 2.1 PARAMETERS WITH DEFAULTS:

MODEL = 6
 ITYPE = 2
 IRLAX = 22
 NOZERO = 1
 NOPRINT = 0
 NMOL = 7
 IPUNCH = 0
 RE = 6371.238 KM
 HSPACE = 100.000 KM
 VBAR = 985.000 CM-1

SLANT PATH SELECTED, ITYPE = 2

CONTROL CARD 2.2: SLANT PATH PARAMETERS

H1 = .0000 KM
 H2 = 20.0000 KM
 ANGLE = .0000 DEG
 RANGE = .0000 KM
 BETA = .0000 DEG
 LEN = 0

ATMOSPHERIC PROFILE SELECTED IS: M - 6 U. S. STANDARD, 1976

Z (KM)	P (MB)	T (K)	REFRACT INDEX-1 -1.566	AIR	H ₂ O	CO ₂	O ₃	N ₂ O	CO	CH ₄	O ₂
1	1013.00000	288.20	271.94	2.55E+19	1.97E+17	8.41E+15	6.78E+11	8.15E+12	3.82E+12	4.33E+13	5.33E+18
2	1.000	281.70	246.92	2.31E+19	1.48E+17	7.63E+15	6.78E+11	7.40E+12	3.35E+12	3.93E+13	4.83E+18
3	2.000	275.20	223.62	2.09E+19	9.78E+16	6.91E+15	6.78E+11	6.78E+12	2.93E+12	3.56E+13	4.38E+18
4	3.000	268.70	202.05	1.89E+19	6.82E+16	6.24E+15	6.27E+11	6.25E+12	2.53E+12	3.21E+13	3.95E+18
5	4.000	262.20	182.11	1.70E+19	3.68E+16	5.62E+15	5.77E+11	5.45E+12	2.22E+12	2.90E+13	3.56E+18
6	5.000	255.70	163.71	1.53E+19	2.14E+16	5.06E+15	5.65E+11	4.90E+12	1.99E+12	2.60E+13	3.20E+18
7	6.000	249.20	146.76	1.37E+19	1.27E+16	4.57E+15	5.65E+11	4.39E+12	1.78E+12	2.33E+13	2.87E+18
8	7.000	242.70	131.20	1.23E+19	7.02E+15	4.05E+15	6.15E+11	3.93E+12	1.54E+12	2.09E+13	2.57E+18
9	8.000	236.20	116.91	1.09E+19	4.07E+15	3.61E+15	6.53E+11	3.50E+12	1.34E+12	1.86E+13	2.29E+18
10	9.000	229.70	103.07	9.71E+18	1.54E+15	3.21E+15	8.91E+11	3.11E+12	1.27E+12	1.65E+13	2.03E+18
11	10.000	223.20	91.93	8.50E+18	6.02E+14	2.84E+15	1.13E+12	2.73E+12	8.68E+11	1.45E+13	1.80E+18
12	11.000	216.00	81.11	7.58E+18	2.74E+14	2.50E+15	1.63E+12	2.38E+12	6.83E+11	1.27E+13	1.59E+18
13	12.000	210.00	69.35	6.48E+18	1.24E+14	2.14E+15	2.01E+12	2.01E+12	5.19E+11	1.08E+13	1.36E+18
14	13.000	216.70	59.27	5.54E+18	5.02E+13	1.83E+15	2.13E+12	1.69E+12	3.62E+11	9.12E+12	1.16E+18
15	14.000	216.70	50.65	4.74E+18	2.81E+13	1.56E+15	2.38E+12	1.42E+12	2.37E+11	7.71E+12	9.90E+17
16	15.000	216.70	43.29	4.05E+18	2.03E+13	1.34E+15	2.63E+12	1.19E+12	1.63E+11	6.50E+12	8.46E+17
17	16.000	216.70	37.00	3.46E+18	1.37E+13	1.14E+15	3.01E+12	9.96E+11	1.44E+11	5.40E+12	7.24E+17
18	17.000	216.70	31.64	2.96E+18	1.14E+13	9.77E+14	3.51E+12	8.74E+11	7.40E+10	4.60E+12	6.19E+17
19	18.000	216.70	27.04	2.53E+18	9.68E+12	8.35E+14	4.02E+12	6.76E+11	5.06E+10	3.85E+12	5.29E+17
20	19.000	216.70	23.12	2.15E+18	8.31E+12	7.14E+14	4.39E+12	5.47E+11	3.24E+10	3.20E+12	4.52E+17
21	20.000	216.70	19.76	1.85E+18	7.21E+12	6.10E+14	4.77E+12	4.37E+11	2.40E+10	2.63E+12	3.86E+17
22	21.000	217.60	16.05	1.57E+18	6.26E+12	5.00E+14	4.77E+12	3.46E+11	1.89E+10	2.13E+12	3.29E+17
23	22.000	218.60	14.34	1.34E+18	5.46E+12	4.43E+14	4.89E+12	2.75E+11	1.61E+10	1.71E+12	2.80E+17
24	23.000	219.50	12.23	1.14E+18	4.80E+12	3.78E+14	4.77E+12	2.25E+11	1.49E+10	1.36E+12	2.39E+17
25	24.000	220.60	10.44	9.76E+17	4.24E+12	3.22E+14	4.57E+12	1.83E+11	1.37E+10	1.09E+12	2.04E+17
26	25.000	221.60	8.91	8.33E+17	3.69E+12	2.75E+14	4.27E+12	1.46E+11	1.33E+10	8.80E+11	1.74E+17
27	26.000	224.00	6.03	5.64E+17	2.59E+12	1.86E+14	3.27E+12	8.96E+10	1.02E+10	5.57E+11	1.18E+17
28	27.000	226.50	4.09	3.83E+17	1.81E+12	1.26E+14	2.51E+12	5.42E+10	7.66E+09	3.50E+11	8.00E+16
29	28.000	230.00	2.70	2.52E+17	1.22E+12	8.33E+13	1.86E+12	2.94E+10	5.73E+09	2.09E+11	5.20E+16
30	29.000	236.50	1.88	1.76E+17	8.63E+11	5.81E+13	1.39E+12	1.63E+10	4.49E+09	1.31E+11	3.68E+16
31	30.000	242.90	1.32	1.24E+17	6.13E+11	4.49E+13	9.66E+11	8.29E+09	3.59E+09	8.19E+10	2.59E+16
32	31.000	250.40	.89	8.30E+16	4.19E+11	2.74E+13	6.07E+11	3.75E+09	4.99E+09	4.69E+10	1.74E+16
33	32.000	257.30	.62	5.80E+16	2.90E+11	1.91E+13	3.60E+11	1.69E+09	5.16E+09	2.68E+10	1.21E+16
34	33.000	264.20	.44	4.09E+16	2.14E+11	1.35E+13	2.15E+11	6.51E+08	5.33E+09	1.43E+10	8.55E+15
35	34.000	270.60	.31	2.92E+16	1.53E+11	9.64E+12	1.20E+11	2.74E+08	5.71E+09	8.10E+09	6.10E+15
36	35.000	278.70	.23	2.13E+16	1.12E+11	7.05E+12	6.62E+10	1.02E+08	6.19E+09	4.49E+09	4.46E+15
37	36.000	286.00	.13	1.18E+16	6.83E+10	3.90E+12	2.13E+10	2.23E+07	5.33E+09	1.95E+09	2.47E+15
38	37.000	293.00	.07	6.42E+15	3.85E+10	2.12E+12	2.07E+09	4.52E+06	4.59E+09	8.20E+08	1.24E+15
39	38.000	299.00	.04	3.38E+15	1.42E+10	1.12E+12	2.07E+09	8.54E+05	4.40E+09	3.50E+08	7.00E+14
40	39.000	305.00	.02	1.72E+15	6.80E+09	5.89E+11	5.17E+08	1.54E+05	4.31E+09	1.42E+08	3.69E+14
41	40.000	311.00	.01	8.34E+14	2.36E+09	2.75E+11	2.09E+08	2.62E+04	2.86E+09	5.49E+07	1.74E+14
42	41.000	317.00	.00	3.83E+14	7.86E+08	1.56E+11	1.15E+08	4.22E+03	1.80E+09	2.01E+07	8.01E+13
43	42.000	323.00	.00	1.71E+14	2.20E+08	5.65E+10	8.56E+07	6.60E+02	1.17E+09	7.10E+06	3.50E+13

TABLE B-2 (Cont.)

44 90.000 .00104 186.90 .00 7.13E+13 6.07E+07 2.35E+10 5.08E+07 9.64E+01 7.14E+08 2.40E+06 1.49E+13
 45 95.000 .00076 188.40 .00 2.92E+13 1.58E+07 9.65E+09 2.05E+07 1.30E+01 3.00E+08 7.05E+05 6.02E+12
 46 100.000 .00032 195.10 .00 1.19E+13 4.04E+06 3.92E+09 4.76E+06 1.97E+00 1.25E+08 2.55E+05 2.30E+12

CASE 2A: GIVEN H1, H2, ANGLE

SLANT PATH PARAMETERS IN STANDARD FORM

H1 = .000 KM
 H2 = 20.000 KM
 ANGLE = .000 DEG
 PHI = 100.000 DEG
 HMIN = .000 KM
 LEN = 0

HALFWIDTH INFORMATION ON THE USER SUPPLIED FASCODE BOUNDARIES

THE FOLLOWING VALUES ARE ASSUMED:
 ALZERO = .100 CM-1 = AVERAGE LORENTZ WIDTH AT STP
 AVNUT = 36.00 = AVERAGE MOLECULAR WEIGHT
 VBAR = 905.00 CM-1 = AVERAGE WAVELENGTH

I	Z (KM)	P (MB)	T (K)	LORENTZ (CM-1)	DOPPLER (CM-1)	ZETA	VOIGT (CM-1)	VOIGT RATIO	TEMP DIFF (K)
1	.000	1013.00000	288.20	.10132	.00092	.991	.10133	1.10	9.8
2	1.500	845.00000	278.45	.00081	.00090	.998	.00602	1.10	9.8
3	3.000	701.00000	268.70	.07263	.00089	.988	.02264	1.19	9.8
4	4.500	577.29741	258.95	.06091	.00087	.986	.06093	1.20	9.8
5	6.000	472.20000	249.20	.05073	.00085	.983	.05080	1.21	9.8
6	7.500	382.82783	239.45	.04201	.00084	.980	.04202	1.22	9.8
7	9.000	308.00000	229.70	.03451	.00082	.977	.03453	1.25	10.3
8	10.000	241.49818	219.40	.02760	.00080	.972	.02771	1.98	2.7
9	15.000	121.10000	216.70	.01397	.00080	.946	.01401	1.98	0
10	19.400	60.74078	216.70	.00701	.00080	.898	.00710	1.90	3.0
11	24.000	29.72000	220.60	.00340	.00080	.809	.00358	2.01	5.6
12	29.700	12.52214	226.20	.00141	.00081	.635	.00178	1.50	11.1
13	35.300	5.52596	237.27	.00061	.00083	.423	.00119	1.15	11.3
14	39.400	3.13644	240.60	.00034	.00085	.284	.00104	1.07	11.5
15	43.500	1.81014	260.06	.00019	.00087	.100	.00097	1.09	1.2
16	55.700	.30733	250.07	.00004	.00087	.045	.00089	1.04	12.4
17	60.200	.21297	246.45	.00002	.00085	.026	.00086	1.03	12.6
18	64.000	.11208	233.85	.00001	.00083	.015	.00083	1.03	12.9
19	69.500	.05619	220.97	.00001	.00080	.008	.00081	1.03	13.2
20	75.300	.02224	207.01	.00000	.00078	.003	.00078	1.04	13.5
21	82.200	.00720	194.33	.00000	.00075	.001	.00075	1.00	.0
22	100.000	.00032	195.10	.00000	.00075	.000	.00075	.00	.0

TABLE B-2 (Cont.)

CALCULATION OF THE REFRACTED PATH THROUGH THE ATMOSPHERE

I	ALTITUDE FROM (KM)	TO (KM)	THETA (DEG)	DRANGE (KM)	RANGE (KM)	DBETA (DEG)	BETA (DEG)	PHI (DEG)	DBEND (DEG)	BENDING (DEG)	PBAR (MB)	TBAR (K)	RHOBAR (MOL CM-3)
H1 TO H2													
1	1.000	1.000	.000	1.000	1.000	.000	.000	180.000	.000	.000	955.603	284.930	2.43E+19
2	1.000	1.500	.000	.500	1.500	.000	.000	180.000	.000	.000	872.802	280.005	2.25E+19
3	1.500	2.000	.000	.500	2.000	.000	.000	180.000	.000	.000	820.105	276.835	2.15E+19
4	2.000	3.000	.000	1.000	3.000	.000	.000	180.000	.000	.000	747.913	271.992	1.99E+19
5	3.000	4.000	.000	1.000	4.000	.000	.000	180.000	.000	.000	658.727	265.493	1.80E+19
6	4.000	4.500	.000	.500	4.500	.000	.000	180.000	.000	.000	596.908	260.586	1.66E+19
7	4.500	5.000	.000	.500	5.000	.000	.000	180.000	.000	.000	558.068	257.336	1.57E+19
8	5.000	6.000	.000	1.000	6.000	.000	.000	180.000	.000	.000	506.204	252.435	1.45E+19
9	6.000	7.000	.000	1.000	7.000	.000	.000	180.000	.000	.000	441.516	245.956	1.30E+19
10	7.000	7.500	.000	.500	7.500	.000	.000	180.000	.000	.000	396.932	241.007	1.19E+19
11	7.500	8.000	.000	.500	8.000	.000	.000	180.000	.000	.000	369.634	237.037	1.13E+19
12	8.000	9.000	.000	1.000	9.000	.000	.000	180.000	.000	.000	332.137	232.999	1.03E+19
13	9.000	10.000	.000	1.000	10.000	.000	.000	180.000	.000	.000	286.399	226.550	9.14E+18
14	10.000	10.500	.000	.500	10.500	.000	.000	180.000	.000	.000	253.215	221.369	8.20E+18
15	10.500	11.000	.000	.500	11.000	.000	.000	180.000	.000	.000	234.235	218.189	7.70E+18
16	11.000	12.000	.000	1.000	12.000	.000	.000	180.000	.000	.000	210.499	216.751	7.02E+18
17	12.000	13.000	.000	1.000	13.000	.000	.000	180.000	.000	.000	179.908	216.700	6.00E+18
18	13.000	14.000	.000	1.000	14.000	.000	.000	180.000	.000	.000	153.758	216.700	5.13E+18
19	14.000	15.000	.000	1.000	15.000	.000	.000	180.000	.000	.000	131.408	216.700	4.30E+18
20	15.000	16.000	.000	1.000	16.000	.000	.000	180.000	.000	.000	112.308	216.700	3.75E+18
21	16.000	17.000	.000	1.000	17.000	.000	.000	180.000	.000	.000	96.000	216.700	3.20E+18
22	17.000	18.000	.000	1.000	18.000	.000	.000	180.000	.000	.000	82.075	216.700	2.74E+18
23	18.000	19.000	.000	1.000	19.000	.000	.000	180.000	.000	.000	70.168	216.700	2.34E+18
24	19.000	19.400	.000	.400	19.400	.000	.000	180.000	.000	.000	62.705	216.700	2.10E+18
25	19.400	20.000	.000	.600	20.000	.000	.000	180.000	.000	.000	58.015	216.700	1.94E+18

TABLE B-2 (Cont.)

INTEGRATED ABSORBER AMOUNTS BY LAYER

I	LAYER BOUNDARIES		INTEGRATED AMOUNTS (MOL CM-2)										O2		
	FROM	TO	AIR	H2O	CO2	O3	N2O	CO	CH4						
1	1.000	1.000	2.426E+24	1.673E+22	8.014E+20	6.779E+16	7.773E+17	3.583E+17	4.129E+18	5.076E+23					
2	1.000	1.500	1.127E+24	6.410E+21	3.723E+20	3.390E+16	3.610E+17	1.622E+17	1.918E+18	2.358E+23					
3	1.500	2.000	1.073E+24	5.377E+21	3.542E+20	3.389E+16	3.435E+17	1.516E+17	1.825E+18	2.244E+23					
4	2.000	3.000	1.990E+24	7.711E+21	6.570E+20	6.323E+16	6.378E+17	2.738E+17	3.384E+18	4.161E+23					
5	3.000	4.000	1.795E+24	4.751E+21	5.926E+20	6.019E+16	5.747E+17	2.380E+17	3.053E+18	3.753E+23					
6	4.000	4.500	8.293E+23	1.611E+21	2.730E+20	2.886E+16	2.655E+17	1.079E+17	1.411E+18	1.734E+23					
7	4.500	5.000	7.862E+23	1.229E+21	2.596E+20	2.885E+16	2.518E+17	1.023E+17	1.337E+18	1.644E+23					
8	5.000	6.000	1.450E+24	1.680E+21	4.780E+20	5.789E+16	4.643E+17	1.886E+17	2.467E+18	3.033E+23					
9	6.000	7.000	1.298E+24	9.506E+20	4.287E+20	5.895E+16	4.157E+17	1.657E+17	2.200E+18	2.715E+23					
10	7.000	7.500	5.260E+23	2.062E+20	1.965E+20	3.222E+16	1.905E+17	7.383E+16	1.013E+18	1.247E+23					
11	7.500	8.000	5.626E+23	2.315E+20	1.858E+20	3.216E+16	1.802E+17	6.827E+16	9.559E+17	1.177E+23					
12	8.000	9.000	1.031E+24	2.501E+20	3.405E+20	7.657E+16	3.295E+17	1.187E+17	1.749E+18	2.156E+23					
13	9.000	10.000	9.142E+23	9.979E+19	3.019E+20	1.006E+17	2.916E+17	9.689E+16	1.545E+18	1.912E+23					
14	10.000	10.600	4.960E+23	2.079E+19	1.641E+20	7.582E+16	1.575E+17	4.820E+16	8.363E+17	1.039E+23					
15	10.600	11.000	3.111E+23	1.289E+19	1.027E+20	6.067E+16	9.799E+16	2.862E+16	5.220E+17	6.506E+22					
16	11.000	12.000	7.020E+23	1.891E+19	2.310E+20	1.813E+17	2.199E+17	5.973E+16	1.172E+18	1.468E+23					
17	12.000	13.000	6.001E+23	8.815E+18	1.982E+20	2.870E+17	1.845E+17	4.350E+16	9.931E+17	1.255E+23					
18	13.000	14.000	5.128E+23	4.211E+18	1.694E+20	2.256E+17	1.552E+17	2.944E+16	8.394E+17	1.073E+23					
19	14.000	15.000	4.383E+23	2.396E+18	1.447E+20	2.507E+17	1.307E+17	1.971E+16	7.886E+17	9.166E+22					
20	15.000	16.000	3.746E+23	1.675E+18	1.237E+20	2.819E+17	1.091E+17	1.308E+16	5.974E+17	7.834E+22					
21	16.000	17.000	3.202E+23	1.250E+18	1.057E+20	3.256E+17	9.072E+16	8.809E+15	5.024E+17	6.697E+22					
22	17.000	18.000	2.738E+23	1.051E+18	9.040E+19	3.759E+17	7.473E+16	6.156E+15	4.211E+17	5.725E+22					
23	18.000	19.000	2.340E+23	8.986E+17	7.720E+19	4.200E+17	6.809E+16	4.085E+15	3.515E+17	4.894E+22					
24	19.000	19.400	8.381E+22	3.237E+17	2.767E+19	1.706E+17	2.092E+16	1.223E+15	1.232E+17	1.753E+22					
25	19.400	20.000	1.163E+23	4.519E+17	3.839E+19	2.791E+17	2.807E+16	1.580E+15	1.676E+17	2.431E+22					
TOTAL	.000	20.000	2.034E+25	4.737E+22	6.710E+21	3.538E+18	6.412E+18	2.369E+18	3.423E+19	4.255E+24					

TABLE B-2 (Cont.)

SUMMARY OF THE GEOMETRY CALCULATION

MODEL = U. S. STANDARD, 1976
 H1 = .000 KM
 H2 = 20.000 KM
 ANGLE = .000 DEG
 RANGE = 20.000 KM
 BETA = .000 DEG
 PHI = 180.000 DEG
 RHIN = .000 KM
 BEND:MG = .000 DEG
 LEN = 0
 AIRMAS = .945 RELATIVE TO A VERTICAL PATH, GROUND TO SPACE

FINAL SET OF LAYERS FOR INPUT TO FASCODE

A LAYER AMOUNT MAY BE SET TO ZERO IF THE CUMULATIVE AMOUNT FOR THAT LAYER AND ABOVE IS LESS THAN 0.1 PERCENT OF THE TOTAL AMOUNT. THIS IS DONE ONLY FOR THE FOLLOWING CASES
 1. IEMIT = 0 (TRANSMITTANCE)
 2. IEMIT = 1 (RADIANCE) AND IPATH = 3 (PATH LOOKING UP)

O2 IS NOT INCLUDED

IF THE AMOUNTS FOR ALL THE MOLECULES BUT O2 ARE ZEROED, THE REMAINING LAYERS ARE ELIMINATED

L	LAYER BOUNDARIES FROM (KM)	TO (KM)	IPATH (MB)	PBAR	TBAR	(K)	AIR	H2O	CO2	O3	N2O	CO	CH4	O2
1	.000	1.500	3	929.14827	283.43	3.55E+24	2.31E+22	1.17E+21	1.02E+17	1.14E+18	5.20E+17	6.05E+18	7.43E+23	
2	1.500	3.000	3	773.19998	273.69	3.00E+24	1.30E+22	1.01E+21	9.91E+16	9.81E+17	4.25E+17	5.21E+18	6.40E+23	
3	3.000	4.500	3	639.19247	263.94	2.62E+24	6.36E+21	8.66E+20	8.91E+16	8.40E+17	3.46E+17	4.46E+18	5.49E+23	
4	4.500	6.000	3	524.71482	254.20	2.24E+24	2.90E+21	7.38E+20	8.60E+16	7.16E+17	2.91E+17	3.80E+18	4.68E+23	
5	6.000	7.500	3	427.48751	244.45	1.89E+24	1.26E+21	6.26E+20	9.02E+16	6.07E+17	2.40E+17	3.22E+18	3.96E+23	
6	7.500	9.000	3	345.37569	234.71	1.59E+24	4.90E+20	5.26E+20	1.09E+17	5.10E+17	1.87E+17	2.70E+18	3.33E+23	
7	9.000	10.600	3	274.71517	224.73	1.41E+24	1.29E+20	4.66E+20	1.76E+17	4.49E+17	1.44E+17	2.38E+18	2.95E+23	
8	10.600	15.000	3	181.34791	216.80	2.56E+24	4.72E+19	8.47E+20	9.25E+17	7.87E+17	1.81E+17	4.24E+18	5.36E+23	
9	15.000	19.400	3	90.91292	216.70	1.29E+24	5.20E+18	4.35E+20	1.50E+18	3.56E+17	3.34E+16	2.00E+18	2.69E+23	
10	19.400	20.000	3	59.01539	216.70	1.16E+23	0.52E+17	3.84E+19	2.79E+17	2.81E+16	1.50E+15	1.60E+17	2.43E+22	

TABLE B-2 (Cont.)

V1(CM-1) = 900.0000
 V2(CM-1) = 910.0000
 SAMPLE = 4.0000
 DVSET = .000000
 ALFAL0 = .1000
 AVMASS = 36.0000
 DPTMIN = .0000E+00
 TBOUND = .0000
 DPTFAC = .000000
 BOUNDARY EMISSIVITY = 1.000000
 SECANT = 1.0000

AER TEST CASE - MULTIPLE SCATTERING - RURAL AEROSOL * 900 - 910 CM-1 FASCO02 06/07/15 16.04.54													
LAYER	P(MB)	T(K)	ALPHL	ALPHD	ALPHV	ZETA	CALC DV	H2OSLF	DV	TYPE	ITYPE	IPATH	SECANT
1	.00 TO 1.50 KM	283.43	.096174	.000009	.096103	.991	.024046	1.0260	.024000	.000	99	3	1.000000
2	1.50 TO 3.00 KM	273.59	.080730	.000094	.080740	.989	.020105	1.0170	.024000	1.109	0	3	1.000000
3	3.00 TO 4.50 KM	263.94	.067469	.000070	.067400	.987	.016070	1.0097	.016000	1.423	2	3	1.000000
4	4.50 TO 6.00 KM	254.20	.056185	.000061	.056190	.985	.014049	1.0052	.016000	1.139	0	3	1.000000
5	6.00 TO 7.50 KM	244.45	.046561	.000045	.046576	.982	.011644	1.0027	.010667	1.374	2	3	1.000000
6	7.50 TO 9.00 KM	234.71	.030335	.000028	.030353	.979	.009588	1.0012	.010667	1.112	0	3	1.000000
7	9.00 TO 10.60 KM	224.73	.031135	.000010	.031156	.975	.007789	1.0004	.007111	1.369	2	3	1.000000
8	10.60 TO 15.00 KM	216.00	.020015	.0000795	.020046	.963	.005236	1.0001	.004741	1.358	2	3	1.000000
9	15.00 TO 19.40 KM	216.70	.010489	.0000795	.010549	.930	.002637	1.0000	.002370	1.798	1	3	1.000000
10	19.40 TO 20.00 KM	216.70	.006594	.0000795	.006787	.894	.001697	1.0000	.001500	1.397	2	3	1.000000

TABLE B-2 (Cont.)

AER TEST CASE - MULTIPLE SCATTERING - RURAL AEROSOL * 900 - 910 CM-1 FASCODE2 86/07/15 16.04.54										
	P (MB)	T (K)	IPATH	H2O	CO2	MOLECULAR AMOUNTS (MOL/CM**2) BY LAYER	CO	CH4	O2	OTHER
1	.00 TO 1.50 KM	283.43	3	2.314E+22	1.174E+21	1.017E+17	1.130E+18	5.205E+17	6.047E+18	7.434E+23 2.706E+24
2	1.50 TO 3.00 KM	273.69	3	1.304E+22	1.011E+21	9.912E+16	9.806E+17	4.254E+17	5.209E+18	6.404E+23 2.408E+24
3	3.00 TO 4.50 KM	263.94	3	6.362E+21	8.665E+20	8.905E+16	8.402E+17	3.459E+17	4.464E+18	5.408E+23 2.060E+24
4	4.50 TO 6.00 KM	254.20	3	2.897E+21	7.385E+20	8.595E+16	7.161E+17	2.909E+17	3.804E+18	4.677E+23 1.765E+24
5	6.00 TO 7.50 KM	244.45	3	1.265E+21	6.256E+20	9.016E+16	6.066E+17	2.395E+17	3.221E+18	3.962E+23 1.496E+24
6	7.50 TO 9.00 KM	234.71	3	4.895E+20	5.263E+20	1.087E+17	5.101E+17	1.870E+17	2.705E+18	3.333E+23 1.259E+24
7	9.00 TO 10.50 KM	224.73	3	1.385E+20	4.660E+20	1.764E+17	4.491E+17	1.443E+17	2.382E+18	2.951E+23 1.115E+24
8	10.50 TO 15.00 KM	216.00	3	4.721E+19	8.469E+20	9.253E+17	7.070E+17	1.810E+17	4.235E+18	5.363E+23 2.027E+24
9	15.00 TO 19.40 KM	216.78	3	5.198E+18	4.249E+20	1.502E+16	3.564E+17	3.335E+16	1.996E+18	2.690E+23 1.017E+24
10	19.40 TO 20.00 KM	216.70	3	4.519E+17	3.839E+19	2.791E+17	2.807E+16	1.580E+15	1.576E+17	2.431E+22 9.191E+22
ACCUMULATED MOLECULAR AMOUNTS FOR TOTAL PATH										
10	.00 TO 20.00 KM	251.73		4.737E+22	6.710E+21	3.530E+18	6.412E+18	2.369E+18	3.423E+19	4.255E+24 1.603E+25

LINE FILE INFORMATION

LINE FILE FOR FASCODE2 PKG FOR 800 - 1199 CM-1

8CDMRG2 86/03/25 12.55.52

H2O = 814
 CO2 = 2008
 O3 = 19025
 N2O = 721
 CO = 0
 CH4 = 226
 O2 = 0
 .0000E+00

LOWEST LINE = 800.000

HIGHEST LINE = 1199.905

TOTAL NUMBER OF LINES = 22794

TABLE B-2 (Cont.)

AER TEST CASE - MULTIPLE SCATTERING - RURAL AEROSOL - 900 - 910 CH-1 FASCODE 86/87/15 16.84.54
 LAYER - 1
 ***** CONTINUA: H2O(T), CO2, N2 (31 JULY 82)
 02(1600CM-1), 03(101FUSE-T), H2O SELF HAS BEEN REDUCED IN THE 800-1200 CM-1 REGION (81 SEPT 1988)

L8LF4 -
 DV FOR L8LF4 = 1.53688 BOUND FOR L8LF4 = 25.8888
 NO. LINES BEFORE SHRINK = 659. NO. LINES AFTER SHRINK = 1148. NO. LINES AFTER REJECT = 114
 TIME 72.612 READ CONVOLUTION .538 PANEL .881
 MIRAC1
 OUTPUT ON FILE 18 DV = .0248888 BOUND(31CM-1) = 6.1248
 LOCATION WAVENUMBER OPT. DEPTH

1825	988.888888	.43862368E-01	1438	989.912888	.52997347E-01
1826	988.824888	.43873529E-01	1439	989.936888	.52234962E-01
1827	988.808888	.43887166E-01	1440	989.960888	.51996562E-01
1828	988.872888	.43983231E-01	1441	989.984888	.52289131E-01
1829	988.896888	.43923428E-01	1442	918.888888	.53181751E-01

TIME 72.758 READ CONVOLUTION .885 PANEL .887
 ----- 14 HALF WIDTH CHANGES
 AVERAGE WIDTH = .862977. AVERAGE ZETA = .982264. NO. LINES = 321. NO. LINES AFTER REJECT = 321. NO. HV CHANGES = 14

AER TEST CASE - MULTIPLE SCATTERING - RURAL AEROSOL - 900 - 910 CH-1 FASCODE 86/87/15 16.84.54

TIME AT THE START OF --EMINIT-- 72.778

INITIAL LAYER 1 FINAL LAYER 1

FILE 25 MERGED WITH FILE 18 ONTO FILE 23 WITH XTYPE = 5.

INITIAL LAYER 1 FINAL LAYER 1

FILE 18 MERGED WITH FILE 11 ONTO FILE

LOCATION WAVENUMBER RADIANCE TRANSMITTANCE

1	988.888888	.61784845E-06	.88682463E+00	414	989.912888	.68365738E-06	.87688888E+00
2	988.824888	.61794864E-06	.88681474E+00	415	989.936888	.67752379E-06	.87746871E+00
3	988.808888	.61805285E-06	.88680271E+00	416	989.960888	.67556485E-06	.87767792E+00
4	926.872888	.61818611E-06	.88598842E+00	417	989.984888	.67795977E-06	.87742118E+00
5	988.896888	.61835301E-06	.88597853E+00	418	918.888888	.68456245E-06	.87668722E+00

LOCATION WAVENUMBER COMP FLUX UP COMP REFLECT UP

LOCATION WAVENUMBER COMP FLUX UP COMP REFLECT UP

TABLE B-2 (Cont.)

AER TEST CASE - MULTIPLE SCATTERING - RURAL AEROSOL * 900 - 910 CH-1 FASCDZ 86/87/15 16.04.54

LAYER = 2

***** CONTINUA: H2O(T), CO2(N2 (31 JULY 82)

O2(1688CM-1), O3(DIFFUSE,T), H2O SELF HAS BEEN REDUCED IN THE 800-1200 CM-1 REGION (31 SEP 1986)

LBLF4 = 1.53600 BOUND FOR LBLF4 = 25.0000

NO. LINES BEFORE SHRINK = 659. NO. LINES AFTER SHRINK = 148. NO. LINES AFTER REJECT = 144

TIME READ CONVOLUTION PANEL

72.932 .026 .000

OUTPUT ON FILE 10 DV = .02400000 BOUND(31CM-1) = 6.1400

LOCATION WAVENUMBER OPT. DEPTH LOCATION WAVENUMBER OPT. DEPTH

1025	900.000000	.17204370E-01	1438	909.912000	.20542306E-01
1026	900.024000	.17209253E-01	1439	909.936000	.20243310E-01
1027	900.048000	.17216103E-01	1440	909.960000	.20223959E-01
1028	900.072000	.17226114E-01	1441	909.984000	.20501043E-01
1029	900.096000	.17239097E-01	1442	910.008000	.20920112E-01

TIME READ CONVOLUTION PANEL

73.852 .013 .007

----- 17 HALF WIDTH CHANGES

AVERAGE WIDTH = .053895. AVERAGE ZETA = .979547. NO. LINES = 1321. NO. LINES AFTER REJECT = 321. NO. HW CHANGES = 17

AER TEST CASE - MULTIPLE SCATTERING - RURAL AEROSOL * 900 - 910 CH-1 FASCDZ 86/87/15 16.04.54

THE TIME AT THE START OF RADMRG IS 73.866

INITIAL LAYER 1 FINAL LAYER 2

FILE 10 MERGED WITH FILE 11 ONTO FILE 12

CNTRL AND IANT 3

LOCATION WAVENUMBER RADIANCE TRANSMITTANCE

1	900.000000	.75756060E-06	.86289760E+00	84112338E-06	.85093451E+00
2	900.024000	.75760397E-06	.86288375E+00	83317599E-06	.85103822E+00
3	900.048000	.75784002E-06	.86286512E+00	83115099E-06	.85205701E+00
4	900.072000	.75803709E-06	.86284358E+00	83527004E-06	.85157257E+00
5	900.096000	.75820060E-06	.86281495E+00	84445302E-06	.85005170E+00

LOCATION WAVENUMBER COMP FLUX UP COMP REFLECT UP

1	900.000000	.30010060E-04	.13672041E-01	414	909.912000	.29462067E-04	.13709410E-01
---	------------	---------------	---------------	-----	------------	---------------	---------------

TABLE B-2 (Cont.)

2 988.824000 .38813749E-04 .1367263E-01 .13737762E-01
 3 988.840000 .38818675E-04 .13671830E-01 .13743334E-01
 4 988.872000 .38818576E-04 .13671865E-01 .1375211E-01
 5 988.896000 .38818443E-04 .13670990E-01 .13688995E-01

THE TIME AT THE END OF RADMRG IS 73.138
 .872 SECS WERE REQUIRED FOR THIS MERGE

AER TEST CASE - MULTIPLE SCATTERING - RURAL AEROSOL * 988 - 918 CM-1 FASC002 86/87/15 16.84.54
 LAYER = 3
 ***** CONTINUA: H2O(T), CO2, N2 (01 JULY 82)
 O2(1688CM-1), O3(DIFFUSE,T), H2O SELF HAS BEEN REDUCED IN THE 888-1208 CM-1 REGION (01 SEPT 1985)

L8LF4 *
 DV FOR L8LF4 = 1.82400 SOUND FOR L8LF4 = 25.8888
 NO. LINES BEFORE SHRINK = 647, NO. LINES AFTER SHRINK = 189, NO. LINES AFTER REJECT = 179

TIME READ CONVOLUTION PANEL
 73.258 .827 .881

HIRACI
 OUTPUT ON FILE 16 DV = .81688888 SOUND F3(CM-1) = 4.8968
 LOCATION WAVENUMBER OPT. DEPTH
 1825 988.888888 .58995146E-02 1646 989.936888 .61512844E-02
 1836 988.816888 .51885681E-02 1647 989.952888 .6186761E-02
 1847 988.832888 .51821875E-02 1648 989.968888 .62111488E-02
 1858 988.848888 .5184555E-02 1649 989.984888 .63469378E-02
 1869 988.864888 .51881618E-02 1658 918.888888 .65153316E-02

TIME READ CONVOLUTION PANEL
 73.364 .814 .888
 ----- 11 HALF WIDTH CHANGES

AVERAGE WIDTH = .845278, AVERAGE ZETA = .975949, NO. LINES = 248, NO. LINES AFTER REJECT = 248, NO. HV CHANGES = 11

AER TEST CASE - MULTIPLE SCATTERING - RURAL AEROSOL * 988 - 918 CM-1 FASC002 86/87/15 16.84.54

THE TIME AT THE START OF RADMRG IS 73.379

INITIAL LAYER 1 FINAL LAYER 3

FILE 10 MERGED WITH FILE 12 ONTO FILE 11
 CNTRL AND TANT 3 0

LOCATION	WAVENUMBER	PADIANCE	TRANSMITTANCE	LOCATION	WAVENUMBER	PADIANCE	TRANSMITTANCE
1	988.888888	.78793664E-06	.65818816E-08	622	989.936888	.86817319E-06	.84629824E-08
2	988.816888	.78801628E-06	.85817899E-08	623	989.952888	.86614973E-06	.84652430E-08
3	988.832888	.7881158E-06	.85816579E-08	624	989.968888	.86723157E-06	.84637788E-08
4	988.848888	.78824286E-06	.85815253E-08	625	989.984888	.87587384E-06	.84533696E-08
5	988.864888	.78838896E-06	.85813518E-08	626	918.888888	.87677568E-06	.84519462E-08

LOCATION	WAVENUMBER	COMP FLUX UP	COMP REFLECT UP
622	989.936888	.86817319E-06	.84629824E-08
623	989.952888	.86614973E-06	.84652430E-08
624	989.968888	.86723157E-06	.84637788E-08
625	989.984888	.87587384E-06	.84533696E-08
626	918.888888	.87677568E-06	.84519462E-08

TABLE B-2 (Cont.)

1 900.000000 .2996320E-04 .13429722E-01 622 909.936000 .29409933E-04 .13445045E-01
 2 900.016000 .29963245E-04 .13429416E-01 623 909.952000 .29410783E-04 .13451417E-01
 3 900.032000 .29963187E-04 .13429081E-01 624 909.968000 .29409700E-04 .13443620E-01
 4 900.048000 .29963114E-04 .13428495E-01 625 909.984000 .29408411E-04 .13410870E-01
 5 900.064000 .29963020E-04 .13427850E-01 626 910.000000 .29403022E-04 .13403054E-01

THE TIME AT THE END OF RADMRG IS 73.483
 .104 SECS WERE REQUIRED FOR THIS MERGE

AER TEST CASE - MULTIPLE SCATTERING - RURAL AEROSOL * 900 - 910 CM-1 FASCODE2 86/87/15 16.04.54

LAYER = 4

***** CONTINUA: H2O(1), CO2, N2 (01 JULY 82)

02(1600CM-1), 03(DIFFUSE,T), H2O SELF HAS BEEN REDUCED IN THE 800-1200 CM-1 REGION (01 SEPT 1985)

LBFL4 * 1.02400 BOUND FOR LBFL4 = 25.0000

NO. LINES BEFORE SHRINK = 647. NO. LINES AFTER SHRINK = 109. NO. LINES AFTER REJECT = 179

TIME READ CONVOLUTION PANEL
 73.599 .026 .000

OUTPUT ON FILE 10 DV = .01688200 ROUND(3(CM-1)) = 3.0960

LOCATION	WAVENUMBER	OPT. DEPTH	LOCATION	WAVENUMBER	OPT. DEPTH
1025	900.000000	.13332791E-02	1646	909.936000	.16636445E-02
1026	900.016000	.13333825E-02	1647	909.952000	.16741265E-02
1027	900.032000	.13338344E-02	1648	909.968000	.17201954E-02
1028	900.048000	.13350451E-02	1649	909.984000	.18063762E-02
1029	900.064000	.13369103E-02	1650	910.000000	.19391071E-02

TIME READ CONVOLUTION PANEL
 73.709 .015 .000

----- 15 HALF WIDTH CHANGES

AVERAGE WIDTH = .038333. AVERAGE ZETA = .972097. NO. LINES = 240. NO. LINES AFTER REJECT = 240. NO. HV CHANGES = 15

AER TEST CASE - MULTIPLE SCATTERING - RURAL AEROSOL * 900 - 910 CM-1 FASCODE2 86/87/15 16.04.54

THE TIME AT THE START OF RADMRG IS 73.724

INITIAL LAYER 1 FINAL LAYER 4

FILE 10 MERGED WITH FILE 11 ONTO FILE 12
 CNTRL AND TANT 3 8

LOCATION	WAVENUMBER	RADIANCE	TRANSMITTANCE	LOCATION	WAVENUMBER	RADIANCE	TRANSMITTANCE
1	900.000000	.79474547E-06	.05691011E-00	622	909.936000	.87610964E-06	.04475063E-00
2	900.016000	.79482551E-06	.05690086E-00	623	909.952000	.87421596E-06	.04497517E-00
3	900.032000	.79493790E-06	.05688030E-00	624	909.968000	.87549063E-06	.04470947E-00
4	900.048000	.79505510E-06	.05687303E-00	625	909.984000	.88422250E-06	.04367647E-00
5	900.064000	.79511044E-06	.05685402E-00	626	910.000000	.88399596E-06	.04342146E-00

LOCATION	WAVENUMBER	COMP FLUX UP	COMP REFLECT UP	LOCATION	WAVENUMBER	COMP FLUX UP	COMP REFLECT UP
1	900.000000	.20946047E-04	.13366305E-01	622	909.936000	.29109157E-04	.13366577E-01

TABLE B-2 (Cont.)

2 988.816000 .29946800E-04 .13366841E-01
 3 988.872000 .29945930E-04 .13365670E-01
 4 988.878000 .29945853E-04 .13365800E-01
 5 988.864000 .29945738E-04 .13364319E-01

THE TIME AT THE END OF RADNRG IS 73.822
 .298 SECS WERE REQUIRED FOR THIS MERGE

AER TEST CASE - MULTIPLE SCATTERING - RURAL AEROSOL - 988 - 918 CM-1 FASC002 86/87/15 16.84.54

LAYER = 5

***** CONTINUA: H2O(T), CO2, H2 (81 JULY 82)

02(168CM-1), O3(DIFFUSE,T), H2O SELF HAS BEEN REDUCED IN THE 888-1288 CM-1 REGION (81 SEPT 1985)

LBLF4 " .68267 BOUND FOR LBLF4 = 25.8888

NO. LINES BEFORE SHRINK = 638. NO. LINES AFTER SHRINK = 234. NO. LINES AFTER REJECT = 219

TIME READ CONVOLUTION PANEL
 -- 959 .026 .088

WIRAC:

OUTPUT ON FILE 18 DV = .81866667 BOUND(3)(CM-1) = 2.7387

LOCATION WAVENUMBER OPT. DEPTH

1825	988.888000	.32966666E-03	1958	989.952000	.44623824E-03
1826	988.818550	.32964266E-03	1959	989.962667	.46848285E-03
1827	988.821333	.32949959E-03	1960	989.973333	.48568193E-03
1828	988.832000	.32961897E-03	1961	989.984000	.52292947E-03
1829	988.842667	.32991837E-03	1962	989.994567	.59472198E-03

TIME READ CONVOLUTION PANEL
 -- 4.863 .013 .012

----- 1: HALF WIDTH CHANGES

AVERAG WIDTH = .231216. AVERAGE ZETA = .964637. NO. LINES = 192. NO. LINES AFTER REJECT = 192. NO. HV CHANGES = 11

AER TEST CASE - MULTIPLE SCATTERING - RURAL AEROSOL - 988 - 918 CM-1 FASC002 86/87/15 16.84.54

THE TIME AT THE START OF RADNRG IS 74.876

INITIAL LAYER : FINAL LAYER 5

FILE IS MERGED WITH FILE 12 ONTO FILE 11
 CENTRE ANGLE 3

LOCATION WAVENUMBER RADIANCE TRANSMITTANCE

1	988.888000	.79635871E-06	.85653588E-08	934	989.952000	.87619631E-06	.84450768E-08
2	988.818667	.79640090E-06	.85653849E-08	935	989.962667	.87645349E-06	.84448999E-08
3	988.821333	.79647188E-06	.85652382E-08	936	989.973333	.88651167E-06	.84393278E-08
4	988.832000	.79654644E-06	.85651422E-08	937	989.984000	.88758159E-06	.84381921E-08
5	988.842667	.79662934E-06	.85658151E-08	938	989.994567	.88775928E-06	.84295869E-08

LOCATION WAVENUMBER COMP FLUX UP COMP REFLECT UP

LOCATION WAVENUMBER COMP FLUX UP COMP REFLECT UP

TABLE B-2 (Cont.)

1 900.000000 .29939846E-04 .13350864E-01 934 909.952000 .29382149E-04 .13350943E-01
 2 900.010667 .29939823E-04 .13349912E-01 935 909.962667 .29381295E-04 .13346148E-01
 3 900.021333 .29939800E-04 .13349622E-01 936 909.973333 .29378045E-04 .13327617E-01
 4 900.032000 .29939777E-04 .13349335E-01 937 909.984000 .29377065E-04 .13324134E-01
 5 900.042667 .29939683E-04 .13348985E-01 938 909.994667 .29372701E-04 .13290828E-01

THE TIME AT THE END OF RADWRG IS 74.222
 .146 SECS WERE REQUIRED FOR THIS MERGE

AER TEST CASE - MULTIPLE SCATTERING - RURAL AEROSOL - 900 - 910 CM-1 FASCODE2 86/87/15 16.84.54

LAYER = 6

CONTINUA: H2O(I7), CO2(M2) (01 JULY 82)

02(150CM-1), O3(DIFFUSE,T), H2O SELF HAS BEEN REDUCED IN THE 800-1200 CM-1 REGION (01 SEPT 1985)

L8LF4 * BOUND FOR L8LF4 = 25.0000

DV FOR L8LF4 = .68267 BOUND FOR L8LF4 = 25.0000
 NO. LINES BEFORE SHRINK = 638. NO. LINES AFTER SHRINK = 234. NO. LINES AFTER REJECT = 219

TIME READ CONVOLUTION PANEL
 74.364 .076 .052 .000

OUTPUT ON FILE 10 DV = .01066667 BOUND F3(CM-1) = 2.7307

LOCATION	WAVENUMBER	OPT. DEPTH	LOCATION	WAVENUMBER	OPT. DEPTH
1025	900.000000	.0008145E-04	1958	909.952000	.17095818E-03
1026	900.010667	.00091934E-04	1959	909.962667	.11617515E-03
1027	900.021333	.00083454E-04	1960	909.973333	.12820501E-03
1028	900.032000	.00094544E-04	1961	909.984000	.14913507E-03
1029	900.042667	.00092499E-04	1962	909.994667	.18566756E-03

TIME READ CONVOLUTION PANEL
 74.457 .074 .048 .011

----- 15 HALF WIDTH CHANGES

AVERAGE WIDTH = .026035. AVERAGE ZETA = .958691. NO. LINES = 192. NO. LINES AFTER REJECT = 192. NO. HV CHANGES = 15

AER TEST CASE - MULTIPLE SCATTERING - RURAL AEROSOL - 900 - 910 CM-1 FASCODE2 86/87/15 16.84.54

THE TIME AT THE START OF RADWRG IS 74.471

INITIAL LAYER 1 FINAL LAYER 6

FILE 10 MERGED WITH FILE 11 ONTO FILE 12
 CTRL AND LANT 3 2

LOCATION	WAVENUMBER	RADIANCE	TRANSMITTANCE	LOCATION	WAVENUMBER	RADIANCE	TRANSMITTANCE
1	900.000000	.79671390E-06	.85643253E-00	934	909.952000	.87663667E-06	.8437320E-00
2	900.010667	.79670903E-06	.85642759E-00	935	909.962667	.87692450E-06	.8438085E-00
3	900.021333	.79682414E-06	.85642029E-00	936	909.973333	.88101697E-06	.8438223E-00
4	900.032000	.79689680E-06	.85641149E-00	937	909.984000	.88806290E-06	.8438509E-00
5	900.042667	.79690197E-06	.85640131E-00	938	909.994667	.88842885E-06	.8437598E-00

LOCATION	WAVENUMBER	COMP FLUX UP	COMP REFLECT UP
1	900.000000	.29937858E-04	.13346366E-01

LOCATION	WAVENUMBER	COMP FLUX UP	COMP REFLECT UP
934	909.952000	.29379560E-04	.13345531E-01

TABLE B-2 (Cont.)

2 908.818667 .29937841E-04 .13346288E-01
 3 908.821333 .29937809E-04 .13345968E-01
 4 908.822000 .29937763E-04 .13345661E-01
 5 908.822667 .29937702E-04 .13345285E-01

THE TIME AT THE END OF RADMRG IS 74.583
 .132 SECS WERE REQUIRED FOR THIS MERGE

AER TEST CASE - MULTIPLE SCATTERING - RURAL AEROSOL * 908 - 910 CM-1 FASCODE2 86/87/15 16.04.54

LAYER = 7

***** CONTINUA: H2O(T), CO2, N2 (01 JULY 82)

02(1680CM-1), O3(DIFFUSE,T), H2O SELF HAS BEEN REDUCED IN THE 808-1200 CM-1 REGION (01 SEPT 1985)

***** IPTS4 = 27 DVR4 = .91822 BOUND4 = 25.0000 *****

LRLF4 =
 DV FOR LRLF4 = .91822 BOUND FOR LRLF4 = 25.0000

NO. LINES BEFORE SHRINK = 645. NO. LINES AFTER SHRINK = 199. NO. LINES AFTER REJECT = 187

TIME READ CONVOLUTION PANEL
 74.752 .026 .001

OUTPUT ON FILE 10 DV = .00711111 BOUND3(CM-1) = 1.8204

LOCATION	WAVENUMBER	OPT. DEPTH	LOCATION	WAVENUMBER	OPT. DEPTH
1825	908.808000	.11917688E-04	2427	909.969778	.38845139E-04
1826	908.807111	.11684389E-04	2428	909.976889	.34792875E-04
1827	908.814222	.11524283E-04	2429	909.984000	.41177885E-04
1828	908.821333	.11424487E-04	2430	909.991111	.48594855E-04
1829	908.828444	.11387777E-04	2431	909.998222	.68433531E-04

TIME READ CONVOLUTION PANEL
 74.841 .012 .013

----- 9 HALF WIDTH CHANGES

AVERAGE WIDTH = .028994, AVERAGE ZETA = .949873, NO. LINES = 150, NO. LINES AFTER REJECT = 150, NO. HV CHANGES = 9

AER TEST CASE - MULTIPLE SCATTERING - RURAL AEROSOL * 908 - 910 CM-1 FASCODE2 86/87/15 16.04.54

THE TIME AT THE START OF RADMRG IS 74.856

INITIAL LAYER 1 FINAL LAYER 7

FILE 10 MERGED WITH FILE 12 ONTO FILE 11
 CNTSL AND IANT 3 0

LOCATION	WAVENUMBER	RADIANCE	TRANSMITTANCE	LOCATION	WAVENUMBER	RADIANCE	TRANSMITTANCE
1	908.808000	.79666032E-06	.85639705E-00	1403	909.969778	.87941256E-06	.84395546E-00
2	908.807111	.79683299E-06	.85639519E-00	1404	909.976889	.88365555E-06	.84340134E-00
3	908.814222	.79687131E-06	.85639103E-00	1405	909.984000	.88840306E-06	.84274608E-00
4	908.821333	.79691541E-06	.85638603E-00	1406	909.991111	.88841965E-06	.84273903E-00
5	908.828444	.79696397E-06	.85638036E-00	1407	909.998222	.88844611E-06	.84272985E-00

TABLE B-2 (Cont.)

LOCATION	WAVENUMBER	COMP FLUX UP	COMP REFLECT UP	LOCATION	WAVENUMBER	COMP FLUX UP	COMP REFLECT UP
1	900.808080	.29936992E-04	.13244216E-01	1403	909.969778	.29375357E-04	.13236179E-01
2	900.807111	.29936987E-04	.13244136E-01	1404	909.976869	.29371536E-04	.13205948E-01
3	900.814000	.29936974E-04	.13244089E-01	1405	909.984722	.29366255E-04	.1320675E-01
4	900.821310	.29936952E-04	.13243844E-01	1406	909.991111	.29366898E-04	.13208281E-01
5	900.828444	.29936925E-04	.13243649E-01	1407	909.998222	.29365847E-04	.13279652E-01

THE TIME AT THE END OF RANGING IS 75.015
1159 SECS WERE REQUIRED FOR THIS MERGE

AER TEST CASE - MULTIPLE SCATTERING - RURAL AEROSOL = 900 - 910 CM-1 FASCODE2 86/07/15 16.04.54

LAYER = 8

***** CONTINUA: H2O(T), CO2, H2 (01 JULY 82)

***** IPTS4 = 41 DVR4 = .68681 BOUND4 = 25.0000 *****

LBLF4 =

BOUND FOR LBLF4 = 25.0000

NO. LINES BEFORE SHRINK = 537. NO. LINES AFTER SHRINK = 253. NO. LINES AFTER REJECT = 238

TIME 75.186 READ CONVOLUTION PANEL .001

WIRAC:

OUT-ON FILE 1P DV = .00000004 BOUND3(CM-1) = 1.2136

LOCATION	WAVENUMBER	OPT. DEPTH	LOCATION	WAVENUMBER	OPT. DEPTH
1025	900.808080	.77439942E-04	2428	906.651259	.10928336E-03
1026	900.807471	.77336895E-04	2429	906.656800	.14229586E-03
1027	900.809461	.77439942E-04	2430	906.660741	.10942459E-03
1028	900.814222	.69299507E-04	2431	906.665481	.84299485E-04
1029	900.818963	.687174E-04	2432	906.670222	.66680408E-04
33	906.674962	.54799433E-04	730	909.979259	.25763872E-04
34	906.681221	.55663634E-04	731	909.984020	.30753202E-04
35	906.684444	.30903181E-04	732	909.988741	.37781872E-04
36	906.689185	.34777147E-04	733	909.993481	.47687442E-04
37	906.693926	.38795061E-04	734	909.998222	.61148931E-04

TIME 75.282 READ CONVOLUTION PANEL .023

***** HALF WIDTH CHANGES

AVERAGE WIDTH = .01024P. AVERAGE ZETA = .92824. NO. LINES = 133. NO. LINES AFTER REJECT = 133. NO. HV CHANGES = 9

AER TEST CASE - MULTIPLE SCATTERING - RURAL AEROSOL = 900 - 910 CM-1 FASCODE2 86/07/15 16.04.54

THE TIME AT THE START OF RANGING IS 75.296

INITIAL LAYER 1 FINAL LAYER 8

FILE 10 MESSAGE "FILE 11 ONTO FILE 12

CTRL AND LANT

LOCATION	WAVENUMBER	RADIANCE	TRANSMITTANCE	LOCATION	WAVENUMBER	RADIANCE	TRANSMITTANCE
900.808080	.77439942E-04	.05628037E-00		1404	906.651259	.95085778E-06	.03510853E-00

TABLE B-2 (Cont.)

LOCATION	WAVENUMBER	COMP FLUX UP	COMP REFLECT UP	LOCATION	WAVENUMBER	COMP FLUX UP	COMP REFLECT UP
2	900.004741	.79700129E-06	.85627907E+00	1405	906.656000	.96297652E-06	.83463638E+00
3	900.005481	.79710337E-06	.85627690E+00	1406	906.660741	.96870217E-06	.83406039E+00
4	900.014222	.79715950E-06	.85627415E+00	1407	906.665481	.97530759E-06	.83338414E+00
5	900.018963	.79715027E-06	.85627099E+00	1408	906.670222	.98343520E-06	.83253651E+00
LOCATION	WAVENUMBER	COMP FLUX UP	COMP REFLECT UP	LOCATION	WAVENUMBER	COMP FLUX UP	COMP REFLECT UP
1	900.000000	.29933956E-04	.13338403E-01	1404	906.651259	.29473014E-04	.12807323E-01
2	900.004741	.29933962E-04	.13338454E-01	1405	906.656000	.29473451E-04	.12877605E-01
3	900.009481	.29933962E-04	.13338395E-01	1406	906.660741	.29473040E-04	.12864501E-01
4	900.014222	.29933956E-04	.13338312E-01	1407	906.665481	.29471950E-04	.12847642E-01
5	900.018963	.29933945E-04	.13338211E-01	1408	906.670222	.29469911E-04	.12825222E-01
1	906.674963	.99340547E-06	.83146130E+00	690	909.979259	.88573981E-06	.84301740E+00
2	906.679704	.10060193E-05	.83007647E+00	699	909.984000	.88871123E-06	.84260223E+00
3	906.684444	.10223497E-05	.82025963E+00	700	909.988741	.88875380E-06	.84258507E+00
4	906.689185	.10439311E-05	.82583531E+00	701	909.993481	.88877141E-06	.84257672E+00
5	906.693926	.10719060E-05	.82267090E+00	702	909.998222	.88879570E-06	.84256530E+00
1	906.674963	.29466535E-04	.12794468E-01	698	909.979259	.29365997E-04	.13289592E-01
2	906.679704	.29461730E-04	.12754341E-01	699	909.984000	.29362531E-04	.13273440E-01
3	906.684444	.29455050E-04	.12701469E-01	700	909.988741	.29362094E-04	.13272409E-01
4	906.689185	.29445567E-04	.12629071E-01	701	909.993481	.29361077E-04	.13271953E-01
5	906.693926	.29432692E-04	.12555931E-01	702	909.998222	.29361582E-04	.13271335E-01

THE TIME AT THE END OF RADMRG IS 75.610
.314 SECS WERE REQUIRED FOR THIS MERGE

TABLE B-2 (Cont.)

AER TEST CASE - MULTIPLE SCATTERING - RURAL AEROSOL * 988 - 918 CM-1 FASCOD2 86/87/15 16.84.54
 LAYER - 9

***** CONTINUA: H2O(T).CO2.W2 (81 JULY 82)
 O2(1688CM-1), O3(DIFFUSE.T), H2O SELF HAS BEEN REDUCED IN THE 888-1288 CM-1 REGION (81 SEPT 1985)

***** IPTS4 = 32 DVR4 = .3834; BOUND4 = 9.78984 *****

LBFL4 *
 DV FOR LBFL4 = .3834; BOUND FOR LBFL4 = 9.7898

NO. LINES BEFORE SHRINK = 471. NO. LINES AFTER SHRINK = 267. NO. LINES AFTER REJECT = 158

TIME 75.788
 READ .826
 CONVOLUTION .854
 PANEL .881

HIRACI
 OUTPUT ON FILE 18 DV = .88237837 BOUNDF3(CH-1) = .5868

LOCATION	WAVENUMBER	OPT. DEPTH	LOCATION	WAVENUMBER	OPT. DEPTH
1025	988.88888	.21348834E-05	2428	983.325630	.13811837E-05
1026	988.882378	.19528896E-05	2429	983.328888	.13799493E-05
1027	988.884741	.18363804E-05	2430	983.330378	.13766508E-05
1028	988.887111	.17508248E-05	2431	983.332741	.13743478E-05
1029	988.889481	.16923168E-05	2432	983.335111	.13738665E-05
33	983.337481	.13768292E-05	2428	989.814519	.66677133E-05
34	983.339852	.13768495E-05	2429	989.816889	.63894382E-05
35	983.342222	.13763982E-05	2430	989.819259	.59688258E-05
36	983.344593	.13778112E-05	2431	989.821638	.56485783E-05
37	983.346963	.13778726E-05	2432	989.824008	.53728422E-05
33	989.825638	.51297728E-05	448	989.991111	.12253728E-04
34	989.828741	.49128663E-05	441	989.993481	.14547873E-04
35	989.831111	.47164351E-05	442	989.995852	.17418142E-04
36	989.833481	.45384742E-05	443	989.998222	.21484888E-04
37	989.835852	.43737789E-05	444	918.888593	.26989883E-04

----- 7 HALF WIDTH CHANGES

AVERAGE WIDTH = .887145, AVERAGE ZETA = .878888, NO. LINES = 118. NO. LINES AFTER REJECT = 118. NO. HW CHANGES = 7

AER TEST CASE - MULTIPLE SCATTERING - RURAL AEROSOL * 988 - 918 CM-1 FASCOD2 86/87/15 16.84.54

THE TIME AT THE START OF RADMRG IS 75.913

INITIAL LAYER 1 FINAL LAYER 9

TABLE B-2 (Cont.)

FILE 18 MERGED WITH FILE 12 ONTO FILE 11
CNTRL AND JANT 3 8

LOCATION	WAVENUMBER	RADIANCE	TRANSMITTANCE	LOCATION	WAVENUMBER	RADIANCE	TRANSMITTANCE
1	900.000000	.79727294E-06	.05618640E+00	1404	903.325630	.78781920E-06	.05654195E+00
2	900.002370	.79727874E-06	.05618604E+00	1405	903.328000	.78776766E-06	.05654778E+00
3	900.004741	.79728745E-06	.05618535E+00	1406	903.330370	.78772295E-06	.05655189E+00
4	900.007111	.79729761E-06	.05618444E+00	1407	903.332741	.78760300E-06	.05655465E+00
5	900.009481	.79730924E-06	.05618332E+00	1408	903.335111	.78764977E-06	.05655625E+00
LOCATION	WAVENUMBER	COMP FLUX UP	COMP REFLECT UP	LOCATION	WAVENUMBER	COMP FLUX UP	COMP REFLECT UP
1	900.000000	.29931377E-04	.13333891E-01	1404	903.325630	.29776057E-04	.13438868E-01
2	900.002370	.29931384E-04	.13333889E-01	1405	903.328000	.29776101E-04	.13439213E-01
3	900.004741	.29931390E-04	.13333876E-01	1406	903.330370	.29776120E-04	.13439700E-01
4	900.007111	.29931395E-04	.13333854E-01	1407	903.332741	.29776145E-04	.13440087E-01
5	900.009481	.29931394E-04	.13333824E-01	1408	903.335111	.29776155E-04	.13441368E-01
1	903.337481	.78762085E-06	.05655657E+00	2396	909.014519	.74190130E-05	.11659032E+00
2	903.339852	.78759618E-06	.05655605E+00	2397	909.016889	.72701287E-05	.13114517E+00
3	903.342222	.78757567E-06	.05655460E+00	2398	909.019259	.71168485E-05	.14630885E+00
4	903.344593	.78755885E-06	.05655235E+00	2399	909.021630	.59617926E-05	.16182807E+00
5	903.346963	.78754598E-06	.05654934E+00	2400	909.024000	.68075892E-05	.17745863E+00
1	903.337481	.29776153E-04	.13442347E-01	409	909.931111	.88901445E-06	.84246264E+00
2	903.339852	.29776149E-04	.13442345E-01	409	909.933481	.88901858E-06	.84246871E+00
3	903.342222	.29776139E-04	.13444655E-01	410	909.935852	.88902375E-06	.84245829E+00
4	903.344593	.29776122E-04	.13444594E-01	411	909.938222	.88903093E-06	.84245493E+00
5	903.346963	.29776100E-04	.13447313E-01	412	910.000593	.88904099E-06	.84245023E+00
1	909.026370	.66545445E-05	.19314697E+00	408	909.931111	.88901445E-06	.84246264E+00
2	909.028741	.65040747E-05	.21875124E+00	409	909.933481	.88901858E-06	.84246871E+00
3	909.031111	.63554784E-05	.24299570E+00	410	909.935852	.88902375E-06	.84245829E+00
4	909.033481	.62082273E-05	.2794600E+00	411	909.938222	.88903093E-06	.84245493E+00
5	909.035852	.60632190E-05	.25517024E+00	412	910.000593	.88904099E-06	.84245023E+00
1	909.026370	.26659025E-04	.11006554E-02	408	909.931111	.29350745E-04	.13266218E-01
2	909.028741	.26932991E-04	.12270630E-02	409	909.933481	.29350691E-04	.13266104E-01
3	909.031111	.27001680E-04	.13511054E-02	410	909.935852	.29350624E-04	.13265972E-01
4	909.033481	.27036040E-04	.14786104E-02	411	909.938222	.29350531E-04	.13265789E-01
5	909.035852	.27017523E-04	.16080311E-02	412	910.000593	.29350401E-04	.13265532E-01

THE TIME AT THE END OF RADMRG IS 76.493
.580 SECS WERE REQUIRED FOR THIS MERGE

TABLE B-2 (Cont.)

AER TEST CASE - MULTIPLE SCATTERING - RURAL AEROSOL * 908 - 918 CM-1 FASCO02 86/87/15 16.84.54
 LAYER = 18
 ***** CONTINUA: H2O(I), CO2, N2 (81 JULY 82)
 O2(1688CM-1), O3(1115CM-1), H2O SELF HAS BEEN REDUCED IN THE 888-1208 CM-1 REGION (81 SEPT 1985)

***** IPTSA = 32 DVA = .28227 BOUND4 = 6.47269 *****
 LBLF4 *
 DV FOR LBLF4 = .28227 BOUND FOR LBLF4 = 6.4727
 NO. LINES BEFORE SHRINK = 441, NO. LINES AFTER SHRINK = 288, NO. LINES AFTER REJECT = 143

TIME READ CONVOLUTION PANEL
 76.688 .824 .856 .881

HIRAC1
 OUTPUT ON FILE 18 DV = .88158825 BOUND(3/CM-1) = .4845

LOCATION	WAVENUMBER	OPT. DEPTH	LOCATION	WAVENUMBER	OPT. DEPTH
1825	988.888888	.12554139E-06	2428	982.217886	.38891819E-05
1826	988.888888	.11621708E-06	2429	982.218567	.34286468E-05
1827	988.883168	.10949777E-06	2430	982.220247	.42199614E-05
1828	988.884741	.10457647E-06	2431	982.221827	.53886814E-05
1829	988.886321	.10094832E-06	2432	982.223487	.69615145E-05
33	982.224988	.93863494E-05	2428	986.889679	.35344142E-06
34	982.226568	.12638317E-04	2429	986.881259	.34845163E-06
35	982.228148	.17288633E-04	2430	986.881284	.32836798E-06
36	982.229728	.22865478E-04	2431	986.881428	.31741517E-06
37	982.231389	.24529381E-04	2432	986.881688	.38755695E-06
33	986.881758	.29875783E-06	2428	989.882272	.9924859E-07
34	986.881918	.29839775E-06	2429	989.883852	.9954126E-07
35	986.882074	.28287488E-06	2430	989.885432	.9986838E-07
36	986.882232	.27619896E-06	2431	989.887812	.99986247E-07
37	986.882391	.27835331E-06	2432	989.888593	.18817112E-06
33	989.881873	.18873431E-06	149	989.993481	.86882498E-06
34	989.881753	.18115821E-06	150	989.993862	.10838428E-05
35	989.881333	.18282825E-06	151	989.996542	.11534512E-05
36	989.881494	.18323856E-06	152	989.998222	.13199642E-05
37	989.881649	.18451685E-06	153	989.999882	.15449143E-05

TIME READ CONVOLUTION PANEL
 76.816 .811 .831 .858

----- 4 HALF WIDTH CHANGES

AVERAGE WIDTH = .824655, AVERAGE ZETA = .817436, NO. LINES = 183, NO. LINES AFTER REJECT = 183, NO. HV CHANGES = 4

AER TEST CASE - MULTIPLE SCATTERING - RURAL AEROSOL * 999 - 918 CM-1 FASCOJ2 86/07/15 16.04.54

THE TIME AT THE START OF RADMRG IS 76.829

INITIAL LAYER 1 FINAL LAYER 10

FILE 10 MERGED WITH FILE 11 ONTO FILE 12
CNTRL AND LANT 3 2

LOCATION	WAVENUMBER	RADIANCE	TRANSMITTANCE	LOCATION	WAVENUMBER	RADIANCE	TRANSMITTANCE
1	900.00000	.79730901E-06	.85617046E-00	1404	902.217056	.83155291E-06	.85102450E+00
2	900.001500	.79731133E-06	.85617027E-00	1405	902.218067	.83240234E-06	.85093402E+00
3	900.003100	.79731642E-06	.85616992E+00	1406	902.220247	.83272127E-06	.85084592E+00
4	900.004741	.79732245E-06	.85616943E+00	1407	902.221877	.83321259E-06	.85076012E+00
5	900.006321	.79732907E-06	.85616885E+00	1408	902.223487	.83367507E-06	.85067694E+00
LOCATION	WAVENUMBER	COMP FLUX UP	COMP REFLECT UP	LOCATION	WAVENUMBER	COMP FLUX UP	COMP REFLECT UP
1	900.00000	.29930870E-04	.13332905E-01	1404	902.217056	.29795517E-04	.13294460E-01
2	900.001500	.29930874E-04	.13332904E-01	1405	902.218067	.29791496E-04	.13290289E-01
3	900.003100	.29930879E-04	.13332900E-01	1406	902.220247	.29793329E-04	.13196235E-01
4	900.004741	.29930883E-04	.13332891E-01	1407	902.221877	.29792148E-04	.13192288E-01
5	900.006321	.29930885E-04	.13332877E-01	1408	902.223487	.29790947E-04	.13188449E-01
1	902.224988	.83411056E-06	.85059627E+00	2396	906.009679	.90857094E-06	.84147561E+00
2	902.226568	.83451276E-06	.85051972E+00	2397	906.011259	.90966279E-06	.84136043E+00
3	902.228148	.83487603E-06	.85044598E+00	2398	906.012840	.91082714E-06	.84123647E+00
4	902.229728	.83518655E-06	.85039297E+00	2399	906.014420	.91205624E-06	.84110460E+00
5	902.231309	.83542908E-06	.85035581E+00	2400	906.016000	.91337121E-06	.84095613E+00
1	906.017500	.91465500E-06	.84082274E+00	2396	906.009679	.29542549E-04	.13086416E-01
2	906.019160	.91604750E-06	.84067250E+00	2397	906.011259	.29543311E-04	.13083476E-01
3	906.020741	.91749586E-06	.84051454E+00	2398	906.012840	.29543136E-04	.13080235E-01
4	906.022321	.91901605E-06	.84034759E+00	2399	906.014420	.29542975E-04	.13076720E-01
5	906.023901	.92061503E-06	.84017111E+00	2400	906.016000	.29542775E-04	.13072997E-01
1	906.017500	.29542459E-04	.13066910E-01	2396	909.002272	.93282373E-06	.83762953E+00
2	906.019160	.29542075E-04	.13064991E-01	2397	909.003852	.93352158E-06	.83732610E+00
3	906.020741	.29541640E-04	.13063014E-01	2398	909.005432	.93578674E-06	.83715874E+00
4	906.022321	.29541163E-04	.13061550E-01	2399	909.007012	.93760800E-06	.83692923E+00
5	906.023901	.29540635E-04	.13060087E-01	2400	909.008593	.93937206E-06	.83670569E+00
1	909.010173	.94106575E-06	.83649086E+00	2396	909.002272	.29340620E-04	.13114006E-01
2	909.011753	.94260033E-06	.83628309E+00	2397	909.003852	.29339200E-04	.13105034E-01
				2398	909.005432	.29337703E-04	.13095117E-01
				2399	909.007012	.29336363E-04	.13087305E-01
				2400	909.008593	.29334951E-04	.13078669E-01
				117	909.993481	.98905602E-06	.84244313E+00
				118	909.995062	.98905954E-06	.84244148E+00

TABLE B-2 (Cont.)

3	909.81333	.94200954E-06	.83608537E+00	119	909.996642	.89386383E-06	.84243948E+00
4	909.814914	.94564897E-06	.83569666E+00	120	909.998222	.88907422E-06	.84243463E+00
5	909.816494	.94698809E-06	.83572859E+00	121	909.999802	.88907462E-06	.84243443E+00
1	909.810173	.29333566E-04	.13070273E-01	117	909.993401	.29358130E-04	.13265004E-01
2	909.811753	.29332209E-04	.13062149E-01	118	909.995062	.29358084E-04	.13264913E-01
3	909.813333	.29330876E-04	.13054305E-01	119	909.996642	.29358028E-04	.13264802E-01
4	909.814914	.29329551E-04	.13046697E-01	120	909.998222	.29357893E-04	.13264536E-01
5	909.816494	.29328281E-04	.13039525E-01	121	909.999802	.29357887E-04	.13264524E-01

THE TIME AT THE END OF RADMRG IS 77.452
.623 SECS WERE REQUIRED FOR THIS MERGE

THE TIME AT THE START OF FLYDOWN IS
FLYDOWN - LAYER 10 WITH 4 PANELS

77.500

LOCATION	WAVENUMBER	COMP FLUX DN	COMP REFLECT DN
1	906.000000	.59189566E-09	.00000000E+00
2	906.001500	.59159670E-09	.00000000E+00
3	906.003100	.59138170E-09	.00000000E+00
4	906.004701	.59122422E-09	.00000000E+00
5	906.006321	.59110913E-09	.00000000E+00
TOTAL FLUX DN			
1	906.000000	.29308700E-04	.00000000E+00
2	906.001500	.29308700E-04	.00000000E+00
3	906.003100	.29308700E-04	.00000000E+00
4	906.004701	.29308700E-04	.00000000E+00
5	906.006321	.29308700E-04	.00000000E+00
1	906.000000	.09658320E-09	.00000000E+00
2	906.001500	.99982720E-09	.00000000E+00
3	906.003100	.11455389E-08	.00000000E+00
4	906.004701	.13081150E-08	.00000000E+00
5	906.006321	.13785301E-08	.00000000E+00
1	906.000000	.29789716E-04	.00000000E+00
2	906.001500	.29783497E-04	.00000000E+00
3	906.003100	.29787358E-04	.00000000E+00
4	906.004701	.29786641E-04	.00000000E+00
5	906.006321	.29786615E-04	.00000000E+00
1	906.000000	.62190959E-09	.00000000E+00
2	906.001500	.62164538E-09	.00000000E+00
3	906.003100	.62140872E-09	.00000000E+00
4	906.004701	.62119796E-09	.00000000E+00
5	906.006321	.62101389E-09	.00000000E+00
1	906.000000	.29542459E-04	.00000000E+00
2	906.001500	.29542075E-04	.00000000E+00
3	906.003100	.29541600E-04	.00000000E+00
4	906.004701	.29541163E-04	.00000000E+00
5	906.006321	.29540635E-04	.00000000E+00
1	909.000000	.62415261E-09	.00000000E+00
2	909.001500	.62417498E-09	.00000000E+00
3	909.003100	.62420099E-09	.00000000E+00
4	909.004701	.62423060E-09	.00000000E+00
5	909.006321	.62427079E-09	.00000000E+00
1	909.000000	.29333256E-04	.00000000E+00
2	909.001500	.29332299E-04	.00000000E+00
3	909.003100	.29330876E-04	.00000000E+00

TABLE B-2 (Cont.)

LOCATION	WAVENUMBER	COMP FLUX DN	COMP REFLECT DN
1484	902.217066	.68687036E-09	.00000000E+00
1485	902.218667	.70659570E-09	.00000000E+00
1486	902.220267	.73178991E-09	.00000000E+00
1487	902.221827	.76899757E-09	.00000000E+00
1488	902.223407	.81507655E-09	.00000000E+00
TOTAL FLUX UP			
1484	902.217066	.29795617E-04	.00000000E+00
1485	902.218667	.29794406E-04	.00000000E+00
1486	902.220267	.29793329E-04	.00000000E+00
1487	902.221827	.29792148E-04	.00000000E+00
1488	902.223407	.29790947E-04	.00000000E+00
2396	906.000679	.62346220E-09	.00000000E+00
2397	906.011259	.62305249E-09	.00000000E+00
2398	906.012840	.62267136E-09	.00000000E+00
2399	906.014420	.62232591E-09	.00000000E+00
2400	906.016000	.62201497E-09	.00000000E+00
2396	906.000679	.29543549E-04	.00000000E+00
2397	906.011259	.29543311E-04	.00000000E+00
2398	906.012840	.29543136E-04	.00000000E+00
2399	906.014420	.29542975E-04	.00000000E+00
2400	906.016000	.29542775E-04	.00000000E+00
2396	906.000679	.62364886E-09	.00000000E+00
2397	906.000679	.62364978E-09	.00000000E+00
2398	906.004332	.62364685E-09	.00000000E+00
2399	906.007812	.62364828E-09	.00000000E+00
2400	906.009593	.62365656E-09	.00000000E+00
2396	909.002272	.29340628E-04	.00000000E+00
2397	909.003852	.29339208E-04	.00000000E+00
2398	909.005432	.29337783E-04	.00000000E+00
2399	909.007012	.29336361E-04	.00000000E+00
2400	909.008593	.29334951E-04	.00000000E+00
117	909.993481	.64808005E-09	.00000000E+00
118	909.995062	.65236273E-09	.00000000E+00
119	909.996642	.65704329E-09	.00000000E+00
120	909.998222	.66224576E-09	.00000000E+00
121	909.999802	.66927481E-09	.00000000E+00
117	909.993481	.29358130E-04	.00000000E+00
118	909.995062	.29358084E-04	.00000000E+00
119	909.996642	.29358028E-04	.00000000E+00

TABLE B-2 (Cont.)

FLYDOWN - LAYER 5 WITH 3 PANELS									
LOCATION	WAVENUMBER	COMP FLUX DN	COMP REFLECT DN	LOCATION	WAVENUMBER	COMP FLUX DN	COMP REFLECT DN	LOCATION	WAVENUMBER
1	989.814914	.29329551E-04	.43371711E-06	1484	989.998222	.29357893E-04	.43344766E-06	1484	989.998222
2	989.816494	.29328281E-04	.43371725E-06	1485	989.998802	.29357887E-04	.43344766E-06	1485	989.998802
3	989.884741	.36823894E-08	.43371734E-06	1486	989.998802	.29357887E-04	.43344766E-06	1486	989.998802
4	989.887111	.35998231E-08	.43371748E-06	1487	989.998802	.29357887E-04	.43344766E-06	1487	989.998802
5	989.889481	.35981871E-08	.43371745E-06	1488	989.998802	.29357887E-04	.43344766E-06	1488	989.998802
LOCATION	WAVENUMBER	TOTAL FLUX UP	TOTAL FLUX DN	LOCATION	WAVENUMBER	TOTAL FLUX UP	TOTAL FLUX DN	LOCATION	WAVENUMBER
1	989.888888	.29931425E-04	.36243218E-08	1484	989.998222	.29776185E-04	.36863764E-08	1484	989.998222
2	989.888888	.29931433E-04	.36188686E-08	1485	989.998802	.29776185E-04	.36863764E-08	1485	989.998802
3	989.884741	.29931438E-04	.36153712E-08	1486	989.998802	.29776185E-04	.36863764E-08	1486	989.998802
4	989.887111	.29931441E-04	.36128848E-08	1487	989.998802	.29776185E-04	.36863764E-08	1487	989.998802
5	989.889481	.29931442E-04	.36118889E-08	1488	989.998802	.29776185E-04	.36863764E-08	1488	989.998802
1	989.337481	.36789719E-08	.43379118E-06	2395	989.814519	.29776185E-04	.36863764E-08	2395	989.814519
2	989.339852	.36789725E-08	.43379118E-06	2396	989.814519	.29776185E-04	.36863764E-08	2396	989.814519
3	989.342252	.36789728E-08	.43379118E-06	2397	989.814519	.29776185E-04	.36863764E-08	2397	989.814519
4	989.344593	.36789731E-08	.43379118E-06	2398	989.814519	.29776185E-04	.36863764E-08	2398	989.814519
5	989.346963	.36789734E-08	.43379118E-06	2399	989.814519	.29776185E-04	.36863764E-08	2399	989.814519
1	989.337481	.29776203E-04	.36918884E-08	2400	989.814519	.29776185E-04	.36863764E-08	2400	989.814519
2	989.339852	.29776203E-04	.36918884E-08	2401	989.814519	.29776185E-04	.36863764E-08	2401	989.814519
3	989.342252	.29776203E-04	.36918884E-08	2402	989.814519	.29776185E-04	.36863764E-08	2402	989.814519
4	989.344593	.29776203E-04	.36918884E-08	2403	989.814519	.29776185E-04	.36863764E-08	2403	989.814519
5	989.346963	.29776203E-04	.36918884E-08	2404	989.814519	.29776185E-04	.36863764E-08	2404	989.814519
1	989.826378	.38853298E-08	.43425764E-06	408	989.991111	.41853398E-08	.43425764E-06	408	989.991111
2	989.828741	.38853298E-08	.43425764E-06	409	989.991111	.41853398E-08	.43425764E-06	409	989.991111
3	989.831111	.38853298E-08	.43425764E-06	410	989.991111	.41853398E-08	.43425764E-06	410	989.991111
4	989.833481	.38853298E-08	.43425764E-06	411	989.991111	.41853398E-08	.43425764E-06	411	989.991111
5	989.835852	.38853298E-08	.43425764E-06	412	989.991111	.41853398E-08	.43425764E-06	412	989.991111
1	989.826378	.26659829E-04	.38979859E-08	408	989.991111	.29357893E-04	.41188928E-08	408	989.991111
2	989.828741	.26659829E-04	.38979859E-08	409	989.991111	.29357893E-04	.41188928E-08	409	989.991111
3	989.831111	.26659829E-04	.38979859E-08	410	989.991111	.29357893E-04	.41188928E-08	410	989.991111
4	989.833481	.26659829E-04	.38979859E-08	411	989.991111	.29357893E-04	.41188928E-08	411	989.991111
5	989.835852	.26659829E-04	.38979859E-08	412	989.991111	.29357893E-04	.41188928E-08	412	989.991111

TABLE B-2 (Cont.)

THE TIME AT THE START OF SRCFCN IS 78.468

SRCFCN - LAYER 18 WITH 4 PANELS

LOCATION	WAVENUMBER	MSCAT SRC FCN	MS TRANS	LOCATION	WAVENUMBER	MSCAT SRC FCN	MS TRANS
1	900.000000	.40583627E-12	.99998158E+00	1484	902.217806	.40384544E-12	.99978433E+00
2	900.001560	.40583630E-12	.99998151E+00	1485	902.218667	.40383717E-12	.99977810E+00
3	900.003160	.40583635E-12	.99998152E+00	1486	902.220247	.40381810E-12	.99977000E+00
4	900.004741	.40583638E-12	.99998152E+00	1487	902.221827	.40380848E-12	.99975850E+00
5	900.006321	.40583640E-12	.99998153E+00	1488	902.223387	.40379198E-12	.99974210E+00
1	902.224988	.40584495E-12	.99997183E+00	2396	906.009679	.40064191E-12	.99998023E+00
2	902.226568	.40399349E-12	.99996859E+00	2397	906.011259	.40063862E-12	.99998025E+00
3	902.228148	.40398331E-12	.99996401E+00	2398	906.012840	.40063622E-12	.99998025E+00
4	902.229728	.40397568E-12	.99995915E+00	2399	906.014420	.40063400E-12	.99998027E+00
5	902.231309	.40397158E-12	.99995669E+00	2400	906.016000	.40063125E-12	.99998028E+00
1	906.017587	.40080008E-12	.99998028E+00	2396	909.802272	.39832113E-12	.99998004E+00
2	906.019160	.40079556E-12	.99998029E+00	2397	909.803852	.39830180E-12	.99998004E+00
3	906.020741	.40078972E-12	.99998029E+00	2398	909.805432	.39828241E-12	.99998004E+00
4	906.022321	.40078322E-12	.99998030E+00	2399	909.807012	.39826320E-12	.99998004E+00
5	906.023901	.40077686E-12	.99998031E+00	2400	909.808593	.39824402E-12	.99998004E+00
1	909.810173	.39834780E-12	.99998002E+00	117	909.993481	.39868338E-12	.99979252E+00
2	909.811753	.39832874E-12	.99998002E+00	118	909.995062	.39868314E-12	.99979152E+00
3	909.813333	.39831061E-12	.99998002E+00	119	909.996642	.39868285E-12	.99978997E+00
4	909.814914	.39829256E-12	.99998002E+00	120	909.998222	.39868285E-12	.99978800E+00
5	909.816494	.39827541E-12	.99998002E+00	121	909.999802	.39868215E-12	.99978590E+00

THE TIME AT THE END OF SRCFCN IS 79.785
1.245 SECS WERE REQUIRED FOR THIS MERGE

FLXDOWN - LAYER 8 WITH 2 PANELS

LOCATION	WAVENUMBER	COMP FLUX DN	COMP REFLECT DN	LOCATION	WAVENUMBER	COMP FLUX DN	COMP REFLECT DN
1	900.000000	.75748798E-08	.98689030E-06	1484	906.651259	.15671805E-07	.98752986E-06
2	900.004741	.75550626E-08	.98689144E-06	1485	906.656800	.13292987E-07	.98767120E-06
3	900.009481	.75426239E-08	.98689224E-06	1486	906.660741	.11812993E-07	.98776527E-06
4	900.014222	.75355434E-08	.98689270E-06	1487	906.665481	.10787900E-07	.98783529E-06
5	900.018963	.75315485E-08	.98689329E-06	1488	906.670222	.10085680E-07	.98788364E-06
LOCATION	WAVENUMBER	TOTAL FLUX UP	TOTAL FLUX DN	LOCATION	WAVENUMBER	TOTAL FLUX UP	TOTAL FLUX DN
1	900.000000	.29934405E-04	.76044215E-08	1484	906.651259	.29473216E-04	.15788911E-07
2	900.004741	.29934403E-04	.75845042E-08	1485	906.656800	.29473623E-04	.13322097E-07
3	900.009481	.29934403E-04	.75721656E-08	1486	906.660741	.29473320E-04	.11842113E-07
4	900.014222	.29934405E-04	.75588871E-08	1487	906.665481	.29473019E-04	.10817019E-07
5	900.018963	.29934406E-04	.75610902E-08	1488	906.670222	.29472743E-04	.10114793E-07
1	906.674363	.56048072E-08	.98836586E-06	698	909.979259	.86251444E-08	.98985627E-06
2	906.679704	.92803619E-08	.98838865E-06	699	909.984800	.80126835E-08	.98984208E-06

TABLE B-2 (Cont.)

3	986.68444	.98381884E-09	.98848659E-06	788	989.988741	.98826891E-08	.98882367E-06
4	986.689185	.88465283E-08	.98841971E-06	781	989.993481	.94889968E-08	.98979635E-06
5	986.693926	.87171488E-08	.98842891E-06	782	989.998222	.10865143E-07	.98975798E-06
1	986.674963	.29466658E-04	.96379311E-08	698	989.979259	.29366112E-04	.86543826E-08
2	926.679784	.29461857E-04	.9384817E-08	699	989.984808	.29362645E-04	.88417479E-08
3	986.68444	.29455152E-04	.9853828E-08	788	989.988741	.29362215E-04	.91116725E-08
4	986.689185	.29445688E-04	.88756338E-08	781	989.993481	.29362883E-04	.95188592E-08
5	986.693926	.29432882E-04	.87462338E-08	782	989.998222	.29361716E-04	.10894584E-07

TABLE B-2 (Cont.)

THE TIME AT THE START OF SRCFCN IS 79.998

SRCFCN - LAYER 9 WITH 3 PANELS

LOCATION	WAVENUMBER	MSCAT SRC FCN	MS TRANS	LOCATION	WAVENUMBER	MSCAT SRC FCN	MS TRANS
1	900.000000	.23617228E-11	.99988897E+00	1404	903.325630	.23481175E-11	.99988833E+00
2	900.000000	.23617228E-11	.99988815E+00	1405	903.328000	.23481209E-11	.99988833E+00
3	900.000000	.23617228E-11	.99988812E+00	1406	903.330370	.23481231E-11	.99988834E+00
4	900.000000	.23617228E-11	.99988813E+00	1407	903.332741	.23481244E-11	.99988834E+00
5	900.000000	.23617228E-11	.99988814E+00	1408	903.335111	.23481253E-11	.99988834E+00
1	903.337481	.23499984E-11	.99988813E+00	2396	909.014519	.16364615E-11	.99987840E+00
2	903.339852	.23499984E-11	.99988813E+00	2397	909.016889	.17491729E-11	.99987876E+00
3	903.342223	.23499984E-11	.99988813E+00	2398	909.019259	.18674989E-11	.99987911E+00
4	903.344593	.23499984E-11	.99988813E+00	2399	909.021630	.19745386E-11	.99987942E+00
5	903.346963	.23499984E-11	.99988812E+00	2400	909.024000	.20523796E-11	.99987978E+00
1	909.026370	.21084724E-11	.99987977E+00	408	909.991111	.23280311E-11	.99987207E+00
2	909.028741	.21281097E-11	.99987999E+00	409	909.993481	.23280314E-11	.99986978E+00
3	909.031111	.21335306E-11	.99988019E+00	410	909.995852	.23280318E-11	.99986991E+00
4	909.033481	.21335306E-11	.99988035E+00	411	909.998222	.23280321E-11	.99986991E+00
5	909.035852	.21335306E-11	.99988053E+00	412	910.000593	.23280324E-11	.99986991E+00

THE TIME AT THE START OF MSEMIS IS 80.822

INITIAL LAYER 1 FINAL LAYER 10

FILE 27 MERGED WITH FILE 26 ONTO FILE 28 WITH XTTYPE -2.5000

LOCATION	WAVENUMBER	MS EMISSION	MS TRANS	LOCATION	WAVENUMBER	MS EMISSION	MS TRANS
1	900.000000	.27675149E-11	.99998150E+00	1404	902.217006	.27540892E-11	.99997843E+00
2	900.001500	.27675149E-11	.99998151E+00	1405	902.218667	.27540813E-11	.99997781E+00
3	900.003160	.27675149E-11	.99998152E+00	1406	902.220247	.27539416E-11	.99997700E+00
4	900.004741	.27675149E-11	.99998153E+00	1407	902.221827	.27538749E-11	.99997585E+00
5	900.006321	.27675149E-11	.99998153E+00	1408	902.223407	.27538176E-11	.99997427E+00
1	902.224900	.27538092E-11	.99997183E+00	2396	906.009679	.27328239E-11	.99988023E+00
2	902.226568	.27538092E-11	.99996959E+00	2397	906.011259	.27328238E-11	.99988025E+00
3	902.228148	.27538105E-11	.99996401E+00	2398	906.012840	.27328094E-11	.99988026E+00
4	902.229728	.27538092E-11	.99995915E+00	2399	906.014420	.27327935E-11	.99988027E+00
5	902.231309	.27538092E-11	.99995669E+00	2400	906.016000	.27327739E-11	.99988028E+00
1	906.017500	.27329176E-11	.99988028E+00	2396	909.002272	.27152407E-11	.99988004E+00
2	906.019160	.27328015E-11	.99988029E+00	2397	909.003952	.27151087E-11	.99988004E+00
3	906.020741	.27328040E-11	.99988029E+00	2398	909.005632	.27149763E-11	.99988004E+00
4	906.022321	.27327952E-11	.99988030E+00	2399	909.007312	.27149460E-11	.99988004E+00
5	906.023901	.27327460E-11	.99988031E+00	2400	909.008992	.27147151E-11	.99988004E+00
1	909.010173	.27147084E-11	.99988002E+00	117	909.993481	.27189458E-11	.99997926E+00
2	909.011753	.27145042E-11	.99988002E+00	118	909.995062	.27189408E-11	.99997913E+00
3	909.013333	.27144605E-11	.99988002E+00	119	909.996642	.27189650E-11	.99997897E+00

TABLE B-2 (Cont.)

TIME TIME AT THE END OF MSEMIS IS .184 SECS WERE REQUIRED FOR THIS MERGE				TIME TIME AT THE END OF SRCFCN IS 1.027 SECS WERE REQUIRED FOR THIS MERGE			
FLXDOWN - LAYER 7 WITH 1 PANELS				FLXDOWN - LAYER 7 WITH 1 PANELS			
LOCATION	WAVENUMBER	COMP FLUX DN	COMP REFLECT DN	LOCATION	WAVENUMBER	COMP FLUX DN	COMP REFLECT DN
4	909.014314	.271423375E-11	.99998002E+00	120	909.990222	.271870188E-11	.99997898E+00
5	909.016494	.27142214E-11	.99998002E+00	121	909.999802	.27187291E-11	.99997858E+00
TIME TIME AT THE END OF MSEMIS IS .184 SECS WERE REQUIRED FOR THIS MERGE				TIME TIME AT THE END OF SRCFCN IS 1.027 SECS WERE REQUIRED FOR THIS MERGE			
FLXDOWN - LAYER 7 WITH 1 PANELS				FLXDOWN - LAYER 7 WITH 1 PANELS			
LOCATION	WAVENUMBER	COMP FLUX DN	COMP REFLECT DN	LOCATION	WAVENUMBER	COMP FLUX DN	COMP REFLECT DN
1	908.000000	.90391840E-08	.98673132E-06	1403	909.969778	.105531555E-07	.98964038E-06
2	908.007111	.90635258E-08	.98673382E-06	1404	909.976889	.10506342E-07	.98960959E-06
3	908.014222	.90449666E-08	.98673527E-06	1405	909.984000	.11409006E-07	.98955500E-06
4	908.021333	.90358930E-08	.98673692E-06	1406	909.991111	.12133593E-07	.98950401E-06
5	908.028444	.90326732E-08	.98673629E-06	1407	909.990222	.13375050E-07	.98948398E-06
LOCATION	WAVENUMBER	TOTAL FLUX UP	TOTAL FLUX DN	LOCATION	WAVENUMBER	TOTAL FLUX UP	TOTAL FLUX DN
1	908.000000	.29937114E-04	.91287239E-08	1403	909.969778	.29375498E-04	.10587727E-07
2	908.007111	.29937108E-04	.90930668E-08	1404	909.976889	.29371681E-04	.10935409E-07
3	908.014222	.29937095E-04	.90745866E-08	1405	909.984000	.29366407E-04	.11430866E-07
4	908.021333	.29937087E-04	.90654330E-08	1406	909.991111	.29366259E-04	.12102751E-07
5	908.028444	.29937074E-04	.90622131E-08	1407	909.990222	.29366026E-04	.13484105E-07

TABLE B-2 (Cont.)

THE TIME AT THE START OF SRCFCN IS 81.161

SRCFCN - LAYER 8 WITH 2 PANELS

LOCATION	WAVENUMBER	MSCAT	SRC FCM	MS TRANS
1	906.000000	.29913370E-11	.99986363E+00	
2	906.004741	.29913353E-11	.99986400E+00	
3	906.009481	.29913337E-11	.99986428E+00	
4	906.014222	.29913321E-11	.99986445E+00	
5	906.018963	.29913305E-11	.99986454E+00	
1	906.674963	.29530790E-11	.99983933E+00	
2	906.679724	.29530774E-11	.99981707E+00	
3	906.684444	.29530758E-11	.99982455E+00	
4	906.689105	.29530742E-11	.99982943E+00	
5	906.693926	.29495632E-11	.99983283E+00	

THE TIME AT THE START OF MSEMIS IS 81.600

INITIAL LAYER 1 FINAL LAYER 10

FILE 27 MERGED WITH FILE 28 ONTO FILE 26 WITH XTYPE=-1.0000

LOCATION	WAVENUMBER	MS EMISSION	MS TRANS
1	902.000000	.57584744E-11	.99998150E+00
2	902.004741	.57584738E-11	.99998151E+00
3	902.009481	.57584732E-11	.99998152E+00
4	902.014222	.57584726E-11	.99998153E+00
5	902.018963	.57584720E-11	.99998154E+00
1	902.224988	.57325301E-11	.99997183E+00
2	902.229728	.57325285E-11	.99996859E+00
3	902.234467	.57324870E-11	.99996401E+00
4	902.239207	.57324854E-11	.99995915E+00
5	902.243947	.57324838E-11	.99995669E+00

1	906.017559	.56922933E-11	.99988028E+00
2	906.022300	.56922917E-11	.99988029E+00
3	906.027041	.56918767E-11	.99988029E+00
4	906.031782	.56917602E-11	.99988030E+00
5	906.036523	.56916604E-11	.99988031E+00
1	909.010173	.56573414E-11	.99988002E+00
2	909.014914	.56570707E-11	.99988003E+00
3	909.019655	.56568237E-11	.99988004E+00
4	909.024396	.56565696E-11	.99988005E+00
5	909.029137	.56563255E-11	.99988006E+00

THE TIME AT THE END OF MSEMIS IS 81.780
.180 SECS WERE REQUIRED FOR THIS MERGE

LOCATION	WAVENUMBER	MSCAT	SRC FCM	MS TRANS
1484	906.651259	.29521113E-11	.99967443E+00	
1485	906.656000	.29518610E-11	.99972141E+00	
1486	906.660741	.29516309E-11	.99975427E+00	
1487	906.665481	.29513803E-11	.99977929E+00	
1488	906.670222	.29510896E-11	.99979700E+00	
698	909.979259	.29460554E-11	.99383526E+00	
699	909.984000	.29457552E-11	.99383827E+00	
700	909.988741	.29454549E-11	.99382325E+00	
701	909.993481	.29451546E-11	.99381334E+00	
702	909.998222	.29448544E-11	.99379988E+00	

LOCATION

WAVENUMBER

MS EMISSION

MS TRANS

1484	902.217086	.57327788E-11	.99997843E+00
1485	902.216667	.57326470E-11	.99997781E+00
1486	902.220247	.57325340E-11	.99997702E+00
1487	902.221827	.57324375E-11	.99997585E+00
1488	902.223407	.57323600E-11	.99997427E+00
2396	906.009679	.56924400E-11	.99998023E+00
2397	906.011259	.56924162E-11	.99998025E+00
2398	906.012840	.56923970E-11	.99998026E+00
2399	906.014420	.56923659E-11	.99998027E+00
2400	906.016000	.56923301E-11	.99998028E+00
2396	909.807272	.56585555E-11	.99988004E+00
2397	909.807352	.56583013E-11	.99988004E+00
2398	909.807432	.56580286E-11	.99988004E+00
2399	909.807512	.56577543E-11	.99988004E+00
2400	909.807593	.56574848E-11	.99988004E+00
117	909.993481	.56642050E-11	.99997926E+00
118	909.995862	.56642073E-11	.99997912E+00
119	909.996642	.56642233E-11	.99997897E+00
120	909.998222	.56642056E-11	.99997800E+00
121	909.999802	.56639858E-11	.99997650E+00

TABLE B-2 (Cont.)

THE TIME AT THE END OF SRCFCM IS 81.781
.620 SECS WERE REQUIRED FOR THIS MERGE

FLXDMN - LAYER 6 WITH 1 PANELS

LOCATION	WAVENUMBER	COMP FLUX DN	COMP REFLECT DN
1	988.800000	.13289832E-07	.27566912E-05
2	988.810667	.13161401E-07	.27566965E-05
3	988.821333	.13128178E-07	.27566991E-05
4	988.832000	.13124471E-07	.27566994E-05
5	988.842667	.13132895E-07	.27566983E-05
LOCATION	WAVENUMBER	TOTAL FLUX UP	TOTAL FLUX DN
1	988.800000	.29938836E-04	.13291562E-07
2	988.810667	.29938817E-04	.13233931E-07
3	988.821333	.29937985E-04	.13218665E-07
4	988.832000	.29937935E-04	.13207183E-07
5	988.842667	.29937878E-04	.13215425E-07

LOCATION	WAVENUMBER	COMP FLUX DN	COMP REFLECT DN
934	989.952000	.15412970E-07	.28586448E-05
935	989.962667	.15903274E-07	.28585733E-05
936	989.973333	.16715744E-07	.28584565E-05
937	989.984000	.18134676E-07	.28582531E-05
938	989.994667	.20762152E-07	.28498980E-05
LOCATION	WAVENUMBER	TOTAL FLUX UP	TOTAL FLUX DN
934	989.952000	.29379766E-04	.15496721E-07
935	989.962667	.29378802E-04	.15907821E-07
936	989.973333	.29375368E-04	.16799477E-07
937	989.984000	.29368778E-04	.18218384E-07
938	989.994667	.29367228E-04	.20845846E-07

TABLE B-2 (Cont.)

THE TIME AT THE START OF SRCFCN IS 81.913				
SRCFCN - LAYER 7 WITH 1 PANELS				
LOCATION	WAVENUMBER	MSCAT SRC FCN	MS TRANS	
1	909.800000	.38130560E-11	.99995972E+00	
2	909.800711	.381308470E-11	.99995996E+00	
3	909.801422	.381308410E-11	.999959812E+00	
4	909.802133	.381308362E-11	.999959822E+00	
5	909.802844	.381308310E-11	.999959825E+00	
THE TIME AT THE START OF MSEMIS IS 82.199				
INITIAL LAYER 1 FINAL LAYER 10				
FILE 27 MERGED WITH FILE 26 ONTO FILE 28 WITH XTYP= -78571				
LOCATION	WAVENUMBER	MS EMISSION	MS TRANS	
1	909.800000	.95720905E-11	.99998150E+00	
2	909.800150	.95720972E-11	.99998151E+00	
3	909.800316	.95720955E-11	.99998152E+00	
4	909.800471	.95720936E-11	.99998152E+00	
5	909.800632	.95720916E-11	.99998153E+00	
1	902.224988	.95645596E-11	.99997103E+00	
2	902.226568	.95646420E-11	.99996859E+00	
3	902.228148	.95647107E-11	.99996401E+00	
4	902.229728	.95647849E-11	.99995916E+00	
5	902.231309	.95648220E-11	.99995669E+00	
1	906.801750	.95746970E-11	.99998028E+00	
2	906.801916	.95744205E-11	.99998029E+00	
3	906.802071	.95741432E-11	.99998029E+00	
4	906.802231	.95739597E-11	.99998030E+00	
5	906.802390	.95737816E-11	.99998031E+00	
1	909.801073	.95740429E-11	.99998002E+00	
2	909.801753	.95736114E-11	.99998002E+00	
3	909.803333	.95731934E-11	.99998002E+00	
4	909.804914	.95727800E-11	.99998002E+00	
5	909.806494	.95723787E-11	.99998002E+00	
THE TIME AT THE END OF MSEMIS IS 82.376				
.177 SECS WERE REQUIRED FOR THIS MERGE				
THE TIME AT THE END OF SRCFCN IS 82.377				
.464 SECS WERE REQUIRED FOR THIS MERGE				
FLXDOWN - LAYER 5 WITH 1 PANELS				
LOCATION	WAVENUMBER	COMP FLUX DN	COMP REFLECT DN	
1	909.800000	.29247665E-07	.65334371E-05	

LOCATION	WAVENUMBER	MSCAT SRC FCN	MS TRANS	
1403	909.969778	.39210621E-11	.99994100E+00	
1404	909.976889	.39214678E-11	.99993625E+00	
1405	909.984000	.39364268E-11	.99992983E+00	
1406	909.991111	.39365967E-11	.99992242E+00	
1407	909.998222	.39367803E-11	.99991058E+00	

LOCATION	WAVENUMBER	MS EMISSION	MS TRANS	
1404	902.217006	.95642573E-11	.99997843E+00	
1405	902.218667	.95641690E-11	.99997781E+00	
1406	902.220247	.95641641E-11	.99997702E+00	
1407	902.221827	.95641970E-11	.99997585E+00	
1408	902.223407	.95642521E-11	.99997427E+00	
2396	906.809679	.95750585E-11	.99998023E+00	
2397	906.811259	.95749905E-11	.99998025E+00	
2398	906.812840	.95749311E-11	.99998026E+00	
2399	906.814420	.95748635E-11	.99998027E+00	
2400	906.816000	.95747606E-11	.99998028E+00	
2396	909.802272	.95761544E-11	.99998004E+00	
2397	909.803052	.95757203E-11	.99998004E+00	
2398	909.805432	.95752676E-11	.99998004E+00	
2399	909.807012	.95748143E-11	.99998004E+00	
2400	909.808593	.95743678E-11	.99998004E+00	
117	909.993481	.96004071E-11	.99997926E+00	
118	909.995062	.96004380E-11	.99997912E+00	
119	909.996642	.96004778E-11	.99997897E+00	
120	909.998222	.96004795E-11	.99997880E+00	
121	909.999802	.96002655E-11	.99997858E+00	

LOCATION	WAVENUMBER	COMP FLUX DN	COMP REFLECT DN	
924	909.952000	.35365020E-07	.681805690E-05	

TABLE B-2 (Cont.)

LOCATION	WAVENUMBER	TOTAL FLUX UP	TOTAL FLUX DN	LOCATION	WAVENUMBER	TOTAL FLUX UP	TOTAL FLUX DN
2	900.010667	.29181747E-07	.65334461E-05	935	909.962667	.36370113E-07	.68182625E-05
3	900.021333	.29153177E-07	.65334451E-05	936	909.973333	.38096034E-07	.68177256E-05
4	900.032250	.29133760E-07	.65334495E-05	937	909.984000	.40073087E-07	.68168986E-05
5	900.042667	.29117321E-07	.65334435E-05	938	909.994667	.45112810E-07	.68153428E-05

LOCATION	WAVENUMBER	TOTAL FLUX UP	TOTAL FLUX DN	LOCATION	WAVENUMBER	TOTAL FLUX UP	TOTAL FLUX DN
1	900.002000	.29940239E-04	.29443278E-07	934	909.952000	.29382624E-04	.35565367E-07
2	900.010667	.29940215E-04	.29377359E-07	935	909.962667	.29381783E-04	.36570446E-07
3	900.021333	.29940180E-04	.29348789E-07	936	909.973333	.29378555E-04	.380297129E-07
4	900.032000	.29940134E-04	.29348773E-07	937	909.984000	.29372324E-04	.41074116E-07
5	900.042667	.29940075E-04	.29368823E-07	938	909.994667	.29371396E-04	.46312994E-07

TABLE B-2 (Cont.)

THE TIME AT THE START OF SRCFCN IS 82.497

SRCFCN - LAYER 6 WITH 1 PANELS

LOCATION	WAVENUMBER	MSCAT SRC FCN	MS TRANS
1	900.000000	.87243026E-11	.99987980E+00
2	900.010667	.87243679E-11	.99988026E+00
3	900.021333	.87243631E-11	.99988035E+00
4	900.032000	.87243322E-11	.99988040E+00
5	900.042667	.87243209E-11	.99988027E+00

THE TIME AT THE START OF MSEMIS IS 82.695

INITIAL LAYER 1 FINAL LAYER 10

FILE 27 MERGED WITH FILE 28 ONTO FILE 26 WITH XTYPE= -.6739;

LOCATION	WAVENUMBER	MS EMISSION	MS TRANS
1	900.000000	.18295351E-10	.99990150E+00
2	900.001500	.18295346E-10	.99990151E+00
3	900.003160	.18295340E-10	.99990152E+00
4	900.004741	.18295334E-10	.99990152E+00
5	900.006321	.18295327E-10	.99990153E+00
1	902.224988	.18346039E-10	.99997103E+00
2	902.226568	.18347310E-10	.99996859E+00
3	902.228148	.18347700E-10	.99996840E+00
4	902.229728	.18347934E-10	.99995915E+00
5	902.231309	.18347835E-10	.99995669E+00
1	906.017500	.18430954E-10	.99990028E+00
2	906.019160	.18430503E-10	.99990029E+00
3	906.020741	.18430849E-10	.99990029E+00
4	906.022321	.18429800E-10	.99990030E+00
5	906.023901	.18429299E-10	.99990031E+00
1	909.010173	.18552418E-10	.99990000E+00
2	909.011753	.18551667E-10	.99990002E+00
3	909.013333	.18550946E-10	.99990002E+00
4	909.014914	.18550257E-10	.99990002E+00
5	909.016494	.18549602E-10	.99990002E+00

THE TIME AT THE END OF MSEMIS IS 82.873
.178 SECS WERE REQUIRED FOR THIS MERGETHE TIME AT THE END OF SRCFCN IS 82.874
.377 SECS WERE REQUIRED FOR THIS MERGE

FLXDOWN - LAYER 4 WITH 1 PANELS

LOCATION WAVENUMBER COMP FLUX DN COMP REFLECT DN

LOCATION	WAVENUMBER	MSCAT SRC FCN	MS TRANS
934	909.952000	.89910105E-11	.99984118E+00
935	909.953667	.89910092E-11	.99983397E+00
936	909.955333	.89906731E-11	.99982194E+00
937	909.957000	.89896950E-11	.99980071E+00
938	909.958667	.89911711E-11	.99976449E+00
LOCATION	WAVENUMBER	MS EMISSION	MS TRANS
1404	902.217006	.18344543E-10	.99997043E+00
1405	902.218667	.18344604E-10	.99997781E+00
1406	902.220247	.18345122E-10	.99997702E+00
1407	902.221827	.18345616E-10	.99997585E+00
1408	902.223407	.18346127E-10	.99997427E+00
2396	906.005679	.18432010E-10	.99990023E+00
2397	906.011259	.18431793E-10	.99990025E+00
2398	906.012840	.18431608E-10	.99990026E+00
2399	906.014420	.18431413E-10	.99990027E+00
2400	906.016000	.18431185E-10	.99990028E+00
2396	909.002272	.18556200E-10	.99990004E+00
2397	909.003852	.18555477E-10	.99990004E+00
2398	909.005432	.18554650E-10	.99990004E+00
2399	909.007012	.18553850E-10	.99990004E+00
2400	909.008593	.18553056E-10	.99990004E+00
117	909.993481	.18589106E-10	.99997926E+00
118	909.995062	.18589362E-10	.99997912E+00
119	909.996642	.18589440E-10	.99997897E+00
120	909.998222	.18589459E-10	.99997880E+00
121	909.999802	.18589247E-10	.99997858E+00

LOCATION WAVENUMBER COMP FLUX DN COMP REFLECT DN

TABLE B-2 (Cont.)

LOCATION	WAVENUMBER	TOTAL FLUX UP	TOTAL FLUX DN
1	900.000000	.88119930E-07	.12044003E-04
2	900.016000	.88039891E-07	.12044091E-04
3	900.032000	.88048300E-07	.12044077E-04
4	900.048000	.88130809E-07	.12044020E-04
5	900.064000	.88268889E-07	.12043949E-04
LOCATION	WAVENUMBER	TOTAL FLUX UP	TOTAL FLUX DN
1	900.080000	.29947230E-04	.88400617E-07
2	900.016000	.29947184E-04	.88400577E-07
3	900.032000	.29947121E-04	.88400506E-07
4	900.048000	.29947035E-04	.88491432E-07
5	900.064000	.29946922E-04	.88626750E-07
LOCATION	WAVENUMBER	TOTAL FLUX UP	TOTAL FLUX DN
622	909.936000	.10515392E-06	.12398354E-04
623	909.952000	.10628437E-06	.12597784E-04
624	909.968000	.10981413E-06	.12595710E-04
625	909.984000	.11700031E-06	.12501612E-04
626	910.000000	.12759827E-06	.12505609E-04
LOCATION	WAVENUMBER	TOTAL FLUX UP	TOTAL FLUX DN
622	909.936000	.29390568E-04	.10552428E-06
623	909.952000	.29391309E-04	.10665464E-06
624	909.968000	.29389762E-04	.11018432E-06
625	909.984000	.29383592E-04	.11737029E-06
626	910.000000	.29380825E-04	.12756805E-06

TABLE B-2 (Cont.)

THE TIME AT THE START OF SRCFCN IS 82.972

SRCFCN - LAYER 5 WITH 1 PANELS

LOCATION	WAVENUMBER	MSCAT SRC FCN	MS TRANS
1	900.000000	.18681305E-10	.99956378E+00
2	900.001500	.18681229E-10	.99956401E+00
3	900.003000	.18681176E-10	.99956415E+00
4	900.004500	.18681155E-10	.99956424E+00
5	900.006000	.18681152E-10	.99956374E+00

THE TIME AT THE START OF MSEMIS IS 83.177

INITIAL LAYER 1 FINAL LAYER 10

FILE 2- MERGED WITH FILE 26 ONTO FILE 28 WITH XTYP= -67391

LOCATION	WAVENUMBER	MS EMISSION	MS TRANS
1	902.000000	.36968676E-10	.99991150E+00
2	902.001500	.36968662E-10	.99990151E+00
3	902.003000	.36968646E-10	.99990152E+00
4	902.004500	.36968638E-10	.99990154E+00
5	902.006000	.36968611E-10	.99990153E+00
1	902.223900	.37162933E-10	.99997103E+00
2	902.225400	.37164094E-10	.99996859E+00
3	902.226900	.37165025E-10	.99996401E+00
4	902.228400	.37165534E-10	.99995915E+00
5	902.230000	.37165272E-10	.99995669E+00
1	906.017500	.37398800E-10	.99998028E+00
2	906.019100	.37397863E-10	.99998029E+00
3	906.020700	.37396909E-10	.99998029E+00
4	906.022300	.37396053E-10	.99998030E+00
5	906.023900	.37395157E-10	.99998031E+00
1	909.010173	.37779242E-10	.99998002E+00
2	909.011753	.37778292E-10	.99998002E+00
3	909.013333	.37777410E-10	.99998002E+00
4	909.014914	.37776555E-10	.99998002E+00
5	909.016494	.37775655E-10	.99998002E+00

THE TIME AT THE END OF MSEMIS IS 93.356
.179 SECS WERE REQUIRED FOR THIS MERGETHE TIME AT THE END OF SRCFCN IS 93.357
.385 SECS WERE REQUIRED FOR THIS MERGE

FLXDUN - LAYER 3 WITH 1 PANELS

LOCATION	WAVENUMBER	COMP FLUX DN	COMP REFLECT DN
1	900.000000	.21915036E-06	.24916381E-04

LOCATION	WAVENUMBER	MSCAT SRC FCN	MS TRANS
934	909.952000	.19254440E-10	.99997255E+00
935	909.952667	.19255187E-10	.99997312E+00
936	909.953333	.19256124E-10	.99997371E+00
937	909.954000	.19256715E-10	.99997427E+00
938	909.954667	.19256931E-10	.99997485E+00

LOCATION	WAVENUMBER	MS EMISSION	MS TRANS
1404	902.212886	.37156090E-10	.99997843E+00
1405	902.210667	.37157154E-10	.99997781E+00
1406	902.222027	.37155580E-10	.99997702E+00
1407	902.221027	.37160050E-10	.99997595E+00
1408	902.223407	.371671480E-10	.99997427E+00
2396	906.009679	.37402050E-10	.99998023E+00
2397	906.011259	.37421300E-10	.99998025E+00
2398	906.012840	.37430764E-10	.99998026E+00
2399	906.014420	.37400156E-10	.99998027E+00
2400	906.016000	.37395520E-10	.99998028E+00
2396	909.007272	.37784590E-10	.99998004E+00
2397	909.007385	.37783417E-10	.99998004E+00
2398	909.005432	.37782264E-10	.99998004E+00
2399	909.007012	.37781155E-10	.99998004E+00
2400	909.009593	.37780095E-10	.99998004E+00
117	909.993481	.37037795E-10	.99997926E+00
118	909.993062	.37038412E-10	.99997912E+00
119	909.993642	.37038624E-10	.99997937E+00
120	909.998222	.37038703E-10	.99997980E+00
121	909.998002	.37038498E-10	.99997958E+00

LOCATION	WAVENUMBER	COMP FLUX DN	COMP REFLECT DN
622	909.993000	.37502655E-06	.20350061E-04

TABLE B-2 (Cont.)

2	900.816000	.31911550E-06	.24916322E-04	623	909.952000	.37595785E-06	.26049804E-04
3	900.832000	.31918874E-06	.24916210E-04	624	909.968000	.38210263E-06	.26043584E-04
4	900.848000	.31927357E-06	.24916007E-04	625	909.984000	.39480693E-06	.26038493E-04
5	900.864000	.31936617E-06	.24915700E-04	626	910.000000	.41222815E-06	.26013478E-04
LOCATION	WAVENUMBER	TOTAL FLUX UP	TOTAL FLUX DN	LOCATION	WAVENUMBER	TOTAL FLUX UP	TOTAL FLUX DN
1	900.880000	.29967594E-04	.31989785E-06	622	909.936000	.29414985E-04	.37579292E-06
2	900.896000	.29967541E-04	.31986218E-06	623	909.952000	.29415851E-04	.37672412E-06
3	900.912000	.29967493E-04	.31993541E-06	624	909.968000	.29414855E-04	.38286978E-06
4	900.928000	.29967413E-04	.32012023E-06	625	909.984000	.29409733E-04	.39557248E-06
5	900.944000	.29967323E-04	.32040836E-06	626	910.000000	.29408637E-04	.41238515E-06

TABLE B-2 (Cont.)[illegible]

TABLE B-2 (Cont.)

LOCATION	WAVELENGTH	TOTAL FLUX UP	TOTAL FLUX DN	LOCATION	WAVELENGTH	TOTAL FLUX UP	TOTAL FLUX DN
414	989.912000	.14264315E-05	.17406411E-02	414	989.912000	.29483254E-04	.14797997E-05
415	989.936000	.14607451E-05	.17415589E-02	415	989.936000	.29485773E-04	.14618964E-05
416	989.960000	.14120519E-05	.17416069E-02	416	989.960000	.29486549E-04	.14634850E-05
417	989.984000	.14395761E-05	.17407561E-02	417	989.984000	.29481638E-04	.14918016E-05
418	918.000000	.14752609E-05	.17404272E-02	418	918.000000	.29488775E-04	.15265693E-05

TABLE B-2 (Cont.)

THE TIME AT THE START OF SECTION IS 83.032				
SECTION - LAYER 3 WITH 1 PANELS				
LOCATION	WAVENUMBER	MSCAT SPC FCN	MS TRANS	MS TRANS
1	909.936000	78413373E-10	.99349759E+00	.99349759E+00
2	909.936000	78415238E-10	.99350000E+00	.99350000E+00
3	909.936000	78443149E-10	.99343012E+00	.99343012E+00
4	909.936000	78443953E-10	.99330323E+00	.99330323E+00
5	909.936000	78565313E-10	.99313598E+00	.99313598E+00
THE TIME AT THE START OF SECTION IS 83.971				
SECTION - LAYER 3 WITH 1 PANELS				
LOCATION	WAVENUMBER	MSCAT SPC FCN	MS TRANS	MS TRANS
1	902.217866	.13331778E-09	.9997813E+00	.9997813E+00
2	902.218667	.13332792E-09	.9997781E+00	.9997781E+00
3	902.220247	.13333791E-09	.9997782E+00	.9997782E+00
4	902.221827	.13334722E-09	.9997585E+00	.9997585E+00
5	902.223427	.13335512E-09	.9997427E+00	.9997427E+00
6	906.809679	.13463777E-09	.99998023E+00	.99998023E+00
7	906.811259	.13463619E-09	.99998025E+00	.99998025E+00
8	906.811840	.13463611E-09	.99998026E+00	.99998026E+00
9	906.811420	.13463443E-09	.99998027E+00	.99998027E+00
10	906.811600	.13463426E-09	.99998028E+00	.99998028E+00
11	909.807272	.13643296E-09	.99998024E+00	.99998024E+00
12	909.807812	.13644310E-09	.99998004E+00	.99998004E+00
13	909.807812	.13645311E-09	.99998004E+00	.99998004E+00
14	909.808593	.13646293E-09	.99998004E+00	.99998004E+00
15	909.992461	.13647408E-09	.9997925E+00	.9997925E+00
16	909.992672	.13647207E-09	.9997912E+00	.9997912E+00
17	909.992642	.13647923E-09	.9997897E+00	.9997897E+00
18	909.992222	.13644574E-09	.9997808E+00	.9997808E+00
19	909.992802	.13645133E-09	.9997858E+00	.9997858E+00
THE TIME AT THE START OF SECTION IS 84.148				
SECTION - LAYER 3 WITH 1 PANELS				
LOCATION	WAVENUMBER	MSCAT SPC FCN	MS TRANS	MS TRANS
1	909.912200	.48279727E-05	.14255144E-01	.14255144E-01

TABLE B-2 (Cont.)

LOCATION	WAVENUMBER	TOTAL FLUX UP	TOTAL FLUX DN	LOCATION	WAVENUMBER	TOTAL FLUX UP	TOTAL FLUX DN
1	909.936000	.48813084E-05	.14375567E-01	415	909.936000	.48813084E-05	.14375567E-01
2	909.960000	.48726931E-05	.14301794E-01	416	909.960000	.48726931E-05	.14301794E-01
3	909.984000	.49091114E-05	.14373579E-01	417	909.984000	.49091114E-05	.14373579E-01
4	910.008000	.49724957E-05	.14360448E-01	418	910.008000	.49724957E-05	.14360448E-01
5	909.912000	.29716535E-04	.53545557E-05	419	909.912000	.29716535E-04	.53545557E-05
6	909.936000	.29718107E-04	.53085238E-05	415	909.936000	.29718107E-04	.53085238E-05
7	909.960000	.29718685E-04	.53011011E-05	416	909.960000	.29718685E-04	.53011011E-05
8	909.984000	.29718339E-04	.53362698E-05	417	909.984000	.29718339E-04	.53362698E-05
9	910.008000	.29716577E-04	.53392338E-05	418	910.008000	.29716577E-04	.53392338E-05

TABLE B-2 (Cont.)

THE TIME AT THE START OF SECTION IS 84.215				
SECTION - LAYER 2 WITH 1 PANELS				
LOCATION	WAVENUMBER	MSCAT SRC FCN	MS TRANS	
414	909.912000	.1110136E-07	.9725147E+00	
415	909.916000	.1106603E-07	.97000506E+00	
416	909.960000	.11062950E-07	.97002305E+00	
417	909.984000	.11112080E-07	.97055489E+00	
418	909.988000	.11196301E-07	.97014591E+00	
THE TIME AT THE START OF SECTION IS 84.318				
SECTION - LAYER 1 FINAL LAYER 10				
FILE - 20 ONTO FILE 20 WITH XTYPE= -57049				
LOCATION	WAVENUMBER	MSCAT SRC FCN	MS TRANS	
1404	902.217000	.10839479E-07	.9997843E+00	
1405	902.218667	.10944497E-07	.93977781E+00	
1406	902.220747	.10846630E-07	.99977802E+00	
1407	902.221807	.10853226E-07	.9997585E+00	
1408	902.223407	.10856950E-07	.9997427E+00	
2396	906.009679	.11305508E-07	.99980023E+00	
2397	906.011299	.11310606E-07	.99980023E+00	
2398	906.012840	.11316481E-07	.99980023E+00	
2399	906.014420	.11321720E-07	.99980023E+00	
2400	906.016000	.1132846E-07	.99980023E+00	
2396	909.002222	.11519233E-07	.99980004E+00	
2397	909.003852	.11520256E-07	.99980004E+00	
2398	909.005432	.11544060E-07	.99980004E+00	
2399	909.007012	.11557589E-07	.99980004E+00	
2400	909.008513	.11568076E-07	.99980004E+00	
117	909.993481	.11261206E-07	.9997926E+00	
118	909.995062	.11266602E-07	.9997912E+00	
119	909.996642	.1126795E-07	.9997807E+00	
120	909.998222	.11297996E-07	.9997800E+00	
121	909.999802	.11303896E-07	.9997850E+00	
THE TIME AT THE START OF SECTION IS 84.406				
SECTION - LAYER 2 WITH 1 PANELS				
LOCATION	WAVENUMBER	MSCAT SRC FCN	MS TRANS	
414	909.912000	.1110136E-07	.9725147E+00	
415	909.916000	.1106603E-07	.97000506E+00	
416	909.960000	.11062950E-07	.97002305E+00	
417	909.984000	.11112080E-07	.97055489E+00	
418	909.988000	.11196301E-07	.97014591E+00	
THE TIME AT THE START OF SECTION IS 84.407				
SECTION - LAYER 2 WITH 1 PANELS				
LOCATION	WAVENUMBER	MSCAT SRC FCN	MS TRANS	
414	909.912000	.1110136E-07	.9725147E+00	
415	909.916000	.1106603E-07	.97000506E+00	
416	909.960000	.11062950E-07	.97002305E+00	
417	909.984000	.11112080E-07	.97055489E+00	
418	909.988000	.11196301E-07	.97014591E+00	

TABLE B-2 (Cont.)

LOCATION	WAVENUMBER	TOTAL FLUX UP	TOTAL FLUX DN	LOCATION	WAVENUMBER	TOTAL FLUX UP	TOTAL FLUX DN
1	909.936000	.48813084E-05	.14375567E-01	415	909.936000	.48813084E-05	.14375567E-01
2	909.960000	.48736931E-05	.14381794E-01	416	909.960000	.48736931E-05	.14381794E-01
3	909.984000	.49091114E-05	.14373579E-01	417	909.984000	.49091114E-05	.14373579E-01
4	910.008000	.49724955E-05	.14360448E-01	418	910.008000	.49724955E-05	.14360448E-01
1	909.912000	.30340070E-04	.53635102E-05	414	909.912000	.30340070E-04	.53635102E-05
2	909.936000	.30340070E-04	.53174756E-05	415	909.936000	.30340070E-04	.53174756E-05
3	909.960000	.30340070E-04	.53100493E-05	416	909.960000	.30340070E-04	.53100493E-05
4	909.984000	.30340070E-04	.53452103E-05	417	909.984000	.30340070E-04	.53452103E-05
5	910.008000	.30340070E-04	.54002400E-05	418	910.008000	.30340070E-04	.54002400E-05

TABLE B-2 (Cont.)

[illegible]

TABLE B-2 (Cont.)

INITIAL LAYER	FINAL LAYER	IF	FILE	20 MERGED WITH FILE	12 ONTO FILE	11 WITH XTYPE=	8.
LOCATION	WAVENUMBER	RADIANCE	TRANSMITTANCE	LOCATION	WAVENUMBER	RADIANCE	TRANSMITTANCE
1	902.2170866	.9539034E-06	.8561704E+00	1404	902.2170866	.95290365E-06	.85102450E+00
2	902.2170866	.9539034E-06	.8561704E+00	1405	902.2170866	.9539034E-06	.85093402E+00
3	902.2170866	.9539034E-06	.8561704E+00	1406	902.2170866	.95406210E-06	.85084592E+00
4	902.2170866	.9539034E-06	.8561704E+00	1407	902.2170866	.95453089E-06	.85076012E+00
5	902.2170866	.9539034E-06	.8561704E+00	1408	902.2170866	.95509917E-06	.85067634E+00
6	902.2170866	.9539034E-06	.8561704E+00	2396	906.009679	.10357103E-05	.84147561E+00
7	902.2170866	.9539034E-06	.8561704E+00	2397	906.011259	.10168826E-05	.84136043E+00
8	902.2170866	.9539034E-06	.8561704E+00	2398	906.012840	.10281555E-05	.84123647E+00
9	902.2170866	.9539034E-06	.8561704E+00	2399	906.014420	.10394271E-05	.84110460E+00
10	902.2170866	.9539034E-06	.8561704E+00	2400	906.016000	.1040024E-05	.84096613E+00
11	902.2170866	.9539034E-06	.8561704E+00	2396	909.002272	.10616034E-05	.83762952E+00
12	902.2170866	.9539034E-06	.8561704E+00	2397	909.003852	.10636313E-05	.83739263E+00
13	902.2170866	.9539034E-06	.8561704E+00	2398	909.005432	.10656460E-05	.83715874E+00
14	902.2170866	.9539034E-06	.8561704E+00	2399	909.007012	.10676136E-05	.83692923E+00
15	902.2170866	.9539034E-06	.8561704E+00	2400	909.008593	.10695003E-05	.83670569E+00
16	902.2170866	.9539034E-06	.8561704E+00	117	909.993401	.10156097E-05	.84244313E+00
17	902.2170866	.9539034E-06	.8561704E+00	118	909.995062	.10157522E-05	.84244148E+00
18	902.2170866	.9539034E-06	.8561704E+00	119	909.996642	.10159244E-05	.84243948E+00
19	902.2170866	.9539034E-06	.8561704E+00	120	909.998222	.10158919E-05	.84243462E+00
20	902.2170866	.9539034E-06	.8561704E+00	121	909.999802	.10159572E-05	.84243443E+00
TIME LEAVING CASCODE				TIME LEAVING CASCODE			
84.9258				84.9258			
TOTAL				TOTAL			
13.2218				13.2218			

THE TIME AT THE END OF THE MERGE IS 84.9258
 13.2218 SECS WERE REQUIRED FOR THIS MERGE

Appendix C

EXAMPLES OF LOWTRAN OUTPUT

Four cases are included as tests for LOWTRAN with multiple scattering. The input cards for the four cases are listed in Table C-1 and the listing of the file OUTPUT (TAPE 6) is in Tables C-2 - C-5. The next section will discuss the output for case 1. Only those details which differ from the standard LOWTRAN output will be discussed.

C.1 Case 1: Thermal Scattering of Downward Radiance

This case demonstrates the new multiple scattering calculation for thermal radiance. The parameters selected for this case are as follows: the atmospheric profile is the 1962 U.S. Standard and the boundary layer aerosol model is RURAL with 5 km meteorological range. The path is a slant path from the ground to 20 km with a zenith angle at the ground of 0.0 degrees.

The output for this case shown in Table C-2 will now be described. The first difference is in CARD 1, which now contains another quantity, IMULT. IMULT is the last variable printed on CARD 1, and is the flag for multiple scattering. When IMULT is 1, the multiple scattering features of the program will be used. A message to this effect is printed in the output directly after the message which tells the user that 'PROGRAM WILL COMPUTE RADIANCE'.

The next four pages which print out the 'ATMOSPHERIC PROFILES' and the 'REFRACTED PATH THROUGH THE ATMOSPHERE' are identical to those printed out by LOWTRAN6. The following three pages are not included in LOWTRAN6. These three pages contain the new slant path parameters for using multiple scattering followed by the refracted path used by the multiple scattering run, and the summary of the multiple scattering geometry calculation. The final page is exactly identical except that the radiance that is printed out is the multiple scattered radiance.

C.2 Case 2: Thermal Scattering of Upward Radiance

This case is directly analogous to Case 1 except that the observer is looking straight down instead of straight up. The output differences are the same as those explained for Case 1.

C.3 Case 3: Solar Scattering of Downward Radiance

Case 3 illustrates the multiple scattered solar radiance calculation. The parameters for this case are the same as those for Case 1, with the addition of the sun at 60 degrees. The output differences are the same as those listed for Case 1, excluding the final radiance output.

The final radiance output has been expanded for the solar case. Two new columns have been added. Under the column heading 'PATH SCATTERED RADIANCE', there are now three columns. These are 'TOTAL' (in both cm^{-1} and microns) and 'S SCAT' (in cm^{-1}). TOTAL is the total path scattered radiance, containing both single and multiple scattered contributions. S SCAT is the single scattered part of the total path scattered radiance. This S SCAT is the quantity that LOWTRAN would provide under the 'PATH SCATTERED' heading if the user were to run LOWTRAN without multiple scattering. Likewise under the header 'GROUND REFLECTED RADIANCE' there are now three columns. These are TOTAL (in both cm^{-1} and microns) and 'DIRECT' (in cm^{-1}). TOTAL is the total ground reflected contribution to the radiance, containing both scattered and direct contributions. DIRECT is the direct ground reflected part of the total reflected radiance. The DIRECT term is the quantity that LOWTRAN would provide under the GROUND REFLECTED heading if the user were to run LOWTRAN without multiple scattering. The significance of the S SCAT and the DIRECT terms is that the user can run one case of multiple scattering and by comparing these quantities to the total quantities can determine the relative importance of multiple scattering for that case. This will allow the user to decide more easily whether or not multiple scattering has a significant contribution for that particular case.

C.4 Case 4: Solar Scattering of Upward Radiance

This case is directly analogous to Case 3 except that the observer is looking straight down instead of straight up. The output differences are the same as those explained for Case 3.

TABLE C-1

INPUT CARDS FOR THE FOUR LOWTRAN TEST CASES

Test Case 1

```

6      2      1      0      0      0      0      0      0      0      0
2      0      0      0      0      0      0      0      0      0      0
      0.0      20.0      5.0      0.000      0.000      0.000      0.000
850.0      950.0      5.0

```

Test Case 2

```

6      2      1      0      0      0      0      0      0      0      0
2      0      0      0      0      0      0      0      0      0      0
      20.0      00.0      100.00      0.000      0.000      0.000      0.000
850.0      950.0      5.0

```

Test Case 3

```

6      2      2      0      0      0      0      0      0      0      0
2      0      0      0      0      0      0      0      0      0      0
      0.0      20.0      0.00      0.000      0.000      0.000      0.000
2      2      1      0      0      0      0      0      0      0      0
000.0      60.00      00.0      20.0      00.0      00.0      00.0      00.0
18100.0      16260.0      10.0

```

Test Case 4

```

6      2      2      0      0      0      0      0      0      0      0
2      0      0      0      0      0      0      0      0      0      0
      20.0      00.0      100.00      0.000      0.000      0.000      0.000
2      2      1      0      0      0      0      0      0      0      0
000.0      60.00      00.0      20.0      00.0      00.0      00.0      00.0
18100.0      16260.0      10.0

```

LOWTRAN OUTPUT FOR CASE 1

C-4

TABLE C-2 (Cont).

ATMOSPHERIC PROFILES								
Z (KM)	P (MB)	T (K)	H2O (SCALED)	CO2+ (LOWTRAN UNITS)	N2 (MOL/CM2 KM)	CNTNSLF MOL SCAT (-)	N-1 (-)	O3 (UV) (ATM CM/KM)
1	1.02	181.2	5.758E-01	2.493E-03	7.378E-01	1.569E+20	9.475E-01	2.722E-04
2	1.02	181.2	5.758E-01	2.493E-03	7.378E-01	1.569E+20	9.475E-01	2.722E-04
3	1.02	181.2	5.758E-01	2.493E-03	7.378E-01	1.569E+20	9.475E-01	2.722E-04
4	1.02	181.2	5.758E-01	2.493E-03	7.378E-01	1.569E+20	9.475E-01	2.722E-04
5	1.02	181.2	5.758E-01	2.493E-03	7.378E-01	1.569E+20	9.475E-01	2.722E-04
6	1.02	181.2	5.758E-01	2.493E-03	7.378E-01	1.569E+20	9.475E-01	2.722E-04
7	1.02	181.2	5.758E-01	2.493E-03	7.378E-01	1.569E+20	9.475E-01	2.722E-04
8	1.02	181.2	5.758E-01	2.493E-03	7.378E-01	1.569E+20	9.475E-01	2.722E-04
9	1.02	181.2	5.758E-01	2.493E-03	7.378E-01	1.569E+20	9.475E-01	2.722E-04
10	1.02	181.2	5.758E-01	2.493E-03	7.378E-01	1.569E+20	9.475E-01	2.722E-04
11	1.02	181.2	5.758E-01	2.493E-03	7.378E-01	1.569E+20	9.475E-01	2.722E-04
12	1.02	181.2	5.758E-01	2.493E-03	7.378E-01	1.569E+20	9.475E-01	2.722E-04
13	1.02	181.2	5.758E-01	2.493E-03	7.378E-01	1.569E+20	9.475E-01	2.722E-04
14	1.02	181.2	5.758E-01	2.493E-03	7.378E-01	1.569E+20	9.475E-01	2.722E-04
15	1.02	181.2	5.758E-01	2.493E-03	7.378E-01	1.569E+20	9.475E-01	2.722E-04
16	1.02	181.2	5.758E-01	2.493E-03	7.378E-01	1.569E+20	9.475E-01	2.722E-04
17	1.02	181.2	5.758E-01	2.493E-03	7.378E-01	1.569E+20	9.475E-01	2.722E-04
18	1.02	181.2	5.758E-01	2.493E-03	7.378E-01	1.569E+20	9.475E-01	2.722E-04
19	1.02	181.2	5.758E-01	2.493E-03	7.378E-01	1.569E+20	9.475E-01	2.722E-04
20	1.02	181.2	5.758E-01	2.493E-03	7.378E-01	1.569E+20	9.475E-01	2.722E-04
21	1.02	181.2	5.758E-01	2.493E-03	7.378E-01	1.569E+20	9.475E-01	2.722E-04
22	1.02	181.2	5.758E-01	2.493E-03	7.378E-01	1.569E+20	9.475E-01	2.722E-04
23	1.02	181.2	5.758E-01	2.493E-03	7.378E-01	1.569E+20	9.475E-01	2.722E-04
24	1.02	181.2	5.758E-01	2.493E-03	7.378E-01	1.569E+20	9.475E-01	2.722E-04
25	1.02	181.2	5.758E-01	2.493E-03	7.378E-01	1.569E+20	9.475E-01	2.722E-04
26	1.02	181.2	5.758E-01	2.493E-03	7.378E-01	1.569E+20	9.475E-01	2.722E-04
27	1.02	181.2	5.758E-01	2.493E-03	7.378E-01	1.569E+20	9.475E-01	2.722E-04
28	1.02	181.2	5.758E-01	2.493E-03	7.378E-01	1.569E+20	9.475E-01	2.722E-04
29	1.02	181.2	5.758E-01	2.493E-03	7.378E-01	1.569E+20	9.475E-01	2.722E-04
30	1.02	181.2	5.758E-01	2.493E-03	7.378E-01	1.569E+20	9.475E-01	2.722E-04
31	1.02	181.2	5.758E-01	2.493E-03	7.378E-01	1.569E+20	9.475E-01	2.722E-04
32	1.02	181.2	5.758E-01	2.493E-03	7.378E-01	1.569E+20	9.475E-01	2.722E-04
33	1.02	181.2	5.758E-01	2.493E-03	7.378E-01	1.569E+20	9.475E-01	2.722E-04

TABLE C-2 (Cont).

ATMOSPHERIC PROFILES

[illegible]

CASE 2A: GIVEN H_1 , H_2 , ANGLE

SLANT PATH PARAMETERS IN STANDARD FORM

H1	=	.000 KM
H2	=	20.000 KM
ANGLE	=	.000 DEG

TABLE C-2 (Cont).

PHI	182.000 DEG
HMIN	.000 KH
LEN	g

TABLE C-2 (Cont).

CALCULATION OF THE REFRACTED PATH THROUGH THE ATMOSPHERE

I	ALTITUDE		THETA (DEG)	ORANGE (KM)	RANGE (KM)	DBETA (DEG)	BETA (DEG)	PHI (DEG)	DBEND (DEG)	BENDING (DEG)	PBAR (MB)	TBAR (K)	RHOBAR (GM CM-3)
	FROM (KM)	TO (KM)											
H1 TO H2													
1	1.000	1.000	.000	1.000	1.000	.000	.000	180.000	.000	.000	955.683	284.99	1.17E-03
2	1.000	2.000	.000	1.000	2.000	.000	.000	180.000	.000	.000	846.698	278.49	1.06E-03
3	2.000	3.000	.000	1.000	3.000	.000	.000	180.000	.000	.000	747.913	271.99	9.57E-04
4	3.000	4.000	.000	1.000	4.000	.000	.000	180.000	.000	.000	658.727	265.49	8.63E-04
5	4.000	5.000	.000	1.000	5.000	.000	.000	180.000	.000	.000	578.391	258.99	7.77E-04
6	5.000	6.000	.000	1.000	6.000	.000	.000	180.000	.000	.000	516.204	252.50	6.98E-04
7	6.000	7.000	.000	1.000	7.000	.000	.000	180.000	.000	.000	471.516	246.00	6.24E-04
8	7.000	8.000	.000	1.000	8.000	.000	.000	180.000	.000	.000	433.677	239.50	5.52E-04
9	8.000	9.000	.000	1.000	9.000	.000	.000	180.000	.000	.000	402.137	233.00	4.96E-04
10	9.000	10.000	.000	1.000	10.000	.000	.000	180.000	.000	.000	376.399	226.55	4.40E-04
11	10.000	11.000	.000	1.000	11.000	.000	.000	180.000	.000	.000	355.987	220.10	3.89E-04
12	11.000	12.000	.000	1.000	12.000	.000	.000	180.000	.000	.000	339.999	213.75	3.38E-04
13	12.000	13.000	.000	1.000	13.000	.000	.000	180.000	.000	.000	328.980	207.50	2.89E-04
14	13.000	14.000	.000	1.000	14.000	.000	.000	180.000	.000	.000	321.750	201.40	2.47E-04
15	14.000	15.000	.000	1.000	15.000	.000	.000	180.000	.000	.000	317.400	195.50	2.11E-04
16	15.000	16.000	.000	1.000	16.000	.000	.000	180.000	.000	.000	314.900	189.90	1.80E-04
17	16.000	17.000	.000	1.000	17.000	.000	.000	180.000	.000	.000	313.200	184.60	1.54E-04
18	17.000	18.000	.000	1.000	18.000	.000	.000	180.000	.000	.000	312.275	179.70	1.32E-04
19	18.000	19.000	.000	1.000	19.000	.000	.000	180.000	.000	.000	311.160	175.20	1.13E-04
20	19.000	20.000	.000	1.000	20.000	.000	.000	180.000	.000	.000	310.000	171.00	9.62E-05

CUMULATIVE ABSORBER AMOUNTS FOR THE PATH FROM H1 TO Z

J	Z (KM)	THETA (DEG)	H2C (SCALED LOWTRAN UNITS)	CO2+ (SCALED LOWTRAN UNITS)	O3 (ATM CM)	HNO3 (ATM CM)	O3 UV (ATM CM)	CNTMSLF1 (MOL CM-2)	CNTMSLF2 (MOL CM-2)	CNTMFRM (MOL CM-2)
1	1.000	284.99	4.664E-01	8.586E-01	2.448E-03	.000E+00	2.520E-03	1.138E+20	3.482E+19	1.629E+22
2	2.000	279.49	7.631E-01	1.561E+00	4.725E-03	.000E+00	5.049E-03	1.700E+20	6.213E+19	3.608E+22
3	3.000	271.99	9.344E-01	2.151E+00	6.924E-03	.000E+00	7.465E-03	1.944E+20	7.842E+19	3.207E+22
4	4.000	265.49	1.037E+00	2.649E+00	8.819E-03	.000E+00	9.764E-03	2.193E+20	8.630E+19	3.631E+22
5	5.000	258.99	1.090E+00	3.043E+00	1.055E-02	.000E+00	1.185E+02	2.371E+20	8.963E+19	3.817E+22
6	6.000	252.50	1.118E+00	3.373E+00	1.218E-02	.000E+00	1.397E+02	2.488E+20	9.407E+19	3.915E+22
7	7.000	246.00	1.132E+00	3.643E+00	1.379E-02	.000E+00	1.617E+02	2.586E+20	9.115E+19	3.965E+22
8	8.000	239.50	1.129E+00	3.861E+00	1.543E-02	2.034E-35	1.852E+02	2.687E+20	9.127E+19	3.990E+22
9	9.000	233.00	1.142E+00	4.030E+00	1.725E-02	1.807E-06	2.139E+02	2.787E+20	9.138E+19	4.001E+22
10	10.000	226.55	1.144E+00	4.179E+00	1.966E-02	8.893E-06	2.515E+02	2.887E+20	9.131E+19	4.005E+22
11	11.000	220.10	1.144E+00	4.297E+00	2.268E-02	2.546E-05	3.028E+02	2.987E+20	9.131E+19	4.006E+22
12	12.000	213.75	1.144E+00	4.388E+00	2.645E-02	5.123E-05	3.785E+02	3.087E+20	9.131E+19	4.007E+22
13	13.000	207.50	1.144E+00	4.446E+00	3.048E-02	8.015E-05	4.475E+02	3.187E+20	9.131E+19	4.007E+22
14	14.000	201.40	1.144E+00	4.497E+00	3.461E-02	1.087E-04	5.315E+02	3.287E+20	9.131E+19	4.007E+22
15	15.000	195.50	1.144E+00	4.535E+00	3.892E-02	1.363E-04	6.248E+02	3.387E+20	9.131E+19	4.007E+22

TABLE C-2 (Cont).

[illegible]

SUMMARY OF THE GEOMETRY CALCULATION

NAME	AGE	SEX	HT	WT	HAIR	EYES	SKIN	TEETH	SCARS	REMARKS
WALSH, JAMES	28	M	5'10"	160	BROWN	BROWN	Fair	Good	None	Normal
SMITH, JOHN	32	M	5'8"	150	BLACK	BLUE	Dark	Good	None	Normal
JOHNSON, ROBERT	25	M	5'12"	170	BROWN	BROWN	Fair	Good	None	Normal
DAVIS, MICHAEL	30	M	5'9"	155	BLACK	BROWN	Dark	Good	None	Normal
WILLIAMS, DAVID	27	M	5'11"	165	BROWN	BROWN	Fair	Good	None	Normal
BROWN, JAMES	31	M	5'7"	145	BLACK	BLUE	Dark	Good	None	Normal
GREEN, ROBERT	29	M	5'10"	160	BROWN	BROWN	Fair	Good	None	Normal
MILLER, JOHN	33	M	5'8"	150	BLACK	BROWN	Dark	Good	None	Normal
WILSON, DAVID	26	M	5'11"	165	BROWN	BROWN	Fair	Good	None	Normal
ANDERSON, MICHAEL	34	M	5'9"	155	BLACK	BROWN	Dark	Good	None	Normal
THOMAS, JAMES	28	M	5'10"	160	BROWN	BROWN	Fair	Good	None	Normal
LEE, ROBERT	30	M	5'8"	150	BLACK	BROWN	Dark	Good	None	Normal
WALKER, DAVID	27	M	5'11"	165	BROWN	BROWN	Fair	Good	None	Normal
PERKINS, JOHN	32	M	5'7"	145	BLACK	BROWN	Dark	Good	None	Normal
ROBERTS, MICHAEL	29	M	5'10"	160	BROWN	BROWN	Fair	Good	None	Normal
TURNER, JAMES	31	M	5'9"	155	BLACK	BROWN	Dark	Good	None	Normal
SCOTT, DAVID	26	M	5'11"	165	BROWN	BROWN	Fair	Good	None	Normal
CRISP, MICHAEL	34	M	5'8"	150	BLACK	BROWN	Dark	Good	None	Normal
COOPER, JAMES	28	M	5'10"	160	BROWN	BROWN	Fair	Good	None	Normal
REED, ROBERT	30	M	5'7"	145	BLACK	BROWN	Dark	Good	None	Normal
BENTLEY, DAVID	27	M	5'11"	165	BROWN	BROWN	Fair	Good	None	Normal
WATSON, MICHAEL	32	M	5'9"	155	BLACK	BROWN	Dark	Good	None	Normal
FRANKS, JAMES	29	M	5'10"	160	BROWN	BROWN	Fair	Good	None	Normal
WELLS, JOHN	33	M	5'8"	150	BLACK	BROWN	Dark	Good	None	Normal
WATSON, DAVID	26	M	5'11"	165	BROWN	BROWN	Fair	Good	None	Normal
COOPER, MICHAEL	34	M	5'9"	155	BLACK	BROWN	Dark	Good	None	Normal
CRISP, JAMES	28	M	5'10"	160	BROWN	BROWN	Fair	Good	None	Normal
REED, ROBERT	30	M	5'7"	145	BLACK	BROWN	Dark	Good	None	Normal
BENTLEY, DAVID	27	M	5'11"	165	BROWN	BROWN	Fair	Good	None	Normal
WATSON, MICHAEL	32	M	5'9"	155	BLACK	BROWN	Dark	Good	None	Normal
FRANKS, JAMES	29	M	5'10"	160	BROWN	BROWN	Fair	Good	None	Normal
WELLS, JOHN	33	M	5'8"	150	BLACK	BROWN	Dark	Good	None	Normal
WATSON, DAVID	26	M	5'11"	165	BROWN	BROWN	Fair	Good	None	Normal
COOPER, MICHAEL	34	M	5'9"	155	BLACK	BROWN	Dark	Good	None	Normal
CRISP, JAMES	28	M	5'10"	160	BROWN	BROWN	Fair	Good	None	Normal
REED, ROBERT	30	M	5'7"	145	BLACK	BROWN	Dark	Good	None	Normal
BENTLEY, DAVID	27	M	5'11"	165	BROWN	BROWN	Fair	Good	None	Normal
WATSON, MICHAEL	32	M	5'9"	155	BLACK	BROWN	Dark	Good	None	Normal
FRANKS, JAMES	29	M	5'10"	160	BROWN	BROWN	Fair	Good	None	Normal
WELLS, JOHN	33	M	5'8"	150	BLACK	BROWN	Dark	Good	None	Normal
WATSON, DAVID	26	M	5'11"	165	BROWN	BROWN	Fair	Good	None	Normal
COOPER, MICHAEL	34	M	5'9"	155	BLACK	BROWN	Dark	Good	None	Normal
CRISP, JAMES	28	M	5'10"	160	BROWN	BROWN	Fair	Good	None	

EQUIVALENT SEA LEVEL TOTAL ABSORBER AMOUNTS

H ₂ O (SCALED LOWTRAN UNITS)	CO ₂ ⁺ O ₃	HNO ₃ (ATM CM)	O ₃ UV (ATM CM)	CNTMSLF1 (MOL CM-2)	CNTMSLF2 (MOL CM-2)	CNTNFAN (MOL CM-2)
1.144E+80	4.626E+80	6.512E+82	2.449E+84	1.318E+81	2.887E+20	4.987E+22

TABLE C-2 (Cont).

N2 CONT	MOL SCAT	AER 1	AER 2	AER 3	AER 4	CIPRUS	MEAN RH (PRCNT)
3.250E+00	7.571E+00	1.080E+00	7.991E-02	6.100E-03	.000E+00	.000E+00	48.25

CASE 2: GIVEN H1, H2, ANGLE

SLANT PATH PARAMETERS IN STANDARD FORM

H1	=	.000 KM
H2	=	100.000 KM
ANGLE	=	.000 DEG
PHI	=	180.000 DEG
HMIN	=	.000 KM
LEN	=	B

TABLE C-2 (Cont).

CALCULATION OF THE REFRACTED PATH THROUGH THE ATMOSPHERE

I	FROM (KM)	A. TITUDE TO (KM)	THEYA (DEG)	ORANGE (KM)	RANGE (KM)	DBETA (DEG)	BETA (DEG)	PHI (DEG)	DBEND (DEG)	BENDING (DEG)	PBAR (MB)	TBAR (K)	RHOBAR (GM CM-3)
H: TO H2													
1	1.000	1.000	.000	1.000	1.000	.000	.000	100.000	.000	.000	955.603	284.99	1.17E-03
2	1.000	2.000	.000	1.000	2.000	.000	.000	100.000	.000	.000	846.698	228.43	1.06E-03
3	2.000	3.000	.000	1.000	3.000	.000	.000	100.000	.000	.000	747.913	271.99	9.57E-04
4	3.000	4.000	.000	1.000	4.000	.000	.000	100.000	.000	.000	658.727	265.49	8.63E-04
5	4.000	5.000	.000	1.000	5.000	.000	.000	100.000	.000	.000	578.391	258.99	7.77E-04
6	5.000	6.000	.000	1.000	6.000	.000	.000	100.000	.000	.000	506.204	252.50	6.98E-04
7	6.000	7.000	.000	1.000	7.000	.000	.000	100.000	.000	.000	441.516	246.00	6.24E-04
8	7.000	8.000	.000	1.000	8.000	.000	.000	100.000	.000	.000	383.677	239.50	5.57E-04
9	8.000	9.000	.000	1.000	9.000	.000	.000	100.000	.000	.000	322.137	232.00	4.96E-04
10	9.000	10.000	.000	1.000	10.000	.000	.000	100.000	.000	.000	266.399	226.50	4.40E-04
11	10.000	11.000	.000	1.000	11.000	.000	.000	100.000	.000	.000	245.907	220.10	3.89E-04
12	11.000	12.000	.000	1.000	12.000	.000	.000	100.000	.000	.000	210.499	216.75	3.38E-04
13	12.000	13.000	.000	1.000	13.000	.000	.000	100.000	.000	.000	179.900	216.70	2.89E-04
14	13.000	14.000	.000	1.000	14.000	.000	.000	100.000	.000	.000	153.750	216.70	2.47E-04
15	14.000	15.000	.000	1.000	15.000	.000	.000	100.000	.000	.000	131.400	216.70	2.11E-04
16	15.000	16.000	.000	1.000	16.000	.000	.000	100.000	.000	.000	112.300	216.70	1.80E-04
17	16.000	17.000	.000	1.000	17.000	.000	.000	100.000	.000	.000	95.000	216.70	1.54E-04
18	17.000	18.000	.000	1.000	18.000	.000	.000	100.000	.000	.000	82.075	216.70	1.32E-04
19	18.000	19.000	.000	1.000	19.000	.000	.000	100.000	.000	.000	70.160	216.70	1.13E-04
20	19.000	20.000	.000	1.000	20.000	.000	.000	100.000	.000	.000	59.990	216.70	9.62E-05
21	20.000	21.000	.000	1.000	21.000	.000	.000	100.000	.000	.000	51.293	217.14	8.21E-05
22	21.000	22.000	.000	1.000	22.000	.000	.000	100.000	.000	.000	43.863	210.09	7.00E-05
23	22.000	23.000	.000	1.000	23.000	.000	.000	100.000	.000	.000	37.572	219.09	5.96E-05
24	23.000	24.000	.000	1.000	24.000	.000	.000	100.000	.000	.000	32.197	220.09	5.09E-05
25	24.000	25.000	.000	1.000	25.000	.000	.000	100.000	.000	.000	27.607	221.09	4.34E-05
26	25.000	26.000	.000	1.000	26.000	.000	.000	100.000	.000	.000	18.754	220.73	3.70E-05
27	26.000	27.000	.000	1.000	27.000	.000	.000	100.000	.000	.000	8.000	220.82	3.10E-05
28	27.000	28.000	.000	1.000	28.000	.000	.000	100.000	.000	.000	4.322	242.52	5.95E-06
29	28.000	29.000	.000	1.000	29.000	.000	.000	100.000	.000	.000	2.187	256.43	2.06E-06
30	29.000	30.000	.000	1.000	30.000	.000	.000	100.000	.000	.000	1.146	267.09	1.45E-06
31	30.000	31.000	.000	1.000	31.000	.000	.000	100.000	.000	.000	.416	253.92	3.21E-07
32	31.000	32.000	.000	1.000	32.000	.000	.000	100.000	.000	.000	.000	217.85	1.60E-08

CUMULATIVE ABSORBER AMOUNTS FOR THE PATH FROM H1 TO Z

J	Z (KM)	TBAR (K)	H2O (SCALED LOWTRAN UNITS)	CO2+ (SCALED LOWTRAN UNITS)	O3 (ATM CM)	HNO3 (ATM CM)	O3 UV (ATM CM)	CNTMSLF1 (MOL CM-2)	CNTMSLF2 (MOL CM-2)	CNTMFRN (MOL CM-2)
H1 TO H2										
1	1.000	284.99	4.664E-01	8.506E-01	2.440E-03	.000E+00	2.520E-03	1.138E+20	3.402E+19	1.629E+22
2	2.000	278.49	7.631E-01	1.561E+00	4.775E-03	.000E+00	5.040E-03	1.700E+20	6.213E+19	2.668E+22
3	3.000	271.99	9.394E-01	2.151E+00	5.924E-03	.000E+00	7.465E-03	1.944E+20	7.842E+19	3.287E+22
4	4.000	265.49	1.037E+00	2.640E+00	8.819E-03	.000E+00	9.704E-03	2.037E+20	8.630E+19	3.631E+22

TABLE C-2 (Cont).

J	Z (K)	NO CONT	MOL SCAT	AER 1	AER 2	AER 3	AER 4	CIRRU	
5	5.000	253.99	1.090E+00	3.343E+00	1.055E-02	.000E+00	1.195E-02	2.071E+20	8.963E+19
6	6.000	252.50	1.110E+00	3.373E+00	1.210E-02	.000E+00	1.397E-02	2.002E+20	9.077E+19
7	7.000	246.00	1.120E+00	3.643E+00	1.379E-02	.000E+00	1.617E-02	2.006E+20	9.115E+19
8	8.000	250.50	1.135E+00	3.861E+00	1.543E-02	2.034E-35	1.852E-02	2.007E+20	9.127E+19
9	9.000	253.00	1.142E+00	4.030E+00	1.732E-02	1.807E-06	2.139E-02	2.007E+20	9.130E+19
10	10.000	256.55	1.144E+00	4.179E+00	1.966E-02	8.893E-06	2.515E-02	2.007E+20	9.131E+19
11	11.000	250.10	1.144E+00	4.294E+00	2.269E-02	2.546E-05	3.008E-02	2.007E+20	9.131E+19
12	12.000	216.75	1.144E+00	4.380E+00	2.645E-02	5.123E-05	3.705E-02	2.007E+20	9.131E+19
13	13.000	216.70	1.144E+00	4.446E+00	3.049E-02	8.015E-05	4.475E-02	2.007E+20	9.131E+19
14	14.000	216.70	1.144E+00	4.497E+00	3.461E-02	1.007E-04	5.315E-02	2.007E+20	9.131E+19
15	15.000	216.70	1.144E+00	4.535E+00	3.892E-02	1.363E-04	6.248E-02	2.007E+20	9.131E+19
16	16.000	216.70	1.144E+00	4.555E+00	4.347E-02	1.621E-04	7.208E-02	2.007E+20	9.131E+19
17	17.000	216.70	1.144E+00	4.587E+00	4.840E-02	1.853E-04	8.512E-02	2.007E+20	9.131E+19
18	18.000	215.70	1.144E+00	4.604E+00	5.375E-02	2.062E-04	9.912E-02	2.007E+20	9.131E+19
19	19.000	216.70	1.144E+00	4.616E+00	5.937E-02	2.253E-04	1.140E-01	2.007E+20	9.131E+19
20	20.000	216.70	1.144E+00	4.627E+00	6.512E-02	2.440E-04	1.308E-01	2.007E+20	9.131E+19
21	21.000	217.14	1.144E+00	4.634E+00	7.074E-02	2.661E-04	1.495E-01	2.007E+20	9.131E+19
22	22.000	218.00	1.144E+00	4.639E+00	7.609E-02	2.874E-04	1.675E-01	2.007E+20	9.131E+19
23	23.000	219.00	1.144E+00	4.643E+00	8.111E-02	3.009E-04	1.854E-01	2.007E+20	9.131E+19
24	24.000	220.00	1.144E+00	4.647E+00	8.564E-02	3.309E-04	2.027E-01	2.007E+20	9.131E+19
25	25.000	221.00	1.144E+00	4.649E+00	8.967E-02	3.472E-04	2.190E-01	2.007E+20	9.131E+19
26	26.000	222.73	1.144E+00	4.655E+00	1.025E-01	3.831E-04	2.406E-01	2.007E+20	9.131E+19
27	27.000	223.00	1.144E+00	4.656E+00	1.079E-01	3.875E-04	2.577E-01	2.007E+20	9.131E+19
28	28.000	224.52	1.144E+00	4.657E+00	1.099E-01	3.876E-04	2.733E-01	2.007E+20	9.131E+19
29	29.000	226.40	1.144E+00	4.657E+00	1.107E-01	3.876E-04	2.884E-01	2.007E+20	9.131E+19
30	30.000	227.00	1.144E+00	4.657E+00	1.107E-01	3.876E-04	3.035E-01	2.007E+20	9.131E+19
31	31.000	228.00	1.144E+00	4.657E+00	1.107E-01	3.876E-04	3.187E-01	2.007E+20	9.131E+19
32	32.000	229.00	1.144E+00	4.657E+00	1.107E-01	3.876E-04	3.340E-01	2.007E+20	9.131E+19
33	33.000	230.00	1.144E+00	4.657E+00	1.107E-01	3.876E-04	3.494E-01	2.007E+20	9.131E+19
34	34.000	231.00	1.144E+00	4.657E+00	1.107E-01	3.876E-04	3.648E-01	2.007E+20	9.131E+19
35	35.000	232.00	1.144E+00	4.657E+00	1.107E-01	3.876E-04	3.802E-01	2.007E+20	9.131E+19
36	36.000	233.00	1.144E+00	4.657E+00	1.107E-01	3.876E-04	3.956E-01	2.007E+20	9.131E+19
37	37.000	234.00	1.144E+00	4.657E+00	1.107E-01	3.876E-04	4.110E-01	2.007E+20	9.131E+19
38	38.000	235.00	1.144E+00	4.657E+00	1.107E-01	3.876E-04	4.264E-01	2.007E+20	9.131E+19
39	39.000	236.00	1.144E+00	4.657E+00	1.107E-01	3.876E-04	4.418E-01	2.007E+20	9.131E+19
40	40.000	237.00	1.144E+00	4.657E+00	1.107E-01	3.876E-04	4.572E-01	2.007E+20	9.131E+19
41	41.000	238.00	1.144E+00	4.657E+00	1.107E-01	3.876E-04	4.726E-01	2.007E+20	9.131E+19
42	42.000	239.00	1.144E+00	4.657E+00	1.107E-01	3.876E-04	4.880E-01	2.007E+20	9.131E+19
43	43.000	240.00	1.144E+00	4.657E+00	1.107E-01	3.876E-04	5.034E-01	2.007E+20	9.131E+19
44	44.000	241.00	1.144E+00	4.657E+00	1.107E-01	3.876E-04	5.188E-01	2.007E+20	9.131E+19
45	45.000	242.00	1.144E+00	4.657E+00	1.107E-01	3.876E-04	5.342E-01	2.007E+20	9.131E+19
46	46.000	243.00	1.144E+00	4.657E+00	1.107E-01	3.876E-04	5.496E-01	2.007E+20	9.131E+19
47	47.000	244.00	1.144E+00	4.657E+00	1.107E-01	3.876E-04	5.650E-01	2.007E+20	9.131E+19
48	48.000	245.00	1.144E+00	4.657E+00	1.107E-01	3.876E-04	5.804E-01	2.007E+20	9.131E+19
49	49.000	246.00	1.144E+00	4.657E+00	1.107E-01	3.876E-04	5.958E-01	2.007E+20	9.131E+19
50	50.000	247.00	1.144E+00	4.657E+00	1.107E-01	3.876E-04	6.112E-01	2.007E+20	9.131E+19
51	51.000	248.00	1.144E+00	4.657E+00	1.107E-01	3.876E-04	6.266E-01	2.007E+20	9.131E+19
52	52.000	249.00	1.144E+00	4.657E+00	1.107E-01	3.876E-04	6.420E-01	2.007E+20	9.131E+19
53	53.000	250.00	1.144E+00	4.657E+00	1.107E-01	3.876E-04	6.574E-01	2.007E+20	9.131E+19
54	54.000	251.00	1.144E+00	4.657E+00	1.107E-01	3.876E-04	6.728E-01	2.007E+20	9.131E+19
55	55.000	252.00	1.144E+00	4.657E+00	1.107E-01	3.876E-04	6.882E-01	2.007E+20	9.131E+19
56	56.000	253.00	1.144E+00	4.657E+00	1.107E-01	3.876E-04	7.036E-01	2.007E+20	9.131E+19
57	57.000	254.00	1.144E+00	4.657E+00	1.107E-01	3.876E-04	7.190E-01	2.007E+20	9.131E+19
58	58.000	255.00	1.144E+00	4.657E+00	1.107E-01	3.876E-04	7.344E-01	2.007E+20	9.131E+19
59	59.000	256.00	1.144E+00	4.657E+00	1.107E-01	3.876E-04	7.498E-01	2.007E+20	9.131E+19
60	60.000	257.00	1.144E+00	4.657E+00	1.107E-01	3.876E-04	7.652E-01	2.007E+20	9.131E+19
61	61.000	258.00	1.144E+00	4.657E+00	1.107E-01	3.876E-04	7.806E-01	2.007E+20	9.131E+19
62	62.000	259.00	1.144E+00	4.657E+00	1.107E-01	3.876E-04	7.960E-01	2.007E+20	9.131E+19
63	63.000	260.00	1.144E+00	4.657E+00	1.107E-01	3.876E-04	8.114E-01	2.007E+20	9.131E+19
64	64.000	261.00	1.144E+00	4.657E+00	1.107E-01	3.876E-04	8.268E-01	2.007E+20	9.131E+19
65	65.000	262.00	1.144E+00	4.657E+00	1.107E-01	3.876E-04	8.422E-01	2.007E+20	9.131E+19
66	66.000	263.00	1.144E+00	4.657E+00	1.107E-01	3.876E-04	8.576E-01	2.007E+20	9.131E+19
67	67.000	264.00	1.144E+00	4.657E+00	1.107E-01	3.876E-04	8.730E-01	2.007E+20	9.131E+19
68	68.000	265.00	1.144E+00	4.657E+00	1.107E-01	3.876E-04	8.884E-01	2.007E+20	9.131E+19
69	69.000	266.00	1.144E+00	4.657E+00	1.107E-01	3.876E-04	9.038E-01	2.007E+20	9.131E+19
70	70.000	267.00	1.144E+00	4.657E+00	1.107E-01	3.876E-04	9.192E-01	2.007E+20	9.131E+19
71	71.000	268.00	1.144E+00	4.657E+00	1.107E-01	3.876E-04	9.346E-01	2.007E+20	9.131E+19
72	72.000	269.00	1.144E+00	4.657E+00	1.107E-01	3.876E-04	9.500E-01	2.007E+20	9.131E+19
73	73.000	270.00	1.144E+00	4.657E+00	1.107E-01	3.876E-04	9.654E-01	2.007E+20	9.131E+19
74	74.000	271.00	1.144E+00	4.657E+00	1.107E-01	3.876E-04	9.808E-01	2.007E+20	9.131E+19
75	75.000	272.00	1.144E+00	4.657E+00	1.107E-01	3.876E-04	9.962E-01	2.007E+20	9.131E+19
76	76.000	273.00	1.144E+00	4.657E+00	1.107E-01	3.876E-04	1.0116E-01	2.007E+20	9.131E+19
77	77.000	274.00	1.144E+00	4.657E+00	1.107E-01	3.876E-04	1.0270E-01	2.007E+20	9.131E+19
78	78.000	275.00	1.144E+00	4.657E+00	1.107E-01	3.876E-04	1.0424E-01	2.007E+20	9.131E+19
79	79.000	276.00	1.144E+00	4.657E+00	1.107E-01	3.876E-04	1.0578E-01	2.007E+20	9.131E+19
80	80.000	277.00	1.144E+00	4.657E+00	1.107E-01	3.876E-04	1.0732E-01	2.007E+20	9.131E+19
81	81.000	278.00	1.144E+00	4.657E+00	1.107E-01	3.876E-04	1.0886E-01	2.007E+20	9.131E+19
82	82.000	279.00	1.144E+00	4.657E+00	1.107E-01	3.876E-04	1.1040E-01	2.007E+20	9.131E+19
83	83.000	280.00	1.144E+00	4.657E+00	1.107E-01	3.876E-04	1.1194E-01	2.007E+20	9.131E+19
84	84.000	281.00	1.144E+00	4.657E+00	1.107E-01	3.876E-04	1.1348E-01	2.007E+20	9.131E+19
85	85.000	282.00	1.144E+00	4.657E+00	1.107E-01	3.876E-04	1.1502E-01	2.007E+20	9.131E+19
86	86.000	283.00	1.144E+00	4.657E+00	1.107E-01	3.876E-04	1.1656E-01	2.007E+20	9.131E+19
87	87.000	284.00	1.144E+00	4.657E+00	1.107E-01	3.876E-04	1.1810E-01	2.007E+20	9.131E+19
88	88.000	285.00	1.144E+00	4.657E+00	1.107E-01	3.876E-04	1.1964E-01	2.007E+20	9.131E+19
89	89.000	286.00	1.144E+00	4.657E+00	1.107E-01	3.876E-04	1.2118E-01	2.007E+20	9.131E+19
90	90.000	287.00	1.144E+00	4.657E+00	1.107E-01	3.876E-04	1.2272E-01	2.007E+20	9.131E+19
91	91.000	288.00	1.144E+00	4.657E+00	1.107E-01	3.876E-04	1.2426E-01	2.007E+20	9.131E+19
92	92.000	289.00	1.144E+00	4.657E+00	1.107E-01	3.876E-04	1.2580E-01	2.007E+20	9.131E+19
93	93.000	290.00	1.144E+00	4.657E+00	1.107E-01	3.876E-04	1.2734E-01	2.007E+20	9.131E+19
94	94.000	291.00	1.144E+00	4.657E+00	1.107E-01	3.876E-04	1.2888E-01	2.007E+20	9.131E+19
95	95.000	292.00	1.144E+00	4.657E+00	1.107E-01	3.876E-04	1.3042E-01	2.007E+20	9.131E+19
96	96.000	293.00	1.144E+00	4.657E+00	1.107E-01	3.876E-04	1.3196E-01	2.007E+20	9.131E+19

SUMMARY OF THE GEOMETRY CALCULATION

C-13

TABLE C-2 (Cont).

RADIANCE (WATTS/CM ² -STER-XXX)				
FREQ WAVLEN (CM-1) (MICRN)	ATMOS RADIANCE (CM-1)	(MICRN)	INTEGRAL TOTAL (CM-1)	TRANS
850. 11.765	2.23E-06	1.61E-04	5.57E-06	.7544
855. 11.696	2.12E-06	1.55E-04	1.63E-05	.7627
860. 11.628	1.98E-06	1.47E-04	2.61E-05	.7727
865. 11.561	1.81E-06	1.35E-04	3.52E-05	.7966
870. 11.494	1.67E-06	1.27E-04	4.35E-05	.7920
875. 11.429	1.66E-06	1.27E-04	5.10E-05	.7969
880. 11.364	1.66E-06	1.28E-04	6.01E-05	.7949
885. 11.299	1.62E-06	1.27E-04	6.82E-05	.7966
890. 11.236	1.56E-06	1.24E-04	7.60E-05	.8010
895. 11.173	1.51E-06	1.21E-04	8.35E-05	.8043
900. 11.111	1.45E-06	1.17E-04	9.09E-05	.8084
905. 11.050	1.46E-06	1.20E-04	9.81E-05	.8052
910. 10.989	1.45E-06	1.20E-04	1.05E-04	.8043
915. 10.929	1.44E-06	1.21E-04	1.13E-04	.8020
920. 10.870	1.41E-06	1.19E-04	1.20E-04	.8035
925. 10.811	1.27E-06	1.09E-04	1.26E-04	.8133
930. 10.753	1.27E-06	1.10E-04	1.32E-04	.8116
935. 10.695	1.20E-06	1.12E-04	1.39E-04	.8079
940. 10.638	1.31E-06	1.15E-04	1.45E-04	.8024
945. 10.582	1.36E-06	1.21E-04	1.52E-04	.7932
950. 10.526	1.39E-06	1.25E-04	1.55E-04	.7857
INTEGRATED ABSORPTION FROM 850 TO 950 CM-1 = 20.32 CM-1				
AVERAGE TRANSMITTANCE = .7968				
INTEGRATED RADIANCE = 1.555E-04 WATTS CM-2 STER-1				
MINIMUM RADIANCE = 1.268E-06 WATTS CM-2 STER-1 (CM-1)-1 AT				
MAXIMUM RADIANCE = 2.229E-06 WATTS CM-2 STER-1 (CM-1)-1 AT				
BOUNDARY TEMPERATURE = .00 K				
BOUNDARY EMISSIVITY = 1.000				
CAPD 5 ***** 0				
17.46.51.UCLP, AA, L02 . 0.960KLMs.				

925.0 CM-1
850.0 CM-1

TABLE C-3

LOWTRAN OUTPUT FOR CASE 2

```

***** LOWTRAN 6 *****
CARD 1 ***** 6 2 1 0 0 0 0 0 0
CARD 2 ***** 2 0 0 0 0 0 0 0 0
CARD 3 ***** 20.000 0.000 180.000 0.000
CARD 4 ***** 850.000 950.000 5.000

PROGRAM WILL COMPUTE RADIANCE
CALCULATIONS WILL BE DONE USING MULTIPLE SCATTERING
ATMOSPHERIC MODEL
TEMPERATURE = 6 1962 U S STANDARD
WATER VAPOR = 6 1962 U S STANDARD
OZONE = 6 1962 U S STANDARD

AEROSOL MODEL REGIME AEROSOL TYPE PROFILE SEASON
BOUNDARY LAYER (0-2 KM) RURAL 5.0 KM VIS AT SEA LEVEL
TROPOSPHERE (2-10KM) TROPOSPHERIC TROPOSPHERIC SPRING-SUMMER
STRATOSPHERE (10-30KM) BACKGROUND STRATO BACKGROUND STRATO SPRING-SUMMER
UPPER ATMOS (30-100KM) METEORIC DUST NORMAL

SLANT PATH. H1 TO H2
H1 = 20.000 KM
H2 = 0.000 KM
ANGLE = 180.000 DEG
RANGE = 0.000 KM
BETA = 0.000 DEG
LEN = 0

FREQUENCY RANGE
V1 = 850.0 CM-1 ( 11.76 MICROMETERS)
V2 = 950.0 CM-1 ( 10.53 MICROMETERS)
DV = 5.0 CM-1

```

TABLE C-3 (Cont).

ATMOSPHERIC PROFILES											
I	Z (KM)	P (MB)	T (K)	H2O (SCALED)	CO2* (LOWTRAN UNITS)	N2 (MOL/CM2 KM)	CNTMSLF (MOL/CM2 KM)	MOL SCAT (-)	N-1 (-)	O3 (UV/ (ATM CM/KM)	
1	1.00	1013.000	288.2	5.750E-01	9.285E-01	2.493E-03	7.370E-01	1.569E+20	9.475E-01	2.722E-04	2.520E-03
2	1.00	898.000	281.7	3.719E-01	7.771E-01	2.387E-03	6.810E-01	7.951E+19	8.601E-01	2.471E-04	2.520E-03
3	2.00	795.000	275.2	2.323E-01	6.474E-01	2.294E-03	4.870E-01	3.791E+19	7.780E-01	2.238E-04	2.520E-03
4	3.00	701.200	268.7	1.302E-01	5.331E-01	2.020E-03	3.922E-01	1.460E+19	7.035E-01	2.822E-04	2.333E-03
5	4.00	616.500	262.2	7.166E-02	4.435E-01	1.774E-03	3.150E-01	5.454E+18	6.340E-01	1.823E-04	2.147E-03
6	5.00	540.500	255.7	3.745E-02	3.646E-01	1.692E-03	2.513E-01	1.846E+18	5.690E-01	1.638E-04	2.147E-03
7	6.00	472.200	249.2	1.992E-02	2.982E-01	1.576E-03	1.994E-01	5.508E+17	5.180E-01	1.469E-04	2.108E-03
8	7.00	411.100	242.7	9.834E-03	2.427E-01	1.632E-03	1.572E-01	1.988E+17	4.566E-01	1.313E-04	2.207E-03
9	8.00	356.500	236.2	5.004E-03	1.963E-01	1.645E-03	1.232E-01	6.490E+16	4.059E-01	1.170E-04	2.427E-03
10	9.00	306.000	229.7	1.703E-03	1.579E-01	2.130E-03	9.506E-02	9.537E+15	3.615E-01	1.040E-04	3.313E-03
11	10.00	265.000	223.3	5.894E-04	1.262E-01	2.557E-03	7.403E-02	1.460E+15	3.195E-01	9.201E-05	4.202E-03
12	11.00	227.000	216.8	2.267E-04	1.002E-01	3.493E-03	5.670E-02	3.031E+14	2.833E-01	8.110E-05	5.067E-03
13	12.00	194.000	216.7	9.275E-05	7.619E-02	4.037E-03	4.150E-02	6.170E+13	2.413E-01	6.941E-05	7.467E-03
14	13.00	165.500	216.7	3.917E-05	5.788E-02	4.028E-03	3.031E-02	1.460E+13	2.063E-01	5.932E-05	7.933E-03
15	14.00	141.700	216.7	1.587E-05	4.397E-02	4.229E-03	2.214E-02	3.180E+12	1.763E-01	5.070E-05	8.867E-03
16	15.00	121.100	216.7	1.181E-05	3.340E-02	4.308E-03	1.617E-02	2.337E+12	1.507E-01	4.333E-05	9.000E-03
17	16.00	103.500	216.7	8.687E-06	2.537E-02	4.710E-03	1.181E-02	1.677E+12	1.280E-01	3.707E-05	1.132E-02
18	17.00	89.500	216.7	6.432E-06	1.929E-02	5.161E-03	0.637E-02	1.219E+12	1.101E-01	3.166E-05	1.307E-02
19	18.00	75.650	216.7	4.725E-06	1.466E-02	5.540E-03	6.311E-03	8.726E+11	9.411E-02	2.707E-05	1.493E-02
20	19.00	64.650	216.7	4.104E-06	1.114E-02	5.591E-03	4.611E-03	8.726E+11	8.245E-02	2.314E-05	1.631E-02
21	20.00	55.290	216.7	3.564E-06	8.470E-03	5.803E-03	3.371E-03	8.726E+11	6.878E-02	1.970E-05	1.773E-02
22	21.00	47.290	217.6	3.371E-06	6.406E-03	5.447E-03	2.451E-03	1.030E+12	5.859E-02	1.685E-05	1.773E-02
23	22.00	40.470	218.6	3.168E-06	4.847E-03	5.240E-03	1.703E-03	1.219E+12	4.991E-02	1.435E-05	1.820E-02
24	23.00	34.670	219.6	3.015E-06	3.675E-03	4.802E-03	1.239E-03	1.464E+12	4.256E-02	1.224E-05	1.773E-02
25	24.00	29.720	220.6	2.803E-06	2.709E-03	4.274E-03	9.402E-04	1.577E+12	3.632E-02	1.044E-05	1.607E-02
26	25.00	25.490	221.6	2.636E-06	2.119E-03	3.792E-03	6.909E-04	1.963E+12	3.181E-02	8.918E-06	1.507E-02
27	30.00	11.970	226.5	7.612E-07	5.476E-04	1.642E-03	1.479E-04	6.500E+11	1.425E-02	4.097E-06	9.333E-03
28	35.00	5.746	236.5	1.624E-07	1.429E-04	6.674E-04	3.193E-05	1.154E+11	6.550E-03	1.884E-06	5.133E-03
29	40.00	2.871	250.4	3.549E-08	3.922E-05	2.227E-04	7.518E-06	2.023E+10	3.091E-03	8.809E-07	2.287E-03
30	45.00	1.491	264.2	9.176E-09	1.157E-05	5.881E-05	1.021E-06	4.615E+09	1.521E-03	4.375E-07	7.933E-04
31	50.00	0.798	270.7	1.939E-09	3.747E-06	1.072E-05	5.007E-07	6.490E+08	7.945E-04	2.205E-07	1.067E-04
32	70.00	0.055	219.7	2.406E-12	4.660E-08	8.259E-07	3.291E-09	1.014E+05	6.773E-05	1.948E-08	4.013E-06
33	100.00	0.000	210.0	1.502E-16	5.420E-12	1.046E-12	1.046E-13	4.507E+00	3.861E-07	1.111E-10	2.007E-09

TABLE C-3 (Cont).

ATMOSPHERIC PROFILES											
I	Z (KM)	P (MB)	T (K)	CHTMFRN MOL/CM2 KM	HNO3 ATM CM/KM	AEROSOL 1 (-)	AEROSOL 2 (-)	AEROSOL 3 (-)	AEROSOL 4 (-)	CIRRUS (-)	RH (PERCENT)
1	1.00	1013.000	289.2	2.010E+22	.000E+00	7.700E-01	.000E+00	.000E+00	3.533E+01	.000E+00	4.589E+01
2	1.00	899.000	281.7	1.301E+22	.000E+00	7.700E-01	.000E+00	.000E+00	3.777E+01	.000E+00	4.966E+01
3	2.00	795.000	275.2	8.143E+21	.000E+00	6.210E-02	.000E+00	.000E+00	3.230E+00	.000E+00	5.201E+01
4	3.00	701.200	269.1	4.513E+21	.000E+00	3.460E-02	.000E+00	.000E+00	.000E+00	.000E+00	.000E+00
5	4.00	616.600	262.2	2.521E+21	.000E+00	.000E+00	1.950E-02	.000E+00	.000E+00	.000E+00	.000E+00
6	5.00	540.500	255.7	1.319E+21	.000E+00	.000E+00	9.310E-03	.000E+00	.000E+00	.000E+00	.000E+00
7	6.00	472.200	249.2	7.025E+20	.000E+00	.000E+00	7.710E-03	.000E+00	.000E+00	.000E+00	.000E+00
8	7.00	411.100	242.7	3.472E+20	.000E+00	.000E+00	6.230E-03	.000E+00	.000E+00	.000E+00	.000E+00
9	8.00	356.500	236.2	1.760E+20	4.069E-35	.000E+00	3.370E-03	.000E+00	.000E+00	.000E+00	.000E+00
10	9.00	308.000	229.7	6.023E+19	3.615E-06	.000E+00	1.820E-03	.000E+00	.000E+00	.000E+00	.000E+00
11	10.00	265.000	223.3	2.006E+19	1.056E-05	.000E+00	.000E+00	1.140E-03	.000E+00	.000E+00	.000E+00
12	11.00	227.000	216.8	8.304E+18	2.258E-05	.000E+00	.000E+00	7.990E-04	.000E+00	.000E+00	.000E+00
13	12.00	194.000	216.7	3.235E+18	2.096E-05	.000E+00	.000E+00	6.410E-04	.000E+00	.000E+00	.000E+00
14	13.00	165.800	216.7	1.345E+18	2.888E-05	.000E+00	.000E+00	5.170E-04	.000E+00	.000E+00	.000E+00
15	14.00	141.700	216.7	5.364E+17	2.820E-05	.000E+00	.000E+00	4.420E-04	.000E+00	.000E+00	.000E+00
16	15.00	121.100	216.7	3.929E+17	2.712E-05	.000E+00	.000E+00	3.950E-04	.000E+00	.000E+00	.000E+00
17	16.00	103.500	216.7	2.845E+17	2.446E-05	.000E+00	.000E+00	3.020E-04	.000E+00	.000E+00	.000E+00
18	17.00	88.500	216.7	2.074E+17	2.222E-05	.000E+00	.000E+00	4.250E-04	.000E+00	.000E+00	.000E+00
19	18.00	75.650	216.7	1.500E+17	1.976E-05	.000E+00	.000E+00	5.200E-04	.000E+00	.000E+00	.000E+00
20	19.00	64.670	216.7	1.202E+17	1.850E-05	.000E+00	.000E+00	5.810E-04	.000E+00	.000E+00	.000E+00
21	20.00	55.290	216.7	1.096E+17	2.063E-05	.000E+00	.000E+00	5.890E-04	.000E+00	.000E+00	.000E+00
22	21.00	47.290	217.6	1.019E+17	2.168E-05	.000E+00	.000E+00	5.020E-04	.000E+00	.000E+00	.000E+00
23	22.00	40.470	218.6	9.401E+16	2.096E-05	.000E+00	.000E+00	4.200E-04	.000E+00	.000E+00	.000E+00
24	23.00	34.670	219.6	8.700E+16	2.213E-05	.000E+00	.000E+00	3.000E-04	.000E+00	.000E+00	.000E+00
25	24.00	29.720	220.6	8.025E+16	2.179E-05	.000E+00	.000E+00	1.980E-04	.000E+00	.000E+00	.000E+00
26	25.00	25.490	221.6	7.414E+16	1.170E-05	.000E+00	.000E+00	1.310E-04	.000E+00	.000E+00	.000E+00
27	30.00	11.970	226.5	1.901E+16	3.704E-06	.000E+00	.000E+00	3.320E-05	.000E+00	.000E+00	.000E+00
28	35.00	5.746	236.5	3.790E+15	1.441E-07	.000E+00	.000E+00	.000E+00	1.640E-05	.000E+00	.000E+00
29	40.00	2.871	250.4	7.507E+14	3.091E-37	.000E+00	.000E+00	.000E+00	7.990E-06	.000E+00	.000E+00
30	45.00	1.491	264.2	1.764E+14	.000E+00	.000E+00	.000E+00	.000E+00	4.010E-06	.000E+00	.000E+00
31	50.00	.798	270.7	3.454E+13	.000E+00	.000E+00	.000E+00	.000E+00	2.100E-06	.000E+00	.000E+00
32	70.00	.055	219.7	3.600E+10	.000E+00	.000E+00	.000E+00	.000E+00	1.600E-07	.000E+00	.000E+00
33	100.00	.000	210.0	1.399E+06	.000E+00	.000E+00	.000E+00	.000E+00	9.310E-10	.000E+00	.000E+00

CASE 2A: GIVEN H1, H2, ANGLE

EITHER A SHORT PATH (LEN=0) OR A LONG PATH THROUGH A TANGENT HEIGHT (LEN=1) IS POSSIBLE: LEN = 0

SLANT PATH PARAMETERS IN STANDARD FORM

TABLE C-3 (Cont).

H1	"	27.000 KM
H2	"	.000 KM
ANGLE	"	187.000 DEG
PHI	"	.000 DEG
AMIN	"	.000 KM
LEN	"	0

TABLE C-3 (Cont).

CALCULATION OF THE REFRACTED PATH THROUGH THE ATMOSPHERE

J	FROM (KM)	ALITUDE (KM)	THETA (DEG)	CRANGE (KM)	RANGE (KM)	DBETA (DEG)	BETA (DEG)	PHI (DEG)	DBEND (DEG)	BENDING (DEG)	PBAR (MB)	TBAR (K)	RHOBAR (GM CM-3)
M2 TO M1													
1	1.000	1.000	.000	1.000	1.000	.000	.000	180.000	.000	.000	955.683	284.99	1.17E-03
2	1.000	1.000	.000	1.000	2.000	.000	.000	180.000	.000	.000	845.598	278.49	1.05E-03
3	1.000	1.000	.000	1.000	3.000	.000	.000	180.000	.000	.000	747.913	271.99	9.57E-04
4	1.000	1.000	.000	1.000	4.000	.000	.000	180.000	.000	.000	658.727	265.49	8.63E-04
5	1.000	1.000	.000	1.000	5.000	.000	.000	180.000	.000	.000	578.361	258.99	7.77E-04
6	1.000	1.000	.000	1.000	6.000	.000	.000	180.000	.000	.000	507.204	252.50	6.98E-04
7	1.000	1.000	.000	1.000	7.000	.000	.000	180.000	.000	.000	441.516	246.00	6.24E-04
8	1.000	1.000	.000	1.000	8.000	.000	.000	180.000	.000	.000	383.677	239.50	5.57E-04
9	1.000	1.000	.000	1.000	9.000	.000	.000	180.000	.000	.000	332.137	233.00	4.90E-04
10	1.000	1.000	.000	1.000	10.000	.000	.000	180.000	.000	.000	286.399	226.55	4.28E-04
11	1.000	1.000	.000	1.000	11.000	.000	.000	180.000	.000	.000	245.907	220.12	3.69E-04
12	1.000	1.000	.000	1.000	12.000	.000	.000	180.000	.000	.000	210.499	216.75	3.18E-04
13	1.000	1.000	.000	1.000	13.000	.000	.000	180.000	.000	.000	179.900	216.70	2.89E-04
14	1.000	1.000	.000	1.000	14.000	.000	.000	180.000	.000	.000	153.750	216.70	2.47E-04
15	1.000	1.000	.000	1.000	15.000	.000	.000	180.000	.000	.000	131.400	216.70	2.11E-04
16	1.000	1.000	.000	1.000	16.000	.000	.000	180.000	.000	.000	112.300	216.70	1.80E-04
17	1.000	1.000	.000	1.000	17.000	.000	.000	180.000	.000	.000	96.800	216.72	1.54E-04
18	1.000	1.000	.000	1.000	18.000	.000	.000	180.000	.000	.000	82.075	216.72	1.32E-04
19	1.000	1.000	.000	1.000	19.000	.000	.000	180.000	.000	.000	78.160	216.70	1.13E-04
20	1.000	1.000	.000	1.000	20.000	.000	.000	180.000	.000	.000	59.900	216.70	9.62E-05

CUMULATIVE ABSORBER AMOUNTS FOR THE PATH FROM M1 TO Z

J	Z (KM)	TBAR (K)	H2O (SCALED LOWTRAN UNITS)	CO2+ (SCALED LOWTRAN UNITS)	O3 (ATM CM)	HNO3 (ATM CM)	O3 UV (ATM CM)	CNTMSLF1 (MOL CM-2)	CNTMSLF2 (MOL CM-2)	CNTMFRM (MOL CM-2)
1	19.000	216.70	3.830E-06	9.745E-03	5.747E-03	1.957E-05	1.703E-02	8.726E+11	8.726E+11	1.187E+17
2	18.000	216.70	8.235E-06	2.257E-02	1.136E-02	3.870E-05	3.267E-02	1.745E+12	1.745E+12	2.575E+17
3	17.000	216.70	1.377E-05	3.944E-02	1.671E-02	5.957E-05	4.667E-02	2.781E+12	2.781E+12	4.347E+17
4	16.000	216.70	2.137E-05	6.163E-02	2.165E-02	8.270E-05	5.800E-02	4.217E+12	4.217E+12	6.706E+17
5	15.000	216.70	3.144E-05	9.083E-02	2.620E-02	1.060E-04	6.530E-02	6.206E+12	6.206E+12	1.014E+18
6	14.000	216.70	4.518E-05	1.293E-01	3.051E-02	1.362E-04	7.863E-02	8.942E+12	8.942E+12	1.475E+18
7	13.000	216.70	7.097E-05	1.799E-01	3.463E-02	1.647E-04	8.703E-02	1.644E+13	1.644E+13	2.355E+18
8	12.000	216.70	1.331E-04	2.465E-01	3.667E-02	1.937E-04	9.473E-02	2.808E+13	2.808E+13	4.508E+18
9	11.000	216.75	2.060E-04	3.342E-01	4.243E-02	2.194E-04	1.015E-01	2.808E+14	2.808E+14	9.915E+18
10	10.000	220.10	6.734E-04	4.469E-01	4.546E-02	2.360E-04	1.066E-01	9.367E+14	9.367E+14	2.360E+19
11	9.000	226.55	1.732E-03	5.883E-01	4.700E-02	2.431E-04	1.103E-01	5.241E+15	5.241E+15	6.073E+19
12	8.000	233.00	4.785E-03	7.847E-01	4.969E-02	2.449E-04	1.133E-01	3.411E+16	3.411E+16	1.690E+20
13	7.000	239.50	1.102E-02	9.824E-01	5.120E-02	2.449E-04	1.156E-01	1.537E+17	1.537E+17	4.215E+20
14	6.000	246.00	2.622E-02	1.253E+00	5.293E-02	2.449E-04	1.178E-01	5.340E+17	5.340E+17	9.566E+20
15	5.000	252.50	5.399E-02	1.583E+00	5.456E-02	2.449E-04	1.199E-01	1.681E+18	1.681E+18	1.984E+21

TABLE C-3 (Cont).

16	4.000	250.99	1.067E-01	1.986E+00	5.630E-02	2.449E-04	1.221E-01	5.012E+10	5.012E+18	3.760E+21
17	3.000	265.49	2.047E-01	2.475E+00	5.819E-02	2.449E-04	1.243E-01	1.430E+19	1.288E+19	7.205E+21
18	2.000	271.99	3.011E-01	3.065E+00	6.034E-02	2.449E-04	1.267E-01	3.873E+19	2.918E+19	1.339E+22
19	1.000	278.49	6.778E-01	3.776E+00	6.260E-02	2.449E-04	1.293E-01	9.489E+19	5.649E+19	2.378E+22
20	.000	284.99	1.144E+00	4.626E+00	6.512E-02	2.449E-04	1.318E-01	2.087E+20	9.131E+19	4.007E+22

J	Z (KM)	N2 CONT	MOL SCAT	AER 1	AER 2	AER 3	AER 4	CIRRUS
1	19.000	3.959E-03	7.445E-02	.000E+00	.000E+00	5.850E-04	.000E+00	.000E+00
2	18.000	9.376E-03	1.616E-01	.000E+00	.000E+00	1.136E-03	.000E+00	.000E+00
3	17.000	1.679E-02	2.639E-01	.000E+00	.000E+00	1.600E-03	.000E+00	.000E+00
4	16.000	2.693E-02	3.826E-01	.000E+00	.000E+00	2.012E-03	.000E+00	.000E+00
5	15.000	4.081E-02	5.221E-01	.000E+00	.000E+00	2.400E-03	.000E+00	.000E+00
6	14.000	5.981E-02	6.852E-01	.000E+00	.000E+00	2.610E-03	.000E+00	.000E+00
7	13.000	8.582E-02	8.761E-01	.000E+00	.000E+00	3.297E-03	.000E+00	.000E+00
8	12.000	1.214E-01	1.099E+00	.000E+00	.000E+00	3.873E-03	.000E+00	.000E+00
9	11.000	1.702E-01	1.361E+00	.000E+00	.000E+00	4.500E-03	.000E+00	.000E+00
10	10.000	2.355E-01	1.661E+00	.000E+00	.000E+00	5.500E-03	.000E+00	.000E+00
11	9.000	3.197E-01	2.002E+00	.000E+00	9.100E-04	6.130E-03	.000E+00	.000E+00
12	8.000	4.286E-01	2.385E+00	.000E+00	3.426E-03	6.130E-03	.000E+00	.000E+00
13	7.000	5.681E-01	2.817E+00	.000E+00	8.000E-03	6.130E-03	.000E+00	.000E+00
14	6.000	7.456E-01	3.300E+00	.000E+00	1.507E-02	6.130E-03	.000E+00	.000E+00
15	5.000	9.700E-01	3.840E+00	.000E+00	2.351E-02	6.130E-03	.000E+00	.000E+00
16	4.000	1.252E+00	4.441E+00	.000E+00	3.609E-02	6.130E-03	.000E+00	.000E+00
17	3.000	1.604E+00	5.109E+00	.000E+00	6.261E-02	6.130E-03	.000E+00	.000E+00
18	2.000	2.042E+00	5.850E+00	3.105E-02	7.991E-02	6.130E-03	.000E+00	.000E+00
19	1.000	2.505E+00	6.668E+00	3.122E-01	7.991E-02	6.130E-03	.000E+00	.000E+00
20	.000	3.253E+00	7.571E+00	1.002E+00	7.991E-02	6.130E-03	.000E+00	.000E+00

SUMMARY OF THE GEOMETRY CALCULATION

H1 = 20.000 KM
 H2 = .000 KM
 ANGLE = 180.000 DEG
 RANGE = 20.000 KM
 BETA = .000 DEG
 PHI = .000 DEG
 HMIN = .000 KM
 BENDING = .000 DEG
 LEN = 0

EQUIVALENT SEA LEVEL TOTAL ABSORBER AMOUNTS

H2O	CO2*	O3	HNO3	O3 UV	CNTMSLF1	CNTMSLF2	CNTMERN
(SCALED LOWTRAN UNIT'S)							
(ATM CM)	(ATM CM)	(ATM CM)	(MOL CM-2)	(MOL CM-2)	(MOL CM-2)	(MOL CM-2)	(MOL CM-2)
1.144E+00	4.626E+00	6.512E-02	2.449E-04	1.318E-01	2.087E+20	9.131E+19	4.007E+22

TABLE C-3 (Cont).

N2 CONT	MOL SCAT	AER 1	AER 2	AER 3	AER 4	CIRRUS	MEAN RH (PRCNT)
3.252E+00	7.571E+00	1.002E+00	7.991E-02	6.120E-03	.000E+00	.000E+00	48.25

ITER	ANGLE (DEG)	BETA (DEG)	RANGE (KM)	HMIN (KM)	PHI (DEG)	BENDING (DEG)
1	.0000	.0000	.0000	.000	180.0000	.0000
2	.0000	.0000	.0000	.000	180.0000	.0000

CASE 2D: GIVEN H1, H2, BETA:

ITERATE AROUND ANGLE UNTIL BETA CONVERGES

SLANT PATH PARAMETERS IN STANDARD FORM

H1	=	100.000 KM
H2	=	.000 KM
ANGLE	=	180.000 DEG
PHI	=	.000 DEG
HMIN	=	.000 KM
LEN	=	0

TABLE C-3 (Cont).

CALCULATION OF THE REFRACTED PATH THROUGH THE ATMOSPHERE

J	FROM (KM)	ALTITUDE C (KM)	THETA (DEG)	DISTANCE (KM)	RANGE (KM)	DBETA (DEG)	BETA (DEG)	PHI (DEG)	DBEND (DEG)	BENDING (DEG)	PBAR (MB)	TBAR (K)	RHOBAR (GM CM-3)
H2 TO H1													
1	1.000	1.000	.000	1.000	1.000	.000	.000	180.000	.000	.000	955.583	284.99	1.17E-03
2	1.000	2.000	.000	1.000	2.000	.000	.000	180.000	.000	.000	846.698	279.49	1.06E-03
3	1.000	3.000	.000	1.000	3.000	.000	.000	180.000	.000	.000	747.913	271.93	9.57E-04
4	3.000	4.000	.000	1.000	4.000	.000	.000	180.000	.000	.000	658.727	265.49	8.63E-04
5	4.000	5.000	.000	1.000	5.000	.000	.000	180.000	.000	.000	578.391	258.99	7.77E-04
6	5.000	6.000	.000	1.000	6.000	.000	.000	180.000	.000	.000	506.284	252.50	6.98E-04
7	6.000	7.000	.000	1.000	7.000	.000	.000	180.000	.000	.000	441.516	246.00	6.24E-04
8	7.000	8.000	.000	1.000	8.000	.000	.000	180.000	.000	.000	383.677	239.50	5.57E-04
9	8.000	9.000	.000	1.000	9.000	.000	.000	180.000	.000	.000	332.137	233.00	4.96E-04
10	9.000	10.000	.000	1.000	10.000	.000	.000	180.000	.000	.000	286.399	226.55	4.40E-04
11	10.000	11.000	.000	1.000	11.000	.000	.000	180.000	.000	.000	245.997	220.10	3.89E-04
12	11.000	12.000	.000	1.000	12.000	.000	.000	180.000	.000	.000	210.499	216.75	3.38E-04
13	12.000	13.000	.000	1.000	13.000	.000	.000	180.000	.000	.000	179.500	216.70	2.89E-04
14	13.000	14.000	.000	1.000	14.000	.000	.000	180.000	.000	.000	153.758	216.70	2.47E-04
15	14.000	15.000	.000	1.000	15.000	.000	.000	180.000	.000	.000	131.400	216.70	2.11E-04
16	15.000	16.000	.000	1.000	16.000	.000	.000	180.000	.000	.000	112.388	216.70	1.80E-04
17	16.000	17.000	.000	1.000	17.000	.000	.000	180.000	.000	.000	96.000	216.70	1.54E-04
18	17.000	18.000	.000	1.000	18.000	.000	.000	180.000	.000	.000	82.075	216.70	1.32E-04
19	18.000	19.000	.000	1.000	19.000	.000	.000	180.000	.000	.000	70.160	216.70	1.13E-04
20	19.000	20.000	.000	1.000	20.000	.000	.000	180.000	.000	.000	59.988	216.70	9.62E-05
21	20.000	21.000	.000	1.000	21.000	.000	.000	180.000	.000	.000	51.793	216.70	8.21E-05
22	21.000	22.000	.000	1.000	22.000	.000	.000	180.000	.000	.000	43.683	216.70	7.02E-05
23	22.000	23.000	.000	1.000	23.000	.000	.000	180.000	.000	.000	37.572	216.70	5.96E-05
24	23.000	24.000	.000	1.000	24.000	.000	.000	180.000	.000	.000	32.197	220.00	5.09E-05
25	24.000	25.000	.000	1.000	25.000	.000	.000	180.000	.000	.000	27.607	221.00	4.24E-05
26	25.000	26.000	.000	1.000	26.000	.000	.000	180.000	.000	.000	23.773	223.70	3.59E-05
27	26.000	27.000	.000	1.000	27.000	.000	.000	180.000	.000	.000	20.888	232.00	3.08E-05
28	27.000	28.000	.000	1.000	28.000	.000	.000	180.000	.000	.000	18.322	242.50	2.69E-05
29	28.000	29.000	.000	1.000	29.000	.000	.000	180.000	.000	.000	16.187	256.43	2.36E-05
30	29.000	30.000	.000	1.000	30.000	.000	.000	180.000	.000	.000	14.146	267.00	2.05E-05
31	30.000	31.000	.000	1.000	31.000	.000	.000	180.000	.000	.000	12.416	283.00	1.81E-05
32	31.000	32.000	.000	1.000	32.000	.000	.000	180.000	.000	.000	10.828	307.85	1.68E-05

CUMULATIVE ABSORBER AMOUNTS FOR THE PATH FROM H1 TO Z

J	Z (KM)	TBAR (K)	H2O (SCALED LOWTRAN UNITS)	CO2 (SCALED LOWTRAN UNITS)	O3 (ATM CM)	NO2 (ATM CM)	O3 UV (ATM CM)	CNTMSLP1 (MOL CM-2)	CNTMSLP2 (MOL CM-2)	CNTMFRN (MOL CM-2)
1	20.000	217.85	7.454E-12	1.543E-07	2.560E-07	.000E+00	1.503E-05	3.076E-05	3.036E+05	1.005E+11
2	50.000	253.92	5.724E-09	1.702E-05	4.390E-05	.000E+00	5.672E-04	1.481E-04	1.481E+09	1.005E+14
3	45.000	267.00	2.407E-08	5.172E-05	1.853E-04	.000E+00	3.064E-03	1.159E-10	9.606E+09	5.950E+14
4	40.000	256.43	1.203E-07	1.650E-04	8.007E-04	7.727E-07	1.012E-02	6.443E+10	6.244E+10	2.517E+15

TABLE C-3 (Cont).

[illegible]

TABLE C-3 (Cont).

18	14.000	7.951E-02	1.125E+00	.000E+00	.000E+00	.000E+00	5.024E-03	1.591E-04	.000E+00
19	13.000	9.652E-02	1.316E+00	.000E+00	.000E+00	.000E+00	5.504E-03	1.591E-04	.000E+00
20	12.000	1.321E-01	1.539E+00	.000E+00	.000E+00	.000E+00	6.001E-03	1.591E-04	.000E+00
21	11.000	1.009E-01	1.790E+00	.000E+00	.000E+00	.000E+00	6.790E-03	1.591E-04	.000E+00
22	10.000	5.450E-01	2.101E+00	.000E+00	.000E+00	.000E+00	7.760E-03	1.591E-04	.000E+00
23	9.000	3.304E-01	2.443E+00	.000E+00	.000E+00	.000E+00	8.320E-03	1.591E-04	.000E+00
24	8.000	4.593E-01	2.925E+00	.000E+00	.000E+00	.000E+00	8.320E-03	1.591E-04	.000E+00
25	7.000	5.760E-01	3.257E+00	.000E+00	.000E+00	.000E+00	8.320E-03	1.591E-04	.000E+00
26	6.000	7.563E-01	3.740E+00	.000E+00	.000E+00	.000E+00	8.320E-03	1.591E-04	.000E+00
27	5.000	9.000E-01	4.200E+00	.000E+00	.000E+00	.000E+00	8.320E-03	1.591E-04	.000E+00
28	4.000	1.263E+00	4.801E+00	.000E+00	.000E+00	.000E+00	8.320E-03	1.591E-04	.000E+00
29	3.000	1.615E+00	5.545E+00	.000E+00	.000E+00	.000E+00	8.320E-03	1.591E-04	.000E+00
30	2.000	2.053E+00	6.220E+00	.000E+00	.000E+00	.000E+00	8.320E-03	1.591E-04	.000E+00
31	1.000	3.550E+00	7.100E+00	.000E+00	.000E+00	.000E+00	8.320E-03	1.591E-04	.000E+00
32	.000	3.662E+00	8.100E+00	.000E+00	.000E+00	.000E+00	8.320E-03	1.591E-04	.000E+00

SUMMARY OF THE GEOMETRY CALCULATION

H1	=	100.000 KM
H2	=	.000 KM
ANGLE	=	100.000 DEG
RANGE	=	100.000 KM
BETA	=	.000 DEG
PHI	=	.000 DEG
HMIN	=	.000 KM
BENDING	=	.000 DEG
LEN	=	0

EQUIVALENT SEA LEVEL TOTAL ABSORBER AMOUNTS:

	H2O	CO2+	O3	HNO3	O3 UV	CINTSLF1	CINTSLF2	CINTFRM
	(SCALED LOWTRAN UNITS)							
1	1.144E+00	4.657E+00	1.107E-01	3.076E-04	3.434E-01	2.007E+20	9.131E+19	4.007E+22
N2 CONT	MOL	SCAT	AER 1	AER 2	AER 3	AER 4	CIRRUS	MEAN RH (PRCNT)
3	2.622E+00	8.012E+00	1.000E+00	7.991E-02	8.320E-03	1.591E-04	.000E+00	48.25

SUMMARY OF THE GEOMETRY CALCULATION

H1 = 100.000 KM
 H2 = .000 KM
 ANGLE = 100.000 DEG
 RANGE = 100.000 KM
 BETA = .000 DEG
 PHI = .000 DEG
 HMIN = .000 KM
 BENDING = .000 DEG
 LEN = 0

TABLE C-3 (Cont).

RADIANCE (WATTS/CM²-STER-XXX)

FREQ WAVLEN (CM-1)	ATMOS RADIANCE (CM-1)	INTEGRAL (CM-1)	TOTAL TRANS
850.	11.765	1.04E-05	7.54E-05
855.	11.696	1.03E-05	7.54E-05
860.	11.628	1.02E-05	7.54E-05
865.	11.561	1.02E-05	7.54E-05
870.	11.494	1.01E-05	7.54E-05
875.	11.429	1.00E-05	7.54E-05
880.	11.364	9.96E-06	7.54E-05
885.	11.299	9.98E-06	7.54E-05
890.	11.236	9.98E-06	7.54E-05
895.	11.173	9.72E-06	7.54E-05
900.	11.111	9.54E-06	7.54E-05
905.	11.050	9.55E-06	7.54E-05
910.	10.989	9.46E-06	7.54E-05
915.	10.929	9.36E-06	7.54E-05
920.	10.870	9.27E-06	7.54E-05
925.	10.811	9.17E-06	7.54E-05
930.	10.753	9.07E-06	7.54E-05
935.	10.695	8.96E-06	7.54E-05
940.	10.638	8.85E-06	7.54E-05
945.	10.582	8.73E-06	7.54E-05
950.	10.526	8.60E-06	7.54E-05

INTEGRATED ABSORPTION FROM 850 TO 950 CM-1 = 28.32 CM-1

AVERAGE TRANSMITTANCE = .7968

INTEGRATED RADIANCE = 9.593E-04 WATTS CM-2 STER-1
 MINIMUM RADIANCE = 8.559E-06 WATTS CM-2 STER-1 (CM-1)-1 AT
 MAXIMUM RADIANCE = 1.835E-05 WATTS CM-2 STER-1 (CM-1)-1 AT
 BOUNDARY TEMPERATURE = 288.20 K
 BOUNDARY EMISSIVITY = 1.000

CARD 5 *****

17.42.38.UCLP, AA, LP2 , 1.824KLS.

950.0 CM-1
850.0 CM-1

LOWTRAN OUTPUT FOR CASE 3

***** LOWTRAN 6 *****

TABLE C-4 (Cont.).

ATMOSPHERIC PROFILES										
I	Z (KM)	P (MB)	T (K)	H ₂ O (SCALED)	CO ₂ ⁺ (LOWTRAN UNITS)	N ₂	CONTMSLF (INOL/CM ² KM)	MOL SCAT (-)	N-1 (-)	O ₃ (UV) (ATM CM/KM)
1	1.00	1013.000	288.2	5.750E-01	9.205E-01	2.493E-03	7.378E-01	1.569E+20	9.475E-21	2.774E-04
2	1.00	898.800	281.7	3.719E-01	7.771E-01	2.387E-03	6.010E-01	7.951E+19	8.601E-01	2.519E-04
3	2.00	795.800	275.2	2.323E-01	6.474E-01	2.284E-03	4.870E-01	3.791E+19	7.788E-01	2.281E-04
4	3.00	701.200	268.7	1.302E-01	5.371E-01	2.020E-03	3.927E-01	1.468E+19	7.035E-01	2.061E-04
5	4.00	616.600	262.2	7.166E-02	4.435E-01	1.774E-03	3.150E-01	5.484E+18	6.348E-01	1.859E-04
6	5.00	540.500	255.7	3.745E-02	3.646E-01	1.621E-03	2.513E-01	1.846E+18	5.638E-01	1.670E-04
7	6.00	472.200	249.2	1.992E-02	2.982E-01	1.576E-03	1.944E-01	9.580E+17	5.188E-01	1.497E-04
8	7.00	411.100	242.7	9.834E-03	2.427E-01	1.632E-03	1.572E-01	1.988E+17	4.566E-01	1.338E-04
9	8.00	356.500	236.2	5.804E-03	1.963E-01	1.645E-03	1.232E-01	6.439E+16	4.069E-01	1.192E-04
10	9.00	308.000	229.7	1.703E-03	1.579E-01	2.130E-03	9.586E-02	9.537E+15	3.615E-01	1.059E-04
11	10.00	265.000	223.3	5.894E-04	1.262E-01	2.557E-03	7.493E-02	1.468E+15	3.199E-01	9.376E-05
12	11.00	227.000	216.8	2.367E-04	1.002E-01	3.493E-03	5.678E-02	3.031E+14	2.823E-01	8.273E-05
13	12.00	194.000	216.7	9.275E-05	7.619E-02	4.037E-03	4.150E-02	6.170E+13	2.413E-01	7.073E-05
14	13.00	165.800	216.7	3.917E-05	5.780E-02	4.028E-03	3.831E-02	1.460E+13	2.063E-01	6.045E-05
15	14.00	141.700	216.7	1.587E-05	4.397E-02	4.220E-03	2.214E-02	3.180E+12	1.753E-01	5.165E-05
16	15.00	121.100	216.7	1.181E-05	3.340E-02	4.388E-03	1.617E-02	2.337E+12	1.587E-01	4.415E-05
17	16.00	103.500	216.7	8.682E-06	2.537E-02	4.710E-03	1.181E-02	1.677E+12	1.288E-01	3.774E-05
18	17.00	88.500	216.7	6.432E-06	1.929E-02	5.161E-03	8.637E-03	1.239E+12	1.101E-01	3.227E-05
19	18.00	75.650	216.7	4.726E-06	1.466E-02	5.540E-03	6.311E-03	8.726E+11	9.411E-02	2.758E-05
20	19.00	64.670	216.7	3.549E-06	1.114E-02	5.691E-03	4.612E-03	8.726E+11	8.045E-02	2.358E-05
21	20.00	55.290	216.7	3.564E-06	8.470E-03	5.803E-03	3.371E-03	8.726E+11	6.978E-02	2.016E-05
22	21.00	47.290	217.6	3.371E-06	6.406E-03	5.447E-03	2.451E-03	1.030E+12	5.059E-02	1.717E-05
23	22.00	40.470	218.6	3.169E-06	4.847E-03	5.248E-03	1.783E-03	1.219E+12	4.991E-02	1.463E-05
24	23.00	34.670	219.6	3.015E-06	3.675E-03	4.802E-03	1.299E-03	1.464E+12	4.266E-02	1.247E-05
25	24.00	29.720	220.6	2.803E-06	2.709E-03	4.274E-03	9.483E-04	1.672E+12	3.622E-02	1.064E-05
26	25.00	25.490	221.6	2.636E-06	2.119E-03	3.792E-03	6.929E-04	1.963E+12	3.101E-02	9.088E-06
27	30.00	11.970	226.5	7.612E-07	5.476E-04	1.642E-03	1.479E-04	6.598E+11	4.455E-02	4.175E-06
28	35.00	5.746	236.5	1.624E-07	1.429E-04	6.674E-04	3.193E-05	1.154E+11	6.550E-03	1.920E-06
29	40.00	2.871	250.4	3.549E-08	3.922E-05	2.227E-04	7.318E-06	2.023E+10	3.091E-03	9.059E-07
30	45.00	1.491	264.2	9.176E-09	1.157E-05	5.801E-05	1.821E-06	4.615E+09	1.521E-03	4.459E-07
31	50.00	.798	270.7	1.939E-09	3.747E-06	1.072E-05	5.827E-07	6.490E+08	7.945E-04	3.328E-07
32	70.00	.055	219.7	2.406E-12	4.660E-08	8.259E-08	3.291E-09	1.014E+05	6.733E-05	1.985E-08
33	100.00	.000	210.0	1.502E-16	5.420E-12	5.180E-12	1.046E-13	4.507E+00	3.061E-07	1.132E-10

TABLE C-4 (Cont).

ATMOSPHERIC PROFILES												
I	Z (KM)	P (MB)	T (K)	CNTMFRN MOL/CM ² KM	HM03 ATM CM/KM	AEROSOL 1 (-)	AEROSOL 2 (-)	AEROSOL 3 (-)	AEROSOL 4 (-)	AEI*RH (...)	CIRRUS (-)	RH (PERCENT)
1	.00	1013.000	288.2	2.010E+22	.000E+00	7.700E-01	.000E+00	.000E+00	.000E+00	3.533E+01	.000E+00	4.509E+01
2	1.00	898.800	281.7	1.301E+22	.000E+00	7.700E-01	.000E+00	.000E+00	.000E+00	3.777E+01	.000E+00	4.906E+01
3	2.00	795.000	275.2	9.143E+21	.000E+00	6.210E-02	.000E+00	.000E+00	.000E+00	3.230E+00	.000E+00	5.201E+01
4	3.00	701.200	268.7	4.573E+21	.000E+00	3.460E-02	.000E+00	.000E+00	.000E+00	.000E+00	.000E+00	.000E+00
5	4.00	616.600	262.2	2.531E+21	.000E+00	1.850E-02	.000E+00	.000E+00	.000E+00	.000E+00	.000E+00	.000E+00
6	5.00	540.500	255.7	1.319E+21	.000E+00	.000E+00	9.210E-03	.000E+00	.000E+00	.000E+00	.000E+00	.000E+00
7	6.00	472.200	249.2	.000E+00	.000E+00	.000E+00	7.710E-03	.000E+00	.000E+00	.000E+00	.000E+00	.000E+00
8	7.00	411.100	242.7	3.472E+20	.000E+00	.000E+00	6.230E-03	.000E+00	.000E+00	.000E+00	.000E+00	.000E+00
9	8.00	356.500	236.2	1.768E+20	4.069E-35	.000E+00	3.370E-03	.000E+00	.000E+00	.000E+00	.000E+00	.000E+00
10	9.00	308.000	229.7	6.023E+19	3.615E-06	.000E+00	1.820E-03	.000E+00	.000E+00	.000E+00	.000E+00	.000E+00
11	10.00	265.000	223.3	2.086E+19	1.055E-05	.000E+00	.000E+00	1.140E-03	.000E+00	.000E+00	.000E+00	.000E+00
12	11.00	227.000	216.8	8.384E+18	2.250E-05	.000E+00	.000E+00	7.950E-04	.000E+00	.000E+00	.000E+00	.000E+00
13	12.00	194.000	216.7	3.235E+18	2.696E-05	.000E+00	.000E+00	6.410E-04	.000E+00	.000E+00	.000E+00	.000E+00
14	13.00	165.800	216.7	1.345E+18	2.080E-05	.000E+00	.000E+00	5.170E-04	.000E+00	.000E+00	.000E+00	.000E+00
15	14.00	141.700	216.7	5.364E+17	2.820E-05	.000E+00	.000E+00	4.420E-04	.000E+00	.000E+00	.000E+00	.000E+00
16	15.00	121.100	216.7	3.923E+17	2.712E-05	.000E+00	.000E+00	3.950E-04	.000E+00	.000E+00	.000E+00	.000E+00
17	16.00	105.500	216.7	2.845E+17	2.446E-05	.000E+00	.000E+00	3.820E-04	.000E+00	.000E+00	.000E+00	.000E+00
18	17.00	88.500	216.7	2.071E+17	2.202E-05	.000E+00	.000E+00	4.250E-04	.000E+00	.000E+00	.000E+00	.000E+00
19	18.00	75.650	216.7	1.507E+17	1.976E-05	.000E+00	.000E+00	5.200E-04	.000E+00	.000E+00	.000E+00	.000E+00
20	19.00	64.670	216.7	1.282E+17	1.850E-05	.000E+00	.000E+00	5.910E-04	.000E+00	.000E+00	.000E+00	.000E+00
21	20.00	55.290	216.7	1.036E+17	2.063E-05	.000E+00	.000E+00	5.830E-04	.000E+00	.000E+00	.000E+00	.000E+00
22	21.00	47.120	216.6	1.019E+17	2.168E-05	.000E+00	.000E+00	5.020E-04	.000E+00	.000E+00	.000E+00	.000E+00
23	22.00	40.470	219.6	9.401E+16	2.095E-05	.000E+00	.000E+00	4.200E-04	.000E+00	.000E+00	.000E+00	.000E+00
24	23.00	34.670	219.6	8.788E+16	2.213E-05	.000E+00	.000E+00	3.000E-04	.000E+00	.000E+00	.000E+00	.000E+00
25	24.00	29.720	220.6	8.035E+16	2.179E-05	.000E+00	.000E+00	1.900E-04	.000E+00	.000E+00	.000E+00	.000E+00
26	25.00	25.490	221.6	7.414E+16	1.170E-05	.000E+00	.000E+00	1.310E-04	.000E+00	.000E+00	.000E+00	.000E+00
27	26.00	21.970	226.5	1.961E+16	3.704E-06	.000E+00	.000E+00	3.320E-05	.000E+00	.000E+00	.000E+00	.000E+00
28	27.00	19.740	236.5	2.796E+15	1.441E-07	.000E+00	.000E+00	.000E+00	1.640E-05	.000E+00	.000E+00	.000E+00
29	28.00	17.871	250.4	7.502E+14	3.091E-37	.000E+00	.000E+00	.000E+00	7.990E-06	.000E+00	.000E+00	.000E+00
30	29.00	16.491	264.2	1.764E+14	.000E+00	.000E+00	.000E+00	.000E+00	4.010E-06	.000E+00	.000E+00	.000E+00
31	30.00	15.798	270.7	3.454E+13	.000E+00	.000E+00	.000E+00	.000E+00	2.100E-06	.000E+00	.000E+00	.000E+00
32	31.00	15.055	219.7	3.688E+10	.000E+00	.000E+00	.000E+00	.000E+00	1.600E-07	.000E+00	.000E+00	.000E+00
33	100.00	.000	.000	1.399E+06	.000E+00	.000E+00	.000E+00	.000E+00	9.310E-10	.000E+00	.000E+00	.000E+00

CASE 2A: GIVEN H1, H2, ANGLE

SLANT PATH PARAMETERS IN STANDARD FORM

H1 = .000 KM
 H2 = 20.000 KM
 ANGLE = .000 DEG
 PHI = 180.000 DEG

TABLE C-4 (Cont).

HMJN
LEN

-

.000 KM
0

TABLE C-4 (Cont).

CALCULATION OF THE REFRACTED PATH THROUGH THE ATMOSPHERE

I	FROM ALTITUDE (KM)	TO ALTITUDE (KM)	THETA (DEG)	RANGE (KM)	DBETA (DEG)	BETA (DEG)	PHI (DEG)	DBEND (DEG)	BENDING (DEG)	PBAR (MB)	TBAR (V)	RHOBAR (GM CM-3)
H1 TO H2												
1	.000	1.000	.000	1.000	.000	.000	180.000	.000	.000	955.603	284.99	1.17E-03
2	1.000	2.000	.000	1.000	.000	.000	180.000	.000	.000	946.698	278.49	1.06E-03
3	2.000	3.000	.000	1.000	.000	.000	180.000	.000	.000	937.293	271.99	9.57E-04
4	3.000	4.000	.000	1.000	.000	.000	180.000	.000	.000	927.888	265.49	8.46E-04
5	4.000	5.000	.000	1.000	.000	.000	180.000	.000	.000	918.483	258.99	7.35E-04
6	5.000	6.000	.000	1.000	.000	.000	180.000	.000	.000	909.078	252.49	6.24E-04
7	6.000	7.000	.000	1.000	.000	.000	180.000	.000	.000	899.673	245.99	5.13E-04
8	7.000	8.000	.000	1.000	.000	.000	180.000	.000	.000	890.268	239.49	4.02E-04
9	8.000	9.000	.000	1.000	.000	.000	180.000	.000	.000	880.863	232.99	2.91E-04
10	9.000	10.000	.000	1.000	.000	.000	180.000	.000	.000	871.458	226.49	1.80E-04
11	10.000	11.000	.000	1.000	.000	.000	180.000	.000	.000	862.053	219.99	6.89E-05
12	11.000	12.000	.000	1.000	.000	.000	180.000	.000	.000	852.648	213.49	3.78E-05
13	12.000	13.000	.000	1.000	.000	.000	180.000	.000	.000	843.243	206.99	2.67E-05
14	13.000	14.000	.000	1.000	.000	.000	180.000	.000	.000	833.838	200.49	1.56E-05
15	14.000	15.000	.000	1.000	.000	.000	180.000	.000	.000	824.433	193.99	4.45E-06
16	15.000	16.000	.000	1.000	.000	.000	180.000	.000	.000	815.028	187.49	1.34E-06
17	16.000	17.000	.000	1.000	.000	.000	180.000	.000	.000	805.623	180.99	2.23E-07
18	17.000	18.000	.000	1.000	.000	.000	180.000	.000	.000	796.218	174.49	1.12E-07
19	18.000	19.000	.000	1.000	.000	.000	180.000	.000	.000	786.813	167.99	3.01E-08
20	19.000	20.000	.000	1.000	.000	.000	180.000	.000	.000	777.408	161.49	9.90E-09

CUMULATIVE ABSORBER AMOUNTS FOR THE PATH FROM H1 TO H2

J	Z (KM)	TBAR (V)	H2O (SCALED LOWTRAN UNITS)	CO2+ (SCALED LOWTRAN UNITS)	O3 (ATM CM)	HNO3 (ATM CM)	O3 UV (ATM CM)	CNTMSLF1 (MOL CM-2)	CNTMSLF2 (MOL CM-2)	CNTMFRM (MOL CM-2)
1	1.000	284.99	4.664E-01	8.506E-01	2.448E-03	.000E+00	2.528E-03	1.138E+20	3.482E+19	1.629E+22
2	2.000	278.49	7.631E-01	1.561E+00	4.755E-03	.000E+00	5.048E-03	1.700E+20	6.213E+19	2.668E+22
3	3.000	271.99	9.394E-01	2.151E+00	6.924E-03	.000E+00	7.465E-03	1.941E+20	7.842E+19	3.287E+22
4	4.000	265.49	1.037E+00	2.648E+00	8.819E-03	.000E+00	9.780E-03	2.037E+20	8.630E+19	3.631E+22
5	5.000	258.99	1.090E+00	3.043E+00	1.055E-02	.000E+00	1.185E-02	2.071E+20	8.963E+19	3.817E+22
6	6.000	252.49	1.118E+00	3.373E+00	1.218E-02	.000E+00	1.397E-02	2.082E+20	9.077E+19	3.915E+22
7	7.000	246.00	1.132E+00	3.643E+00	1.379E-02	.000E+00	1.617E-02	2.086E+20	9.115E+19	3.965E+22
8	8.000	239.50	1.139E+00	3.861E+00	1.543E-02	2.034E-05	1.852E-02	2.087E+20	9.127E+19	3.990E+22
9	9.000	233.00	1.142E+00	4.038E+00	1.732E-02	1.087E-05	2.139E-02	2.087E+20	9.136E+19	4.001E+22
10	10.000	226.55	1.144E+00	4.179E+00	1.966E-02	8.893E-06	2.515E-02	2.087E+20	9.131E+19	4.005E+22
11	11.000	220.10	1.144E+00	4.292E+00	2.268E-02	5.545E-06	3.028E-02	2.087E+20	9.131E+19	4.005E+22
12	12.000	213.75	1.144E+00	4.380E+00	2.655E-02	5.123E-06	3.705E-02	2.087E+20	9.131E+19	4.005E+22
13	13.000	216.78	1.144E+00	4.446E+00	3.048E-02	8.015E-06	4.475E-02	2.087E+20	9.131E+19	4.005E+22
14	14.000	216.70	1.144E+00	4.497E+00	3.461E-02	1.087E-05	5.315E-02	2.087E+20	9.131E+19	4.005E+22
15	15.000	216.70	1.144E+00	4.535E+00	3.892E-02	1.363E-05	6.248E-02	2.087E+20	9.131E+19	4.005E+22

TABLE C-4 (Cont).

J	Z (KM)	NZ CONT	MOL SCAT	AER 1	AEP 2	AER 3	AER 4	CIRRU5
16	16.000	216.70	1.144E+00	4.565E+00	4.347E-02	1.621E-04	7.290E-02	2.007E+20 9.131E+19 4.007E+22
17	17.000	216.70	1.144E+00	4.507E+00	4.040E-02	1.853E-04	8.512E-02	2.007E+20 9.131E+19 4.007E+22
18	18.000	216.70	1.144E+00	4.604E+00	5.325E-02	2.062E-04	9.912E-02	2.007E+20 9.131E+19 4.007E+22
19	19.000	216.70	1.144E+00	4.616E+00	5.937E-02	2.253E-04	1.140E-01	2.007E+20 9.131E+19 4.007E+22
20	20.000	216.70	1.144E+00	4.626E+00	6.512E-02	2.449E-04	1.310E-01	2.007E+20 9.131E+19 4.007E+22

SUMMARY OF THE GEOMETRY CALCULATION

H1 = 20.000 KM
 H2 = 20.000 KM
 ANGLE = .000 DEG
 RANGE = 20.000 KM
 BETA = .000 DEG
 PHI = 180.000 DEG
 HMIN = .000 KM
 BENDING = .000 DEG
 LEN = 0

EQUIVALENT SEA LEVEL TOTAL ABSORBER AMOUNTS

H2O (SCALED LOWTRAN UNITS) O3
 HNO3 (ATM CM) O3 UV (ATM CM) CNTMSLF1 (MOL CM-2) CNTMSLF2 (MOL CM-2) CNTMFR4 (MOL CM-2)
 1.144E+00 4.626E+00 6.512E-02 2.449E-04 1.310E-01 2.007E+20 9.131E+19 4.007E+22

TABLE C-4 (Cont).

N2 CONT	MOL SCAT	AER 1	AER 2	AER 3	AER 4	CIRRUS	MEAN RH (PPCNT)
3.253E+00	7.571E+00	1.002E+00	7.991E-02	6.120E-03	.000E+00	.000E+00	48.25
SINGLE SCATTERING POINT TO SOURCE PATHS							
POINT ALT	SCATR ANGLE	SUBTENDED SOLAR PATH ZENITH	RELATIVE AZIMUTH	SCATR ANGLE	MOLECULAR PHASE ϕ		
1	.00	.00	.00	1 50.00	.740E-01		
2	1.00	.00	.00	1 50.00	.740E-01		
3	2.00	.00	.00	1 50.00	.740E-01		
4	3.00	.00	.00	1 50.00	.740E-01		
5	4.00	.00	.00	1 50.00	.740E-01		
6	5.00	.00	.00	1 50.00	.740E-01		
7	6.00	.00	.00	1 50.00	.740E-01		
8	7.00	.00	.00	1 50.00	.740E-01		
9	8.00	.00	.00	1 50.00	.740E-01		
10	9.00	.00	.00	1 50.00	.740E-01		
11	10.00	.00	.00	1 50.00	.740E-01		
12	11.00	.00	.00	1 50.00	.740E-01		
13	12.00	.00	.00	1 50.00	.740E-01		
14	13.00	.00	.00	1 50.00	.740E-01		
15	14.00	.00	.00	1 50.00	.740E-01		
16	15.00	.00	.00	1 50.00	.740E-01		
17	16.00	.00	.00	1 50.00	.740E-01		
18	17.00	.00	.00	1 50.00	.740E-01		
19	18.00	.00	.00	1 50.00	.740E-01		
20	19.00	.00	.00	1 50.00	.740E-01		
21	20.00	.00	.00	1 50.00	.740E-01		

CASE 2A: GIVEN H1, H2, ANGLE

SLANT PATH PARAMETERS IN STANDARD FORM

H1	=	.000 KM
H2	=	100.000 KM
ANGLE	=	.000 DEG
PHI	=	180.000 DEG
HMIN	=	.000 KM
LEN	=	0

TABLE C-4 (Cont).

CALCULATION OF THE REFRACTED PATH THROUGH THE ATMOSPHERE

I	FROM (KM)	ALITUDE TO (KM)	THETA (DEG)	DRANGE (KM)	RANGE (KM)	DBETA (DEG)	BETA (DEG)	PHI (DEG)	DBEND (DEG)	BENDING (DEG)	PBAR (MB)	TBAR (K)	RHOBAR (CM CM-3)
H1 TO H2													
1	1.000	1.000	.000	1.000	1.000	.000	.000	180.000	.000	.000	955.603	284.99	1.17E-03
2	1.000	2.000	.000	1.000	2.000	.000	.000	180.000	.000	.000	846.600	278.49	1.04E-03
3	2.000	3.000	.000	1.000	3.000	.000	.000	180.000	.000	.000	747.913	271.99	9.57E-04
4	3.000	4.000	.000	1.000	4.000	.000	.000	180.000	.000	.000	658.727	265.49	8.63E-04
5	4.000	5.000	.000	1.000	5.000	.000	.000	180.000	.000	.000	578.391	258.99	7.77E-04
6	5.000	6.000	.000	1.000	6.000	.000	.000	180.000	.000	.000	506.204	252.50	6.98E-04
7	6.000	7.000	.000	1.000	7.000	.000	.000	180.000	.000	.000	441.516	246.00	6.24E-04
8	7.000	8.000	.000	1.000	8.000	.000	.000	180.000	.000	.000	383.677	239.50	5.57E-04
9	8.000	9.000	.000	1.000	9.000	.000	.000	180.000	.000	.000	332.137	233.00	4.96E-04
10	9.000	10.000	.000	1.000	10.000	.000	.000	180.000	.000	.000	286.339	226.55	4.40E-04
11	10.000	11.000	.000	1.000	11.000	.000	.000	180.000	.000	.000	245.907	220.10	3.89E-04
12	11.000	12.000	.000	1.000	12.000	.000	.000	180.000	.000	.000	210.499	216.75	3.38E-04
13	12.000	13.000	.000	1.000	13.000	.000	.000	180.000	.000	.000	179.900	216.70	2.89E-04
14	13.000	14.000	.000	1.000	14.000	.000	.000	180.000	.000	.000	153.750	216.70	2.47E-04
15	14.000	15.000	.000	1.000	15.000	.000	.000	180.000	.000	.000	131.400	216.70	2.11E-04
16	15.000	16.000	.000	1.000	16.000	.000	.000	180.000	.000	.000	112.300	216.70	1.80E-04
17	16.000	17.000	.000	1.000	17.000	.000	.000	180.000	.000	.000	96.000	216.70	1.54E-04
18	17.000	18.000	.000	1.000	18.000	.000	.000	180.000	.000	.000	82.075	216.70	1.32E-04
19	18.000	19.000	.000	1.000	19.000	.000	.000	180.000	.000	.000	70.160	216.70	1.13E-04
20	19.000	20.000	.000	1.000	20.000	.000	.000	180.000	.000	.000	59.900	216.70	9.62E-05
21	20.000	21.000	.000	1.000	21.000	.000	.000	180.000	.000	.000	51.253	217.14	8.21E-05
22	21.000	22.000	.000	1.000	22.000	.000	.000	180.000	.000	.000	43.883	218.09	7.00E-05
23	22.000	23.000	.000	1.000	23.000	.000	.000	180.000	.000	.000	37.572	219.09	5.96E-05
24	23.000	24.000	.000	1.000	24.000	.000	.000	180.000	.000	.000	32.197	220.09	5.09E-05
25	24.000	25.000	.000	1.000	25.000	.000	.000	180.000	.000	.000	27.607	221.09	4.34E-05
26	25.000	26.000	.000	5.000	30.000	.000	.000	180.000	.000	.000	18.754	223.73	2.79E-05
27	30.000	35.000	.000	5.000	35.000	.000	.000	180.000	.000	.000	8.800	230.82	1.20E-05
28	35.000	40.000	.000	5.000	40.000	.000	.000	180.000	.000	.000	4.322	242.52	5.95E-06
29	40.000	45.000	.000	5.000	45.000	.000	.000	180.000	.000	.000	2.107	256.43	2.86E-06
30	45.000	50.000	.000	5.000	50.000	.000	.000	180.000	.000	.000	1.146	267.09	1.45E-06
31	50.000	70.000	.000	20.000	70.000	.000	.000	180.000	.000	.000	.416	253.92	3.81E-07
32	70.000	100.000	.000	30.000	100.000	.000	.000	180.000	.000	.000	.000	217.85	1.60E-08

CUMULATIVE ABSORBER AMOUNTS FOR THE PATH FROM H1 TO Z

Z (KM)	TBAR (K)	H2O (SCALED LOWTRAN UNITS)	CO2+ (SCALED LOWTRAN UNITS)	O3 (ATM CM)	HNO3 (ATM CM)	O3 UV (ATM CM)	CNTMSLF1 (MOL CM-2)	CNTMSLF2 (MOL CM-2)	CNTMFRM (MOL CM-2)
1	1.000	4.604E-01	8.506E-01	2.440E-03	.000E+00	2.520E-03	1.130E+20	3.482E+19	1.629E+22
2	2.000	7.631E-01	1.561E+00	4.775E-03	.000E+00	5.040E-03	1.700E+20	6.213E+19	2.660E+22
3	3.000	9.394E-01	2.151E+00	6.924E-03	.000E+00	7.465E-03	1.944E+20	7.842E+19	3.287E+22
4	4.000	1.037E+00	2.640E+00	8.819E-03	.000E+00	9.704E-03	2.037E+20	8.630E+19	3.631E+22

3

C-34

TABLE C-4 (Cont).

18	18.000	3.242E+00	7.410E+00	1.082E+00	7.991E-02	4.904E-03	.000E+00
19	19.000	3.240E+00	7.497E+00	1.082E+00	7.991E-02	5.535E-03	.000E+00
20	20.000	3.252E+00	7.571E+00	1.082E+00	7.991E-02	6.120E-03	.000E+00
21	21.000	3.254E+00	7.635E+00	1.082E+00	7.991E-02	6.641E-03	.000E+00
22	22.000	3.257E+00	7.689E+00	1.082E+00	7.991E-02	7.121E-03	.000E+00
23	23.000	3.258E+00	7.735E+00	1.082E+00	7.991E-02	7.481E-03	.000E+00
24	24.000	3.259E+00	7.775E+00	1.082E+00	7.991E-02	7.726E-03	.000E+00
25	25.000	3.260E+00	7.808E+00	1.082E+00	7.991E-02	7.868E-03	.000E+00
26	26.000	3.262E+00	7.818E+00	1.082E+00	7.991E-02	8.245E-03	.000E+00
27	27.000	3.262E+00	7.966E+00	1.082E+00	7.991E-02	8.328E-03	.000E+00
28	28.000	3.262E+00	7.989E+00	1.082E+00	7.991E-02	8.328E-03	.000E+00
29	29.000	3.262E+00	8.000E+00	1.082E+00	7.991E-02	8.328E-03	.000E+00
30	30.000	3.262E+00	8.005E+00	1.082E+00	7.991E-02	8.328E-03	.000E+00
31	31.000	3.262E+00	8.011E+00	1.082E+00	7.991E-02	8.328E-03	.000E+00
32	32.000	3.262E+00	8.012E+00	1.082E+00	7.991E-02	8.328E-03	.000E+00

SUMMARY OF THE GEOMETRY CALCULATION

H1 = .000 KM
 H2 = 100.000 KM
 ANGLE = 100.000 DEG
 RANGE = 100.000 KM
 BETA = .000 DEG
 PHI = 100.000 DEG
 HMIN = .000 KM
 BENDING = .000 DEG
 LEN = R

EQUIVALENT SEA LEVEL TOTAL ABSORBER AMOUNTS

EQUIVALENT SEA LEVEL TOTAL AEROSOL OPTICAL DEPTH								
W20	CO2*	O3	HNO3	O3 UV	CNTMSLF1	CNTMSLF2	CNTMFRN	
(SCALED LOWTRAN UNITS)								
		(ATM CM)	(ATM CM)	(ATM CM)	(MOL CM-2)	(MOL CM-2)	(MOL CM-2)	
1.144E+00	4.657E+00	1.107E-01	3.876E-04	3.434E-01	2.007E+20	9.131E+19	4.007E+22	

SINGLE SCATTERING POINT TO SOURCE PATHS

POINT ALT	SCATR SUSTENDED ANGLE	SOLA* ZENITH ANGLE	PATH RELATIVE ZENITH	SCATR MOLECULAR PHASE F
1	.00	.00	.00	.748E-01
2	1.00	.00	.00	.748E-01
3	2.00	.00	.00	.748E-01
4	3.00	.00	.00	.748E-01
5	4.00	.00	.00	.748E-01
6	5.00	.00	.00	.748E-01

TABLE C-4 (Cont).

7	6.00	.00	60.00	.00	.00	1	60.00	.740E-01
8	7.00	.00	60.00	.00	.00	1	60.00	.740E-01
9	8.00	.00	62.00	.00	.00	1	60.00	.740E-01
10	9.00	.00	60.00	.00	.00	1	60.00	.740E-01
11	10.00	.00	60.00	.00	.00	1	60.00	.740E-01
12	11.00	.00	60.00	.00	.00	1	60.00	.740E-01
13	12.00	.00	60.00	.00	.00	1	60.00	.740E-01
14	13.00	.00	60.00	.00	.00	1	60.00	.740E-01
15	14.00	.00	60.00	.00	.00	1	60.00	.740E-01
16	15.00	.00	60.00	.00	.00	1	60.00	.740E-01
17	16.00	.00	60.00	.00	.00	1	60.00	.740E-01
18	17.00	.00	62.00	.00	.00	1	60.00	.740E-01
19	18.00	.00	60.00	.00	.00	1	60.00	.740E-01
20	19.00	.00	60.00	.00	.00	1	60.00	.740E-01
21	20.00	.00	60.00	.00	.00	1	60.00	.740E-01
22	21.00	.00	60.00	.00	.00	1	60.00	.740E-01
23	22.00	.00	62.00	.00	.00	1	60.00	.740E-01
24	23.00	.00	60.00	.00	.00	1	60.00	.740E-01
25	24.00	.00	60.00	.00	.00	1	60.00	.740E-01
26	25.00	.00	60.00	.00	.00	1	60.00	.740E-01
27	26.00	.00	62.00	.00	.00	1	60.00	.740E-01
28	27.00	.00	60.00	.00	.00	1	60.00	.740E-01
29	28.00	.00	60.00	.00	.00	1	60.00	.740E-01
30	29.00	.00	62.00	.00	.00	1	60.00	.740E-01
31	30.00	.00	60.00	.00	.00	1	60.00	.740E-01
32	31.00	.00	60.00	.00	.00	1	60.00	.740E-01
33	32.00	.00	62.00	.00	.00	1	60.00	.740E-01

TABLE C-4 (Cont).

RADIANCE(WATTS/CM2-STER-XXX)

FREQ (CM-1)	WAVLEN (MICRN)	ATMOS RADIANCE (CM-1)	(MICRN)	PATH (CM-1)	SCATTERED RADIANCE TOTAL (MICRN)	S SCAT (CM-1)	GROUND REFLECTED RADIANCE TOTAL (CM-1)	(MICRN)	RADIANCE DIRECT (CM-1)	TOTAL RADIANCE (CM-1)	(MICRN)	INTEGRAL (CM-1)	TOTAL TRANS
18100.	.552	5.26E-40	1.72E-35	3.05E-07	1.00E-02	8.09E-08	.00E+00	.00E+00	.00E+00	3.05E-07	1.00E-02	1.53E-06	.2020
18110.	.552	5.01E-40	1.64E-35	3.05E-07	1.00E-02	8.00E-08	.00E+00	.00E+00	.00E+00	3.05E-07	1.00E-02	4.50E-06	.2018
18120.	.552	4.70E-40	1.57E-35	3.05E-07	1.00E-02	8.07E-08	.00E+00	.00E+00	.00E+00	3.05E-07	1.00E-02	7.53E-06	.2016
18130.	.552	4.56E-40	1.50E-35	3.05E-07	1.00E-02	8.07E-08	.00E+00	.00E+00	.00E+00	3.05E-07	1.00E-02	1.07E-05	.2013
18140.	.551	4.34E-40	1.43E-35	3.05E-07	1.00E-02	8.06E-08	.00E+00	.00E+00	.00E+00	3.05E-07	1.00E-02	1.37E-05	.2011
18150.	.551	4.14E-40	1.36E-35	3.05E-07	1.00E-02	8.05E-08	.00E+00	.00E+00	.00E+00	3.05E-07	1.00E-02	1.68E-05	.2009
18160.	.551	3.95E-40	1.30E-35	3.05E-07	1.00E-02	8.04E-08	.00E+00	.00E+00	.00E+00	3.05E-07	1.00E-02	1.98E-05	.2007
18170.	.550	3.77E-40	1.24E-35	3.05E-07	1.00E-02	8.03E-08	.00E+00	.00E+00	.00E+00	3.05E-07	1.00E-02	2.29E-05	.2005
18180.	.550	3.59E-40	1.19E-35	3.05E-07	1.00E-02	8.03E-08	.00E+00	.00E+00	.00E+00	3.05E-07	1.00E-02	2.59E-05	.2003
18190.	.550	3.42E-40	1.13E-35	3.05E-07	1.00E-02	8.03E-08	.00E+00	.00E+00	.00E+00	3.05E-07	1.00E-02	2.90E-05	.2000
18200.	.549	3.27E-40	1.08E-35	3.05E-07	1.00E-02	8.02E-08	.00E+00	.00E+00	.00E+00	3.05E-07	1.00E-02	3.20E-05	.2797
18210.	.549	3.12E-40	1.03E-35	3.05E-07	1.00E-02	8.02E-08	.00E+00	.00E+00	.00E+00	3.05E-07	1.00E-02	3.51E-05	.2793
18220.	.549	2.97E-40	9.85E-36	3.05E-07	1.00E-02	8.01E-08	.00E+00	.00E+00	.00E+00	3.05E-07	1.00E-02	3.81E-05	.2788
18230.	.549	2.83E-40	9.43E-36	3.05E-07	1.00E-02	8.01E-08	.00E+00	.00E+00	.00E+00	3.05E-07	1.00E-02	4.12E-05	.2787
18240.	.549	2.70E-40	9.09E-36	3.05E-07	1.00E-02	8.00E-08	.00E+00	.00E+00	.00E+00	3.05E-07	1.00E-02	4.42E-05	.2783
18250.	.548	2.58E-40	8.58E-36	3.05E-07	1.00E-02	7.99E-08	.00E+00	.00E+00	.00E+00	3.05E-07	1.00E-02	4.73E-05	.2780
18260.	.548	2.46E-40	8.20E-36	3.05E-07	1.00E-02	7.99E-08	.00E+00	.00E+00	.00E+00	3.05E-07	1.00E-02	4.88E-05	.2777

INTEGRATED ABSORPTION FROM 18100 TO 18260 CM-1 = 115.19 CM-1
AVERAGE TRANSMITTANCE = .2801

INTEGRATED RADIANCE = 4.881E-05 WATTS CM-2 STER-1
MINIMUM RADIANCE = 3.045E-07 WATTS CM-2 STER-1 (CM-1)-1 AT 18100.0 CM-1

MAXIMUM RADIANCE = 3.058E-07 WATTS CM-2 STER-1 (CM-1)-1 AT 18260.0 CM-1
BOUNDARY TEMPERATURE = .80 K
BOUNDARY EMISSIVITY = .600

CARD 5 *****

16.43.38.UCLP. AA. LP2 , 1.024KLS.

LOWTRAN OUTPUT FOR CASE 4

C-34

TABLE C-5 (Cont.).

ATMOSPHERIC PROFILES										
I	Z (KM)	P (MB)	T (K)	H2O (SCALED)	CO2+ (LOWTRAN UNITS)	N2 (MOL/CM2 KM)	CH4 (MOL/CM2 KM)	MOL SCAT (-)	N-1 (-)	O3 (UV) (ATM CM/KM)
1	1.00	1013.000	288.2	5.750E-01	9.285E-01	2.493E-03	7.378E-01	1.569E+28	9.475E-01	2.774E-04
2	1.00	898.800	281.7	3.719E-01	7.771E-01	2.387E-03	6.870E-01	7.951E+19	8.501E-01	2.519E-04
3	2.00	795.000	275.2	2.323E-01	6.474E-01	2.284E-03	4.870E-01	3.791E+19	7.788E-01	2.281E-04
4	3.00	701.200	268.7	1.302E-01	5.371E-01	2.020E-03	3.927E-01	1.460E+19	7.035E-01	2.061E-04
5	4.00	616.600	262.2	7.165E-02	4.435E-01	1.774E-03	3.150E-01	5.450E+18	5.348E-01	1.857E-04
6	5.00	540.500	255.7	3.745E-02	3.646E-01	1.692E-03	2.513E-01	1.046E+18	5.698E-01	1.670E-04
7	6.00	472.200	249.2	1.992E-02	2.902E-01	1.576E-03	1.994E-01	6.500E+17	5.100E-01	1.497E-04
8	7.00	411.100	242.7	9.834E-03	2.427E-01	1.532E-03	1.522E-01	1.988E+17	4.566E-01	1.338E-04
9	8.00	356.500	236.2	5.004E-03	1.963E-01	1.645E-03	1.232E-01	6.490E+16	4.066E-01	1.192E-04
10	9.00	308.000	229.7	1.703E-03	1.579E-01	2.130E-03	9.586E-02	9.537E+15	3.615E-01	1.059E-04
11	10.00	265.000	223.3	5.894E-04	1.262E-01	2.557E-03	7.483E-02	1.460E+15	3.199E-01	9.376E-05
12	11.00	227.000	216.8	2.367E-04	1.002E-01	3.493E-03	5.678E-02	3.031E+14	2.823E-01	8.272E-05
13	12.00	194.000	216.7	9.275E-05	7.619E-02	4.037E-03	4.150E-02	6.170E+13	2.413E-01	7.073E-05
14	13.00	165.800	216.7	3.917E-05	5.788E-02	4.020E-03	3.031E-02	1.460E+13	2.063E-01	6.045E-05
15	14.00	141.700	216.7	1.507E-05	4.397E-02	4.220E-03	2.214E-02	3.180E+12	1.763E-01	5.166E-05
16	15.00	121.100	216.7	1.181E-05	3.340E-02	4.380E-03	1.617E-02	2.337E+12	1.507E-01	4.415E-05
17	16.00	103.500	216.7	0.682E-05	2.537E-02	4.710E-03	1.101E-02	1.677E+12	1.288E-01	3.774E-05
18	17.00	88.500	216.7	6.432E-06	1.929E-02	5.161E-03	8.637E-03	1.219E+12	1.101E-01	3.227E-05
19	18.00	75.650	216.7	4.725E-06	1.466E-02	5.540E-03	6.311E-03	8.726E+11	9.411E-02	2.758E-05
20	19.00	64.670	216.7	4.104E-06	1.114E-02	5.971E-03	5.612E-03	8.726E+11	8.045E-02	2.265E-05
21	20.00	55.290	216.7	3.564E-06	8.470E-03	5.803E-03	3.371E-03	8.726E+11	6.878E-02	2.018E-05
22	21.00	47.290	217.6	3.371E-06	6.486E-03	5.447E-03	2.451E-03	1.038E+12	5.859E-02	1.717E-05
23	22.00	40.470	218.5	3.160E-06	4.847E-03	5.240E-03	1.703E-03	1.219E+12	4.991E-02	1.463E-05
24	23.00	34.670	219.6	3.015E-06	3.675E-03	4.802E-03	1.299E-03	1.464E+12	4.256E-02	1.247E-05
25	24.00	29.720	220.6	2.803E-06	2.789E-03	4.374E-03	9.403E-04	1.677E+12	3.633E-02	1.064E-05
26	25.00	25.490	221.6	2.636E-06	2.119E-03	3.792E-03	6.929E-04	1.963E+12	3.101E-02	9.088E-06
27	30.00	11.970	226.5	7.612E-07	5.476E-04	1.542E-03	1.479E-04	6.508E+11	1.425E-02	4.175E-06
28	35.00	5.746	236.5	1.621E-07	1.429E-04	5.674E-04	3.193E-05	1.154E+11	6.550E-03	1.920E-06
29	40.00	2.871	248.4	3.549E-08	2.922E-05	2.227E-05	7.310E-06	2.023E+10	3.091E-03	9.059E-07
30	45.00	1.491	264.2	9.176E-09	1.157E-05	5.801E-05	1.821E-06	4.615E+09	1.521E-03	4.659E-07
31	50.00	.798	278.7	1.939E-09	3.747E-06	1.072E-05	5.077E-07	6.498E+08	7.945E-04	2.328E-07
32	70.00	.055	219.7	2.466E-10	4.660E-08	8.259E-08	3.291E-09	1.071E+09	6.773E-05	1.985E-08
33	100.00	.000	216.0	1.500E-16	5.420E-12	5.190E-12	1.046E-13	4.507E+00	3.861E-07	1.132E-10

TABLE C-5 (Cont.).

ATMOSPHERIC PROFILES											
I	Z (KM)	P (MB)	T (K)	CONTNERN MOI/CH2 KM	HNO3 ATM CM/KM	AEROSOL 1 {-}	AEROSOL 2 {-}	AEROSOL 3 {-}	AEROSOL 4 AER1*RH {-}	CIRRHUS {-}	RH {PERCENT}
1	0.00	1013.000	280.2	2.010E+22	.000E+00	7.700E-01	.000E+00	.000E+00	3.533E+01	.000E+00	4.589E+01
2	1.00	898.000	281.7	1.301E+22	.000E+00	7.700E-01	.000E+00	.000E+00	3.777E+01	.000E+00	4.906E+01
3	2.00	795.000	275.2	8.143E+21	.000E+00	6.210E-02	.000E+00	.000E+00	3.230E+00	.000E+00	5.201E+01
4	3.00	701.200	268.7	4.573E+21	.000E+00	3.460E-02	.000E+00	.000E+00	.000E+00	.000E+00	.000E+00
5	4.00	616.600	262.2	2.521E+21	.000E+00	.000E+00	.000E+00	.000E+00	.000E+00	.000E+00	.000E+00
6	5.00	540.500	255.7	1.319E+21	.000E+00	.000E+00	.000E+00	.000E+00	.000E+00	.000E+00	.000E+00
7	6.00	472.200	249.2	7.025E+20	.000E+00	.000E+00	.000E+00	.000E+00	.000E+00	.000E+00	.000E+00
8	7.00	411.100	242.7	3.472E+20	.000E+00	.000E+00	.000E+00	.000E+00	.000E+00	.000E+00	.000E+00
9	8.00	356.500	236.2	1.768E+20	4.069E-35	.000E+00	3.370E-03	.000E+00	.000E+00	.000E+00	.000E+00
10	9.00	308.000	229.7	6.023E+19	3.615E-06	.000E+00	1.070E-02	.000E+00	.000E+00	.000E+00	.000E+00
11	10.00	265.000	223.3	2.086E+19	1.056E-05	.000E+00	.000E+00	1.142E-03	.000E+00	.000E+00	.000E+00
12	11.00	227.000	216.8	8.384E+18	2.258E-05	.000E+00	1.240E-04	7.990E-04	.000E+00	.000E+00	.000E+00
13	12.00	194.000	216.7	3.235E+18	2.096E-05	.000E+00	.000E+00	6.410E-04	.000E+00	.000E+00	.000E+00
14	13.00	165.000	216.7	1.345E+18	2.000E-05	.000E+00	.000E+00	5.170E-04	.000E+00	.000E+00	.000E+00
15	14.00	141.700	216.7	5.364E+17	2.020E-05	.000E+00	.000E+00	4.420E-04	.000E+00	.000E+00	.000E+00
16	15.00	121.100	216.7	3.929E+17	2.712E-05	.000E+00	.000E+00	3.950E-04	.000E+00	.000E+00	.000E+00
17	16.00	103.500	216.7	2.845E+17	2.446E-05	.000E+00	.000E+00	3.820E-04	.000E+00	.000E+00	.000E+00
18	17.00	88.500	216.7	2.074E+17	2.202E-05	.000E+00	.000E+00	4.250E-04	.000E+00	.000E+00	.000E+00
19	18.00	75.500	216.7	1.508E+17	1.976E-05	.000E+00	.000E+00	5.200E-04	.000E+00	.000E+00	.000E+00
20	19.00	64.670	216.7	1.202E+17	1.050E-05	.000E+00	.000E+00	5.810E-04	.000E+00	.000E+00	.000E+00
21	20.00	55.730	216.7	1.096E+17	2.063E-05	.000E+00	.000E+00	5.890E-04	.000E+00	.000E+00	.000E+00
22	21.00	47.630	217.6	1.019E+17	2.168E-05	.000E+00	.000E+00	5.020E-04	.000E+00	.000E+00	.000E+00
23	22.00	40.470	218.6	9.401E+16	2.096E-05	.000E+00	.000E+00	4.200E-04	.000E+00	.000E+00	.000E+00
24	23.00	34.670	219.6	8.700E+16	2.213E-05	.000E+00	.000E+00	3.800E-04	.000E+00	.000E+00	.000E+00
25	24.00	29.720	220.6	8.025E+16	2.179E-05	.000E+00	.000E+00	1.980E-04	.000E+00	.000E+00	.000E+00
26	25.00	25.490	221.6	7.414E+16	1.170E-05	.000E+00	.000E+00	1.310E-04	.000E+00	.000E+00	.000E+00
27	26.00	21.970	226.5	1.961E+16	3.704E-06	.000E+00	.000E+00	3.320E-05	.000E+00	.000E+00	.000E+00
28	27.00	18.740	236.5	3.796E+15	1.441E-07	.000E+00	.000E+00	1.640E-05	.000E+00	.000E+00	.000E+00
29	28.00	15.950	250.4	7.502E+14	3.091E-37	.000E+00	.000E+00	.000E+00	7.950E-06	.000E+00	.000E+00
30	29.00	13.490	264.2	1.764E+14	.000E+00	.000E+00	.000E+00	.000E+00	4.010E-06	.000E+00	.000E+00
31	30.00	11.490	270.7	3.454E+13	.000E+00	.000E+00	.000E+00	.000E+00	2.100E-06	.000E+00	.000E+00
32	31.00	9.550	279.7	3.608E+10	.000E+00	.000E+00	.000E+00	.000E+00	1.600E-07	.000E+00	.000E+00
33	100.00	.000	218.0	1.399E+06	.000E+00	.000E+00	.000E+00	.000E+00	9.310E-10	.000E+00	.000E+00

CASE 2A: GIVEN H1, H2, ANGLE

EITHER A SHORT PATH (LEN=0) OR A LONG PATH THROUGH A TANGENT WEIGHT (LEN=1) IS POSSIBLE: LEN = 0

SLANT PATH PARAMETERS IN STANDARD FORM

TABLE C-5 (Cont).

H1	20.000 KM
H2	.000 KM
ANGLE	180.000 DEG
PHI	.000 DEG
HMIN	.000 KM
LEN	0

• • • •

TABLE C-5 (Cont.).

CALCULATION OF THE REFRACTED PATH THROUGH THE ATMOSPHERE

I	ALTITUDE FROM (KM)	TO (KM)	THETA (DEG)	DISTANCE (KM)	RANGE (KM)	DBETA (DEG)	BETA (DEG)	PHI (DEG)	DBEND (DEG)	BENDING (DEG)	PBAR (MB)	TBAR (K)	KHOBAR (CM CM-3)
H2 TO H1													
1	1.000	1.000	.000	1.000	1.000	.000	.000	182.000	.000	.000	555.603	204.95	1.17E-03
2	1.000	2.000	.000	1.000	2.000	.000	.000	180.000	.000	.000	846.698	278.49	1.06E-03
3	2.000	3.000	.000	1.000	3.000	.000	.000	180.000	.000	.000	747.913	271.99	9.57E-04
4	3.000	4.000	.000	1.000	4.000	.000	.000	180.000	.000	.000	658.727	265.49	8.63E-04
5	4.000	5.000	.000	1.000	5.000	.000	.000	180.000	.000	.000	578.331	258.99	7.77E-04
6	5.000	6.000	.000	1.000	6.000	.000	.000	180.000	.000	.000	506.284	252.50	6.98E-04
7	6.000	7.000	.000	1.000	7.000	.000	.000	180.000	.000	.000	441.516	246.00	6.24E-04
8	7.000	8.000	.000	1.000	8.000	.000	.000	180.000	.000	.000	383.677	239.50	5.57E-04
9	8.000	9.000	.000	1.000	9.000	.000	.000	180.000	.000	.000	332.137	233.00	4.96E-04
10	9.000	10.000	.000	1.000	10.000	.000	.000	180.000	.000	.000	286.399	226.55	4.40E-04
11	10.000	11.000	.000	1.000	11.000	.000	.000	180.000	.000	.000	245.907	220.10	3.89E-04
12	11.000	12.000	.000	1.000	12.000	.000	.000	180.000	.000	.000	210.499	216.75	3.38E-04
13	12.000	13.000	.000	1.000	13.000	.000	.000	180.000	.000	.000	179.908	216.70	2.89E-04
14	13.000	14.000	.000	1.000	14.000	.000	.000	180.000	.000	.000	153.750	216.70	2.47E-04
15	14.000	15.000	.000	1.000	15.000	.000	.000	180.000	.000	.000	131.400	216.70	2.11E-04
16	15.000	16.000	.000	1.000	16.000	.000	.000	180.000	.000	.000	112.300	216.70	1.80E-04
17	16.000	17.000	.000	1.000	17.000	.000	.000	180.000	.000	.000	96.000	216.70	1.54E-04
18	17.000	18.000	.000	1.000	18.000	.000	.000	180.000	.000	.000	82.075	216.70	1.32E-04
19	18.000	19.000	.000	1.000	19.000	.000	.000	180.000	.000	.000	70.160	216.70	1.13E-04
20	19.000	20.000	.000	1.000	20.000	.000	.000	180.000	.000	.000	59.908	216.70	9.62E-05

CUMULATIVE ABSORBER AMOUNTS FOR THE PATH FROM H1 TO Z

J	Z (KM)	TBAR (K)	H2O (SCALED LOWTRAN UNITS)	CO2+ (SCALED LOWTRAN UNITS)	O3 (ATM CM)	HNO3 (ATM CM)	O3 UV (ATM CM)	CNTMSLF1 (MOL CM-2)	CNTMSLF2 (MOL CM-2)	CNTMFRM (MOL CM-2)
1	19.000	216.70	3.020E-06	9.745E-03	5.747E-03	1.957E-05	1.703E-02	8.725E+11	8.725E+11	1.187E+17
2	18.000	216.70	0.235E-06	2.257E-02	1.136E-02	3.870E-05	3.267E-02	1.745E+12	1.745E+12	2.575E+17
3	17.000	216.70	1.377E-05	3.944E-02	1.671E-02	5.957E-05	4.667E-02	2.781E+12	2.781E+12	4.347E+17
4	16.000	216.70	2.127E-05	6.163E-02	2.165E-02	8.279E-05	5.800E-02	4.217E+12	4.217E+12	6.786E+17
5	15.000	216.70	3.144E-05	9.003E-02	2.620E-02	1.085E-04	6.930E-02	6.205E+12	6.205E+12	1.014E+18
6	14.000	216.70	4.510E-05	1.293E-01	3.051E-02	1.363E-04	7.863E-02	8.942E+12	8.942E+12	1.475E+18
7	13.000	216.70	7.097E-05	1.799E-01	3.463E-02	1.647E-04	8.703E-02	1.644E+13	1.644E+13	2.355E+18
8	12.000	216.70	1.331E-04	2.465E-01	3.867E-02	1.937E-04	9.473E-02	4.912E+13	4.912E+13	4.508E+18
9	11.000	216.75	2.860E-04	3.342E-01	4.243E-02	2.194E-04	1.015E-01	2.000E+14	2.000E+14	9.915E+18
10	10.000	220.10	6.734E-04	4.469E-01	4.544E-02	2.360E-04	1.066E-01	9.367E+14	9.367E+14	2.360E+19
11	9.000	226.55	1.723E-03	5.803E-01	4.780E-02	2.431E-04	1.104E-01	5.241E+15	5.241E+15	6.073E+19
12	8.000	233.00	4.785E-03	7.647E-01	4.960E-02	2.449E-04	1.133E-01	3.411E+16	3.411E+16	1.690E+20
13	7.000	239.50	1.193E-02	9.834E-01	5.130E-02	2.449E-04	1.156E-01	1.537E+17	1.537E+17	4.215E+20
14	6.000	246.00	2.622E-02	1.253E+00	5.293E-02	2.449E-04	1.170E-01	5.340E+17	5.340E+17	9.256E+20

TABLE C-5 (Cont).

J	Z (KM)	N2 CONT	MOL SCAT	AER 1	AER 2	AER 3	AER 4	CIRRUS		
15	5.000	252.50	5.399E-02	1.583E+00	5.456E-02	2.449E-04	1.199E-01	1.661E-18	1.601E+18	1.904E+21
16	4.000	258.99	1.067E-01	1.986E+00	5.630E-02	2.449E-04	1.221E-01	5.012E-18	5.012E+18	3.760E+21
17	3.000	265.49	2.047E-01	2.475E+00	5.819E-02	2.449E-04	1.243E-01	1.430E+19	1.280E+19	7.205E+21
18	2.000	271.99	3.811E-01	3.065E+00	6.034E-02	2.449E-04	1.267E-01	3.073E+19	2.910E+19	1.339E+22
19	1.000	278.49	6.778E-01	3.776E+00	6.260E-02	2.449E-04	1.293E-01	9.489E+19	5.649E+19	2.378E+22
20	.000	284.99	1.144E+00	4.626E+00	6.512E-02	2.449E-04	1.318E-01	2.007E+20	9.131E+19	4.007E+22
1	19.000	3.959E-03	7.446E-02	.000E+00	.000E+00	5.855E-04	.000E+00	.000E+00		
2	18.000	9.376E-03	1.616E-01	.000E+00	.000E+00	1.136E-03	.000E+00	.000E+00		
3	17.000	1.679E-02	2.635E-01	.000E+00	.000E+00	1.600E-03	.000E+00	.000E+00		
4	16.000	2.693E-02	3.826E-01	.000E+00	.000E+00	2.012E-03	.000E+00	.000E+00		
5	15.000	4.001E-02	5.221E-01	.000E+00	.000E+00	2.810E-03	.000E+00	.000E+00		
6	14.000	5.981E-02	6.852E-01	.000E+00	.000E+00	2.810E-03	.000E+00	.000E+00		
7	13.000	8.502E-02	8.761E-01	.000E+00	.000E+00	3.297E-03	.000E+00	.000E+00		
8	12.000	1.214E-01	1.099E+00	.000E+00	.000E+00	3.873E-03	.000E+00	.000E+00		
9	11.000	1.762E-01	1.361E+00	.000E+00	.000E+00	4.590E-03	.000E+00	.000E+00		
10	10.000	2.352E-01	1.661E+00	.000E+00	.000E+00	5.550E-03	.000E+00	.000E+00		
11	9.000	3.197E-01	2.002E+00	.000E+00	9.100E-04	6.120E-03	.000E+00	.000E+00		
12	8.000	4.266E-01	2.385E+00	.000E+00	3.426E-03	6.120E-03	.000E+00	.000E+00		
13	7.000	5.681E-01	2.817E+00	.000E+00	8.000E-03	6.120E-03	.000E+00	.000E+00		
14	6.000	7.456E-01	3.300E+00	.000E+00	1.502E-02	6.120E-03	.000E+00	.000E+00		
15	5.000	9.780E-01	3.840E+00	.000E+00	2.351E-02	6.120E-03	.000E+00	.000E+00		
16	4.000	1.252E+00	4.441E+00	.000E+00	3.689E-02	6.120E-03	.000E+00	.000E+00		
17	3.000	1.604E+00	5.109E+00	.000E+00	6.261E-02	6.120E-03	.000E+00	.000E+00		
18	2.000	2.042E+00	5.850E+00	3.105E-02	7.991E-02	6.120E-03	.000E+00	.000E+00		
19	1.000	2.585E+00	6.668E+00	3.122E-01	7.991E-02	6.120E-03	.000E+00	.000E+00		
20	.000	3.252E+00	7.571E+00	1.082E+00	7.991E-02	6.120E-03	.000E+00	.000E+00		

SUMMARY OF THE GEOMETRY CALCULATION

H1	-	20.000 KM
H2	-	.000 KM
ANGLE	-	180.000 DEG
RANGE	-	20.000 KM
BETA	-	.090 DEG
PHI	-	.000 DEG
HMIN	-	.000 KM
BENDING	-	.000 DEG
LEN	-	?

EQUIVALENT SEA LEVEL TOTAL ABSORBER AMOUNTS

H2O CO2+ O3
(SCALED LOWTRAN UNITS)

O ₃ UV	CNTMSLF1	CNTMSLF2	CNTMFRN
(ATM CM)	(MOL CM-2)	(MOL CM-2)	(MOL CM-2)
0.00	0.00	0.00	0.00
0.01	0.01	0.01	0.01
0.02	0.02	0.02	0.02
0.03	0.03	0.03	0.03
0.04	0.04	0.04	0.04
0.05	0.05	0.05	0.05
0.06	0.06	0.06	0.06
0.07	0.07	0.07	0.07
0.08	0.08	0.08	0.08
0.09	0.09	0.09	0.09
0.10	0.10	0.10	0.10
0.11	0.11	0.11	0.11
0.12	0.12	0.12	0.12
0.13	0.13	0.13	0.13
0.14	0.14	0.14	0.14
0.15	0.15	0.15	0.15
0.16	0.16	0.16	0.16
0.17	0.17	0.17	0.17
0.18	0.18	0.18	0.18
0.19	0.19	0.19	0.19
0.20	0.20	0.20	0.20
0.21	0.21	0.21	0.21
0.22	0.22	0.22	0.22
0.23	0.23	0.23	0.23
0.24	0.24	0.24	0.24
0.25	0.25	0.25	0.25
0.26	0.26	0.26	0.26
0.27	0.27	0.27	0.27
0.28	0.28	0.28	0.28
0.29	0.29	0.29	0.29
0.30	0.30	0.30	0.30
0.31	0.31	0.31	0.31
0.32	0.32	0.32	0.32
0.33	0.33	0.33	0.33
0.34	0.34	0.34	0.34
0.35	0.35	0.35	0.35
0.36	0.36	0.36	0.36
0.37	0.37	0.37	0.37
0.38	0.38	0.38	0.38
0.39	0.39	0.39	0.39
0.40	0.40	0.40	0.40
0.41	0.41	0.41	0.41
0.42	0.42	0.42	0.42
0.43	0.43	0.43	0.43
0.44	0.44	0.44	0.44
0.45	0.45	0.45	0.45
0.46	0.46	0.46	0.46
0.47	0.47	0.47	0.47
0.48	0.48	0.48	0.48
0.49	0.49	0.49	0.49
0.50	0.50	0.50	0.50
0.51	0.51	0.51	0.51
0.52	0.52	0.52	0.52
0.53	0.53	0.53	0.53
0.54	0.54	0.54	0.54
0.55	0.55	0.55	0.55
0.56	0.56	0.56	0.56
0.57	0.57	0.57	0.57
0.58	0.58	0.58	0.58
0.59	0.59	0.59	0.59
0.60	0.60	0.60	0.60
0.61	0.61	0.61	0.61
0.62	0.62	0.62	0.62
0.63	0.63	0.63	0.63
0.64	0.64	0.64	0.64
0.65	0.65	0.65	0.65
0.66	0.66	0.66	0.66
0.67	0.67	0.67	0.67
0.68	0.68	0.68	0.68
0.69	0.69	0.69	0.69
0.70	0.70	0.70	0.70
0.71	0.71	0.71	0.71
0.72	0.72	0.72	0.72
0.73	0.73	0.73	0.73
0.74	0.74	0.74	0.74
0.75	0.75	0.75	0.75
0.76	0.76	0.76	0.76
0.77	0.77	0.77	0.77
0.78	0.78	0.78	0.78
0.79	0.79	0.79	0.79
0.80	0.80	0.80	0.80
0.81	0.81	0.81	0.81
0.82	0.82	0.82	0.82
0.83	0.83	0.83	0.83
0.84	0.84	0.84	

TABLE C-5 (Cont).

1.144E+00 4.626E+00 6.512E-02 2.449E-04 1.318E-01 2.087E+00 9.131E+19 4.007E+22

N2 CONT MOL SCAT AER 1 AER 2 AER 3 AER 4 CIRRUS MEAN RH (PRCNT)

3.252E+00 7.571E+00 1.082E+00 7.991E-02 6.128E-03 .000E+00 .000E+00

SINGLE SCATTERING POINT TO SOURCE PATHS
SCATR SCATR SUBTENDED SOLAR PATH RELATIVE SCATR MOLECULAR
POINT ALT ANGLE ZENITH ZENITH AZIMUTH ANGLE PHASE F

1	20.00	.00	60.00	180.00	1	120.00	.748E-01
2	19.00	.00	60.00	180.00	1	120.00	.748E-01
3	18.00	.00	60.00	180.00	1	120.00	.748E-01
4	17.00	.00	60.00	180.00	1	120.00	.748E-01
5	16.00	.00	60.00	180.00	1	120.00	.748E-01
6	15.00	.00	60.00	180.00	1	120.00	.748E-01
7	14.00	.00	60.00	180.00	1	120.00	.748E-01
8	13.00	.00	60.00	180.00	1	120.00	.748E-01
9	12.00	.00	60.00	180.00	1	120.00	.748E-01
10	11.00	.00	60.00	180.00	1	120.00	.748E-01
11	10.00	.00	60.00	180.00	1	120.00	.748E-01
12	9.00	.00	60.00	180.00	1	120.00	.748E-01
13	8.00	.00	60.00	180.00	1	120.00	.748E-01
14	7.00	.00	60.00	180.00	1	120.00	.748E-01
15	6.00	.00	60.00	180.00	1	120.00	.748E-01
16	5.00	.00	60.00	180.00	1	120.00	.748E-01
17	4.00	.00	60.00	180.00	1	120.00	.748E-01
18	3.00	.00	60.00	180.00	1	120.00	.748E-01
19	2.00	.00	60.00	180.00	1	120.00	.748E-01
20	1.00	.00	60.00	180.00	1	120.00	.748E-01
21	.00	.00	60.00	180.00	1	120.00	.748E-01

CASE 20: GIVEN H1, H2, BETA.

ITERATE AROUND ANGLE UNTIL BETA CONVERGES

ITER	ANGLE (DEG)	BETA (DEG)	DBETA (DEG)	RANGE (KM)	HMIN (KM)	PHI (DEG)	BENDING (DEG)
1	.0000	.0000	.0000	180.000	.000	180.0000	.0000
2	.0000	.0000	.0000	180.000	.000	180.0000	.0000

SLANT PATH PARAMETERS IN STANDARD FORM

H1	=	100.000 KM
H2	=	.000 KM
ANGLE	=	180.000 DEG
PHI	=	.000 DEG
HMIN	=	.000 KM
LEN	=	#

TABLE C-5 (Cont).

CALCULATION OF THE REFRACTED PATH THROUGH THE ATMOSPHERE

I	ALTITUDE FROM (KM)	TO (KM)	THETA (DEG)	DANCE (KM)	RANGE (KM)	DBETA (DEG)	BETA (DEG)	PHI (DEG)	DBEND (DEG)	BENDING (DEG)	PBAR (MB)	TBAR (K)	RHOBAR (GM CM-3)
H2 TO H1													
1	1.000	1.000	.000	1.000	1.000	.000	.000	100.000	.000	.000	955.603	294.99	1.17E-03
2	1.000	2.000	.000	1.000	2.000	.000	.000	100.000	.000	.000	846.698	278.49	1.06E-03
3	2.000	3.000	.000	1.000	3.000	.000	.000	100.000	.000	.000	747.913	271.99	9.57E-04
4	3.000	4.000	.000	1.000	4.000	.000	.000	100.000	.000	.000	658.727	265.49	8.63E-04
5	4.000	5.000	.000	1.000	5.000	.000	.000	100.000	.000	.000	578.391	258.99	7.77E-04
6	5.000	6.000	.000	1.000	6.000	.000	.000	100.000	.000	.000	506.204	252.50	6.98E-04
7	6.000	7.000	.000	1.000	7.000	.000	.000	100.000	.000	.000	441.516	246.00	6.24E-04
8	7.000	8.000	.000	1.000	8.000	.000	.000	100.000	.000	.000	383.677	239.50	5.57E-04
9	8.000	9.000	.000	1.000	9.000	.000	.000	100.000	.000	.000	332.137	233.00	4.96E-04
10	9.000	10.000	.000	1.000	10.000	.000	.000	100.000	.000	.000	286.399	226.55	4.40E-04
11	10.000	11.000	.000	1.000	11.000	.000	.000	100.000	.000	.000	245.907	220.10	3.89E-04
12	11.000	12.000	.000	1.000	12.000	.000	.000	100.000	.000	.000	210.499	216.75	3.38E-04
13	12.000	13.000	.000	1.000	13.000	.000	.000	100.000	.000	.000	179.900	216.70	2.89E-04
14	13.000	14.000	.000	1.000	14.000	.000	.000	100.000	.000	.000	153.750	216.70	2.47E-04
15	14.000	15.000	.000	1.000	15.000	.000	.000	100.000	.000	.000	131.400	216.70	2.11E-04
16	15.000	16.000	.000	1.000	16.000	.000	.000	100.000	.000	.000	112.300	216.70	1.80E-04
17	16.000	17.000	.000	1.000	17.000	.000	.000	100.000	.000	.000	96.000	216.70	1.54E-04
18	17.000	18.000	.000	1.000	18.000	.000	.000	100.000	.000	.000	82.075	216.70	1.32E-04
19	18.000	19.000	.000	1.000	19.000	.000	.000	100.000	.000	.000	70.160	216.70	1.13E-04
20	19.000	20.000	.000	1.000	20.000	.000	.000	100.000	.000	.000	59.900	216.70	9.62E-05
21	20.000	21.000	.000	1.000	21.000	.000	.000	100.000	.000	.000	51.293	217.14	8.21E-05
22	21.000	22.000	.000	1.000	22.000	.000	.000	100.000	.000	.000	43.803	218.05	7.00E-05
23	22.000	23.000	.000	1.000	23.000	.000	.000	100.000	.000	.000	37.572	219.09	5.96E-05
24	23.000	24.000	.000	1.000	24.000	.000	.000	100.000	.000	.000	32.197	220.09	5.09E-05
25	24.000	25.000	.000	1.000	25.000	.000	.000	100.000	.000	.000	27.607	221.09	4.34E-05
26	25.000	30.000	.000	5.000	30.000	.000	.000	100.000	.000	.000	18.754	223.73	2.79E-05
27	30.000	35.000	.000	5.000	35.000	.000	.000	100.000	.000	.000	8.800	230.02	1.20E-05
28	35.000	40.000	.000	5.000	40.000	.000	.000	100.000	.000	.000	4.322	242.52	5.95E-06
29	40.000	45.000	.000	5.000	45.000	.000	.000	100.000	.000	.000	2.107	256.43	2.06E-06
30	45.000	50.000	.000	5.000	50.000	.000	.000	100.000	.000	.000	1.146	257.09	1.45E-06
31	50.000	70.000	.000	20.000	70.000	.000	.000	100.000	.000	.000	.416	253.92	3.01E-07
32	70.000	100.000	.000	30.000	100.000	.000	.000	100.000	.000	.000	.028	217.05	1.60E-08

CUMULATIVE ABSORBER AMOUNTS FOR THE PATH FROM H1 TO Z

J	Z (KM)	TBAR (K)	H2O (SCALED LOWTRAN UNITS)	CO2+ (SCALED LOWTRAN UNITS)	O3 (ATM CM)	NO2 (ATM CM)	O3 UV (ATM CM)	CNTMSLE1 (MOL CM-2)	CNTMSLE2 (MOL CM-2)	CNTMFRN (MOL CM-2)
1	70.000	217.05	7.454E-12	1.543E-07	2.560E-07	.000E+00	1.583E-05	3.036E+05	3.036E+05	1.085E+11
2	50.000	253.92	5.794E-09	1.702E-05	4.399E-05	.000E+00	9.672E-04	1.481E+09	1.481E+09	1.009E+14
3	45.000	267.09	2.907E-08	5.172E-05	1.853E-04	.000E+00	3.064E-03	1.159E+10	9.600E+09	5.350E+14

TABLE C-5 (Cont).

J	Z (km)	N2 CONT	MOL SCAT	AER 1	AER 2	AER 3	AER 4	CIRRUS																																																																																																																																																																																																																																																																																																																																																																																																																																																																																																																																																																																																																																																																																																																																																																
1	70.000	9.534E-09	3.910E-04	.000E+00	.000E+00	.000E+00	9.272E-07	.000E+00	.000E+00	.000E+00	.000E+00	.000E+00	.000E+00	.000E+00	.000E+00	.000E+00	.000E+00	.000E+00	.000E+00	.000E+00	.000E+00	.000E+00	.000E+00	.000E+00	.000E+00	.000E+00	.000E+00	.000E+00	.000E+00	.000E+00	.000E+00	.000E+00	.000E+00	.000E+00	.000E+00	.000E+00	.000E+00	.000E+00	.000E+00	.000E+00	.000E+00	.000E+00	.000E+00	.000E+00	.000E+00	.000E+00	.000E+00	.000E+00	.000E+00	.000E+00	.000E+00	.000E+00	.000E+00	.000E+00	.000E+00	.000E+00	.000E+00	.000E+00	.000E+00	.000E+00	.000E+00	.000E+00	.000E+00	.000E+00	.000E+00	.000E+00	.000E+00	.000E+00	.000E+00	.000E+00	.000E+00	.000E+00	.000E+00	.000E+00	.000E+00	.000E+00	.000E+00	.000E+00	.000E+00	.000E+00	.000E+00	.000E+00	.000E+00	.000E+00	.000E+00	.000E+00	.000E+00	.000E+00	.000E+00	.000E+00	.000E+00	.000E+00	.000E+00	.000E+00	.000E+00	.000E+00	.000E+00	.000E+00	.000E+00	.000E+00	.000E+00	.000E+00	.000E+00	.000E+00	.000E+00	.000E+00	.000E+00	.000E+00	.000E+00	.000E+00	.000E+00	.000E+00	.000E+00	.000E+00	.000E+00	.000E+00	.000E+00	.000E+00	.000E+00	.000E+00	.000E+00	.000E+00	.000E+00	.000E+00	.000E+00	.000E+00	.000E+00	.000E+00	.000E+00	.000E+00	.000E+00	.000E+00	.000E+00	.000E+00	.000E+00	.000E+00	.000E+00	.000E+00	.000E+00	.000E+00	.000E+00	.000E+00	.000E+00	.000E+00	.000E+00	.000E+00	.000E+00	.000E+00	.000E+00	.000E+00	.000E+00	.000E+00	.000E+00	.000E+00	.000E+00	.000E+00	.000E+00	.000E+00	.000E+00	.000E+00	.000E+00	.000E+00	.000E+00	.000E+00	.000E+00	.000E+00	.000E+00	.000E+00	.000E+00	.000E+00	.000E+00	.000E+00	.000E+00	.000E+00	.000E+00	.000E+00	.000E+00	.000E+00	.000E+00	.000E+00	.000E+00	.000E+00	.000E+00	.000E+00	.000E+00	.000E+00	.000E+00	.000E+00	.000E+00	.000E+00	.000E+00	.000E+00	.000E+00	.000E+00	.000E+00	.000E+00	.000E+00	.000E+00	.000E+00	.000E+00	.000E+00	.000E+00	.000E+00	.000E+00	.000E+00	.000E+00	.000E+00	.000E+00	.000E+00	.000E+00	.000E+00	.000E+00	.000E+00	.000E+00	.000E+00	.000E+00	.000E+00	.000E+00	.000E+00	.000E+00	.000E+00	.000E+00	.000E+00	.000E+00	.000E+00	.000E+00	.000E+00	.000E+00	.000E+00	.000E+00	.000E+00	.000E+00	.000E+00	.000E+00	.000E+00	.000E+00	.000E+00	.000E+00	.000E+00	.000E+00	.000E+00	.000E+00	.000E+00	.000E+00	.000E+00	.000E+00	.000E+00	.000E+00	.000E+00	.000E+00	.000E+00	.000E+00	.000E+00	.000E+00	.000E+00	.000E+00	.000E+00	.000E+00	.000E+00	.000E+00	.000E+00	.000E+00	.000E+00	.000E+00	.000E+00	.000E+00	.000E+00	.000E+00	.000E+00	.000E+00	.000E+00	.000E+00	.000E+00	.000E+00	.000E+00	.000E+00	.000E+00	.000E+00	.000E+00	.000E+00	.000E+00	.000E+00	.000E+00	.000E+00	.000E+00	.000E+00	.000E+00	.000E+00	.000E+00	.000E+00	.000E+00	.000E+00	.000E+00	.000E+00	.000E+00	.000E+00	.000E+00	.000E+00	.000E+00	.000E+00	.000E+00	.000E+00	.000E+00	.000E+00	.000E+00	.000E+00	.000E+00	.000E+00	.000E+00	.000E+00	.000E+00	.000E+00	.000E+00	.000E+00	.000E+00	.000E+00	.000E+00	.000E+00	.000E+00	.000E+00	.000E+00	.000E+00	.000E+00	.000E+00	.000E+00	.000E+00	.000E+00	.000E+00	.000E+00	.000E+00	.000E+00	.000E+00	.000E+00	.000E+00	.000E+00	.000E+00	.000E+00	.000E+00	.000E+00	.000E+00	.000E+00	.000E+00	.000E+00	.000E+00	.000E+00	.000E+00	.000E+00	.000E+00	.000E+00	.000E+00	.000E+00	.000E+00	.000E+00	.000E+00	.000E+00	.000E+00	.000E+00	.000E+00	.000E+00	.000E+00	.000E+00	.000E+00	.000E+00	.000E+00	.000E+00	.000E+00	.000E+00	.000E+00	.000E+00	.000E+00	.000E+00	.000E+00	.000E+00	.000E+00	.000E+00	.000E+00	.000E+00	.000E+00	.000E+00	.000E+00	.000E+00	.000E+00	.000E+00	.000E+00	.000E+00	.000E+00	.000E+00	.000E+00	.000E+00	.000E+00	.000E+00	.000E+00	.000E+00	.000E+00	.000E+00	.000E+00	.000E+00	.000E+00	.000E+00	.000E+00	.000E+00	.000E+00	.000E+00	.000E+00	.000E+00	.000E+00	.000E+00	.000E+00	.000E+00	.000E+00	.000E+00	.000E+00	.000E+00	.000E+00	.000E+00	.000E+00	.000E+00	.000E+00	.000E+00	.000E+00	.000E+00	.000E+00	.000E+00	.000E+00	.000E+00	.000E+00	.000E+00	.000E+00	.000E+00	.000E+00	.000E+00	.000E+00	.000E+00	.000E+00	.000E+00	.000E+00	.000E+00	.000E+00	.000E+00	.000E+00	.000E+00	.000E+00	.000E+00	.000E+00	.000E+00	.000E+00	.000E+00	.000E+00	.000E+00	.000E+00	.000E+00	.000E+00	.000E+00	.000E+00	.000E+00	.000E+00	.000E+00	.000E+00	.000E+00	.000E+00	.000E+00	.000E+00	.000E+00	.000E+00	.000E+00	.000E+00	.000E+00	.000E+00	.000E+00	.000E+00	.000E+00	.000E+00	.000E+00	.000E+00	.000E+00	.000E+00	.000E+00	.000E+00	.000E+00	.000E+00	.000E+00	.000E+00	.000E+00	.000E+00	.000E+00	.000E+00	.000E+00	.000E+00	.000E+00	.000E+00	.000E+00	.000E+00	.000E+00	.000E+00	.000E+00	.000E+00	.000E+00	.000E+00	.000E+00	.000E+00	.000E+00	.000E+00	.000E+00	.000E+00	.000E+00	.000E+00	.000E+00	.000E+00	.000E+00	.000E+00	.000E+00	.000E+00	.000E+00	.000E+00	.000E+00	.000E+00	.000E+00	.000E+00	.000E+00	.000E+00	.000E+00	.000E+00	.000E+00	.000E+00	.000E+00	.000E+00	.000E+00	.000E+00	.000E+00	.000E+00	.000E+00	.000E+00	.000E+00	.000E+00	.000E+00	.000E+00	.000E+00	.000E+00	.000E+00	.000E+00	.000E+00	.000E+00	.000E+00	.000E+00	.000E+00	.000E+00	.000E+00	.000E+00	.000E+00	.000E+00	.000E+00	.000E+00	.000E+00	.000E+00	.000E+00	.000E+00	.000E+00	.000E+00	.000E+00	.000E+00	.000E+00	.000E+00	.000E+00	.000E+00	.000E+00	.000E+00	.000E+00	.000E+00	.000E+00	.000E+00	.000E+00	.000E+00	.000E+00	.000E+00	.000E+00	.000E+00	.000E+00	.000E+00	.000E+00	.000E+00	.000E+00	.000E+00	.000E+00	.000E+00	.000E+00	.000E+00	.000E+00	.000E+00	.000E+00	.000E+00	.000E+00	.000E+00	.000E+00	.000E+00	.000E+00	.000E+00	.000E+00	.000E+00	.000E+00	.000E+00	.000E+00	.000E+00	.000E+00	.000E+00	.000E+00	.000E+00	.000E+00	.000E+00	.000E+00	.000E+00	.000E+00	.000E+00	.000E+00	.000E+00	.000E+00	.000E+00	.000E+00	.000E+00	.000E+00	.000E+00	.000E+00	.000E+00	.000E+00	.000E+00	.000E+00	.000E+00	.000E+00	.000E+00	.000E+00	.000E+00	.000E+00	.000E+00	.000E+00	.000E+00	.000E+00	.000E+00	.000E+00	.000E+00	.000E+00	.000E+00	.000E+00	.000E+00	.000E+00	.000E+00	.000E+00	.000E+00	.000E+00	.000E+00	.000E+00	.000E+00	.000E+00	.000E+00	.000E+00	.000E+00	.000E+00	.000E+00	.000E+00	.000E+00	.000E+00	.000E+00	.000E+00	.000E+00	.000E+00	.000E+00	.000E+00	.000E+00	.000E+00	.000E+00	.000E+00	.000E+00	.000E+00	.000E+00	.000E+00	.000E+00	.000E+00	.000E+00	.000E+00	.000E+00	.000E+00	.000E+00	.000E+00	.000E+00	.000E+00	.000E+00	.000E+00	.000E+00	.000E+00	.000E+00	.000E+00	.000E+00	.000E+00	.000E+00	.000E+00	.000E+00	.000E+00	.000E+00	.000E+00	.000E+00	.000E+00	.000E+00	.000E+00	.000E+00	.000E+00	.000E+00	.000E+00	.000E+00	.000E+00	.000E+00	.000E+00	.000E+00	.000E+00	.000E+00	.000E+00	.000E+00	.000E+00	.000E+00	.000E+00	.000E+00	.000E+00	.000E+00	.000E+00	.000E+00	.000E+00	.000E+00	.000E+00	.000E+00	.000E+00	.000E+00	.000E+00	.000E+00	.000E+00	.000E+00	.000E+00	.000E+00	.000E+00	.000E+00	.000E+00	.000E+00	.000E+00	.000E+00	.000E+00	.000E+00	.000E+00	.00

TABLE C-5 (Cont).

17	15.000	5.150E-02	9.621E-01	.000E+00	.000E+00	4.600E-03	1.591E-04	.000E+00
18	14.000	7.051E-02	1.125E+00	.000E+00	.000E+00	5.026E-03	1.591E-04	.000E+00
19	13.000	9.652E-02	1.316E+00	.000E+00	.000E+00	5.504E-03	1.591E-04	.000E+00
20	12.000	1.21E-01	1.539E+00	.000E+00	.000E+00	6.081E-03	1.591E-04	.000E+00
21	11.000	1.009E-01	1.801E+00	.000E+00	.000E+00	6.798E-03	1.591E-04	.000E+00
22	10.000	2.859E-01	2.101E+00	.000E+00	.000E+00	7.758E-03	1.591E-04	.000E+00
23	9.000	3.304E-01	2.442E+00	.000E+00	.000E+00	8.328E-03	1.591E-04	.000E+00
24	8.000	4.393E-01	2.825E+00	.000E+00	.000E+00	8.328E-03	1.591E-04	.000E+00
25	7.000	5.788E-01	3.257E+00	.000E+00	.000E+00	8.328E-03	1.591E-04	.000E+00
26	6.000	7.563E-01	3.740E+00	.000E+00	.000E+00	8.328E-03	1.591E-04	.000E+00
27	5.000	9.807E-01	4.180E+00	.000E+00	.000E+00	8.328E-03	1.591E-04	.000E+00
28	4.000	1.263E+00	4.881E+00	.000E+00	.000E+00	8.328E-03	1.591E-04	.000E+00
29	3.000	1.615E+00	5.549E+00	.000E+00	.000E+00	8.328E-03	1.591E-04	.000E+00
30	2.000	2.053E+00	6.190E+00	.000E+00	.000E+00	8.328E-03	1.591E-04	.000E+00
31	1.000	2.595E+00	7.108E+00	.000E+00	.000E+00	8.328E-03	1.591E-04	.000E+00
32	.000	3.262E+00	8.012E+00	.000E+00	.000E+00	8.328E-03	1.591E-04	.000E+00

SUMMARY OF THE GEOMETRY CALCULATION

H1 = 100.000 KM
 H2 = .000 KM
 ANGLE = 190.000 DEG
 RANGE = 100.000 KM
 BETA = .000 DEG
 PHI = .000 DEG
 HMIN = .000 KM
 BENDING = .000 DEG
 LEN = 0

EQUIVALENT SEA LEVEL TOTAL ABSORBER AMOUNTS

H2O	CO2+	O3	HNO3	O3 UV	CNTMSLF1	CNTMSLF2	CNTMFRN
(SCALED LOWTRAN UNITS)	(ATM CM)	(ATM CM)	(ATM CM)	(ATM CM)	(MOL CM-2)	(MOL CM-2)	(MOL CM-2)
1.144E+00	4.657E+00	1.107E-01	3.876E-04	3.434E-01	2.807E+20	9.131E+19	4.007E+22
N2 CONT	MOL SCAT	AER 1	AER 2	AER 3	AER 4	CIRRUS	MEAN RH (PRCNT)
3.262E+00	8.012E+00	1.002E+00	7.991E-02	8.328E-03	1.591E-04	.000E+00	48.25

SINGLE SCATTERING POINT TO SOURCE PATHS

POINT	ALT	SCATR ANGLE	SUBTENDED ANGLE	SOLAR ZENITH	PATH ZENITH	RELATIVE AZIMUTH	SCATR ANGLE	MOLECULAR PHASE F
1	100.00	.00	.00	60.00	180.00	1	120.00	.748E-01
2	70.00	.00	.00	60.00	180.00	1	120.00	.748E-01
3	50.00	.00	.00	60.00	180.00	1	120.00	.748E-01
4	45.00	.00	.00	60.00	180.00	1	120.00	.748E-01
5	40.00	.00	.00	60.00	180.00	1	120.00	.748E-01

TABLE C-5 (Cont.).

6	35.00	.00	60.00	100.00	1	120.00	.748E-01
7	30.00	.00	60.00	100.00	1	120.00	.748E-01
8	25.00	.00	60.00	100.00	1	120.00	.748E-01
9	24.50	.00	60.00	100.00	1	120.00	.748E-01
10	23.00	.00	60.00	100.00	1	120.00	.748E-01
11	22.00	.00	60.00	100.00	1	120.00	.748E-01
12	21.00	.00	60.00	100.00	1	120.00	.748E-01
13	20.00	.00	60.00	100.00	1	120.00	.748E-01
14	19.00	.00	60.00	100.00	1	120.00	.748E-01
15	18.00	.00	60.00	100.00	1	120.00	.748E-01
16	17.00	.00	60.00	100.00	1	120.00	.748E-01
17	16.00	.00	60.00	100.00	1	120.00	.748E-01
18	15.00	.00	60.00	100.00	1	120.00	.748E-01
19	14.00	.00	60.00	100.00	1	120.00	.748E-01
20	13.00	.00	60.00	100.00	1	120.00	.748E-01
21	12.00	.00	60.00	100.00	1	120.00	.748E-01
22	11.00	.00	60.00	100.00	1	120.00	.748E-01
23	10.00	.00	60.00	100.00	1	120.00	.748E-01
24	9.00	.00	60.00	100.00	1	120.00	.748E-01
25	8.00	.00	60.00	100.00	1	120.00	.748E-01
26	7.00	.00	60.00	100.00	1	120.00	.748E-01
27	6.00	.00	60.00	100.00	1	120.00	.748E-01
28	5.00	.00	60.00	100.00	1	120.00	.748E-01
29	4.00	.00	60.00	100.00	1	120.00	.748E-01
30	3.00	.00	60.00	100.00	1	120.00	.748E-01
31	2.00	.00	60.00	100.00	1	120.00	.748E-01
32	1.00	.00	60.00	100.00	1	120.00	.748E-01
33	.00	.00	60.00	100.00	1	120.00	.748E-01

TABLE C-5 (Cont).

RADIANCE(WATTS/CM²-STER-XXX)

FREQ (CM-1)	WAVLEN (MICRN)	ATMOS RADIANCE (CM-1)	PATH SCATTERED RADIANCE TOTAL (CM-1)	S SCAT (CM-1)	GROUND REFLECTED RADIANCE TOTAL (CM-1)	RADIANCE DIRECT (CM-1)	TOTAL RADIANCE (CM-1)	INTEGRAL TOTAL (CM-1)	TRANS				
18100	.552	1.35E-39	4.41E-35	2.05E-07	6.72E-03	4.70E-08	1.37E-07	4.49E-03	8.01E-08	3.42E-07	1.12E-02	1.71E-06	.2020
18110	.552	1.28E-39	4.21E-35	2.05E-07	6.73E-03	4.70E-08	1.37E-07	4.49E-03	8.79E-08	3.42E-07	1.12E-02	5.13E-06	.2010
18120	.552	1.22E-39	4.02E-35	2.05E-07	6.73E-03	4.71E-08	1.37E-07	4.49E-03	8.73E-08	3.42E-07	1.12E-02	9.55E-06	.2016
18130	.552	1.17E-39	3.83E-35	2.05E-07	6.74E-03	4.71E-08	1.36E-07	4.48E-03	8.77E-08	3.41E-07	1.12E-02	1.20E-05	.2013
18140	.551	1.11E-39	3.66E-35	2.05E-07	6.75E-03	4.71E-08	1.36E-07	4.48E-03	8.75E-08	3.41E-07	1.12E-02	1.54E-05	.2011
18150	.551	1.06E-39	3.49E-35	2.05E-07	6.75E-03	4.71E-08	1.36E-07	4.48E-03	8.74E-08	3.41E-07	1.12E-02	1.88E-05	.2009
18160	.551	1.01E-39	3.33E-35	2.05E-07	6.76E-03	4.71E-08	1.36E-07	4.48E-03	8.73E-08	3.41E-07	1.12E-02	2.22E-05	.2007
18170	.550	9.62E-40	3.16E-35	2.05E-07	6.76E-03	4.71E-08	1.36E-07	4.48E-03	8.72E-08	3.41E-07	1.12E-02	2.56E-05	.2005
18180	.550	9.17E-40	3.03E-35	2.05E-07	6.77E-03	4.71E-08	1.35E-07	4.48E-03	8.70E-08	3.40E-07	1.12E-02	2.90E-05	.2003
18190	.550	8.74E-40	2.89E-35	2.05E-07	6.79E-03	4.72E-08	1.35E-07	4.48E-03	8.70E-08	3.40E-07	1.13E-02	3.24E-05	.2000
18200	.549	8.33E-40	2.76E-35	2.05E-07	6.80E-03	4.73E-08	1.35E-07	4.48E-03	8.69E-08	3.40E-07	1.13E-02	3.58E-05	.2007
18210	.549	7.94E-40	2.63E-35	2.05E-07	6.81E-03	4.73E-08	1.35E-07	4.48E-03	8.68E-08	3.40E-07	1.13E-02	3.92E-05	.2003
18220	.549	7.57E-40	2.51E-35	2.06E-07	6.82E-03	4.74E-08	1.35E-07	4.48E-03	8.67E-08	3.40E-07	1.13E-02	4.26E-05	.2000
18230	.549	7.21E-40	2.40E-35	2.06E-07	6.83E-03	4.74E-08	1.35E-07	4.48E-03	8.66E-08	3.40E-07	1.13E-02	4.60E-05	.2007
18240	.548	6.87E-40	2.29E-35	2.06E-07	6.85E-03	4.74E-08	1.35E-07	4.48E-03	8.65E-08	3.40E-07	1.13E-02	4.94E-05	.2004
18250	.548	6.55E-40	2.19E-35	2.06E-07	6.86E-03	4.75E-08	1.34E-07	4.48E-03	8.64E-08	3.40E-07	1.13E-02	5.28E-05	.2000
18260	.548	6.25E-40	2.08E-35	2.06E-07	6.87E-03	4.75E-08	1.34E-07	4.48E-03	8.63E-08	3.40E-07	1.13E-02	5.62E-05	.2007

INTEGRATED ABSORPTION FROM 18100 TO 18260 CM-1 = 115.19 CM-1
AVERAGE TRANSMITTANCE = .28F1

INTEGRATED RADIANCE = 5.455E-05 WATTS CM-2 STER-1
MINIMUM RADIANCE = 3.403E-07 WATTS CM-2 STER-1 (CM-1)-1 AT 18100.0 CM-1
MAXIMUM RADIANCE = 3.421E-07 WATTS CM-2 STER-1 (CM-1)-1 AT 18100.0 CM-1
BOUNDARY TEMPERATURE = 280.28 K
BOUNDARY EMISSIVITY = .689

CARD 5 *****

16.40.21.UCLP. AA. LP2 1.024K LMS.

END

12-86

DTIC